Molecular Mechanisms of Childhood Idiopathic Nephrotic Syndrome

Thesis format: Thesis by article

Robert Myette

Graduate Program in
Cellular and Molecular Medicine

Thesis submitted to the University of Ottawa
in partial fulfillment of the requirements for the
Doctorate in Philosophy Degree in Cellular and Molecular Medicine.

School of Graduate and Postdoctoral Studies
Cellular and Molecular Medicine
Faculty of Medicine
University of Ottawa

i. Abstract

Idiopathic nephrotic syndrome (iNS), a podocytopathy, is the most common glomerulopathy in children, characterized by significant proteinuria, hypoalbuminemia, and edema, and is managed with steroid therapy. Despite the prevalence of iNS, it remains poorly understood, with no definitive etiology, and no reliable biomarkers for predicting relapse, remission, or long-term outcome. This thesis investigated the role of podocyte-derived extracellular vesicles (EVs), particularly large EVs (LEVs), as biomarkers of iNS disease activity, and as indicators of fundamental biological processes in the podocyte. I used integrated and novel approaches to further the molecular understanding of iNS, including *in vitro* models of podocyte stress, an *in vivo* rat nephrosis model, and urinary specimens from children with iNS. I identified that *in vitro,* podocytes respond to puromycin aminonucleoside (PAN)-induced injury by increasing vesiculation, and further that PAN induces a mitochondrial bioenergetic stress linked with packaging of LEVs with mitochondrial DNA (mtDNA). Prednisolone, the gold-standard immunomodulatory agent used in pediatric iNS, was shown to attenuate these PAN-induced impacts *in vitro*. Lastly, proteomic profiling of LEVs from podocytes, as well as those derived from urinary specimens from children, revealed hundreds of proteins specific to disease relapse, as well as PAN-induced podocyte stress. These novel observations suggest that LEVs reflect dynamic podocyte states which might reflect disease conditions in humans. This work provides the impetus for future studies directed at further understanding the LEV mtDNA and proteomic cargo which will offer further insights into iNS pathophysiology.

ii. Graphical Abstract

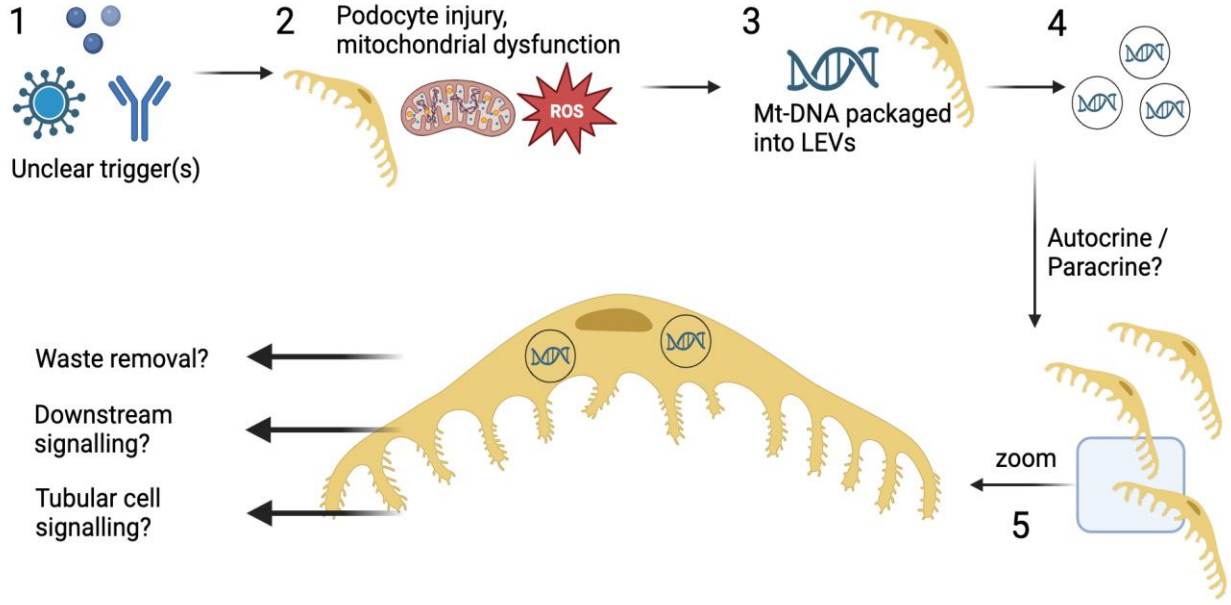

Graphical Abstract 1: Extracellular vesicles (EVs) containing mitochondrial DNA (mtDNA) are released from stressed podocytes.

(1) Nephrotic syndrome (NS) in children has an unclear pathogenesis. (2) Mitochondrial stress has been linked with proteinuric glomerular diseases, and we hypothesized that mitochondrial stress is an important driver of NS. (3, 4, 5) We discovered that podocytes with stressed mitochondria release mtDNA into EVs. The role of mtDNA within LEVs remains unclear, and future studies are directed at better understanding this. A version of this is published in IJMS (https://doi.org/10.3390/ijms26157245).

iii. Acknowledgment

I am indebted to so many people that it would be difficult to name them all. First and foremost, Monica, my wife, for supporting and loving me along the way; I'm finally finishing after 20 years of education. Next, my family. My parents and siblings have been stalwart supporters of my academic journey for the last 20 years. My PhD supervisors who took me in with my crazy ideas and gave me the time and support to see this through, Dr. Dylan Burger and Dr. Chris Kennedy. Mentors along the way, especially including Drs. Feber, Berman, Alexander, Jankov, Menzies, Stanford, Takano, Gadde, Roussel. Next, to the KRC Scientists for welcoming me with open arms. I'd like to thank the entire Burger and Kennedy labs for the innumerable answers to questions, camaraderie, coffee, and general conversation. I'd like to particularly thank Dr. Chet Holterman, Dr. Mayra Trentin-Sonoda, Dr. Fengxia Xiao, and Dr. Julie Zhu for significant support along the way.

iv. Statement of co-authorship

Dr. Fengxia Xiao performed the flow cytometry experiments outlined in Chapter 2.

Dr. Chet Holterman assisted with rat experiments in Chapter 3.

Dr. Tyler T. Cooper performed the proteomics described in Chapter 4.

All other experiments were performed by myself.

v. List of publications during PhD.

1: Tracey Bushnik, Robert Myette, Janine Clark. From BpTRU to OMRON: The impact of changing automated blood pressure measurement devices on blood pressure estimates among children and youth. Health Rep. 2024 Dec 18; 35(12): 16-30.

2: Myette RL, Trentin-Sonoda M, Landry C, Holterman CE, Lin T, Burger D, Kennedy CRJ. Damage-Associated Molecular Patterns and Pattern Recognition Receptors in the Podocyte. J Am Soc Nephrol. 2024 Sep 27. doi: 10.1681/ASN.0000000531. Epub ahead of print. PMID: 39331471.

3: Myette RL, Obrycki Ł, Litwin M, Seeman T, Šuláková T, Feber J. Ambulatory isolated diastolic hypertension and risk of left ventricular hypertrophy in children with primary and secondary hypertension. Pediatr Nephrol. 2024 Jul 18. doi: 10.1007/s00467-024-06457-8. Epub ahead of print. PMID: 39023539.

4: Myette RL, Lamarche C, Odutayo A, Verdin N, Canney M. Cardiovascular Risk in Patients With Glomerular Disease: A Narrative Review of the Epidemiology, Mechanisms, Management, and Patient Priorities. Can J Kidney Health Dis. 2024 Feb 22;11:20543581241232472. doi: 10.1177/20543581241232472. PMID: 38404647; PMCID: PMC10894549.

5: Myette RL, Flynn JT. The ongoing impact of obesity on childhood hypertension. Pediatr Nephrol. 2024 Aug;39(8):2337-2346. doi: 10.1007/s00467-023-06263-8. Epub

2024 Jan 8. PMID: 38189961.

6: Dion R, Myette RL. An afebrile seizure in a previously healthy 9-year-old boy. Paediatr Child Health. 2023 Mar 22;28(5):268-269. doi: 10.1093/pch/pxad009. PMID: 37484039; PMCID: PMC10362961.

7: Myette RL, Xiao F, Geier P, Feber J, Burger D, Kennedy CRJ. Urinary podocyte-derived large extracellular vesicles are increased in paediatric idiopathic nephrotic syndrome. Nephrol Dial Transplant. 2023 Aug 31;38(9):2089-2091. doi: 10.1093/ndt/gfad086. PMID: 37120731; PMCID: PMC10468739.

8: Seeman T, Myette RL, Feber J. Hypertension in pediatric kidney transplantation. Pediatr Transplant. 2023 Aug;27(5):e14522. doi:10.1111/petr.14522. Epub 2023 Apr 28. PMID: 37118862.

9: Abolbaghaei A, Mohammad S, da Silva DF, Hutchinson KA, Myette RL, Adamo KB, Burger D. Impact of acute moderate-intensity aerobic exercise on circulating extracellular vesicles in pregnant and non-pregnant women. Appl Physiol Nutr Metab. 2023 Feb 1;48(2):198-208. doi: 10.1139/apnm-2022-0288. Epub 2022 Nov 18. PMID: 36661228.

10: Burger D, Abdelrasoul A, Alexander RT, Ballermann B, Bridgewater D, Chan JSD, Cunanan J, Cybulsky AV, Gerarduzzi C, Gunaratnam L, Hartwig S, Kapus A, Kennedy

CRJ, Lamarche C, Myette RL, Nmecha IK, Stalker L, Szaszi K, Torban E, Zhang SL, Takano T. Advancing Discovery Research in Nephrology in Canada: A Conference Report From the 2021 Molecules and Mechanisms Mediating Kidney Health and Disease (M3K) Scientific Meeting and Investigator Summit. Can J Kidney Health Dis. 2022 Dec 17;9:20543581221144824. doi: 10.1177/20543581221144824. PMID: 36545249; PMCID: PMC9761209.

11: Constantinescu AR, Mattoo TK, Smoyer WE, Greenbaum LA, Niu J, Howard N, Muff-Luett M, Benoit EB, Traum A, Annaim AA, Wenderfer SE, Plautz E, Rheault MN, Myette RL, Twombley KE, Kamigaki Y, Wandique-Rapalo B, Kallash M, Vasylyeva TL. Clinical presentation and management of nephrotic syndrome in the first year of life: A report from the Pediatric Nephrology Research Consortium. Front Pediatr. 2022 Sep 14;10:988945. doi: 10.3389/fped.2022.988945. PMID: 36210940; PMCID: PMC9534228.

12: Holterman CE, Myette RL, Burger D, Kennedy CR. A letter to the editor about "dopamine 1 receptor activation protects mouse diabetic podocytes injury via regulating the PKA/NOX-5/p38 MAPK axis". Exp Cell Res. 2022 Jun 1;415(1):113065. doi: 10.1016/j.yexcr.2022.113065. Epub 2022 Mar 14. PMID: 35300856.

13: Myette RL, Feber J, Blinder H, Bendiak GN, Foster BJ, MacLean JE, Constantin E, Katz SL. Blood pressure variability in children with obesity and sleep-disordered breathing following positive airway pressure treatment. Pediatr Res.

2022 Sep;92(3):810-815. doi: 10.1038/s41390-021-01841-8. Epub 2021 Nov 16. PMID: 34785780.

14. Pediatric antihypertensives: a short overview – Learning the Ropes. RL Myette, ISH Hypertension News, 26-27.

15: Myette RL, Burger D. Relapse in steroid-sensitive nephrotic syndrome: are extracellular vesicles the missing link? Am J Physiol Renal Physiol. 2021 Nov 1;321(5):F656-F658. doi: 10.1152/ajprenal.00349.2021. Epub 2021 Sep 27. PMID: 34569254.

16: Myette RL, Burger D, Geier P, Feber J. Diastolic hypertension is associated with proteinuria in pediatric patients. Health Sci Rep. 2021 Aug 9;4(3):e346. doi: 10.1002/hsr2.346. PMID: 34401524; PMCID: PMC8351612.

vi. List of Figures

vii. List of Tables

Table of Contents

1 Introduction

1.1 NEPHROTIC SYNDROME

Nephrotic syndrome (NS) is a disease characterized by multiple signs and symptoms which are the result of injury to the glomerular podocyte [1]. NS is comprised of proteinuria, hypoalbuminemia, and significant edema, which make up the diagnostic criteria [2–5]. There are distinct differences, and commonalities, between pediatric and adult NS. Importantly, NS in adults is most commonly a secondary form, often associated with infection, malignancy, and medication side effects [6]. However, NS diagnosed as minimal change disease (MCD), the most common lesion seen in childhood cases, does occur [7]. In children, NS is most commonly idiopathic and associates with histopathological hallmarks including MCD or focal segmental glomerulosclerosis (FSGS) [8], discussed further in Chapter 1.5. The overall focus of this thesis will be on NS in childhood.

1.2 NEPHROTIC SYNDROME OF CHILDHOOD

Childhood NS is the most common glomerulopathy in children [9]. Children present in a similar fashion to the description above, with significant edema associated with proteinuria and hypoalbuminemia. Parents often describe foamy urine, due to the degree of proteinuria. While being the most common glomerulopathy in children, it is still considered a rare disease [8] with an incidence of ~1.4-6.1 per 100,000 children, worldwide, with significant differences observed due to ethnical backgrounds [10]. In Canada, the incidence is approximately 1:5,000. A major classification approach is response to steroids. Importantly, this is a heterogeneous disease where some children will develop a relapsing-remitting course, and others will have a single episode;

and, following treatment, will not relapse again. Specifically, approximately 40% have a single episode, or infrequently relapsing NS while up to 60% will have a frequently relapsing course [8]. Underlying reasons for these vastly different courses for the same disease are unclear. Further complications stem from resistance to the primary form of treatment, steroids, so called steroid resistant NS (SRNS). Indeed, up to 20% of children with NS will be resistant to steroids. This resistance can be primary, where it is most likely related to a monogenic disease [11], while in other cases this is an acquired, secondary resistance to steroids. Genetic NS will be discussed in the following chapter.

1.3 GENETIC NS IN CHILDREN

As mentioned, monogenic forms of NS in children exist, but are rare. However, these cases are generally identified if children are diagnosed at an early age (<1 year) or have steroid resistant disease [11]. Importantly, if caring for a child with NS from a consanguineous family, the chance of a genetic origin increases substantially to nearly 30% [8]. These monogenic forms result in structural abnormalities of the podocyte, which are irreparable, and thus not responsive to immunosuppressive therapy. This becomes obvious after 4-6 weeks of steroids without any clear histological (if biopsy is available) or clinical response. Further clues to a genetic origin of NS include altered kidney function, as in most instances non-genetic, so-called idiopathic NS (iNS) patients have normal kidney function.

Most common genetic findings include mutations in the Nephrin (*NPHS1)* gene, the so-called “Finnish Nephrotic Syndrome”, as well as Podocin (*NPHS2*); however, other genes have been identified and showed causal for monogenic forms of NS, including Phospholipase C epsilon 1 (*PLCE1),* Laminin Subunit Beta 2 (*LAMB2),* and Wilms Tumour 1 (*WT1)* [12]. Interestingly,

collagen mutations, though most related to Alport Syndrome, have also been identified as a monogenic cause of NS [13]. Importantly, particularly for this thesis, is the observation that mitochondrial genes, including several of the Coenzyme *Q* genes, are associated with monogenic forms of NS [14]. This directly supports the role of mitochondria in podocyte health and disease. **Figure 1** outlines several of the monogenic diseases associated with SRNS, of which there are over 50 [1].

It is clear that several genetic mutations can cause podocytopathies which results in a steroid resistant form of NS; however, what about the genetics of steroid sensitive NS (SSNS)? Indeed, the search for genetic associations with SSNS have been ongoing for some time [15]; however, to date, no definitive genetic cause has been identified [8].

While genetic causes of NS are rare, there is a certain phenotype associated with monogenic forms. The search for a genetic association with SSNS is ongoing; however, has yet to be identified. What then makes up the significantly larger group of children with NS? Having been studied for over 60 years, idiopathic nephrotic syndrome (iNS) makes up the most significant proportion of children diagnosed with NS and is the topic of the next section.

1.4 INS IN CHILDREN

Upwards of 85% of children presenting with iNS between the ages of 1-15 will have SSNS. Because the associated presentation with SSNS is well known, a biopsy is rarely undertaken, and if done, reveals the classic histopathology of MCD. The pathophysiology of iNS in children remains mysterious; however, mounting evidence suggests the immune system plays a role [16]. Indeed, as defined, SSNS is steroid sensitive, and thus the pathomechanism seems to be related to a process amenable to immunosuppressive therapy. Recent evidence suggests that

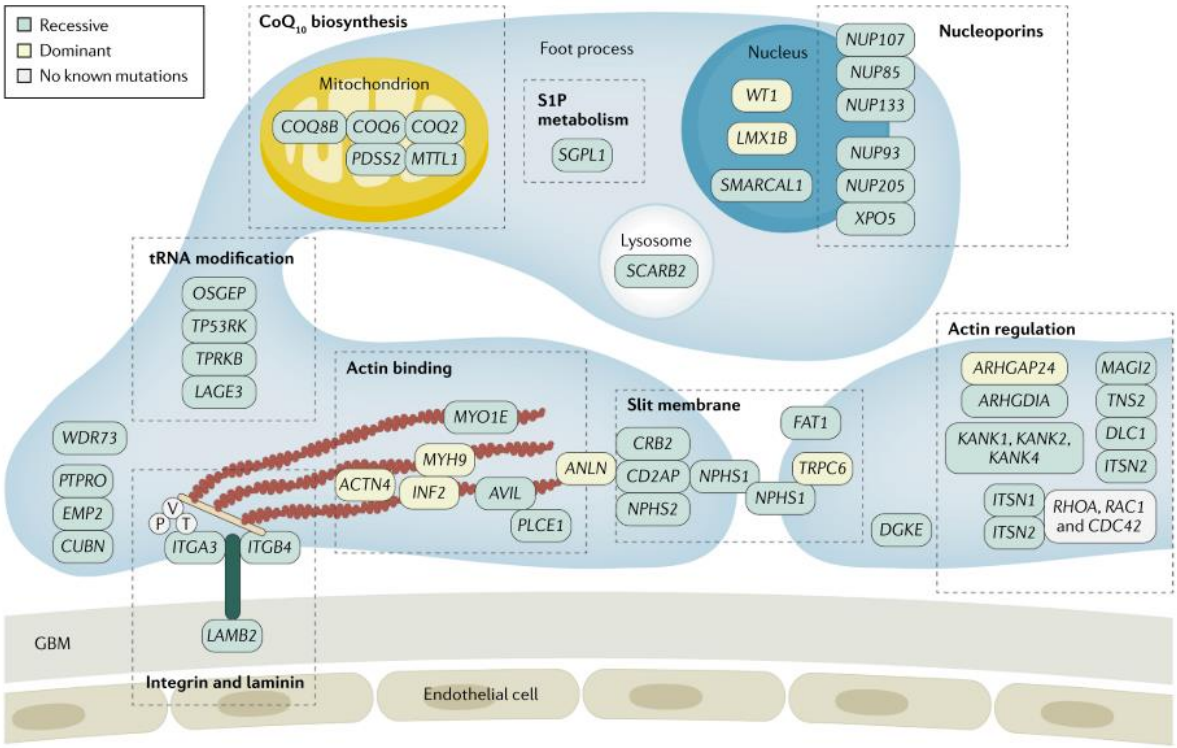

Figure 1. Monogenetic diseases and SRNS

Identification of single-gene causes of steroid-resistant nephrotic syndrome (SRNS) placed the podocyte at the centre of SRNS pathogenesis because most of the implicated genes are expressed in podocytes. Foot processes interdigitate with those from neighbouring podocytes, forming the glomerular slit membrane, which is critical for filtering and retention of protein in the blood-stream. Its integrity is lost in nephrotic syndrome. Proteins encoded by genes that, if mutated, cause monogenic SRNS localize to specific subcellular sites of podocytes depicted here. CoQ10, coenzyme Q10; GBM, glomerular basement membrane; P, paxillin; T, talin; V, vilin. Figure and figure legend reproduced, with permission, Springer Nature [1].

in certain instances, this may represent an autoimmune disease [17–19]. Contrary to these opinions are questions related to how the anti-Nephrin [20] or anti-Ubiquitin Carboxyl-Terminal Hydrolase L1 (UCHL1) [21] antibodies, for example, are made, given the podocyte is relatively 'immune privileged'. Further, if this is a true immune process, particularly involving antibody-mediated damage, why is there only minimal evidence of immune complex deposition or inflammatory infiltrate on biopsy?

In support of the autoimmune, anti-podocyte antibody theory are the countless reports of children having recurrence of their disease post-kidney transplant, suggesting the trigger for disease remains present even after removal of failed kidneys. The most impressive example includes the implantation of a kidney which showed immediate recurrence; however, once explanted and re-implanted into another patient who did not previously have NS, the kidney did not show any signs of recurrence, and the patient did not develop NS [22].

While the autoantibody theory gains traction, and undergoes necessary scrutiny, it is important to recognize previous theories over the past 60 years, including a virally mediated, post-Epstein Barr Virus induced glomerulopathy [23], or the presence of a 'circulating factor' which, when present, leads to the podocyte effacement seen in biopsy specimens (identified as MCD) [24]. This circulating factor has been regarded as the proverbial, 'holy grail' of iNS, and many groups have wondered whether it is in fact an antibody (which aligns well with the most recent autoimmune mechanisms discussed above [17, 21]), a cytokine [25], or potentially extracellular vesicles [26].

1.5 CLINICAL MANIFESTATIONS, IN-DEPTH BIOPSY FINDINGS, AND TREATMENT APPROACHES

As briefly mentioned, children with iNS have a very uniform and 'classic' presentation which comprises proteinuria, hypoalbuminemia, and edema. Associated with these signs and symptoms are hallmark secondary characteristics, which includes hypercholesterolemia [9], hypercoagulability [27], increased risk of infection [28], increased risk of cardiovascular disease, and acute kidney injury (AKI) [9]. Importantly, blood pressure differences have been observed, with children with NS having increases in diastolic blood pressure [29].

Hypercholesterolemia is found in all children with iNS, and the severity of the dyslipidemia is directly proportional to the degree of proteinuria [30]. In a study by Ashoor *et al.*, among the children with glomerulopathies who had lipids measured, a staggering 71% had dyslipidemia with 62% having hypercholesterolemia [31]. The second leading glomerulopathy in the study with elevated cholesterol was iNS (labelled here as MCD); with the first being membranous nephropathy (a rare cause of NS in children). Further, of these children with dyslipidemia, only 9% were prescribed a lipid-lowering agent. This is largely due to the limited use of statins in children [9], which perhaps may be associated with provider hesitation, and a lack of clear interventional studies showing benefit. The Ashoor *et al*., study [31] identified a high prevalence of modifiable cardiovascular disease risk factors in primary childhood glomerulopathies with iNS being one of them.

Often, children present with hypovolemia and require fluid resuscitation, which is challenging due to hypoalbuminemia, and thus low oncotic pressure. What is paradoxical is these children are often massively fluid overloaded with significant edema, and therefore a delicate balance must be struck [3, 32, 33]. As a result, children receive intravenous human albumin followed by furosemide as a means to both refill the intravascular space but also coax the

interstitial edema fluid back into the vasculature for expulsion in the urine [33]. Indeed, many studies have interrogated the best approach to this clinical conundrum. Kapur *et al.,* devised an approach taking into consideration sodium excretion, and aldosterone induction [34]. The importance of this intricate balance is best evidenced when considering the prevalence of AKI in children with iNS [35], which is ~30%.

An additional concern for children with iNS includes the heightened risk of infection [28]. Indeed, through overlapping mechanisms of immunodeficiency (in the setting of immunoglobulin losses from the kidney) and immunosuppression (steroid therapy, and steroid-sparing therapies), children are at increased risk of opportunistic infections. Lastly, children with iNS are at increased risk of venous thromboembolism (VTE), again related to the non-specific loss of coagulation-related proteins in the urine [36]. While infection and VTE are distinct entities, there appears to be an association between infections and VTE in hospitalized patients with NS [28].

Overall, clinical features of iNS in children are homogeneous in that all children with iNS will present with proteinuria, hypoalbuminemia, edema, and some degree of hypercholesterolemia; however, there is some variability in who will present with AKI, infection, or VTE. Unfortunately, there are no good clinical biomarkers to assist in prognostication in children with this unique and mysterious disease [37]. I will next discuss another homogeneous aspect of this disease, which relates to the most common biopsy findings in children with iNS.

A challenging aspect with understanding the histopathology of iNS in children is the fact that we do not perform biopsies on all children at presentation; rather, most will have a biopsy if they are not responding to steroids by 4-6 weeks. However, almost universally, when a biopsy is performed in a child with SSNS, the histopathological diagnosis will be MCD [8]. MCD was first coined prior to the invention of the electron microscope as it comprises relatively normal appearing

pathology findings on light microscopy. Specifically, children with MCD will often have normal appearing glomeruli on light microscopy, with the possibility of light IgM positivity [38]. However, overwhelmingly, there is no evidence of immune complex deposition nor immunofluorescence positivity [2]. On the contrary, in those children with steroid resistance after 4-6 weeks, a biopsy will be performed, usually showing FSGS. In either case, there is distinct and clear evidence of podocyte effacement on biopsy. In SSNS cases, if pre-treatment, and post-treatment biopsies were performed, the distinguishing feature would be resolution of podocyte foot process effacement on the follow up biopsy. It is therefore clear that, as stated earlier, the podocyte is central to the disease process in children with iNS. Overall, clinical features are somewhat homogeneous in children with iNS, and this associates with a relatively similar clustering of biopsy findings; however, what is not homogenous is the response to steroids. We will next discuss approaches to therapy in children with iNS.

Children presenting with iNS will universally be started on steroid therapy. Usually this is prednisone, or prednisolone, at a dose of 60 mg/m^2 daily for 6 weeks (maximum dose 60 mg), followed by 40 mg/m^2 (maximum dose 40 mg) every other day for 6 weeks. Next steps are based on how the child responds to therapy. Unfortunately, while there have been studies in the past assessing initial response to steroids, time to remission, and other clinical variables, there has yet to be discovered a definitive clinical marker to predict prognosis or steroid responsiveness in iNS. If the child responds to steroids, and has infrequent relapses, they will likely go on to have exposure only to steroids with minimal to no side effects. If frequently relapsing NS (FRNS), or steroid-dependent NS (SDNS), children will remain on steroids, usually targeting a low-dose, every other day approach of ~5-10 mg. This associates with an increased risk for sequelae not only associated with iNS but also with prednisone. Side effects are severe and include poor linear growth, weight

gain, increased appetite, hirsutism, fragile bones, and ocular complications [2]. Should steroid-induced side effects become a rate limiting step in the ongoing treatment of a child with FRNS or SDNS, initiation of steroid-sparing therapy is required (**Figure 2)**.

Commonly used steroid-sparing agents include cyclophosphamide, tacrolimus, or mycophenolate mofetil [2, 38, 39]. Once proteinuria is controlled, there is consideration for B-cell depleting agents (**Figure 2**), including Rituximab [40]. Each therapy for iNS comes with a significant toxicity profile, and thus, children with iNS are at increased risk of treatment side effects. Importantly, these are closely monitored. An important consideration is for children with iNS who will ultimately be steroid resistant; these children will be exposed to 4-6 weeks of high dose steroids, and in some instances, likely longer treatment courses to ensure no late response, without any realized benefit. **It is therefore clear that prognosticating factors are needed, and a biomarker of steroid resistance *a priori* is urgently needed.**

In summary, iNS in childhood has several unifying clinical and histopathological features; however, the response to therapy greatly differs, particularly the response to steroids. There is no good biomarker to prognosticate who will respond to steroids, and as such, there is an unmet need to discover one. In doing so, children destined to have a steroid resistant phenotype will be spared a considerable amount of ineffective steroids, thus improving their quality of life, and limiting their exposure to unwanted side effects. We next turn our attention to the cell centrally implicated in the disease pathogenesis, the podocyte.

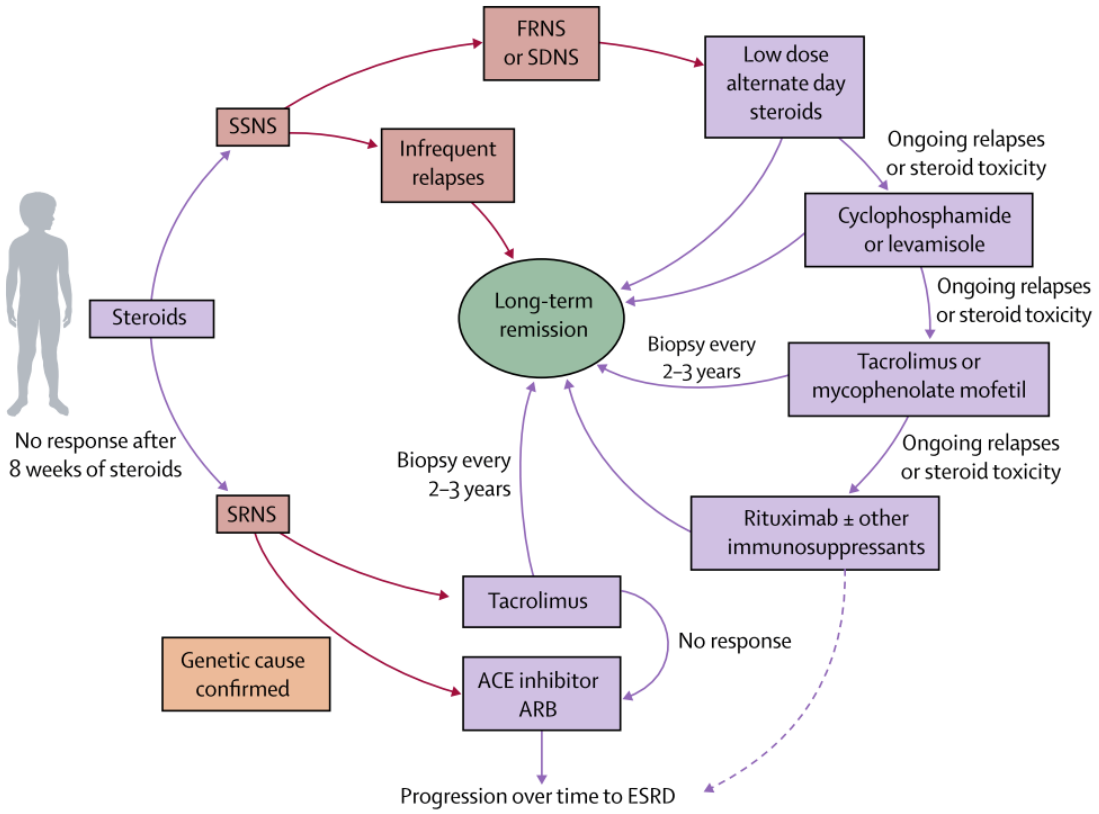

Figure 2. Principal treatments for nephrotic syndrome at diagnosis and follow-up.

After initial therapy with steroids, children are classified as having SSNS or SRNS after at least 8 weeks of therapy. Frequently relapsing SSNS can first be treated with low-dose alternate-day steroids prior to consideration of steroid-sparing agents. Typically, the steroid-sparing agents include cyclophosphamide, or levamisole, and if this fails and the child continues to relapse or is steroid dependent, then a calcineurin inhibitor is often the next agent, or mycophenolate mofetil. The scarcity of trial evidence has resulted in substantial variation in choice of steroid-sparing agents based on physicians' preference, drug availability by country, and cost. SSNS=steroid sensitive nephrotic syndrome. SRNS=steroid resistant nephrotic syndrome. FRNS=frequently relapsing nephrotic syndrome. SDNS=steroid dependent nephrotic syndrome. ACE=angiotensin converting enzyme inhibitor. ARB=angiotensin receptor blocker. Figure and figure legend reproduced with permission, Lancet, Elsevier [2].

1.6 THE PODOCYTE

In order to provide a complete overview of the podocyte, we should first start at the level of the kidney and work our way inwards. The human kidney is a highly specialized organ which is paramount for human health, and is implicated as the cause of disease, and, as an innocent bystander during systemic disease. The kidney is separated into cortex and medulla. The cortex houses the functional tissue for filtration and elimination of waste. Specifically, the glomerulus is the filtering unit of the kidney, and while contentious, it appears there are approximately 1,000,000 glomeruli per kidney [41]. The glomerulus connects with the tubules which allows for passage of urine to the medullary pyramids, and subsequently to the confluence of pyramids, the pelvis, followed by removal into the ureters and bladder. For the purposes of this thesis, the focus will remain on the glomerulus, and specifically the specialized epithelial cells known as podocytes (**Figure 3**).

The glomerulus is comprised of several cell types of varying origins. The podocytes are terminally differentiated and epithelial in nature [42]. The glomerular filtration barrier includes the podocyte foot processes which line the outer aspect of the glomerular basement membrane (GBM) which subsequently abuts with the fenestrated glomerular endothelium. The glomerulus houses a confluence of capillaries allowing for efficient delivery of blood to the filtration apparatus, made up of the interdigitating podocyte foot processes effectively forming slit diaphragms [42].

iNS is categorized as a podocytopathy [1], with the understanding that despite the inciting pathomechanism, the histopathological presentation is that of podocyte structural abnormalities represented as effacement on biopsy. The podocyte has a cell body, major processes, secondary processes, and finally, interdigitating foot processes which creates the slit diaphragm. Within the foot processes, there is copious actin linking adjacent processes [43]. Intermediate fibers make up

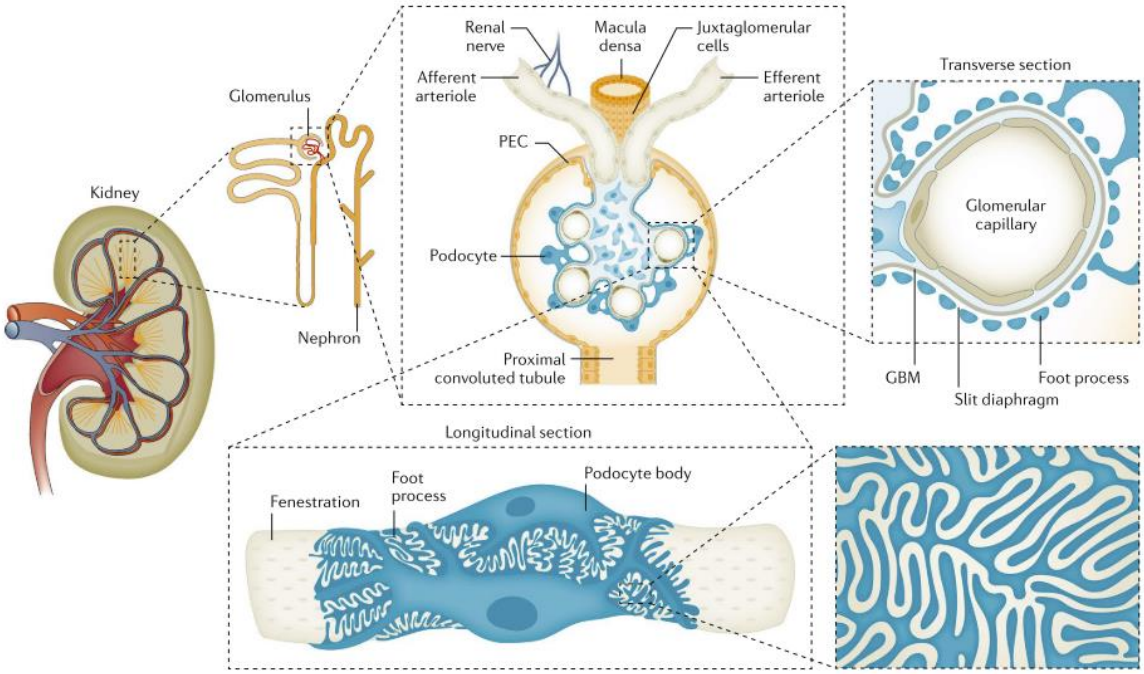

Figure 3. Structure of the nephron, the glomerulus and the filtration barrier.

The kidney is comprised of functional units, nephrons, each of which is made of a glomerulus and a tubule. In healthy humans, the average number of nephrons is ~1 million (range 250,000 to <2.5 million). The glomerulus is composed of a tuft of capillaries covered by visceral epithelial cells — the podocytes — and surrounded by a capsule lined on the inner surface by parietal epithelial cells (PECs). The latter cell population contains podocyte progenitors, which are motile and progressively differentiate into podocytes in the region near the vascular pole of the glomerulus. The vascular pole of the glomerulus includes both the afferent and efferent arterioles (transverse section). The outermost layer is composed of podocytes adhering to the glomerular basement membrane (GBM) and interdigitating (longitudinal section), with the slit diaphragm spanning each gap between pairs of foot processes. The innermost layer is constituted by fenestrated endothelial cells. Figure and figure legend reproduced with permission, Springer Nature [1].

the structural components of the remaining podocyte compartments (cell body) [43]. Microtubules are responsible for the intricate and dynamic intracellular cytoskeletal network of podocytes, assisting in the cell's motility, as well as maintaining cell polarity [43]. Podocytes are also subjected to both tensile and shear stress, given their precise location along the GBM. Specifically, shear stress is a result of ultrafiltrate exposure, while tensile stress stems from stretching of the glomerular capillaries [44]. It is therefore clear that podocytes must remain adaptable in the face of such stressors. Indeed, they are enriched with several mechanosensitive proteins, including Rho-GTPase interacting proteins, Actin bundling proteins, and focal adhesion complex associated proteins [44, 45]. As such, the cytoskeletal structure of podocytes is important for appropriate functioning. Disease processes that interrupt cytoskeletal networks result in a unifying histopathological process, foot process effacement.

Outside of the structural role that podocytes play as part of the glomerulus is their role as immune effectors. The podocyte has been shown to possess functional arms of the immune system [46, 47]. Podocytes exhibit the capacity to recognize and respond to various signaling molecules associated with inflammation and express several cytokines and their receptors, including interleukin 1 alpha (IL-1α), IL-1β, and tumour necrosis factor alpha (TNF-α) [48–50]. Moreover, podocytes express chemokine receptor 1 (CCR1), CCR2, and CXCR4 which play a pivotal role in immune cell recruitment [49]. Podocytes also express major histocompatibility complex (MHC) class I and II genes, key components of the adaptive immune system [51]. Lastly, podocytes possess functional Toll Like Receptors (TLRs), NOD-like receptor pyrin domain-containing protein 3 (NLRP3), cyclic GMP-AMP synthase – stimulator of interferon genes (cGAS-STING), Receptor for Advanced Glycation End Products (RAGE), Retinoic acid-inducible gene I (RIG-1), and Podoplanin (which is pattern recognition receptor (PRR)-like in its interaction with CLEC-2).

The function of these specific PRRs and their roles as innate immune effectors in podocytes is summarized in a published review **Damage associated molecular patterns and pattern recognition receptors in the podocyte** [52], in the Appendix.

Several key takeaways from this review paper include the importance of specific mitochondrial DAMPs, particularly mitochondrial DNA (mtDNA), and its role as an intracellular effector through stimulation of PRRs. This will be further exemplified in **Chapter 3**. However, prior to getting to this, it is imperative to introduce the role of the mitochondria in the cell, in health and disease, and to discuss its importance in the podocyte.

1.7 MITOCHONDRIA IN HEALTH AND DISEASE

Prior to discussing the important roles that mitochondria play in the podocyte, it is important to review mitochondria themselves. Mitochondria are the 'powerhouses' of the cell, producing ATP as well as many other important biosynthetic intermediates. Beyond the direct association with bioenergetics, mitochondria have also been identified as important signalling hubs relating to cellular stress responses and immune mechanisms [53]. **Figure 4** provides a broad overview of the important functions of the mitochondrion.

Mitochondria are derived from a common bacterial ancestor, thought most likely to be an alpha-proteobacterium [54]. Many of the bacterial genes have been lost, and further, many mitochondrial specific proteins are a product of nuclear genes. However, 13 proteins are encoded by the mtDNA, and their roles are specific to ATP production via oxidative phosphorylation (OXPHOS) [54]. In addition to this role, mitochondria are also integral to reactive oxygen species (ROS) signalling; growth and repair signalling, via amino acid metabolites; redox regulation, via

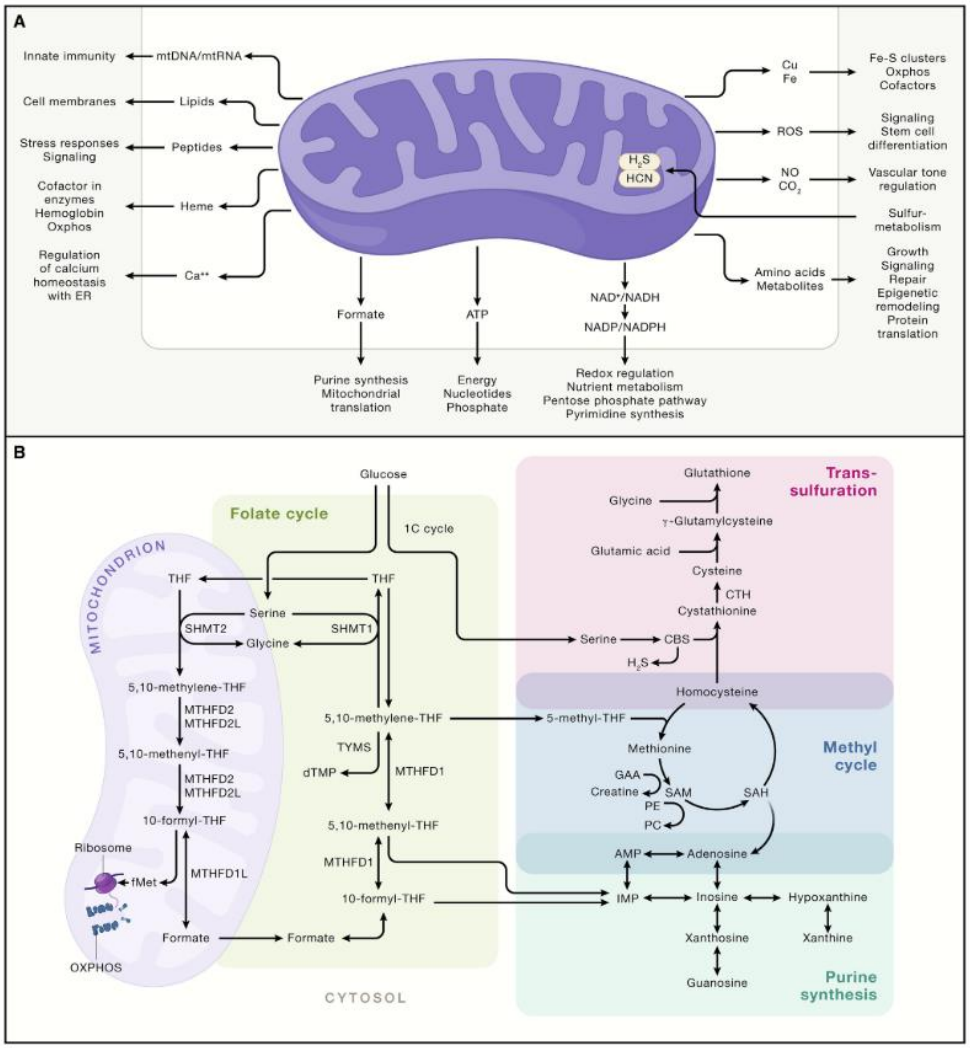

Figure 4. Multifaceted mitochondrial contributions to cellular homeostasis.

(A) Mitochondria produce cofactors and metabolites to cells and tissues, as well as releasing them as systemic signals to tune metabolism. Mitochondria are also a storage site for metals and contain high amounts of B-vitamin derivatives (folates, NAD-forms) and the redox-regulator glutathione. (B) Mitochondrial-cytoplasmic folate- and one-carbon cycle. Mitochondria have an essential role in providing forms of folate for the major biosynthetic, anabolic pathways that provide growth components for the whole cell. Figure and figure legend reproduced without need for permission (Creative Commons CC-BY). Taken directly from [54].

NAD/NADH, purine synthesis, regulation of calcium, stress response signalling, and innate immunity [54].

Oxidative phosphorylation (OXPHOS) and the production of ATP is by far the most well described function of mitochondria. The OXPHOS machinery is housed in the inner mitochondrial membrane and comprises 5 multiprotein complexes (I-V), coupled together with electron carriers Coenzyme Q, and Cytochrome C [55]. Altogether, there are approximately 85 proteins making up OXPHOS, some proteins from the nuclear genome, and others from the mitochondrial genome. The ultimate goal of OXPHOS is to create ATP by moving electrons and protons [55]. It is through this highly complex pathway that energy for both mitochondria, and the cell, is created.

OXPHOS involves several other complexes with unique roles. Specifically, Complex I transfers electrons from NADH, while complex II transfers them from $FADH_2$. Both transfer to Coenzyme Q, which acts like a shuttle, and carries electrons to Complex III [56]. ROS production is also a result of OXPHOS, specifically thought driven by processes linked to complexes I and III [57]. ROS can both impact the respiratory chain and is also a product of it. Mitochondrial ROS (mtROS) can also cause lipid peroxidation, can induce the mitochondrial permeability transition pore (mPTP), and can lead to Cytochrome C-dependent apoptosis and necrosis [57]. Overall, mtROS can contribute to mitochondrial dysfunction, which in turn can contribute to worsening health, or the development of disease. In turn, this process is also thought to be involved in the aging process. In addition to this, mtROS contributes to redox signalling pathways, impacting not only itself, but processes in the cytosol and nucleus [57]. Mitochondria are also responsible for significant biosynthetic processes, and both produce and modify metabolites and cofactors from the Folate Cycle, the Trans-sulphuration process, the Methyl Cycle; and they are involved in purine

synthesis. Altogether, this interlinked metabolic fingerprint directly relates to overall cellular homeostasis [54, 57, 58].

Lastly, it is essential to discuss the role mitochondria play in innate immunity and inflammatory processes. Importantly, the innate immune mechanisms tie together with those of the podocyte, as discussed above (**1.7**). Specifically, components of the mitochondrial genome are pro-inflammatory agonists when released either as a result of damage, or physiologically. mtDNA, RNA, as well as formyl peptides act as damage associated molecular patterns (DAMPs) and bind pattern recognition receptors (PRRs) thus eliciting downstream biological pathways associated with interferon responses.

1.8 THE ROLE OF THE MITOCHONDRIA IN PODOCYTE DISEASE: GENETIC AND IDIOPATHIC NS.

Linking together the bioenergetic and metabolic roles alongside the immune functions of mitochondria showcases their vital importance to the cell's overall health and wellbeing, but also, their role in disease pathogenesis. Podocytes possess mitochondria; however, compared to other, more highly energetic kidney cells, like proximal tubular cells, the podocyte has a relatively lower abundance of mitochondria [59]. Despite this, there are several monogenic forms of NS in children (and adults) which are a result of mitochondrial gene disruptions. Specifically, Coenzyme Q deficiency is associated with a SRNS phenotype, and can be responsive to ubiquinone supplementation [60]. Most commonly, this associates with a FSGS histopathology. When considering the condition 'myopathy, encephalopathy, lactic acidosis, and stroke-like episodes' (MELAS), the implicated mutation is mitochondrial, and this is recognized as a mitochondrial disease. Coupled with this presentation are FSGS lesions in the kidney [60]. Further, mutations in Decaprenyl Diphosphate Synthase Subunit 2 and mitochondrially encoded tRNA leucine 1 (UUA/G) both result in

SRNS phenotypes [61]. Mitochondrial DNA mutations can cause SRNS associating with FSGS. However, what is the role of the podocyte mitochondria in the context of iNS, or SSNS?

The literature is sparse related to mitochondrial dysfunction in childhood iNS. A study from the 1980's revealed that mitochondrial swelling was observed in 24/45 renal biopsies taken from a mixed population of people with iNS. Limited information is available to outline the significance, and most of these altered mitochondria were present in tubular cells [62]. Another study sought to determine the role of Prohibitin 2 (PHB2) as a mitochondrial protective entity in iNS [63]. Exome sequencing of 5 patients with FRNS revealed a heterozygous PHB2 polymorphism in 1 patient, thought perhaps related to the frequently relapsing nature of the disease. However, the value of this observation remains contentious. Aside from this observation, there are few other studies linking mitochondria and iNS. There are some *in vitro* studies linking the mitochondria to podocyte injury in models of iNS, but none do so in a definitive manner.

iNS in children remains a mysterious disease with an unclear fundamental mechanism leading to podocyte effacement. What is most challenging clinically is the inability to predict who will respond to steroids, and who will not. The podocyte is centrally implicated in this condition. Podocytes have diverse roles, both structurally, and as immune effectors. Mitochondria are present in podocytes but are sparse when compared to more energy-dependent cells, like proximal tubules. Despite this, mitochondria are implicated in genetic NS with less clear roles in the pathogenesis of iNS. Mitochondria themselves have specific bioenergetic roles, and it is therefore clear that through mutation of a mitochondrial gene there would likely be catastrophic failure of the cell, including podocytes. However, given the sparse nature of mitochondria in podocytes, perhaps their role is less important for energy requirements, but more important in signalling and immune mechanisms?

Because iNS is a remitting condition (those that are medication-responsive and non-genetic), it is tempting to hypothesize that perhaps the mitochondria in podocytes are stressed, resulting in an intermittent immune-mediated effacement (through PRR engagement) that is responsive to immune suppression. Therefore, understanding and studying the immune effector role of the podocyte, particularly with respect to mitochondria in a non-classic role (immune mediator, not bioenergetic powerhouse) might uncover novel mechanistic pathways underlying iNS. Signalling within, and between cells is important when considering these disease pathways. Cells are capable of autocrine, paracrine, and endocrine signalling using extracellular vesicles (EVs). EVs, and their links to iNS, podocytes, and mitochondria will be discussed next.

1.9 EVS

EVs are important mediators of a variety of inter- and intra-cellular processes linked to their ability to communicate in an auto-, para-, and endocrine-like manner. Further, they are not limited in their role as physiological communicators but are also emerging biomarkers of a variety of diseases [64]. In truly defining EVs, there are several unifying features, as highlighted by the minimal information for studies of EVs (MISEV2023) paper [65]. In summary, EVs:

- Are released from cells
- Are delimited by a lipid bilayer
- Cannot replicate on their own

Importantly, defining EVs stems directly from their properties and methods of biogenesis. Broadly, definitions include exosomes for those EVs originating from the endosomal system,

Ectosomes or Large EVs (LEVs) for those originating from the plasma membrane, and apoptotic bodies for those EVs originating from dying cells. Newer forms of EVs have been uncovered in recent years and include exophers and blebbisomes. Exophers range in size from 2 to 15 μm, and contain organelles, protein complexes, and protein aggregates [66]. Initially, when observed to remove neurotoxic components from neurons of C. elegans, they were deemed as waste disposal units. However, they may play a role during embryo development [66]. Blebbisomes, another form of EV which is enriched in organelles and possesses cell-like properties [67], was recently described. These blebbisomes are ~20 μm, are membrane delimited, and themselves exhibit blebbing behavior. They also were shown to possess functional organelles, including the multivesicular endosome; however, they did not possess a nucleus [67]. While MISEV2023 advises against the use of this nomenclature in a silo, for the purposes of clarity and ease, this thesis will use the term LEVs in later chapters made up of already submitted or published papers. LEVs are traditionally thought to be 100 – 1000 nm in size, bud from the parent cell of origin, and retain characteristics of the parental cell of origin [64]. As such, LEVs represent a unique biomolecule which may be utilized as a biomarker, and in the context of diseases of the kidney, can be obtained from urine and thus can act as a liquid biopsy.

Prior to discussing the roles of LEVs in childhood iNS, we will first review the role of EVs in kidney disease, working our way towards childhood iNS. Indeed, the role of EVs in kidney disease is unclear, and several clinical and *in vitro* studies have been performed attempting to delineate their role [67]. The role of serum EVs in kidney disease is less well understood. Many studies link serum EVs with underlying vascular damage or note that the EVs are related to the plethora of serum cells including platelets, leukocytes, monocytes and T- and B-cells [64]. Contrarily, urine is specifically enriched with EVs thought to arise directly from urine-facing

kidney cells from the nephron through to the bladder. The next section will therefore discuss urinary EVs in the context of kidney disease.

1.10 URINARY EVS IN KIDNEY DISEASE

Urinary EVs were first identified in the 1980's [68], although their complex role is not fully elucidated even today [69]. It is clear that EVs released from urine-facing cells could potentially provide insights into both physiological and pathological processes if collected and examined (**Figure 5)**. Indeed, EVs as biomarkers have been studied in the context of kidney fibrosis, systemic lupus erythematosus (SLE) activity, post-kidney transplant graft monitoring, and risk of AKI following kidney transplantation [69]. Each of these indications reveals the unique characteristics of EVs relating to their source. Of particular importance, for example in lupus, would be whether there is a signal in urinary EVs that would allow for diagnosis of tubular or podocyte damage in advance of a clinical flare, or without the need for an invasive kidney biopsy. Perez-Hernandez *et al.* investigated urinary exosomal microRNAs in patients with SLE and identified that urinary exosomal miR-146a is the most discriminatory for active SLE [70]. By comparing the urinary exosomes between control individuals, those with SLE without nephritis, and those with SLE nephritis, they were able to differentially identify which miR was most specific to active disease. This is just a single example of how a urinary EV population could be exploited in the face of disease. Next, a multi-target approach was taken whereby Dwivedi *et al.* explored the use of genome wide mRNA profiling of urinary EVs and created a 'stress score' to help in the prediction of long-term reductions in kidney function in patients with diabetic kidney disease [71]. Indeed, their stress score included 6 different genes (Glutathione Peroxidase 3, GPX3; NADPH Oxidase 4, NOX4; Methionine Sulfoxide Reductase B and A, MSRB, MSRA; Heat-responsive

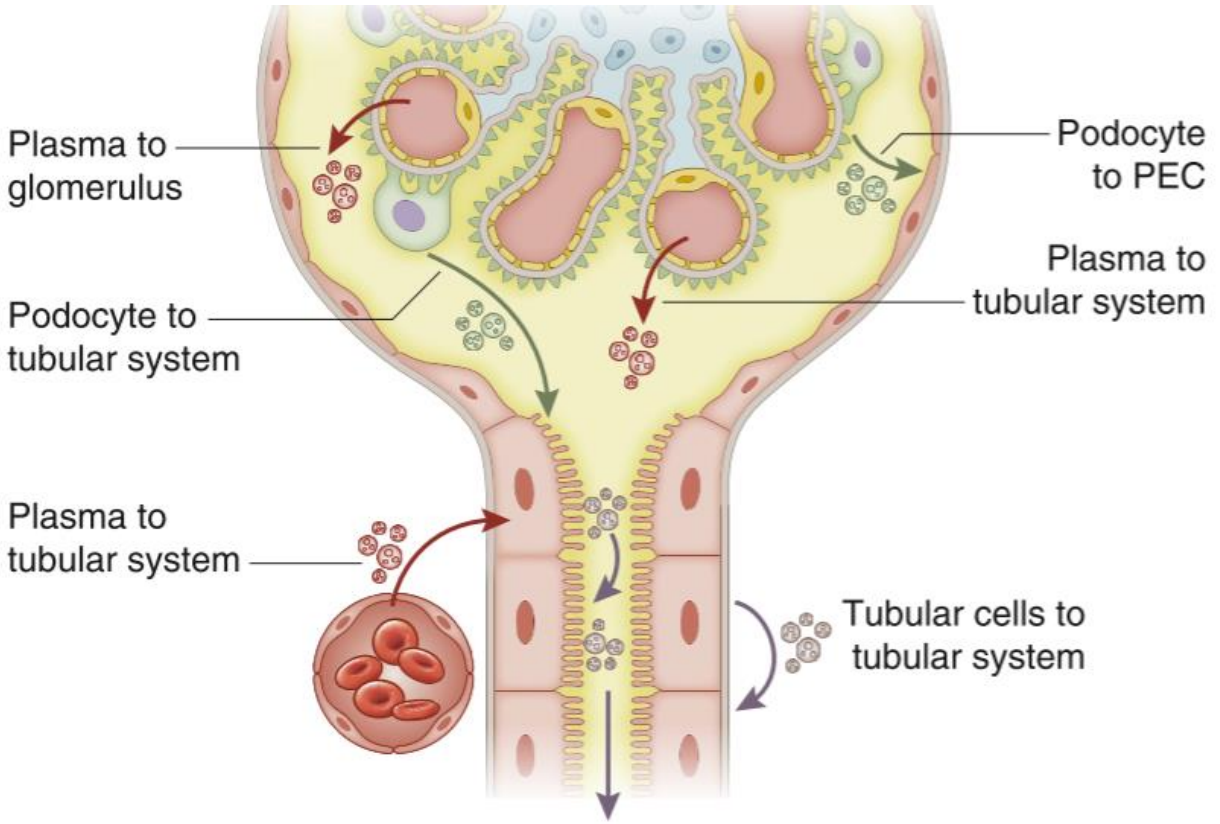

Figure 5. Intranephron and interorgan signaling via extracellular vesicles (EVs).

Potential pathways of intranephron signaling. Reproduced from Ng et al., [69]. Permission not required under CC BY open access license.

protein 12, HRSP12, and Alpha-crystallin B chain, CRYAB) which was strong enough to identify patients who remained normoalbuminuric but were showing early decline in kidney function. While too advanced for the clinic, this work highlights both the unmet need to develop more predictive biomarkers in kidney disease, and the utility of urinary EVs in non-invasive disease research.

Regarding the use of EVs in NS, there are fewer studies with less clear results. A non-EV urinary biomarker risk score thought predictive for SRNS was developed and validated in adults, using the Nephrotic Syndrome Study Network (NEPTUNE) cohort [72]. The authors had previously identified 5 urinary biomarkers, neutrophil gelatinase-associated lipocalin (NGAL), vitamin D binding protein (VDBP), Fetuin-A (FetA), Transthyretin (TTR), and alpha-1 acid glycoprotein 2 (AGP2), which were associative with steroid resistance in children. Using this same signature, but with a new cohort of adult patients with NS, the authors showed the biomarker risk score predicted development of steroid resistance with AUC 0.79 [72]. This same group then applied a similar approach investigating α 1-B glycoprotein (A1BG), specifically a 13.8 kDa fragment found in the urine of children with NS. Indeed, they found that this 13.8 kDa fragment was found in 7/19 patients with SRNS, and in none of the SSNS patients and none of the controls [73]. Previous to this, urinary CD80 concentration was identified as a potential non-invasive diagnostic marker in children with SSNS [74]. While these studies do not highlight the use of EVs, there is a precedent to study urine from patients with NS as a means to determine steroid resistance, or as a marker of disease activity. It is possible that some of these markers were present within urinary EVs when identified in the above studies; however, this is speculation. When considering true urinary EV studies in nephrotic syndrome, there are few, especially in children. One is a study by Santorelli *et al.* whereby this group examined urinary EVs and found specific protein signatures using gel

electrophoresis that discriminated clinical subgroups, namely those steroid sensitive, and steroid resistant [75]. Chen *et al.* reported that certain urinary EV miRs were increased in children with nephrotic syndrome when compared to healthy controls [76]. Another study is our own, where we discovered that podocyte-specific large EVs were increased in the urine of children with iNS [77]. Please see **Chapter 2** for the full manuscript.

1.11 EV CONTENT

While the above studies identified miRNA species within EVs from children with iNS, there are other biomolecules present inside EVs. Indeed, EV content is cell specific and can be enriched under times of physiological or pathological cellular stress. Under physiological conditions, EVs may represent auto-, para-, or endocrine effectors, and thus would be enriched with biomolecules most applicable to the signal of interest. As an example, EVs have been implicated in enhancing coagulation, allowing for their participation in hemostasis [78]. Interestingly, these same pro-coagulant capabilities can be harvested opportunistically by tumour cells, thus increasing the risk of coagulopathies under pathological conditions [78]. This serves simply as an example of how EVs can carry physiological signals, and further, how they can be pathological under other circumstances.

EVs are generally enriched with a variety of proteins, regardless of the cell of origin, including cytoskeletal, cytosolic, heat shock, and plasma membrane proteins [78]. While there have been some studies linking specific proteomic profiles of EVs to specific cells, it remains unclear whether protein cargo can be used to classify an EV's origin. What is commonly accepted is a description of the EVs being studied (cell culture or biological fluid origin), how they were isolated or enriched, and which protein markers were probed for [65]. What is unanimously accepted is

that it is not only miRNA cargo that is enriched in EVs, but also RNA, protein, DNA, and lipids [79]. The following section will discuss proteins and mtDNA.

When considering EVs originating from the kidney and urogenital tract, much work has been done to interrogate the functional importance of released EVs, as described above. Considering a focus on cargo, several examples exist outlining specific cargo that points to a cellular origin. Specifically, kidney tubular cells were shown to release EVs with functional aquaporin 2 [80]. In another interesting study in patients with FSGS, urinary EVs were isolated and shown to have increased amounts of WT1, a podocyte marker [81]. Aside from protein markers in the EVs, there are also some studies examining the presence of mtDNA within EVs as markers of cellular and mitochondrial stress [82]. mtDNA has been described within EVs in the context of aging [82] and malignancy [83], most often. However, it has also been shown as marker of gestational diabetes in a rodent model [84]. Cellular stress, and indeed mitochondrial stress, has been shown to lead to extrusion of mtDNA, as well as other mitochondrial parts (or whole, intact mitochondria) [85]. The purpose of packaging mtDNA, and in fact, the mechanism behind how mtDNA exits mitochondria and is packaged remains quite elusive [86]. Given the role of mitochondria in supporting energy-dependent processes within cells, and the fact that podocytes have robust cytoskeletal networks, I examined the role of mitochondrial stress in podocytes in a model of iNS and discovered that mtDNA is extruded into LEVs. This is the topic of **Chapter 3**, which is published in *The International Journal of Molecular Sciences*. Further, **Chapter 4** is a study aimed at determining differences in the hPod proteome in an experimental model of iNS, with comparisons to urinary LEVs from children with iNS. This paper is under review at *Disease Models & Mechanisms*.

1.12 OVERALL OBJECTIVES AND HYPOTHESES

Taken together, iNS in children is both a homogeneous and heterogeneous disease depending on which aspect is analyzed. Children present in a usual fashion, with significant proteinuria and hypoalbuminemia, which leads to edema. Complications are uniform, however which children will develop these complications is unclear. What is heterogeneous about this disease is the response to steroids. There is a clear unmet need to develop a biomarker which is not only capable of better diagnosing nephrotic syndrome in children but is specifically able to classify their response to steroids *a priori* or be used as a marker to predict relapse or remission. Beyond this, using podocyte-derived EVs will also allow for a deeper fundamental understand of podocyte biology at times of injury. Urinary proteins have been studied and linked back to urine facing cells of interest in the urogenital tract, and these proteins have provided an impetus for future studies looking at improving diagnostic approaches to disease. However, only some of these studies have used EVs. Podocytes which are urinary facing glomerular epithelial cells secrete EVs into the urine, and the natural course of flow allows for isolation, purification, and enumeration from the urine. The podocyte is the centrally implicated cell in nephrotic syndrome and histopathology reveals effacement during nephrotic syndrome. This represents podocyte stress which can lead to the release of EVs. Further, different stresses can lead to the enrichment of specific cargo inside EVs. Mitochondrial stress can lead to the extrusion of mtDNA and packaging into EVs. I therefore hypothesized that **LEVs from children with iNS will be enriched in the urine during times of relapse, will be measurable, and will contain mtDNA, a reflection of podocyte mitochondrial stress. This mitochondrial stress will be measurable *in vitro*. Further, the proteomic profile of the urinary LEVs will differ between relapse and remission in children with iNS.**

I have addressed this overarching hypothesis through 3 aims across 3 chapters.

- **Chapter 2:** Children with iNS were enrolled into my prospective study. I collected urine specimens during times of relapse and remission (paired samples per patient). I collected appropriate anthropometric and clinical data. Thereafter, using Flow Cytometry, we showed that children with iNS have increased levels of podocyte-specific LEVs in their urine. Chapter 2 is published in the journal *Nephrology, Dialysis, Transplantation*.
- **Chapter 3:** Next, knowing that increased podocyte-specific LEV levels in the urine were indicative of relapse, and understanding that podocyte LEVs are released during times of stress, I next used an *in vitro* and *in vivo* approach to study this observation under experimental conditions. We identified that hPod LEVs are enriched with mtDNA following treatment with puromycin aminonucleoside (PAN). This associates with mitochondrial stress as evidenced by increased mitochondrial ROS (mtROS), a decreasing mitochondrial membrane potential (MMP), and evidence of a bioenergetic stress on Seahorse analysis. The presence of mtDNA within LEVs was also observed in a murine model of nephrosis. Next, we examined mtDNA levels in LEVs from children with iNS and observed that this too is increased during relapse. Chapter 3 is published in *The International Journal of Molecular Sciences*.
- **Chapter 4**: Lastly, given the observation the mtDNA is packaged into LEVs in a human cell culture model, is also found in a murine nephrosis model, and was seen to differentiate relapse versus remission in children with iNS, I next applied LEV proteomics using both an *in vitro* and human urine sample model. The proteomic cargo differed greatly between relapse and remission samples, thus providing the impetus for future mechanistic biomarker studies targeting early prediction of steroid responsiveness. Chapter 4 is submitted to *Disease Models & Mechanisms.*

1.13 REFERENCES

1. Kopp JB, Anders HJ, Susztak K, et al (2020) Podocytopathies. Nat Rev Dis Primers 6:. https://doi.org/10.1038/s41572-020-0196-7
2. Noone DG, Iijima K, Parekh R (2018) Idiopathic nephrotic syndrome in children. The Lancet 392:61–74. https://doi.org/10.1016/S0140-6736(18)30536-1
3. Doucet A, Favre G, Deschênes G (2007) Molecular mechanism of edema formation in nephrotic syndrome: Therapeutic implications. Pediatric Nephrology 22:1983–1990. https://doi.org/10.1007/s00467-007-0521-3
4. Trautmann A, Boyer O, Hodson E, et al (2023) IPNA clinical practice recommendations for the diagnosis and management of children with steroid-sensitive nephrotic syndrome
5. Trautmann A, Vivarelli M, Samuel S, et al (2020) IPNA clinical practice recommendations for the diagnosis and management of children with steroid-resistant nephrotic syndrome. Pediatric Nephrology
6. Glassock RJ (2003) Secondary minimal change disease. Nephrology Dialysis Transplantation 18
7. Maas RJ, Deegens JK, Beukhof JR, et al (2017) The Clinical Course of Minimal Change Nephrotic Syndrome With Onset in Adulthood or Late Adolescence: A Case Series. American Journal of Kidney Diseases 69:637–646. https://doi.org/10.1053/j.ajkd.2016.10.032
8. Vivarelli M, Gibson K, Sinha A, Boyer O (2023) Childhood nephrotic syndrome
9. Myette RL, Lamarche C, Odutayo A, et al (2024) Cardiovascular Risk in Patients With Glomerular Disease: A Narrative Review of the Epidemiology, Mechanisms, Management, and Patient Priorities. Can J Kidney Health Dis 11
10. Veltkamp F, Rensma LR, Bouts AHM (2021) Incidence and Relapse of Idiopathic Nephrotic Syndrome: Meta-analysis. Pediatrics 148:2020030494. https://doi.org/10.1542/2020-029249

11. Constantinescu AR, Mattoo TK, Smoyer WE, et al (2022) Clinical presentation and management of nephrotic syndrome in the first year of life: A report from the Pediatric Nephrology Research Consortium. Front Pediatr 10:. https://doi.org/10.3389/FPED.2022.988945
12. Boyer O, Schaefer F, Haffner D, et al (2021) Management of congenital nephrotic syndrome: consensus recommendations of the ERKNet-ESPN Working Group. Nat Rev Nephrol 17:277–289
13. Li S, Hu M, He C, et al (2024) A multicenter study investigating the genetic analysis of childhood steroid-resistant nephrotic syndrome: Variants in COL4A5 may not be coincidental. PLoS One 19:. https://doi.org/10.1371/journal.pone.0304864
14. Drovandi S, Lipska-Ziętkiewicz BS, Ozaltin F, et al (2022) Oral Coenzyme Q10 supplementation leads to better preservation of kidney function in steroid-resistant nephrotic syndrome due to primary Coenzyme Q10 deficiency. Kidney Int 102:604–612. https://doi.org/10.1016/j.kint.2022.04.029
15. Downie ML, Gupta S, Voinescu C, et al (2023) Common Risk Variants in AHI1 Are Associated With Childhood Steroid Sensitive Nephrotic Syndrome. Kidney Int Rep 8:1562–1574. https://doi.org/10.1016/j.ekir.2023.05.018
16. Shimada M, Araya C, Rivard C, et al (2011) Minimal change disease: A “two-hit” podocyte immune disorder? Pediatric Nephrology 26:645–649. https://doi.org/10.1007/s00467-010-1676-x
17. Watts A, Keller K, Lerner G, et al (2021) Discovery of Autoantibodies Targeting Nephrin in Minimal Change Disease Supports a Novel Autoimmune Etiology. Journal of the American Society of Nephrology ASN.2021060794. https://doi.org/10.1681/ASN.2021060794
18. Hengel FE, Dehde S, Lassé M, et al (2024) Autoantibodies Targeting Nephrin in Podocytopathies. New England Journal of Medicine. https://doi.org/10.1056/NEJMoa2314471

19. Al-Aubodah TA, Aoudjit L, Pascale G, et al (2023) The extrafollicular B cell response is a hallmark of childhood idiopathic nephrotic syndrome. Nat Commun 14:. https://doi.org/10.1038/s41467-023-43504-8

20. Cui Z, Zhao MH (2024) Anti-nephrin autoantibodies: a paradigm shift in podocytopathies. Nat Rev Nephrol 20:639–640

21. Jamin A, Berthelot L, Couderc A, et al (2018) Autoantibodies against podocytic UCHL1 are associated with idiopathic nephrotic syndrome relapses and induce proteinuria in mice. J Autoimmun 89:149–161. https://doi.org/10.1016/j.jaut.2017.12.014

22. Gallon L, Leventhal J, Skaro A, et al (2012) Resolution of recurrent focal segmental glomerulosclerosis after retransplantation. N Engl J Med 366:1648–9. https://doi.org/10.1056/NEJMc1202500

23. Dossier C, Jamin A, Deschênes G (2016) Idiopathic nephrotic syndrome: the EBV hypothesis. Pediatric Research 2017 81:1 81:233–239. https://doi.org/10.1038/pr.2016.200

24. Shalhoub RJ (1974) Pathogenesis of lipoid nephrosis: a disorder of T-cell function. Lancet 2:556–60. https://doi.org/10.1016/s0140-6736(74)91880-7

25. Agrawal S, Brier ME, Kerlin BA, et al (2021) Plasma Cytokine Profiling to Predict Steroid Resistance in Pediatric Nephrotic Syndrome. Kidney Int Rep 6:785–795. https://doi.org/10.1016/j.ekir.2020.12.027

26. Myette R, Burger D (2021) Relapse in steroid-sensitive nephrotic syndrome: are extracellular vesicles the missing link? American Journal of Physiology-Renal Physiology 656–658. https://doi.org/10.1152/ajprenal.00349.2021

27. Loscalzo J (2013) Venous thrombosis in the nephrotic syndrome. N Engl J Med 368:956–958. https://doi.org/10.1056/NEJMcibr1209459

28. Carpenter SL, Goldman J, Sherman AK, et al (2019) Association of infections and venous thromboembolism in hospitalized children with nephrotic syndrome. Pediatric Nephrology 34:261–267. https://doi.org/10.1007/s00467-018-4072-6

29. Myette RL, Burger D, Geier P, Feber J (2021) Diastolic hypertension is associated with proteinuria in pediatric patients. Health Sci Rep 4:. https://doi.org/10.1002/hsr2.346

30. Vaziri ND (2016) Disorders of lipid metabolism in nephrotic syndrome: mechanisms and consequences. Kidney Int 90:41–52. https://doi.org/10.1016/j.kint.2016.02.026

31. Ashoor IF, Mansfield SA, O'Shaughnessy MM, et al (2019) Prevalence of Cardiovascular Disease Risk Factors in Childhood Glomerular Diseases. J Am Heart Assoc 8:. https://doi.org/10.1161/JAHA.119.012143

32. Vande Walle JGJ, Donckerwolcke RA, Walle JGJ Vande, et al (2001) Pathogenesis of edema formation in the nephrotic syndrome. Pediatric Nephrology 16:283–293. https://doi.org/10.1007/s004670000512

33. Kallash M, Mahan JD (2020) Mechanisms and management of edema in pediatric nephrotic syndrome. Pediatric Nephrology. https://doi.org/10.1007/s00467-020-04779-x

34. Kapur G, Valentini RP, Imam AA, Mattoo TK (2009) Treatment of severe edema in children with nephrotic syndrome with diuretics alone--a prospective study. Clin J Am Soc Nephrol 4:907–13. https://doi.org/10.2215/CJN.04390808

35. Chen C, Qiu B, Wang J, et al (2024) Incidence and risk factors for acute kidney injury in children with nephrotic syndrome: a meta-analysis. Front Pediatr 12

36. Kerlin BA, Haworth K, Smoyer WE (2014) Venous thromboembolism in pediatric nephrotic syndrome. Pediatric Nephrology 29:989–997. https://doi.org/10.1007/s00467-013-2525-5

37. Carter SA, Mistry S, Fitzpatrick J, et al (2019) Prediction of short and long-term outcomes in childhood nephrotic syndrome. Kidney Int Rep 5:426–434. https://doi.org/10.1016/j.ekir.2019.12.015

38. Geier P, Roushdi A, Skálová S, et al (2012) Is cyclophosphamide effective in patients with IgM-positive minimal change disease? Pediatr Nephrol 27:2227–2231. https://doi.org/10.1007/S00467-012-2234-5

39. Wang H, Liu M, Wang X, et al (2024) Optimal Trough Concentration of Tacrolimus in Pediatric Patients With Primary Nephrotic Syndrome. Clin Pharmacol Ther. https://doi.org/10.1002/cpt.3448

40. Sinha A, Bagga A (2013) Rituximab therapy in nephrotic syndrome: implications for patients' management. Nat Rev Nephrol 9:154–169. https://doi.org/10.1038/nrneph.2012.289

41. Basgen JM, Steffes MW, Stillman AE, Mauer SM (1994) Estimating glomerular number in situ using magnetic resonance imaging and biopsy. Kidney Int 45:1668–1672. https://doi.org/10.1038/KI.1994.218

42. Pavenstädt H, Kriz W, Kretzler M (2003) Cell biology of the glomerular podocyte. Physiol Rev 83:253–307. https://doi.org/10.1152/physrev.00020.2002

43. Welsh GI, Saleem MA (2012) The podocyte cytoskeleton-key to a functioning glomerulus in health and disease. Nat Rev Nephrol 8:14–21. https://doi.org/10.1038/nrneph.2011.151

44. Haydak J, Azeloglu EU (2024) Role of biophysics and mechanobiology in podocyte physiology. Nat Rev Nephrol 20:371–385

45. Matsuda J, Asano-Matsuda K, Kitzler TM, Takano T (2021) Rho GTPase regulatory proteins in podocytes. Kidney Int 99:336–345. https://doi.org/10.1016/j.kint.2020.08.035

46. Bruno V, Mühlig AK, Oh J, Licht C (2023) New insights into the immune functions of podocytes: the role of complement. Mol Cell Pediatr 10

47. Bhargava R, Tsokos GC (2019) The immune podocyte. Curr Opin Rheumatol 31:167–174. https://doi.org/10.1097/BOR.0000000000000578

48. Niemir ZI, Stein H, Dworacki G, et al (1997) Podocytes are the major source of IL-1 alpha and IL-1 beta in human glomerulonephritides. Kidney Int 52:393–403. https://doi.org/10.1038/ki.1997.346

49. Huber TB, Reinhardt HC, Exner M, et al (2002) Expression of Functional CCR and CXCR Chemokine Receptors in Podocytes. The Journal of Immunology 168:6244–6252. https://doi.org/10.4049/jimmunol.168.12.6244

50. Srivastava T, Sharma M, Yew KH, et al (2013) LPS and PAN-induced podocyte injury in an in vitro model of minimal change disease: Changes in TLR profile. J Cell Commun Signal 7:49–60. https://doi.org/10.1007/s12079-012-0184-0

51. Coers W, Brouwer E, Vos JT, et al (1994) Podocyte expression of MHC class I and II and intercellular adhesion molecule-1 (ICAM-1) in experimental pauci-immune crescentic glomerulonephritis. Clin Exp Immunol 98:279–86. https://doi.org/10.1111/j.1365-2249.1994.tb06138.x

52. Myette RL, Trentin-Sonoda M, Landry C, et al (2024) Damage-Associated Molecular Patterns and Pattern Recognition Receptors in the Podocyte. J Am Soc Nephrol. https://doi.org/10.1681/ASN.0000000531

53. Nunnari J, Suomalainen A (2012) Mitochondria: In Sickness and in Health. Cell 148:1145–1159. https://doi.org/10.1016/J.CELL.2012.02.035

54. Suomalainen A, Nunnari J (2024) Mitochondria at the crossroads of health and disease. Cell 187:2601–2627. https://doi.org/10.1016/J.CELL.2024.04.037

55. Smeitink J, Van Den Heuvel L, DiMauro S (2001) The genetics and pathology of oxidative phosphorylation. Nature Reviews Genetics 2001 2:5 2:342–352. https://doi.org/10.1038/35072063

56. Nolfi-Donegan D, Braganza A, Shiva S (2020) Mitochondrial electron transport chain: Oxidative phosphorylation, oxidant production, and methods of measurement. Redox Biol 37:101674. https://doi.org/10.1016/J.REDOX.2020.101674

57. Murphy MP (2008) How mitochondria produce reactive oxygen species. Biochemical Journal 417:1. https://doi.org/10.1042/BJ20081386

58. Schmidt CA, Fisher-Wellman KH, Darrell Neufer P (2021) From OCR and ECAR to energy: Perspectives on the design and interpretation of bioenergetics studies. Journal of Biological Chemistry 297:101140. https://doi.org/10.1016/j.jbc.2021.101140

59. Brinkkoetter PT, Bork T, Salou S, et al (2019) Anaerobic Glycolysis Maintains the Glomerular Filtration Barrier Independent of Mitochondrial Metabolism and Dynamics. Cell Rep 27:1551-1566.e5. https://doi.org/10.1016/j.celrep.2019.04.012

60. Govers LP, Toka HR, Hariri A, et al (2021) Mitochondrial DNA mutations in renal disease: an overview. Pediatr Nephrol 36:9–17. https://doi.org/10.1007/S00467-019-04404-6

61. Machuca E, Benoit G, Antignac C (2009) Genetics of nephrotic syndrome: connecting molecular genetics to podocyte physiology. Hum Mol Genet 18:. https://doi.org/10.1093/HMG/DDP328

62. Chedid A, Jao W, Port J (1980) Megamitochondria in hepatic and renal disease. Am J Gastroenterol 73:319–24

63. Sugimoto K, Miyazawa T, Miyazaki K, et al (2017) Minimal change nephrotic syndrome and prohibitin-2 gene polymorphism. Clin Exp Nephrol 21:665–670. https://doi.org/10.1007/S10157-016-1325-1

64. Medeiros T, Myette RL, Almeida JR, et al (2020) Extracellular Vesicles: Cell-Derived Biomarkers of Glomerular and Tubular Injury. Cell Physiol Biochem 54:88–109. https://doi.org/10.33594/000000207

65. Welsh JA, Goberdhan DCI, O'Driscoll L, et al (2024) Minimal information for studies of extracellular vesicles (MISEV2023): From basic to advanced approaches. J Extracell Vesicles 13:e12404. https://doi.org/10.1002/JEV2.12404

66. Wu Z, Cardona EA, Cohn JA, Pierce JT (2025) Caenorhabditis elegans as a model for studying intercellular communication via extracellular vesicles. J Biosci 50:e2407909122. https://doi.org/10.1073/pnas.2407909122

67. Jeppesen DK, Sanchez ZC, Kelley NM, et al (2025) Blebbisomes are large, organelle-rich extracellular vesicles with cell-like properties. Nat Cell Biol. https://doi.org/10.1038/s41556-025-01621-0

68. Blijdorp CJ, Burger D, Llorente A, Martens-uzunova ES (2022) Extracellular Vesicles as Novel Players in Kidney Disease

69. Wiggins RC, Glatfelter A, Kshirsagar B, Brukman J (1986) Procoagulant activity in normal human urine associated with subcellular particles

70. Ng MSY, Burger D, Svenningsen P, et al (2024) Unlocking the potential of extracellular vesicles in nephrology: what does MISEV2023 add? Kidney Int

71. Perez-Hernandez J, Forner MJ, Pinto C, et al (2015) Increased Urinary Exosomal MicroRNAs in Patients with Systemic Lupus Erythematosus. PLoS One 10:e0138618. https://doi.org/10.1371/JOURNAL.PONE.0138618

72. Dwivedi OP, Barreiro K, Käräjämäki A, et al (2023) Genome-wide mRNA profiling in urinary extracellular vesicles reveals stress gene signature for diabetic kidney disease. iScience 26:. https://doi.org/10.1016/j.isci.2023.106686

73. Stone HK, Huang B, Chen C, et al (2023) External Validation of a Urinary Biomarker Risk Score for the Prediction of Steroid Responsiveness in Adults With Nephrotic Syndrome. Kidney Int Rep 8:2458–2468. https://doi.org/10.1016/J.EKIR.2023.08.039

74. Piyaphanee N, Ma Q, Kremen O, et al (2011) Discovery and initial validation of α 1-B glycoprotein fragmentation as a differential urinary biomarker in pediatric steroid-resistant nephrotic syndrome. Proteomics Clin Appl 5:334. https://doi.org/10.1002/PRCA.201000110

75. Ling C, Liu X, Shen Y, et al (2015) Urinary CD80 levels as a diagnostic biomarker of minimal change disease. Pediatr Nephrol 30:309–16. https://doi.org/10.1007/s00467-014-2915-3

76. Santorelli L, Morello W, Barigazzi E, et al (2021) Urinary Extracellular Vesicle Protein Profiles Discriminate Different Clinical Subgroups of Children with Idiopathic Nephrotic Syndrome. Diagnostics 11:456. https://doi.org/10.3390/diagnostics11030456

77. Chen T, Wang C, Yu H, et al (2019) Increased urinary exosomal microRNAs in children with idiopathic nephrotic syndrome. EBioMedicine 39:552–561. https://doi.org/10.1016/j.ebiom.2018.11.018

78. Myette RL, Xiao F, Geier P, et al (2023) Urinary podocyte-derived large extracellular vesicles are increased in paediatric idiopathic nephrotic syndrome. Nephrology Dialysis Transplantation 38:2089–2091. https://doi.org/10.1093/ndt/gfad086

79. Yáñez-Mó M, Siljander PRM, Andreu Z, et al (2015) Biological properties of extracellular vesicles and their physiological functions. J Extracell Vesicles 4:10.3402/jev.v4.27066. https://doi.org/10.3402/JEV.V4.27066

80. Iraci N, Leonardi T, Gessler F, et al (2016) Focus on Extracellular Vesicles: Physiological Role and Signalling Properties of Extracellular Membrane Vesicles. Int J Mol Sci 17:171. https://doi.org/10.3390/IJMS17020171

81. Street JM, Birkhoff W, Menzies RI, et al (2011) Exosomal transmission of functional aquaporin 2 in kidney cortical collecting duct cells. J Physiol 589:6119–6127. https://doi.org/10.1113/JPHYSIOL.2011.220277

82. Zhou H, Kajiyama H, Tsuji T, et al (2013) Urinary exosomal Wilms' tumor-1 as a potential biomarker for podocyte injury. Am J Physiol Renal Physiol 305:F553. https://doi.org/10.1152/AJPRENAL.00056.2013

83. Lazo S, Noren Hooten N, Green J, et al (2021) Mitochondrial DNA in extracellular vesicles declines with age. Aging Cell 20:1–15. https://doi.org/10.1111/acel.13283

84. Arance E, Ramírez V, Rubio-Roldan A, et al (2022) Determination of exosome mitochondrial dna as a biomarker of renal cancer aggressiveness. Cancers (Basel) 14:1–13. https://doi.org/10.3390/cancers14010199

85. Kereliuk SM, Xiao F, Burger D, Dolinsky VW (2022) Extracellular Vesicles as An Index for Endothelial Injury and Cardiac Dysfunction in a Rodent Model of GDM

86. Li J, Wang T, Hou X, et al (2024) Extracellular vesicles: opening up a new perspective for the diagnosis and treatment of mitochondrial dysfunction. J Nanobiotechnology 22:. https://doi.org/10.1186/S12951-024-02750-8

87. Kim J, Gupta R, Blanco LP, et al (2019) VDAC oligomers form mitochondrial pores to release mtDNA fragments and promote lupus-like disease. Science 366:1531–1536. https://doi.org/10.1126/science.aav4011

2 Urinary podocyte-derived large extracellular vesicles are increased in pediatric idiopathic nephrotic syndrome

Robert L. Myette[1,2], Fengxia Xiao[2], Pavel Geier[1], Janusz Feber[1], Dylan Burger[2*] & Christopher R.J. Kennedy[2*] *Nephrology Dialysis Transplantation*, Volume 38, Issue 9, September 2023, Pages 2089–2091, https://doi.org/10.1093/ndt/gfad086

[1]Children's Hospital of Eastern Ontario, Division of Pediatric Nephrology, University of Ottawa, Ottawa, Ontario, Canada. [2]Kidney Research Center, Ottawa Hospital Research Institute, University of Ottawa, Ottawa, Ontario, Canada.

*Equal contribution.

Correspondence: Dylan Burger & Christopher R.J. Kennedy, Kidney Research Center, Ottawa Hospital Research Institute, Department of Cellular and Molecular Medicine, University of Ottawa, 2513-451 Smyth Rd. Ottawa, ON, Canada.

Email: dburger@uottawa.ca & ckennedy@uottawa.ca.

Pediatric idiopathic nephrotic syndrome (iNS), commonly described histopathologically as minimal change disease, is one of the most common glomerular diseases in children[1]. Complicating this condition is the lack of a clear etiology, with several competing pathomechanisms, including autoimmune[2], infectious[3], and aberrant cellular signalling[1] currently being investigated. Clinically, this disease is more commonly observed in males, is diagnosed when children are of toddler age, and presents with proteinuria and hypoalbuminemia, and usually significant edema. Children with iNS will usually have relapsing and remitting disease necessitating steroid therapy, and sometimes, steroid-sparing intensified immunosuppression[1]. There are no well characterized prognostication tools, nor specific biomarkers of relapse and remission currently in use.

Extracellular vesicles (EV) are small, membrane-bound structures released from cells[4]. A subpopulation of ~100-1000 nm large EVs (LEVs, historically termed microparticles or microvesicles) are comprised in large part of EVs actively shed from their parent cell of origin retaining their characteristics. LEVs contain biologically active cargo, as well as signalling molecules associated with their membranes[4]. Podocyte LEVs have been shown as markers of pre-albuminuric glomerular injury in mouse models[5], and were elevated in the urine of pre-albuminuric type 1 diabetic patients[6]. Urinary EVs have been investigated in pediatric iNS, and it was shown that certain EV protein signatures might discriminate steroid resistance from steroid sensitive disease[7]. Further, it was shown that some miRNAs were increased in EVs isolated from children with iNS[8]. However, in both instances, there was no specificity towards LEVs, nor the podocyte.

As such, we sought to quantify urinary podocyte-derived LEVs in a consecutively enrolled cohort of 14 pediatric patients with iNS, all of whom contributed a relapse sample, and a remission

sample. We first characterized the LEVs from patients using western blot analysis and nanoparticle tracking analysis (NTA). We then assessed the levels of both total and podocyte-specific LEVs in the matched urine samples using flow cytometry. We identified urinary, podocyte-specific LEVs by flow cytometry targeting both Annexin V (to label vesicles) as well as Podoplanin (to label podocyte-specific vesicles).

We enrolled 14 children with iNS into this study. At the time of enrolment, all children had minimal change disease (ten biopsy confirmed, four clinically suspected). Our cohort is heterogeneous (reflective of the patient population seen in the clinic) in that four were steroid sensitive and ten were steroid dependent. Of these ten, four required Tacrolimus, three were on mycophenolate mofetil, and three were treated with cyclophosphamide which induced remission. The median age was 8 years [IQR 4, 13], with 4/14 patients (29%) being female. Using groupwise and pairwise comparisons, there was no difference in renal function during relapse, or during remission ($p>0.05$). Additionally, there were no differences in either systolic blood pressure or diastolic blood pressure, or their Z-scores, between relapse and remission ($p>0.05$). The protein to creatinine ratio was significantly higher in relapse ($p<0.001$) using both groupwise and pairwise comparisons (Table S1).

In order to confirm isolation of LEVs, western blotting for positive and negative markers of EVs was performed. We observed enrichment of flotillin, with absence of calnexin and tumour susceptibility gene (TSG)-101, consistent with an LEV enriched isolation. Urinary total LEVs were also assessed using NTA, as described previously[6]. The mean total LEV size on NTA was 112 ($\pm$25) nm. Those in relapse had LEVs 106 ($\pm$23) nm in diameter, while those in remission had LEVs 118 ($\pm$26) nm in size ($p>0.05$).

The median total LEV value for all patients was $4.15x10^6$ LEVs/mmol of Cr [IQR $1.39x10^6$, $10.8x10^6$]. For those in relapse, total LEV value was $13.5x10^6$ LEVs/mmol of Cr [IQR $4.83x10^6$, $41.1x10^6$] and for those in remission, $2.36x10^6$ LEVs/mmol of Cr [$0.72x10^6$, $4.18x10^6$] ($p < 0.01$). Wilcoxon matched pairs signed rank test yielded a significant difference, with the relapse sample LEV levels being higher than in remission ($p < 0.01$, Figure 1A).

We observed differences in the amounts of podocyte-specific LEVs in the urine from patients in remission, compared to relapse, with those in relapse having significantly higher median values. The median podocyte-specific LEV value for all patients was $5.87x10^3$ LEVs/mmol of Cr [IQR 0, $35.7x10^3$]. For those in relapse, the value was $22.8x10^3$ LEVs/mmol of Cr [IQR $1.11x10^3$, $74.6x10^3$], while for those in remission, it was 0 LEVs/mmol of Cr [0, $14.7x10^3$] ($p < 0.01$). Similarly, we employed Wilcoxon matched-pairs signed rank test and observed statistically significant differences between podocyte-specific LEVs, with those in relapse having higher LEV levels compared to those in remission ($p < 0.02$, Figure 1B).

The key results from this study include the confirmation that LEVs, and specifically podocyte-derived LEVs, can be obtained and quantified from the urine of children with iNS, and that they are differential markers of relapse and remission. To date, only a few studies have evaluated urinary EVs in the context of iNS in children. Santorelli *et al*[7], employed a non-specific approach to assessing total EVs isolated by ultracentrifugation. This qualitative assessment of EVs was limited to sodium dodecyl sulfate polyacrylamide gel electrophoresis with a ruby protein gel stain, allowing for characterization of protein profiles, but the inability for confirmation of specific EV subpopulations (small vs. LEVs), or for absolute quantification. Further, Chen *et al*[8], looked specifically at "exosomes" and their contents, with the focus on miRNA. They were able to identify five miRNAs elevated in urinary "exosomes" from children with relapse. However, neither group

commented on attempts to specifically enrich for LEVs, the quantities of the EVs being released during iNS relapse, nor did they specifically look at podocyte-derived EVs.

Previous work from our group showed that LEVs are found in the urine of normotensive patients with Type 1 diabetes[6], in the absence of albuminuria, suggesting that these molecules may act as an early biomarker of podocyte dysfunction in diabetes. We have shown here that urinary podocyte-derived LEVs can differentiate relapse and remission in children with iNS and may act as early-warning markers of disease. The implications for this are far reaching and may impact our approach to diagnosis and treatment of children with iNS.

This present study is limited by its small sample size but is strengthened by the use of matched samples, and its prospective nature. While we are unable to determine the 'normal' LEV number in the urine of these children, we can compare their relapse states to their remission states. Another strength of this study was the lack of significant renal insufficiency in any of the patients which might confound the podocyte-derived LEV numbers. Future studies are aimed at uncovering mechanisms leading to podocyte-derived LEV formation, release, and their cargo.

References

1. Noone, D. G., Iijima, K. & Parekh, R. Idiopathic nephrotic syndrome in children. *Lancet* **392**, 61–74 (2018).
2. Watts, A. *et al.* Discovery of Autoantibodies Targeting Nephrin in Minimal Change Disease Supports a Novel Autoimmune Etiology. *J. Am. Soc. Nephrol.* ASN.2021060794 (2021) doi:10.1681/ASN.2021060794.
3. Dossier, C., Jamin, A. & Deschênes, G. Idiopathic nephrotic syndrome: The EBV hypothesis. *Pediatr. Res.* **81**, 233–239 (2017).
4. Medeiros, T., Myette, R. L., Almeida, J. R., Silva, A. A. & Burger, D. Extracellular Vesicles: Cell-Derived Biomarkers of Glomerular and Tubular Injury. *Cell. Physiol. Biochem.* **54**, 88–109 (2020).
5. Burger, D. *et al.* Urinary Podocyte Microparticles Identify Prealbuminuric Diabetic Glomerular Injury. *J. Am. Soc. Nephrol.* **25**, 1401–1407 (2014).
6. Lytvyn, Y. *et al.* Assessment of urinary microparticles in normotensive patients with type 1 diabetes. *Diabetologia* **60**, 581–584 (2017).
7. Santorelli, L. *et al.* Urinary Extracellular Vesicle Protein Profiles Discriminate Different Clinical Subgroups of Children with Idiopathic Nephrotic Syndrome. *Diagnostics* **11**, 456 (2021).
8. Chen, T. *et al.* Increased urinary exosomal microRNAs in children with idiopathic nephrotic syndrome. *EBioMedicine* **39**, 552–561 (2019).

Disclosures

DB received funding from CIHR (153224). CK received funding from CIHR (162107). RLM is supported by the Kidney Foundation of Canada Krescent Research Scholarship. The authors otherwise declare no conflicts of interest or competing interests.

Acknowledgments

The authors would like to acknowledge the technical support provided by Dr. Lihua Zhu. The authors also wish to thank the Children's Hospital of Eastern Ontario, Division of Nephrology Nursing staff, as well as the patients and families.

Supplementary Material

Supplementary File (PDF): Supplementary Methods

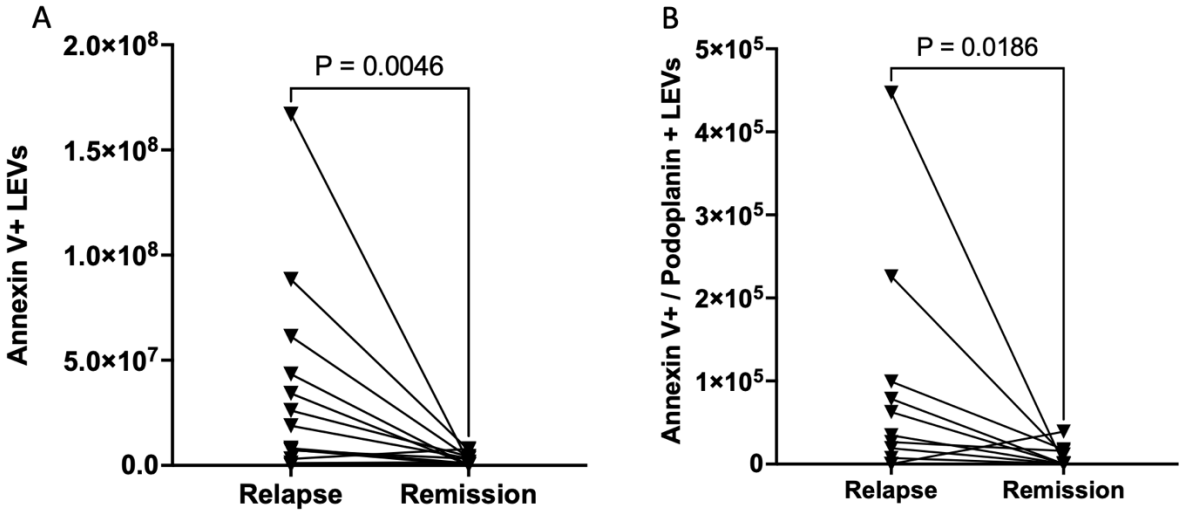

Figure 6. Figure 1. Paired comparison of large extracellular vesicles (LEVs) from urine samples from patients when in relapse and remission.

*Panel A: total LEVs (all Annexin V positive events). Panel B: Podocyte specific LEVs (all Annexin V+ and Podoplanin+ events). All LEV numbers were corrected to urine creatinine (mmol/L). * p < 0.05, ** p<0.01.*

Supplementary Table:

Table 1. Table S1. Anthropometric and clinical variables for the 14 patients enrolled in this study, stratified by their relapse or remission samples.

UPrCr, urinary protein to creatinine ratio.

	Overall	Relapse	Remission	P value
n	28	14	14	
Age (median [IQR])	8 [4, 13]	8 [4, 12]	8 [4, 12]	1
Sex (female %)	8 (29)	4 (29)	4 (29)	1
Weight (median [IQR])	27 [18, 47]	27 [19, 47]	27 [18, 47]	0.647
Height (median [IQR])	128 [102, 155]	128 [103, 150]	127 [104, 156]	0.836
Systolic BP (median [IQR])	100 [95, 105]	97 [95, 104]	102 [96, 105]	0.662
Systolic BP Z-score (mean (SD))	0.30 (1.3)	0.55 (1.2)	0.05 (1.3)	0.308
Diastolic BP (mean (SD))	65 (10.7)	66 (10.4)	65 (11.3)	0.763
Diastolic BP Z-score (mean (SD))	0.95 (1.0)	1.04 (1.0)	0.86 (1.1)	0.660
UPrCr (median [IQR])	0.06 [0.02, 0.51]	0.62 [0.20, 1.12]	0.01 [0.01, 0.03]	**<0.001**
Creatinine (mean (SD))	39 (12.2)	40 (12.8)	39 (12.1)	0.845

Supplementary Material

Methods

Recruitment of patients

Patients were consecutively recruited from the Children's Hospital of Eastern Ontario Pediatric Nephrology Clinic and in-patient service, following Research Ethics Board approval (CHEO REB 18/168X). A Redcap database is in use for storage of appropriate biochemical, anthropometric, clinical and laboratory data for analysis. In some instances, blood work or anthropometric information was not obtained, and urine samples were simply dropped off. In this case, for example, the Cr from the time point before, and the time point after the urine drop off date were averaged. In all cases, the Cr was normal.

Patient Characteristics:

Patient samples were divided based on relapse, with a urine protein to creatinine ratio (UPrCr) > 0.05 g/mmol and remission, characterized by a UPrCr $\leq$ 0.05 g/mmol.

Urine sample processing

Urine samples were collected and centrifuged at 2,500 *x g*, to pellet any cellular debris or sediment, within 4 hours of collection. The supernatant was then frozen at -80ºC until used for down-stream experimentation.

Extracellular vesicle isolation

Urine samples were thawed on ice and then centrifuged again at 2,500 *x g*, for 10 minutes. Three hundred microliters were then aliquoted and subjected to a large extracellular vesicles (LEVs) ultracentrifugation spin, which is 20,000 *x g* for 20 minutes at 4ºC. LEVs were then resuspended in 50 microlitres of phosphate buffered saline that had been filtered using a 0.1 micrometer filter.

Flow Cytometry

LEVs resuspended in filtered PBS were quantified at the University of Ottawa Flow Cytometry and Virometry Facility, using the Cytoflex Flow Cytometer (Beckman Coulter Inc, Indianapolis, IN). We used ApogeeMix beads (Apogee Flow Systems, Hertfordshire, UK) for an appropriate gate size. We specifically used FITC-Annexin V (1:50; Biolegend, San Diego, CA) to identify LEV events, and APC-conjugated podoplanin antibody (1:100; Biolegend) for podocyte-specific LEVs. Samples were then analyzed using FlowJo™ version 7.6.5 (FlowJo, LLC, Ashland, OR). We defined LEVs as 100-1000 nm in size and having greater Annexin V positivity than the negative controls.

Nanoparticle Tracking Analysis

LEV size was assessed using nanoparticle tracking analysis (NTA). The ZetaView PMX110 Multiple Parameter Particle Tracking Analyzer (Particle Metrix, Meerbusch, Germany) was used. We employed size-mode analysis using ZetaView software (version 8.02.28). The already resuspended LEVs in filtered PBS were diluted to the working range of the system. Prior to analysis, the system was calibrated using polystyrene beads (105 nm). We then analyzed the total urinary LEVs at 11 camera positions with 2-second video length at 21ºC.

Western Blot Analysis

LEVs which were resuspended in radioimmunoprecipitation assay (RIPA) buffer following isolation were subjected to western blot analysis. The following primary antibodies were used: anti-flotillin (1:1000, Abcam, Cambridge, UK), anti-tsg-101 (1:500, Systems Biosciences, Palo Alto, CA, USA), anti-calnexin (1:500, Abcam). Following incubation overnight, the membranes were washed in tris-buffered saline with tween-20 (TBS-T) thoroughly with gentle agitation, and then were incubated in the appropriate horseradish peroxidase-conjugated secondary antibodies (1:2000) for 1 hour at room temperature. Thereafter, immunoreactivity was assessed by chemiluminescence.

Statistical Analysis

Continuous variables were summarized as mean (SD) for normally distributed data, or median [IQR] if non-normally distributed. Normality was assessed using the Shapiro-Wilk test. Group differences in LEVS between proteinuria and non-proteinuria were assessed using Student's t-test for normally distributed variables or the Wilcoxon rank-sum test for non-normally distributed variables. For paired comparisons, Wilcoxon matched pairs signed rank test was employed. A p-value of < 0.05 was considered as statistically significant. All tests were performed using statistical software R (version 1.1.456) and Prism (version 9.4.1).

3 Extracellular vesicle mitochondrial DNA reflects podocyte mitochondrial stress and associates with relapse in nephrotic syndrome

Robert L. Myette[1,2,3], Chet E. Holterman[2], Mayra Trentin-Sonoda[2], Tyler T. Cooper[4,5], Gilles A. Lajoie[5], George Cairns[3], Yan Burelle[3], Nour El Khatib[2], Joanna Raman-Nair[2], Dylan Burger[2,3†] & Christopher R.J. Kennedy[2,3†]

A version of this is now published in The International Journal of Molecular Science.

Int J Mol Sci. 2025 Jul 26;26(15):7245. doi: 10.3390/ijms26157245. Open Access.

[1]Children's Hospital of Eastern Ontario Research Institute & Children's Hospital of Eastern Ontario, Division of Pediatric Nephrology, University of Ottawa, Ottawa, Ontario, Canada.

[2]Kidney Research Center, Ottawa Hospital Research Institute, University of Ottawa, Ottawa, Ontario, Canada

[3]Department of Cellular & Molecular Medicine, Faculty of Medicine, University of Ottawa, Ottawa, ON K1H 8M5, Canada.

[4]Department of Biomedical and Molecular Sciences, Queen's University, 99 University Avenue, Kingston, Ontario K7L 3N6, Canada.

[5]Department of Biochemistry, The University of Western Ontario, 1151 Richmond Street, London, Ontario N6A 5B7, Canada.

†Senior authors contributed equally

Correspondence: Dr. Dylan Burger, Kidney Research Center, Ottawa Hospital Research Institute, Department of Cellular and Molecular Medicine, University of Ottawa, 2513-451 Smyth Rd. Ottawa, ON, Canada. Email: dburger@uottawa.ca

The authors have declared that no conflict of interest exists.

Abstract

Idiopathic childhood nephrotic syndrome is a common glomerulopathy comprised of proteinuria, hypoalbuminemia, and edema. Podocyte dysfunction is central to this disease process. Extracellular vesicles are released from stressed cells and can represent a molecular snapshot of the parent cell of origin. We previously showed that urinary large extracellular vesicles (LEVs) derived from podocytes are increased in patients with nephrotic syndrome relapse. Here, we investigated the role of mitochondrial DNA (mtDNA) within LEVs both *in vitro* and *in vivo*, revealing the novel finding that podocytes release LEVs containing mtDNA, driven by mitochondrial stress. A puromycin aminonucleoside nephrosis rat model showed foot process effacement on electron microscopy, and urinary LEVs with significantly increased mtDNA. Prednisolone which drives remission in nephrotic syndrome in children, attenuated mitochondrial stress and reduced the amount of mtDNA content within LEVs. Lastly, urinary LEVs from children with nephrotic syndrome also contain mtDNA, and it is the podocyte LEV-fraction which is preferentially enriched. Overall, these data support a potential mechanism of podocyte mitochondrial stress in non-genetic, idiopathic pediatric nephrotic syndrome.

Introduction

Idiopathic nephrotic syndrome (iNS) is a prevalent glomerulopathy in children and is comprised of proteinuria, hypoalbuminemia, and edema *(1)*, with the most common being minimal change disease (MCD). Several etiologies of MCD have been proposed, and many implicate different components of the immune system; however, our understanding of downstream signalling within the podocyte, in the context of MCD, and other glomerulopathies, is still significantly lacking.

Podocytes are terminally differentiated epithelial cells and are indispensable as key members of the glomerular slit diaphragm *(2, 3)*. Indeed, podocytes act not only as support structures for appropriate filtration; they have also been shown as robust communicators with the underlying glomerular slit diaphragm and are capable of antigen presentation and signalling via common immune pathways *(4–8)*.

Mitochondria are responsible for energy production in the form of ATP, and they maintain their own circular DNA *(9)*. They also act as signalling hubs, contributing to important immune crosstalk within the cell *(10)*. The podocyte has fewer mitochondria than tubular cells, for example, which has prompted some groups to hypothesize that podocytes are less reliant upon mitochondria for energy needs *(11)*. A study by Brinkkoetter *et al*., *(11)* revealed that perturbation of mitochondrial biogenesis, inducing defective fission-fusion capacity, and reduced stability in mitochondrial DNA (mtDNA) did not lead to a pathologic phenotype under physiological and non-stressed conditions. Contrarily, other groups showed that changes to mitochondrial aerobic respiration does lead to a pathologic phenotype seen in diseases such as diabetic kidney disease and focal segmental glomerulosclerosis *(12)*. It is therefore tempting to hypothesize that podocytes rely on anaerobic respiration during times of stability, but switch to a mode requiring more energy, and thus become more dependent on mitochondria, during times of stress. With regards to their

roles in immune signalling, mitochondria can respond to exogenous stimuli, and when damaged, can secrete damage associated molecular patterns (DAMPs), including mtDNA, which interact with pattern recognition receptors (PRRs) *(13)*. These PRRs include the cyclic GMP-AMP synthase–stimulator of interferon genes (cGAS-STING), and Toll-like Receptor 9 (TLR9) *(13)*, all of which are found within podocytes.

Extracellular vesicles (EVs) are small, membrane-enclosed effector molecules released from cells. Some EVs are actively shed from their parent cell of origin, are ~100-1000 nm in size, and are preferentially isolated following a 20,000x *g* centrifugation (called large extracellular vesicles (LEV) here-forward) *(14)*. LEVs retain characteristics of the parent cells and are packaged with biomolecules including DNA. LEVs are released from stressed cells and can act as liquid biopsies. Indeed, we showed recently that children with iNS have elevated levels of podocyte LEVs in their urine during relapse, and these podocyte LEVs are reduced to near-zero during remission *(15)*.

The role of mitochondria, and particularly of mtDNA in the pathogenesis of MCD is an underexplored area of research. The content of EVs has been studied extensively, and lately, there has been a particular interest in mtDNA within EVs (including plasma EVs and monocytic EVs) reflecting mitochondrial stress *(16–18)*. We therefore sought to determine if mtDNA was present in LEVs from human podocytes (hPods) *in vitro* as a marker of mitochondrial stress. We used puromycin aminonucleoside (PAN) as a podocyte toxin and accepted cellular model of nephrosis as it also induces mitochondrial stress *(19–23)*.

We discovered that mitochondrial oxygen consumption rate is increased in hPods in the presence of PAN, and this associates with a marked increase in mtDNA within LEVs from hPods, hinting at a possible unique mechanism of podocyte injury in iNS. We next observed mtDNA

within urinary LEVs from rats following treatment with PAN, associating with podocyte foot process effacement on electron microscopy (EM) and significant proteinuria. Lastly, in a cohort of children with iNS we observed elevated levels of mtDNA in urinary LEVs, and preferentially those from podocytes, during relapse. We show here for the first time the novel use of digital droplet PCR (ddPCR) in the quantification of mtDNA in urinary LEVs from children with iNS, possibly representing a novel approach to disease monitoring.

Results

PAN induces global oxidative stress in hPods which impacts PRR gene expression levels: Following PAN treatment, mean MDA levels were elevated when compared to control hPods ($P=0.01$), indicating that PAN treatment induces oxidative stress in podocytes *in vitro*. Next, we assessed the impact of PAN treatment on PRR gene expression, including TLR9 and cGAS-STING. PAN increased TLR9 ($P<0.05$; Figure 1A), cGAS ($P<0.05$; Figure 1B), and STING ($P<0.01$; Figure 1C) mRNA levels, relative to control.

IL-1ß mRNA levels are increased, but IL-6 levels are decreased, and TNF-alpha levels are minimally increased following PAN treatment: We next looked at downstream inflammatory signatures associated with PRR signalling and discovered that 24-hours of PAN treatment leads to an upregulation of IL-1ß mRNA compared to control ($P<0.0001$; Figure 1D). IL-6 was decreased significantly ($P<0.0001$; Figure 1E) and TNF-alpha mRNA levels were borderline increased ($P=0.059$, Figure 1F).

PAN treatment led to an increase in mitochondrial-specific ROS at 1 hour, but not 24-hours: We observed that following a 1-hour PAN treatment, there was an obvious spike in mitoROS production when compared to control ($P<0.05$; Figure 2A); however, this was attenuated by 24-hours ($P>0.05$; Figure 2A).

PAN induced an acute bioenergetic stress that subsides over time. Oxygen consumption was then monitored to assess the impact of PAN on mitochondrial bioenergetics. Acute 1h exposure of hPods to PAN induced a rapid increase in baseline respiration indicating that PAN's impacts on mitochondria are immediate. This was caused by stimulation of oxidative phosphorylation (OXPHOS), as evidenced by an increased oligomycin-sensitive respiration. Furthermore, PAN also induced a significant increase in OXPHOS-independent mitochondrial respiration, pointing to an increased proton leak through the inner membrane. Maximal respiration induced by uncoupling with the protonophore CCCP was also increased following 1h treatment with PAN. In contrast, aside from a mildly increased proton leak, no discernable differences in mitochondrial respiratory parameters were observed following 24h exposure to PAN.

Bioenergetics were also assessed by monitoring mitochondrial membrane potential (MMP) with TMRE. As shown in Figure 2C, MMP followed a downward trend after 1h exposure to PAN and became significantly lower after 24h hours. Altogether, these results suggest that PAN induced a rapid and robust bioenergetic stress that subsided over time.

Protein levels of Complexes I-V of the electron transport chain and total mitochondrial mass, fission, and fusion machinery are seemingly unaffected by PAN treatment: We next sought to evaluate differences in oxidative phosphorylation proteins using a total OXPHOS western blot antibody cocktail. We did not observe differences in protein expression for each complex between control and 24-hour PAN treatments (data not shown).

We next assessed the impact of 24-h PAN treatments on TOM20 (total mitochondrial mass), DRP1 (fission), and MFN1 (fusion). We initially observed a decrease in MFN1 protein expression relative to control; however, this observation was attenuated when normalizing for total mitochondrial mass (MFN1/TOM20) (data not shown).

hPod proteomics revealed differences in other mitochondrial proteins following 24-hours of PAN treatment: We next applied GPF-DIA proteomics to the hPods treated with PAN to specifically determine changes to mitochondrial proteins in a more sensitive manner. Specifically, we identified 4531 total proteins, of which, 727 were differentially abundant proteins following PAN treatment. Next, utilizing MitoMiner (https://www.mrc-mbu.cam.ac.uk/research-resources-and-facilities/mitominer), a mitochondrial protein database, we determined that 82 differentially abundant proteins were mitochondrial in nature, and of those, 58 were upregulated, and 24 were downregulated (Figure 2D). Many of the proteins were associated with the electron transport chain, the mitochondrial membrane, mitochondrial inner membrane, and the mitochondrial matrix, among others (Figure S1A, B). Specifically, we observed significant upregulation of 58 proteins, including voltage dependent anion channel (VDACs) 1 ($P<0.05$), 2 ($P<0.001$), and 3 ($P<0.05$; Figure 2D) and several mitochondrial ribosomal proteins (MRPLs), including MRPL19 ($P<0.05$), MRPL34 ($P<0.05$), and MRPL44 ($P<0.05$). TFAM was also significantly upregulated ($P=0.02$)

following PAN treatment. We also observed 24 significantly downregulated mitochondrial proteins. Altogether, this suggests that PAN-injury leads to mitochondrial stress.

LEVs from stressed hPods are enriched in mtDNA following treatment with PAN: Having established that mitochondrial stress is present in hPods treated with PAN, we next hypothesized that mtDNA would be present in hPod-LEVs and would associate with hPod injury. We therefore assessed for the presence of two mitochondrial genes within LEVs from hPods (ND2 and COX2). Following preliminary studies showing a similar trend in both genes (data not shown) we focused on a single gene, ND2. The LEV-ND2 gene content was higher following 24-h PAN treatment ($P=0.0002$) compared to control (Figure 3A). We next explored whether LEVs from the urine of rats treated with PAN contained mtDNA.

SD rats are susceptible to PAN treatment, are grossly albuminuric after PAN treatment, and have significant podocyte foot process effacement on EM: Following treatment with PAN, there were no obvious differences between the control animals and those treated with PAN at Day 0. However, at the time of euthanasia and organ harvesting (Day 9), it was apparent that those animals who received PAN had ascites (data not shown). At endpoint (Day 9), urinary ACR was elevated in those animals who received PAN compared to control animals ($P<0.05$; Figure 3B). Representative transmission EM images revealed classic podocyte ultrastructure in control animals (Figure 3B), while those treated with PAN had significant podocyte foot process effacement (Figure 3B).

Urinary LEVs from SD rats treated with PAN have increased levels of mtDNA: We next isolated urinary LEVs from both PAN-treated and control rats. Relative to control animals, at day 9, PAN-treated rat urinary LEV mtDNA levels were ~1000 fold higher (P=0.0087, Figure 3C). Importantly, there was not enough urine to do podocyte-specific LEV pulldowns to determine the relative amounts of mtDNA in total LEVs versus podocyte-specific LEVs. Given the above observations, we next returned to our patient cohort and examined mtDNA levels in urinary LEVs from children with iNS.

Mitochondrial DNA is enriched in LEVs from patients with MCD: We compared the biochemical parameters between 11 patients when they were in relapse vs. remission, and no significant differences were observed in renal function or blood pressure between these states *(15)*. LEVs were isolated from urine samples provided by children with nephrotic syndrome enrolled in this prospective study. We previously showed that urinary, podocyte-specific LEVs were increased in the urine of children with nephrotic syndrome relapse. Using both qPCR and ddPCR, we show here that the mtDNA is present in total urinary LEVs and associates with disease relapse in MCD. The mean copy number per 10,000 total LEVs was 2.9 (± 3.1) in relapse and 0.92 (±0.6) in remission ($p<0.05$; Figure 3D).

mtDNA is markedly increased in urinary podocyte LEVs compared to all other urinary LEVs: We next pooled relapse urine samples, and separately, remission urine samples. LEVs were isolated and treated with DNase and then subjected to magnetic bead conjugation with Anti-Podoplanin antibody to select for podocyte-specific LEVs. We then isolated the DNA from the

LEVs and performed ddPCR to quantify mtDNA copy number. We observed that total urinary LEVs increased approximately 33-fold in relapse, and this was coupled to a 4-fold increase in mtDNA copies per LEV. Podocyte-specific LEVs increased approximately 9-fold, with a 3-fold increase in mtDNA copy number per LEV. Relatively, we observed more mtDNA species per LEV from podocytes.

Prednisolone decreases oxidative stress, hPod LEV-mtDNA content, and mitochondrial stress *in vitro*: Lastly, given its role as the gold standard therapy for children with iNS, and the presence of glucocorticoid receptors on podocytes, we assessed the effectiveness of prednisolone treatment in our cell culture model. When reanalyzing our data from figures 2 and 3, we observed that pre-treatment with prednisolone inhibited the production of mitoROS following a 1-hour treatment with PAN ($P<0.05$; Figure 4A). Further, pre-treatment of hPods with prednisolone attenuated the change in some but not all mitochondrial bioenergetic parameters observed in response to PAN (Figure 4B). Specifically, prednisolone treatment dampened the rise of ATP dependent and maximal OCR observed in response to PAN treatment without significantly affecting proton leak, basal and non-mitochondrial OCR (Figure 4B). Lastly, prednisolone pre-treatment attenuated the packaging of mtDNA into LEVs (Figure 4C).

Discussion

The key findings from this study include the novel discovery of mtDNA within LEVs from stressed podocytes *in vitro*, a recapitulation of these findings in a rat nephrosis model, and lastly, the observation that urinary LEVs from children with iNS and relapse have increased mtDNA compared to remission. Using podocyte-specific magnetic beads, we showed that there was enrichment of mtDNA in podocyte EVs compared with other urinary EV populations. We

previously showed that podocyte-specific LEVs are increased in the urine from children with NS during times of relapse, and that these LEV levels were drastically reduced in remission *(15)*. The presence of mtDNA within non-podocyte EVs has been described by our group *(24)* and others *(25, 26)*; however, this is the only description of LEV-mtDNA in podocytes to our knowledge.

Herein, we have further linked the early production of mitoROS and early increases in OCR followed by later findings of mitochondrial membrane depolarization in hPods treated with PAN. This suggests that PAN may induce mitochondrial stress at an early time point leading to an initial overactive phenotype, perhaps related to compensation as a result of cellular stress *(27)*. Indeed, after 1 hour of PAN treatment, we observed increases in ATP dependent, basal, and maximal OCR when compared to control cells. The timing aligns with an early increase in mitoROS, which may be a result of the increase in mitochondrial OCR. Interestingly, there is an increase in proton leak after 1 hour of PAN, relative to control, which may be an attempt to buffer ROS production *(28)*, and the persistence of a mild proton leak at 24-hours ties together with the lower MMP at 24-hours and might represent a mild, yet persistent signature of cell stress and bioenergetic dysfunction.

In association with these changes, we have observed that PRR genes are induced, suggesting an increase in mtDNA within the cytosol. Within the podocyte, there is ample evidence that cytosolic mtDNA elicits immune responses via inherent immune pathways, including cGAS-STING and TLR9 *(6, 29–32)*. Herein, we describe increases in TLR9 and cGAS-STING mRNA levels following treatment with PAN. We further confirmed that PAN induces oxidative stress in hPods which associates with the induction of TLR9, and cGAS-STING mRNA expression. Ultimately, expression of the downstream effector IL-1β is induced. This is consistent with prior

reports by Mitrofanova *et al.*, who showed that podocytes express all components of the cGAS-STING signalling pathway *(30)*.

Our results suggest that PAN-induced podocyte injury leads to extrusion of mtDNA into the cytosol with subsequent packaging into LEVs. The process by which mtDNA is released from mitochondria is not completely elucidated; however, it is thought that this can occur either via transport pores in the outer mitochondrial membrane *(33)*, or, via fission events that cause mtDNA to leak from the mitochondria into the cytosol *(34)*. We posit that in the context of PAN-induced podocyte injury that this occurs via mitochondrial membrane pores as we did not see any changes in fission and fusion machinery. It is therefore possible that our novel finding of mtDNA within podocyte LEVs may represent a unique self-preservation mechanism. Importantly, our work shows that preventative treatment with prednisolone led to a decrease in mitoROS and attenuated increased OCR in the context of CCCP treatment. This is perhaps not surprising given that podocytes express the glucocorticoid receptor *(35)*. In turn, prednisolone treatment of podocytes prior to injury with PAN led to a marked reduction in the amount of LEV-mtDNA. Consistent with this, we saw similar reductions in LEV-mtDNA from the urine of children with nephrotic syndrome who entered remission following treatment with prednisone.

We next sought to determine if LEVs are packaged with mtDNA in a rodent model of nephrotic syndrome, the PAN-nephrosis model *(36, 37)*. Indeed, the SD rats in our cohort were significantly nephrotic, with ascites, and elevated urinary ACR. Coupled with this significant proteinuria was an ~1000-fold increase in LEV-mtDNA species when compared to control animals injected with saline. To our knowledge, this is the first time that LEVs have been isolated from rat urine and their mtDNA content examined. While the direct mechanism of mtDNA packaging

remains elusive, this appears to be a conserved mechanism, observed in both human podocytes and this murine model, as well as in children with iNS.

Our paper is not without limitations. Much of this work was performed using conditionally immortalized hPods which may not accurately reflect the glomerular environment. Further, we were unable to determine whether the mtDNA-containing urinary LEVs in our rat model were of podocyte origin. Conversely, the strengths of this paper include the use of *in vitro* and *in vivo* studies, as well as human specimens to describe a conserved mechanism associated with podocyte stress in iNS. Much work remains to understand how the mtDNA is extruded from hPod mitochondria. Our proteomic data hints at a potential mechanism, specifically, VDAC1. We observed increases in VDAC1 levels in the cellular proteome, indicating an increase in protein expression following PAN treatment. Given reports that VDAC1 can interact with mtDNA, and VDAC oligomers have been shown to form mitochondrial pores to release mtDNA fragments, we speculate this may represent the mechanism by which mtDNA is extruded from mitochondria into the cytosol in living cells *(33)*. By showing that LEV-mtDNA levels are increased in podocytes *in vitro*, in the urine of rats with nephrotic syndrome, and then in children with iNS, we have provided a foundation for future mechanistic studies.

In summary, the key findings from this study include the novel discovery of mtDNA within LEVs from stressed podocytes *in vitro*, in a rat nephrosis model, and in children with iNS. Our data suggests that early mitochondrial stress drives an increase in OCR, in this model, with subsequent mitochondrial membrane depolarization. We posit that this results in mtDNA extrusion which triggers packaging into LEVs for release. Prednisolone appears to prevent this process from happening; however, it remains unclear whether it is possible to more specifically target the

mtDNA release. Future studies should seek to identify the mtDNA extrusion pathway to better understand this response in the setting of pediatric iNS.

Methods

Sex as a biological variable: All children (after consent or assent) presenting with iNS were enrolled consecutively and prospectively without consideration for sex. In the rat model, 6 animals (3 male, 3 female) were controls, and 6 animals (3 male, 3 female) were treated with PAN.

Patient Cohort: Children (both males and females) with nephrotic syndrome were prospectively and consecutively enrolled from the Children's Hospital of Eastern Ontario (CHEO), Ottawa, Canada. The study was approved by the CHEO Research Institute Research Ethics Board (Protocol 18/168X) and is in accordance with the Declaration of Helsinki. Enrolment is ongoing, and for all patients enrolled, informed consent was obtained. Fifteen patients were initially enrolled, but one was excluded due to a missing urine sample. A further three patients were subsequently shown on follow up biopsy to have focal segmental glomerulosclerosis lesions and were thus excluded. This cohort contains 11 children with MCD on biopsy, or clinically suspected MCD in the absence of a biopsy. These children were heterogeneous in their presentation and response to steroid therapy. Following enrollment, clinical, biological, and anthropometric information was captured, and a urine sample was collected. Urine samples were subsequently collected from children again once they entered remission (defined as a urine protein to creatinine ratio of ≤ 0.05 g/mmol).

LEV Isolation: LEVs were isolated using sequential centrifugation as described previously *(15, 39)*. Briefly, urine or cell culture media was centrifuged at 2,500 x *g* for 10 minutes, the supernatant was then collected and centrifuged at 20,000 x *g* for 20 minutes to pellet LEVs. These LEVs were resuspended in sterile, pre-filtered (0.1 μm) phosphate buffered saline (PBS) and frozen at -80°C until used.

To isolate podocyte-derived LEVs from urine samples, a magnetic conjugation protocol was employed. Briefly, Anti-Podoplanin antibody (Human; Biolegend, San Diego, California, 337003) was conjugated to magnetic beads using the Magnetic Conjugation Kit (Abcam, Cambridge, UK, ab26989). LEVs were incubated with the Anti-Podoplanin antibody-magnetic conjugated beads for 4 hours prior to being applied to a magnetic column. The Anti-Podoplanin antibody was diluted to 0.4 mg/mL with Mag Antibody diluent (Abcam), and 50 μL was added to a 20 μg vial of beads. The protocol was followed verbatim from the manufacturer.

Nanoparticle Tracking Analysis (NTA): NTA was performed as previously described *(15)*. Briefly, the ZetaView PMX110 Multiple Parameter Particle Tracking Analyzer (Particle Metrix, Meerbusch, Germany) was used. We used size-mode analysis with ZetaView software (version 8.02.28) following calibration with polystyrene beads (105 and 500 nm). Samples were analyzed at 11 camera positions with 2-second video length at 21°C.

mtDNA isolation from LEVs: mtDNA levels in LEVs were measured as described previously, with modifications *(24)*. Briefly, isolated LEVs were treated with 2U of DNase-I to ensure coronal and attached DNA specimens were removed. Subsequently, LEVs were resuspended in 200 μL of

PBS and treated with 20 µL of Proteinase K (Quiagen, Venlo, The Netherlands, 19131) and 2 µL of RNAse (10 mg/mL; Quiagen, 19101) and subjected to DNA isolation using a QIAmp DNA Mini Kit (Quiagen) according to the manufacturer's instructions. Total DNA specimens from the LEVs were then resuspended in Buffer AE and subjected to downstream quantitative polymerase chain reaction (qPCR) and ddPCR.

mtDNA qPCR: For qPCR analyses, samples were run in duplicate using mitochondrial-gene specific primers for the mitochondrial genes:

Table 2. Primers for mtDNA.

Gene	Forward	Reverse
Human NADH Dehydrogenase Subunit 2 (ND2)	CCAAGGAATTCCCCTACACA	GAAATTGCGAGAATGGTGGT
Human Cytochrome C Oxidase 2 (COX2)	AGACGCCACATCACCTATCA	CTTGGGCGTCTATTGTGCTT
Rat ND2	CCAAGGAATTCCCCTACACA	GAAATTGCGAGAATGGTGGT

qPCR was performed using SYBR™ Green Master Mix (Applied Biosystems, Waltham, Massachusetts, A25742) and 3 µL of DNA per reaction in a total reaction volume of 20 µL. Samples were run as follows: 2 min at 50°C, 2 min at 95°C followed by 40 cycles of 15 s at 95°C, and 1 min at 60°C, and the dissociation step (15 s at 95°C, 30s at 60°C, and 15 s at 95°C). The relative level of each mtDNA gene was calculated using the formula $2^{-(Ct-X)}$, that is a derivation of the $2^{-\Delta\Delta Ct}$ method. Results were normalized on the mean of the Ct for each primer.

For ddPCR reactions, a similar set-up was used as described above; however, with important differences. EvaGreen™ Master Mix (BioRad, Hercules, California, 1864033), a proprietary master mix specific to ddPCR reactions was used. Next, the DNA samples were added to the master mix preparations, including the same forward and reverse primers as highlighted above. Next, droplets were created using ddPCR Oil™ and the QX200 Droplet Generator™ (BioRad). Following droplet generation, the samples were moved to a PCR plate and run as follows: 5 min at 95°C followed by 40 cycles of 30s at 95°C and 1 min at 60°C. Thereafter, 4°C for 5 mins, 90°C for 5 mins, 4°C for 10 mins, and then 4°C until removed from the machine. The PCR plate was read using the QX200 Droplet Reader™. This method allows for absolute quantification of copy number reported as copies/μL.

RNA Isolation, cDNA creation, qPCR: mRNA was isolated using an RNA-easy Mini Kit (Qiagen, 74104) according to the manufacturer's instructions. Following isolation, 200 ng mRNA was converted to cDNA using a high-capacity RNA to cDNA reverse transcription kit (ThermoFisher, Waltham, MA, USA, 4368814). The resultant cDNA was used for qPCR. qPCR was performed using SYBR™ Green Master Mix (Applied Biosystems, 4309155) and 2 μL of DNA per reaction in a total reaction volume of 20 μL. Samples were run as follows: 2 min at 50°C, 2 min at 95°C followed by 40 cycles of 15 s at 95°C, 20 s at 58°C, and 40 s at 72°C, and the dissociation step (15 s at 95°C, 30s at 60°C, and 15 s at 95°C). The relative level of each mtDNA gene was calculated using the $2^{-\Delta\Delta Ct}$ method and normalized to glyceraldehyde 3-phosphate dehydrogenase (GAPDH) as a housekeeping gene.

PRR and Effector Pathway qPCR: Following cDNA creation, the following human genes were targeted: TLR9, cGAS, STING, IL-1ß, IL-6, and TNF-α. Their primer sequences are as follows:

Table 3. Primers for qPCR and ddPCR.

Gene	Forward	Reverse
TLR9	GCTGGACCTGAGTGAGAACT	GAGTGAGCGGAAGAAGATGC
cGAS	TAACCCTGGCTTTGGAATCA	TAGCCGCCATGTTTCTTCTT
STING	ACTGTGGGGTGCCTGATAAC	CTTGCAGACTTTGTTTGCCA
IL-1ß:	ACGAATCTCCGACCACCAC	CTTGCAGACTTTGTTTGCCA
IL-6	GGTACATCCTCGACGGCATCT	GTGCCTCTTTGCTGCTTTCAC
TNF-α	ATCTACCTGGGAGGCGTCTT	GAGTGGCACAAGGAACTGGT

Cell Culture: Conditionally immortalized human podocytes (hPods) were obtained with permission of Prof. Moin Saleem (University of Bristol, Bristol, UK) *(40)*. Cells (5x10^4) were grown in RPMI-1640 medium supplemented with 10% Fetal Bovine Serum (Gibco, Carlsbad, CA, 12633012) and penicillin-streptomycin (1:100; Gibco, 15140122). Podocytes were proliferated at 33°C in the presence of 10 U/mL Recombinant Human Interferon Gamma (γ-IFN; Invitrogen, RIFNG100). For induction of podocyte differentiation, cells were maintained at 38°C for 13-14 days in the absence of γ-IFN with the experiment performed, in all cases, between days 13-14.

Cell pre-treatment and toxin treatment: Puromycin aminonucleoside (PAN; 25 ug/mL; Cayman Chemicals, Ann Arbour, Michigan, 15509) is a well characterized and ubiquitously employed podocyte toxin and models iNS in the laboratory. Prednisolone pre-treatment occurred 1-hour prior to treatment with PAN. Prednisolone (Pred, 1 μM; Cayman Chemicals, 20866) was resuspended in PBS, aliquoted, and used immediately or frozen. Dose selection was based on dose-response analysis and was consistent with prior studies. PAN treatments occurred for 1-hour, or 24-hours, as indicated. After treatment, the media was collected, and LEVs were isolated as described above. Cell plates were washed with ice cold PBS immediately after media collection and were frozen at -80°C until protein isolation. A minimum of three biological replicates were employed for all conditions.

Western Blot Analysis: Cell pellets were resuspended in 50 μl of radioimmunoprecipitation assay (RIPA) buffer, with 1:100 protease cocktail (PIC). Samples were mixed thoroughly, and the protein concentration was assessed using a BCA standard curve. Five micrograms of cell lysate were added to 6x Laemmli sample buffer and incubated at 95ºC (for Mitofusin-2 (MFN2), Dynamin-related protein 1 (DRP1), Translocase of the Outer Membrane 20 (TOM20), and β-actin probing) or 37ºC (for Oxidative Phosphorylation (OxPhos) protein probing). For each sample, protein was loaded onto a gel and subjected to sodium-dodecyl sulfate polyacrylamide gel electrophoresis (SDS-PAGE), with a stacking gel of 4% and a separating gel of 10% or 12%. This was followed by transfer to PVDF (OxPhos) or Nitrocellulose (MFN2, DRP1, TOM20). Blots were then washed thrice and blocked in 5% non-fat milk in tris-buffered saline with Tween-20 (TBS-T; pH 7.6). Thereafter, the blots were washed again, thoroughly, and then placed into primary antibody (diluted in 5% milk, as above) for overnight incubation at 4ºC. This was followed

by incubation with 1:10,000 anti-rabbit IgG or anti-mouse IgG (Jackson ImmunoResearch, West Grove, PA, USA, 115-005-003). Chemiluminescence was induced by adding SuperSignal West Pico PLUS (ThermoFisher Scientific, 34580). Chemiluminescence was captured on a BioRad ChemiDoc Imaging system. Band densitometry was performed on ImageLab Software.

Antibodies used were as follows:

Mitofusin-2 (D2D10) Rabbit mAb #9482 1:1000

TOM20 (D8T4N) Rabbit mAb #42406 1:1000

DRP1 (D6C7) Rabbit mAb #8570 1:1000

β-Actin (13E5) Rabbit mAb #4970 1:3000

OxPhos Antibody Cocktail Mouse mAb #ab110411 1:5000

Liquid chromatography and tandem mass spectrometry: The MS/MS spectra were obtained using the following protocol *(41)*. Briefly, 50ug of cell lysates in radioimmunoprecipitation assay buffer (150 mM NaCl, 1% Triton X-100, 0.5% sodium deoxycholate, 0.1% SDS, 50 mM Tris, pH 8.0) were isolated via single-pot protein precipitation (SP3) using 50% ethanol and proteolysis buffer (50 mM Ammonium Bicarbonate, 1:50 TrypLysC, 18 hours, 37°C) and analyzed on a Thermo Eclipse using Gas-phase Fractionation operating in Data-Independent Acquisition mode (GPF-DIA). Spectral libraries were searched in DIA-NN (v19.0) against the human proteome using a precursor mass tolerance of 20 ppm and fragment ion mass tolerance of 10 ppm. The search parameters allowed for up to 2 missed cleavages and a maximum of 2 post-translational

modifications per peptide. Missing value imputation, transformations, and proteomic data visualizations were performed using in-house Python code.

Reactive Oxygen Species Kits (Malondialdehyde and Mitochondrial ROS): Malondialdehyde (MDA), a marker of oxidative stress, was analyzed according to manufacturer's instructions (Cayman Chemicals, TBARS Assay Kit, 10009055). Mitochondrial ROS was also assessed according to manufacturer's instructions (Cayman Chemicals, Mitochondrial ROS Detection Kit, 701600).

Tetramethyl rhodamine ethyl ester (TMRE) Assay: The TMRE mitochondrial membrane potential assay kit was purchased from Cayman Chemicals (701310). Briefly, cells were plated onto 96-well, black bottom plates and subjected to pre-treatment and toxin treatments as described. The assay was performed as described in the instruction booklet from the manufacturer.

Seahorse Assay: Oxygen consumption rates (OCR) were measured in hPods (1x10^4 cells per well) using the Seahorse XF96 extracellular flux analyzer. Baseline OCR was recorded in the presence and absence of PAN, and thereafter Oligomycin (Oligo; Final Concentration 1 μM), Carbonyl cyanide-p-trifluoromethoxyphenylhydrazone (CCCP; Final Concentration 1 μM) and antimycin-A/rotenone (AA/R; Final Concentration 0.5 μM) were successively added to determine the impact on ATP-dependent (Oligo), maximal (CCCP), and non-mitochondrial (AA/R) respiration *(42)*. ATP Dependent respiration was calculated as Baseline OCR – Oligo OCR; Proton Leak was calculated as OCR Oligo – OCR AA/R; Basal OCR was calculated as Baseline OCR –

AA/R; Maximum Respiration was calculated as CCCP OCR – Basal OCR; Non-mitochondrial OCR is equal to AA/R OCR. Results were normalized to cellular protein concentration (μg). Multiple, independent Seahorse runs were performed to collect the presented data (N=3 for 1-hour, N=3 for 24-hour).

Experimental Design for Rat Studies: Animal experiments were performed with adherence to, and approval by, the University of Ottawa Animal Care Committee (MEe-4256; Ottawa, ON, Canada). Experiments were conducted according to guidelines of the Canadian Council on Animal Care. Male and female Sprague-Dawley (SD) rats weighing 100-150g were housed 2 animals per cage and had free access to food and water. Animals were randomly assigned to receive PAN or normal saline injection *(37)*. Of the 12 animals, 6 were injected with PAN (3 males, 3 females) and 6 were injected with saline (3 males, 3 females). The PAN injection was a single injection of 100 mg/kg and occurred on Day 0. Animals were housed thereafter for 9 days. Urine was obtained at Day 0 and 9. On Day 9, blood samples were obtained, and all rats were euthanized; kidneys were excised, decapsulated, and subsequently the renal cortex was dissected. Samples were taken for EM imaging. Albumin to creatinine ratio (ACR) was determined using the following kits from Abcam (Creatinine ab204537, Albumin ab235642).

Transmission EM imaging: All steps were performed at room temperature unless otherwise specified. After fixation, tissue portions were incubated for 1 hour in a solution of 1.5% potassium ferrocyanide (Bioshop, Burlington, ON, Canada, PFC232.250) and 2% osmium tetroxide (prepared from 4% osmium tetroxide (aqueous) stock solution, Electron Microscopy Sciences,

Hatfield, PA, USA, 19151). The tissue was then washed in ddH_2O and incubated for 20 minutes in a 10 mg/mL solution of thiocarbohydrazide (Electron Microscopy Sciences, Hatfield, PA, USA, 21900). Following another wash in ddH_2O, the tissue was incubated for 30 minutes in 2% osmium tetroxide. Finally, tissues were washed one last time in ddH_2O before performing a series of dehydrations in increasing concentrations of ice-cold anhydrous ethanol (30%, 50%, 70%, 80%, 90%, and 3x 100%), where they were incubated in each concentration for 2 minutes. The tissue was then further dehydrated in propylene oxide (Sigma-Aldrich, St. Louis, MO, USA, 110205) for 5 minutes before being transferred to aluminum dishes containing Durcupan™ ACM resin (Electron Microscopy Sciences, Hatfield, PA, USA, 14040) overnight. The following day, the tissue was transferred to molds containing fresh Durcupan™ ACM resin and placed in a 55°C oven for 72 hours. Once removed from the oven, samples were sectioned with a diamond knife (80 nm) using an ultramicrotome. Sections were collected on 300-mesh copper grids (Electron Microscopy Sciences, Hatfield, PA, USA, G300-Cu) and imaged with a JEOL JEM1400-Flash electron microscope at 80kV.

Statistical Analysis: Continuous variables were analyzed as mean (±standard deviation, SD) if normally distributed. When non-normally distributed, medians with interquartile ranges (IQR) were analyzed. P-values were generated using student t-tests or one-way analysis of variance (ANOVA) with multiple comparisons which were corrected using Tukey's method if normally distributed. If non-normally distributed, data were analyzed for significance using Mann-Whitney U test or Kruskal-Wallis. Tests were performed using R (version 1.1.456) or Prism (version 9.4.1).

Study Approval: The study was approved by the CHEO Research Institute Research Ethics Board (Protocol 18/168X) and is in accordance with the Declaration of Helsinki. Animal experiments were performed with adherence to, and approval by, the University of Ottawa Animal Care Committee (MEe-4256; Ottawa, ON, Canada). Experiments were conducted according to guidelines of the Canadian Council on Animal Care.

Data Availability: This work does not contain algorithms, or big data sets. We, the authors, declare that the data supporting the findings of our study are available within this article. The authors will share details around animal models and experimental procedure with anyone who wishes to use these models. These models are highly published, with references herein. Please contact RLM, DB, or CRJK for any further information.

Author contributions: RLM conceptualized the study with DB and CRJK. RLM performed experiments and data analysis. CEH assisted with the animal study. MTS assisted with western blot analyses. TTC and GAL completed the proteomics component of this manuscript. GC and YB assisted with Seahorse assays. NEK and JRN completed the electron microscopy. DB and CRJK conceptualized the study with RLM, and provided oversight and guidance, as well as funding for the work.

Acknowledgements: RLM was funded by The Kidney Foundation of Canada (KFOC) KRESCENT Postdoctoral Award (Salary). DB and CRJK are funded by KFOC and Canadian Institutes of Health Research (Operational).

References

1. D. G. Noone, K. Iijima, R. Parekh, Idiopathic nephrotic syndrome in children. *The Lancet* **392**, 61–74 (2018).

2. W. Kriz, I. Shirato, M. Nagata, M. LeHir, K. V. Lemley, The podocyte's response to stress: The enigma of foot process effacement. *Am J Physiol Renal Physiol* **304**, 333–347 (2013).

3. C. E. Martin, N. Jones, Nephrin signaling in the podocyte: An updated view of signal regulation at the slit diaphragm and beyond. *Front Endocrinol (Lausanne)* **9**, 1–12 (2018).

4. V. Bruno, A. K. Mühlig, J. Oh, C. Licht, New insights into the immune functions of podocytes: the role of complement. *Mol Cell Pediatr* **10**, 3 (2023).

5. W. Xiong, X. F. Meng, C. Zhang, Inflammasome activation in podocytes: a new mechanism of glomerular diseases. *Inflammation Research* **69**, 731–743 (2020).

6. G. W. Burke, A. Mitrofanova, A. Fontanella, G. Ciancio, D. Roth, P. Ruiz, C. Abitbol, J. Chandar, S. Merscher, A. Fornoni, The podocyte: glomerular sentinel at the crossroads of innate and adaptive immunity*Front Immunol* **14** (2023), doi:10.3389/fimmu.2023.1201619.

7. H. Xia, W. Bao, S. Shi, Innate immune activity in glomerular podocytes. *Front Immunol* **8**, 1–5 (2017).

8. R. Bhargava, G. C. Tsokos, The immune podocyte. *Curr Opin Rheumatol* **31**, 167–174 (2019).

9. N. A. Gujarati, J. M. Vasquez, D. F. Bogenhagen, S. K. Mallipattu, The complicated role of mitochondria in the podocyte. *Am J Physiol Renal Physiol* **319**, F955–F965 (2020).

10. E. Marques, R. Kramer, D. G. Ryan, Multifaceted mitochondria in innate immunity. *npj Metabolic Health and Disease* **2** (2024), doi:10.1038/s44324-024-00008-3.

11. P. T. Brinkkoetter, T. Bork, S. Salou, W. Liang, A. Mizi, C. Özel, S. Koehler, H. H. Hagmann, C. Ising, A. Kuczkowski, S. Schnyder, A. Abed, B. Schermer, T. Benzing, O. Kretz, V. G. Puelles, S. Lagies, M. Schlimpert, B. Kammerer, C. Handschin, C. Schell, T. B. Huber, Anaerobic Glycolysis Maintains the Glomerular Filtration Barrier Independent of Mitochondrial Metabolism and Dynamics. *Cell Rep* **27**, 1551-1566.e5 (2019).

12. Y. T. Zhu, C. Wan, J. H. Lin, H. P. Hammes, C. Zhang, Mitochondrial Oxidative Stress and Cell Death in Podocytopathies. *Biomolecules* **12** (2022), doi:10.3390/biom12030403.

13. R. L. Myette, M. Trentin-Sonoda, C. Landry, C. E. Holterman, T. Lin, D. Burger, C. R. J. Kennedy, Damage-Associated Molecular Patterns and Pattern Recognition Receptors in the Podocyte. *J Am Soc Nephrol* (2024), doi:10.1681/ASN.0000000531.

14. T. Medeiros, R. L. Myette, J. R. Almeida, A. A. Silva, D. Burger, C. Physiology, Extracellular Vesicles: Cell-Derived Biomarkers of Glomerular and Tubular Injury. *Cell Physiol Biochem* **54**, 88–109 (2020).

15. R. L. Myette, F. Xiao, P. Geier, J. Feber, D. Burger, C. R. J. Kennedy, Urinary podocyte-derived large extracellular vesicles are increased in paediatric idiopathic nephrotic syndrome. *Nephrol Dial Transplant* **38**, 2089–2091 (2023).

16. S. Lazo, N. Noren Hooten, J. Green, E. Eitan, N. A. Mode, Q. R. Liu, A. B. Zonderman, N. Ezike, M. P. Mattson, P. Ghosh, M. K. Evans, Mitochondrial DNA in extracellular vesicles declines with age. *Aging Cell* **20**, 1–15 (2021).

17. H. Konaka, Y. Kato, T. Hirano, K. Tsujimoto, J. Park, T. Koba, W. Aoki, Y. Matsuzaki, M. Taki, S. Koyama, E. Itotagawa, T. Jo, T. Hirayama, T. Kawai, K. J. Ishii, M. Ueda, S. Yamaguchi, S. Akira, T. Morita, Y. Maeda, M. Nishide, S. Nishida, Y. Shima, M. Narazaki, H. Takamatsu, A. Kumanogoh, Secretion of mitochondrial DNA via exosomes promotes inflammation in Behçet's syndrome. *EMBO J* (2023), doi:10.15252/embj.2022112573.

18. E. Arance, V. Ramírez, A. Rubio-Roldan, F. M. Ocaña-Peinado, C. Romero-Cachinero, A. B. Jódar-Reyes, F. Vazquez-Alonso, L. J. Martinez-Gonzalez, M. J. Alvarez-Cubero, Determination of exosome mitochondrial dna as a biomarker of renal cancer aggressiveness. *Cancers (Basel)* **14**, 1–13 (2022).

19. J. Maeda, P. Bartlett, Effects of the potent nephrotogenic aminonucleoside of puromycin on mitochondrial mechanochemistry. *Biochem Pharmacol* **16**, 761–768 (1967).

20. Y. Fujii, H. Matsumura, S. Yamazaki, A. Shirasu, H. Nakakura, T. Ogihara, A. Ashida, Efficacy of a mitochondrion-targeting agent for reducing the level of urinary protein in rats with puromycin aminonucleoside-induced minimal-change nephrotic syndrome. *PLoS One* **15**, e0227414 (2020).

21. A. Stacchiotti, G. Favero, A. Lavazza, M. Monsalve, L. F. Rodella, R. Rezzani, Taurine Supplementation Alleviates Puromycin Aminonucleoside Damage by Modulating Endoplasmic Reticulum Stress and Mitochondrial-Related Apoptosis in Rat Kidney. *Nutrients 2018, Vol. 10, Page 689* **10**, 689 (2018).

22. L. Yu, Y. Liu, Y. Wu, Q. Liu, J. Feng, X. Gu, Y. Xiong, Q. Fan, J. Ye, Smad3/Nox4-mediated mitochondrial dysfunction plays a crucial role in puromycin aminonucleoside-induced podocyte damage. *Cell Signal* **26**, 2979–2991 (2014).

23. M. Hagiwara, K. Yamagata, R. A. Capaldi, A. Koyama, Mitochondrial dysfunction in focal segmental glomerulosclerosis of puromycin aminonucleoside nephrosis. *Kidney Int* **69**, 1146–1152 (2006).

24. S. M. Kereliuk, F. Xiao, D. Burger, V. W. Dolinsky, Extracellular Vesicles as An Index for Endothelial Injury and Cardiac Dysfunction in a Rodent Model of GDM. (2022).

25. A. Picca, R. Calvani, H. J. Coelho-Júnior, F. Landi, R. Bernabei, E. Marzetti, Mitochondrial Dysfunction, Oxidative Stress, and Neuroinflammation: Intertwined Roads to Neurodegeneration. *Antioxidants (Basel)* **9**, 1–21 (2020).

26. I. Tsilioni, T. C. Theoharides, Extracellular vesicles are increased in the serum of children with autism spectrum disorder, contain mitochondrial DNA, and stimulate human microglia to secrete IL-1β. *J Neuroinflammation* **15**, 1–8 (2018).

27. E. D. Williams, S. C. Rogers, X. Zhang, G. Azhar, J. Y. Wei, Elevated oxygen consumption rate in response to acute low-glucose stress: Metformin restores rate to normal level. *Exp Gerontol* **70**, 157–62 (2015).

28. A. S. Divakaruni, M. D. Brand, The regulation and physiology of mitochondrial proton leak.*Physiology (Bethesda)* **26**, 192–205 (2011).

29. N. Zang, C. Cui, X. Guo, J. Song, H. Hu, M. Yang, M. Xu, L. Wang, X. Hou, Q. He, Z. Sun, C. Wang, L. Chen, cGAS-STING activation contributes to podocyte injury in diabetic kidney disease. *iScience* **25**, 105145 (2022).

30. A. Mitrofanova, A. Fontanella, M. Tolerico, S. Mallela, J. M. David, Y. Zuo, M. Boulina, J. J. Kim, J. Santos, M. Ge, A. Sloan, W. Issa, M. Gurumani, J. Pressly, M. Ito, M. Kretzler, S.

Eddy, R. Nelson, S. Merscher, G. Burke, A. Fornoni, Activation of Stimulator of IFN Genes (STING) Causes Proteinuria and Contributes to Glomerular Diseases. *Journal of the American Society of Nephrology* **33**, 2153–2173 (2022).

31. J. Wu, A. Raman, N. J. Coffey, X. Sheng, J. Wahba, M. J. Seasock, Z. Ma, P. Beckerman, D. Laczkó, M. B. Palmer, J. B. Kopp, J. J. Kuo, S. S. Pullen, C. M. Boustany-Kari, A. Linkermann, K. Susztak, The key role of NLRP3 and STING in APOL1-associated podocytopathy. *Journal of Clinical Investigation* **131** (2021), doi:10.1172/JCI136329.

32. W. Bao, H. Xia, Y. Liang, Y. Ye, Y. Lu, X. Xu, A. Duan, J. He, Z. Chen, Y. Wu, X. Wang, C. Zheng, Z. Liu, S. Shi, Toll-like Receptor 9 Can be Activated by Endogenous Mitochondrial DNA to Induce Podocyte Apoptosis. *Sci Rep* **6**, 1–11 (2016).

33. J. Kim, R. Gupta, L. P. Blanco, S. Yang, A. Shteinfer-Kuzmine, K. Wang, J. Zhu, H. E. Yoon, X. Wang, M. Kerkhofs, H. Kang, A. L. Brown, S.-J. Park, X. Xu, E. Zandee van Rilland, M. K. Kim, J. I. Cohen, M. J. Kaplan, V. Shoshan-Barmatz, J. H. Chung, VDAC oligomers form mitochondrial pores to release mtDNA fragments and promote lupus-like disease. *Science* **366**, 1531–1536 (2019).

34. H. Liu, D. Feng, Cells dispose of cytoplasmic mitochondrial DNA by nucleoid-phagy. *Nature Cell Biology 2024 26:6* **26**, 849–850 (2024).

35. J. C. McCaffrey, N. J. Webb, T. M. Poolman, M. Fresquet, C. Moxey, L. A. H. Zeef, I. J. Donaldson, D. W. Ray, R. Lennon, Glucocorticoid therapy regulates podocyte motility by inhibition of Rac1. *Sci Rep* **7**, 1–15 (2017).

36. S. Bhayan, J. A. Dougherty, Y. Kamigaki, S. Agrawal, S. Wijeratne, J. Fitch, A. P. Waller, K. J. Wolfgang, P. White, B. A. Kerlin, W. E. Smoyer, Glucocorticoid- and Pioglitazone-

Induced Proteinuria Reduction in Experimental Nephrotic Syndrome Both Correlate with Glomerular ECM Modulation. *iScience* , 108631 (2023).

37. M. Yamanaka, Y. Tamura, E. Kuribayashi-Okuma, S. Uchida, S. Shibata, Nicorandil protects podocytes via modulation of antioxidative capacity in acute puromycin aminonucleoside-induced nephrosis in rats. *Am J Physiol Renal Physiol* **324**, F168–F178 (2023).

38. R. L. Myette, F. Xiao, P. Geier, J. Feber, D. Burger, C. R. J. Kennedy, Urinary podocyte-derived large extracellular vesicles are increased in paediatric idiopathic nephrotic syndrome. *Nephrology Dialysis Transplantation* **38**, 2089–2091 (2023).

39. M. N. Munkonda, S. Akbari, C. Landry, S. Sun, F. Xiao, M. Turner, C. E. Holterman, R. Nasrallah, R. L. Hébert, C. R. J. Kennedy, D. Burger, Podocyte-derived microparticles promote proximal tubule fibrotic signaling via p38 MAPK and CD36. *J Extracell Vesicles* **7** (2018), doi:10.1080/20013078.2018.1432206.

40. M. A. Saleem, M. J. O'Hare, J. Reiser, R. J. Coward, C. D. Inward, T. Farren, Y. X. Chang, L. Ni, P. W. Mathieson, P. Mundel, A conditionally immortalized human podocyte cell line demonstrating nephrin and podocin expression. *Journal of the American Society of Nephrology* **13**, 630–638 (2002).

41. T. T. Cooper, D. Z. Dieters-Castator, J. Liu, G. M. Siegers, D. Pink, L. Veliz, J. D. Lewis, F. Lagugné-Labarthet, Y. Fu, H. Steed, G. A. Lajoie, L.-M. Postovit, Targeted proteomics of plasma extracellular vesicles uncovers MUC1 as combinatorial biomarker for the early detection of high-grade serous ovarian cancer. *J Ovarian Res* **17**, 149 (2024).

42. G. Cairns, M. Thumiah-Mootoo, M. R. Abbasi, M. Gourlay, J. Racine, N. Larionov, A. Prola, M. Khacho, Y. Burelle, PINK1 deficiency alters muscle stem cell fate decision and muscle regenerative capacity. *Stem Cell Reports* **19**, 673–688 (2024).

Figures and Figure Legends

Figure 7. **Figure 1. Puromycin aminonucleoside (PAN) significantly induces specific pattern recognition receptor genes, as well as some of their downstream effectors in conditionally immortalized human podocytes (hPods).**

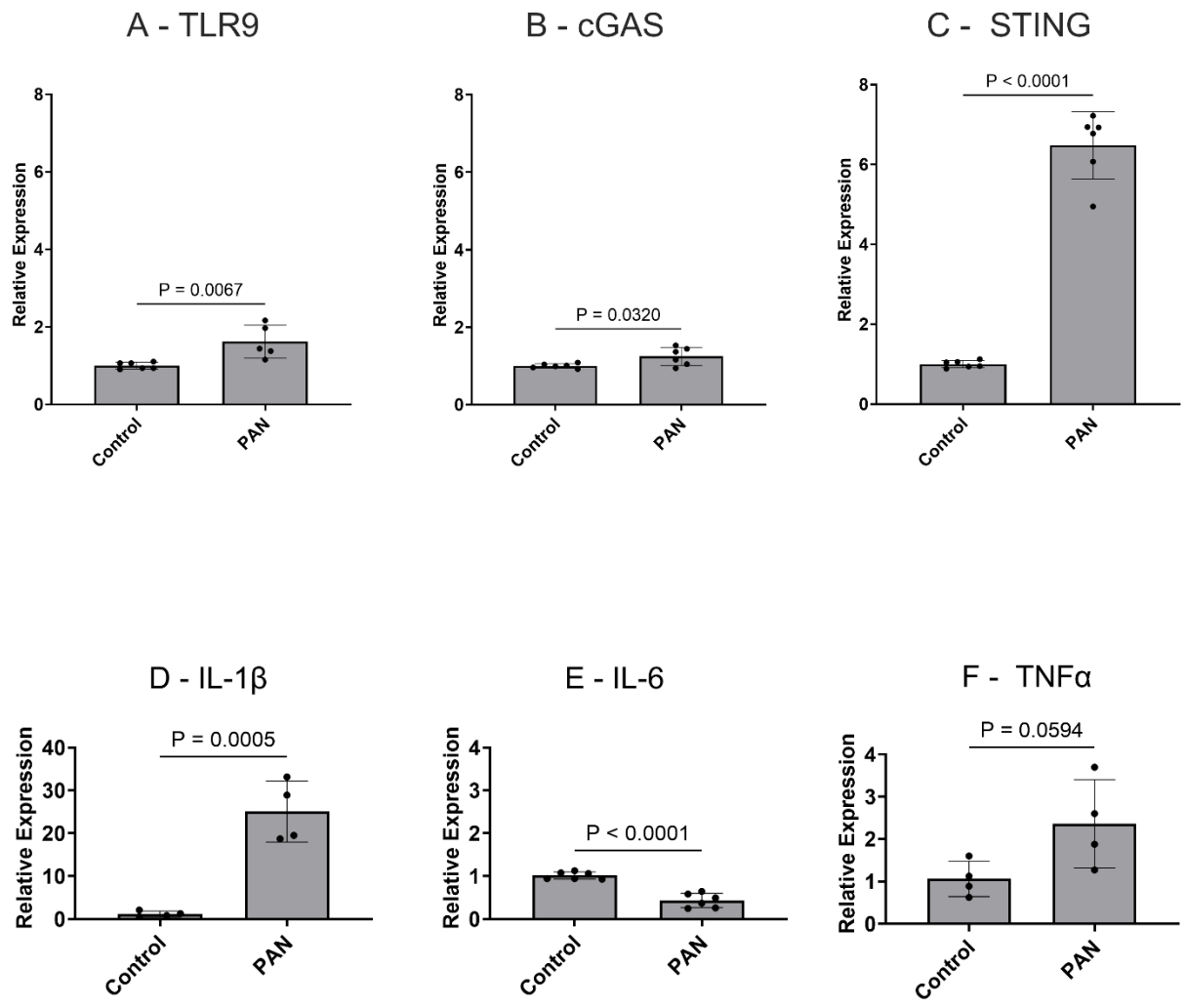

Figure 1. Puromycin aminonucleoside (PAN) significantly induces specific pattern recognition receptor genes, as well as some of their downstream effectors in conditionally immortalized human podocytes (hPods). (A) Toll like receptor 9 (TLR9) was significantly induced following PAN treatment (25 μg/mL; N=3) compared to control (N=3). P=0.0365, two tailed t test. (B) cGAS, cyclic GMP-AMP synthase, was similarly induced following PAN treatment (25 μg/mL; N=3) compared to control (N=3). P=0.0255, two tailed t test. (C) STING, stimulator of interferon genes, was most prominently induced following PAN (25 μg/mL; N=3) compared to control (N=3). P<0.0001, two tailed t test. Next, we assessed downstream effectors, including (D) IL-1ß, Interleukin 1-beta, which was significantly induced following PAN treatment (25 μg/mL; N=3) compared to control (N=3). P=0.0005, two tailed t test. IL-6, interleukin 6 (E), was significantly decreased following treatment with PAN (25 μg/mL; N=3) compared to control (N=3). P<0.0001, two tailed t test. TNF-alpha levels were unaffected by PAN treatment (F). Relative expression = relative fold change using the delta-delta CT method.

Figure 8. Figure 2. Mitochondrial dynamics are altered following treatment of conditional immortalized human podocytes with PAN

Figure 2A.

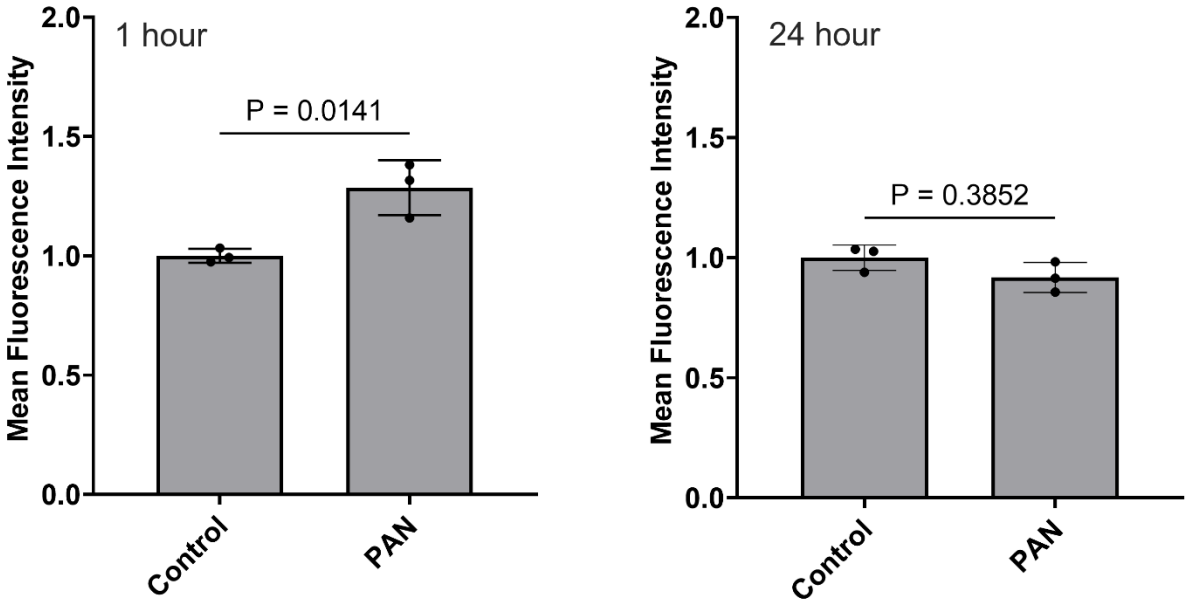

Figure 2B.

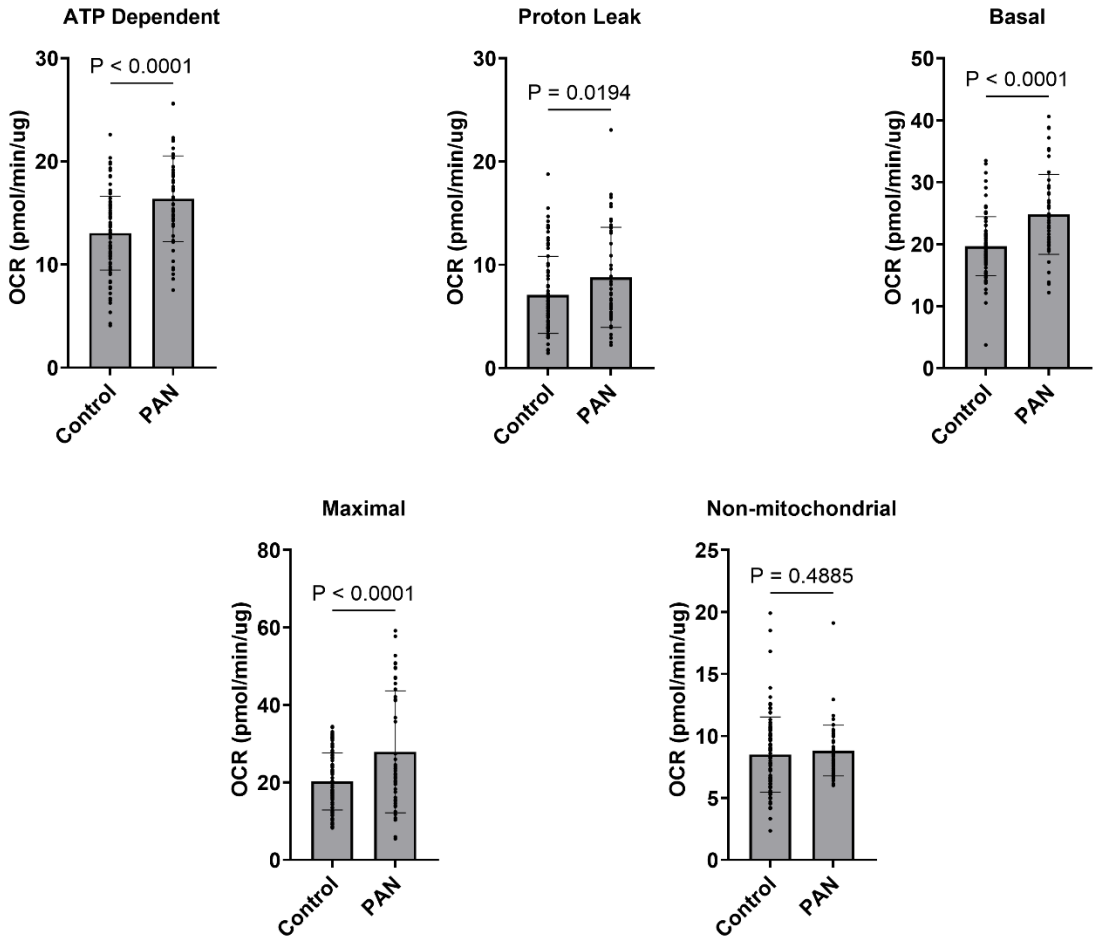
ATP Dependent
P < 0.0001
OCR (pmol/min/ug)
Control
PAN
Proton Leak
P = 0.0194
Basal
P < 0.0001
Maximal
P < 0.0001
Non-mitochondrial
P = 0.4885

Figure 2C.

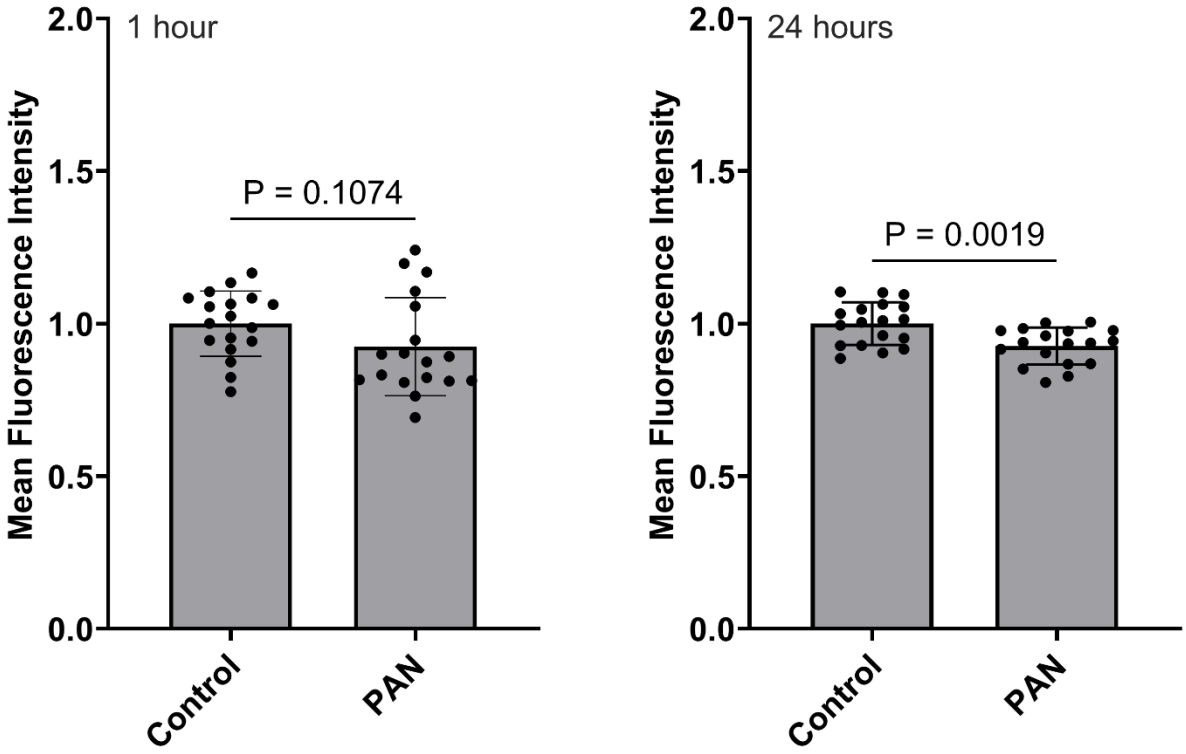
1 hour
Mean Fluorescence Intensity
2.0
1.5
1.0
0.5
0.0
P = 0.1074
Control
PAN
24 hours
Mean Fluorescence Intensity
2.0
1.5
1.0
0.5
0.0
P = 0.0019
Control
PAN

Figure 2D

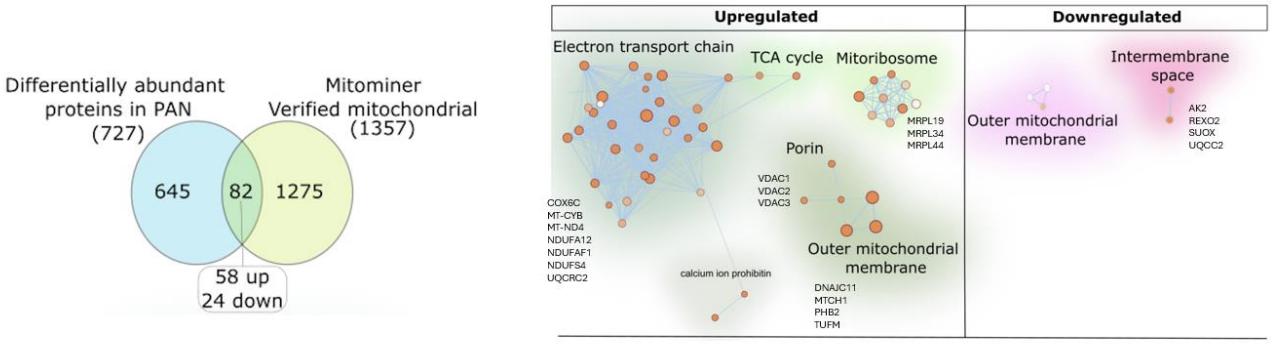
Differentially abundant proteins in PAN (727)
Mitominer Verified mitochondrial (1357)
645
82
1275
58 up
24 down
Upregulated
Downregulated
Electron transport chain
TCA cycle
Mitoribosome
MRPL19
MRPL34
MRPL44
Porin
VDAC1
VDAC2
VDAC3
COX6C
MT-CYB
MT-ND4
NDUFA12
NDUFAF1
NDUFS4
UQCRC2
Outer mitochondrial membrane
calcium ion prohibitin
DNAJC11
MTCH1
PHB2
TUFM
Intermembrane space
AK2
REXO2
SUOX
UQCC2
Outer mitochondrial membrane

Figure 2. Mitochondrial dynamics are altered following treatment of conditional immortalized human podocytes with PAN (A) Mitochondrial ROS (mitoROS) production following PAN treatment of hPods for 1 hour, or 24 hours. mitoROS was significantly increased following 1-hour of PAN treatment (25 μg/mL, N=6) compared to control (N=6). P=0.0141, two tailed t test. **(B)** The impact of 1-hour puromycin aminonucleoside (PAN, 25 μg/mL) treatment on oxygen consumption rate (OCR) using the Seahorse Assay. Basal oxygen consumption rate was increased following treatment with PAN (25 μg/mL, N=3, P<0.0001, two tailed t test). Similarly, for ATP Dependent OCR, we observed an increase following PAN (25 μg/mL, N=3, P<0.0001, two tailed t test). Maximal OCR was increased following treatment with PAN (25 μg/mL, N=3, P<0.0001, two tailed t test). There was no impact on non-mitochondrial OCR following treatment with PAN (25 μg/mL, N=3). There was an increase in Proton Leak (P=0.02). **(C)** Tetramethyl rhodamine, ester (TMRE) assay revealing decreases in mitochondrial membrane potential (MMP) following 24-hours of PAN treatment, but not 1 hour. Specifically, after 24-hours of PAN (25 μg/mL) there was a significant decrease in mean fluorescence intensity representing decreased MMP (N=6, P=0.0053, two tailed t test) **(D)** Proteomic assessment of hPods following treatment with PAN (25 μg/mL, N=4), compared to control (N=4). 727 proteins were differentially abundant, with 82 overlapping with the MitoMiner database (https://www.mrc-mbu.cam.ac.uk/research-resources-and-facilities/mitominer). Of the 82 overlapping proteins, 58 were upregulated, and 24 were downregulated. Upregulated proteins comprised those associated with the electron transport chain (cytochrome c oxidase subunit 6C, COX6C; mitochondrially encoded cytochrome b, MT-CYB; mitochondrially encoded NADH dehydrogenase 4, MT-ND4; NADH dehydrogenase [ubiquinone] 1 alpha subcomplex subunit 12, NDUFA12; NDUFAF1, NDUFS4, Ubiquinol-Cytochrome c Reductase Core Protein 2, UQCRC2), mitoribosomes (Mitochondrial Ribosomal

Protein L19, MRPL19; MRPL34, MRPL44), porins (Voltage-Dependent Anion Channel 1, VDAC1; VDAC2, VDAC3), and the outer mitochondrial membrane (DnaJ Heat Shock Protein Family (Hsp40) Member C11, DNJAC11; Mitochondrial Carrier Homolog 1, MTCH1; Prohibitin 2, PHB2; Tu Translation Elongation Factor, Mitochondrial, TUFM), for example. Those associated with downregulation were related to the outer mitochondrial membrane, and intermembrane space (Adenylate Kinase 2, AK2; RNA Exonuclease 2, REXO2; Sulfite Oxidase, SUOX; Ubiquinol-Cytochrome c Reductase Complex Assembly Factor 2, UQCC2), for example.

Figure 9. Figure 3. Large extracellular vesicles (LEVs) from conditionally immortalized human podocytes contain significantly elevated mtDNA content after treatment with PAN, and this is recapitulated in a rat nephrosis model. Further, urinary LEVs from children with nephrotic syndrome also have elevated levels of mtDNA

Figure 3A.

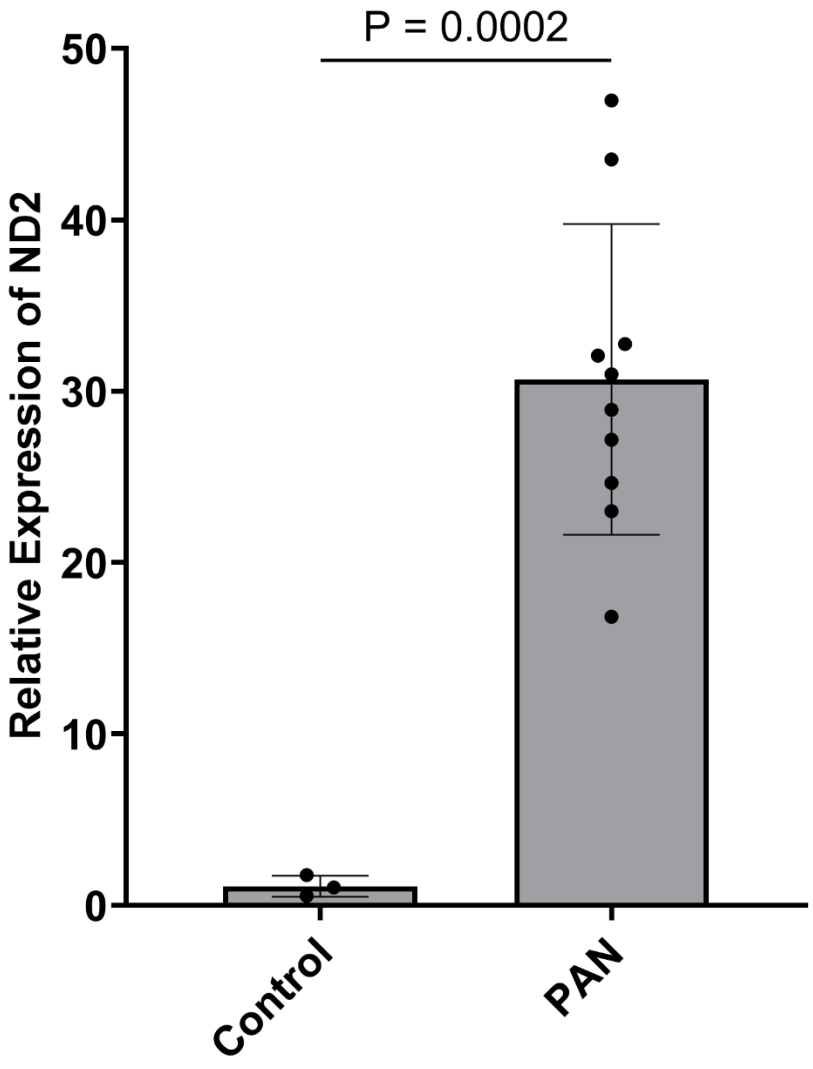

Figure 3B.

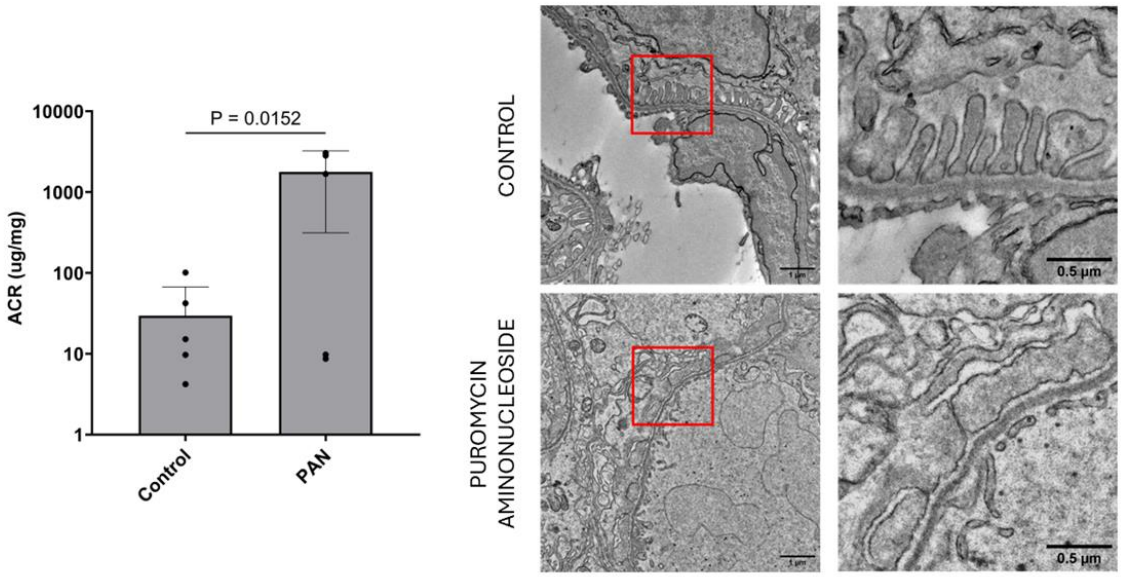
P = 0.0152
ACR (ug/mg)
10000
1000
100
10
1
Control
PAN
CONTROL
PUROMYCIN AMINONUCLEOSIDE
0.5 µm
0.5 µm

Figure 3C.

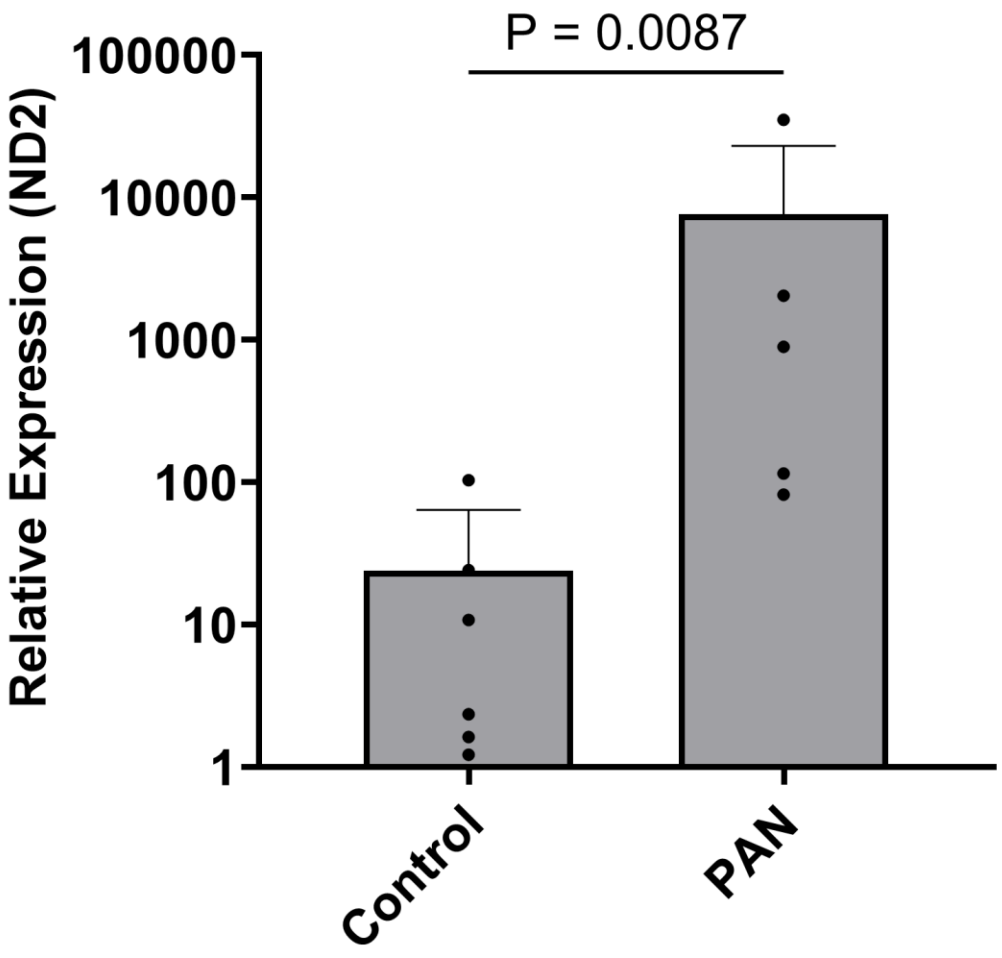
P = 0.0087
Relative Expression (ND2)
100000
10000
1000
100
10
1
Control
PAN

Figure 3D.

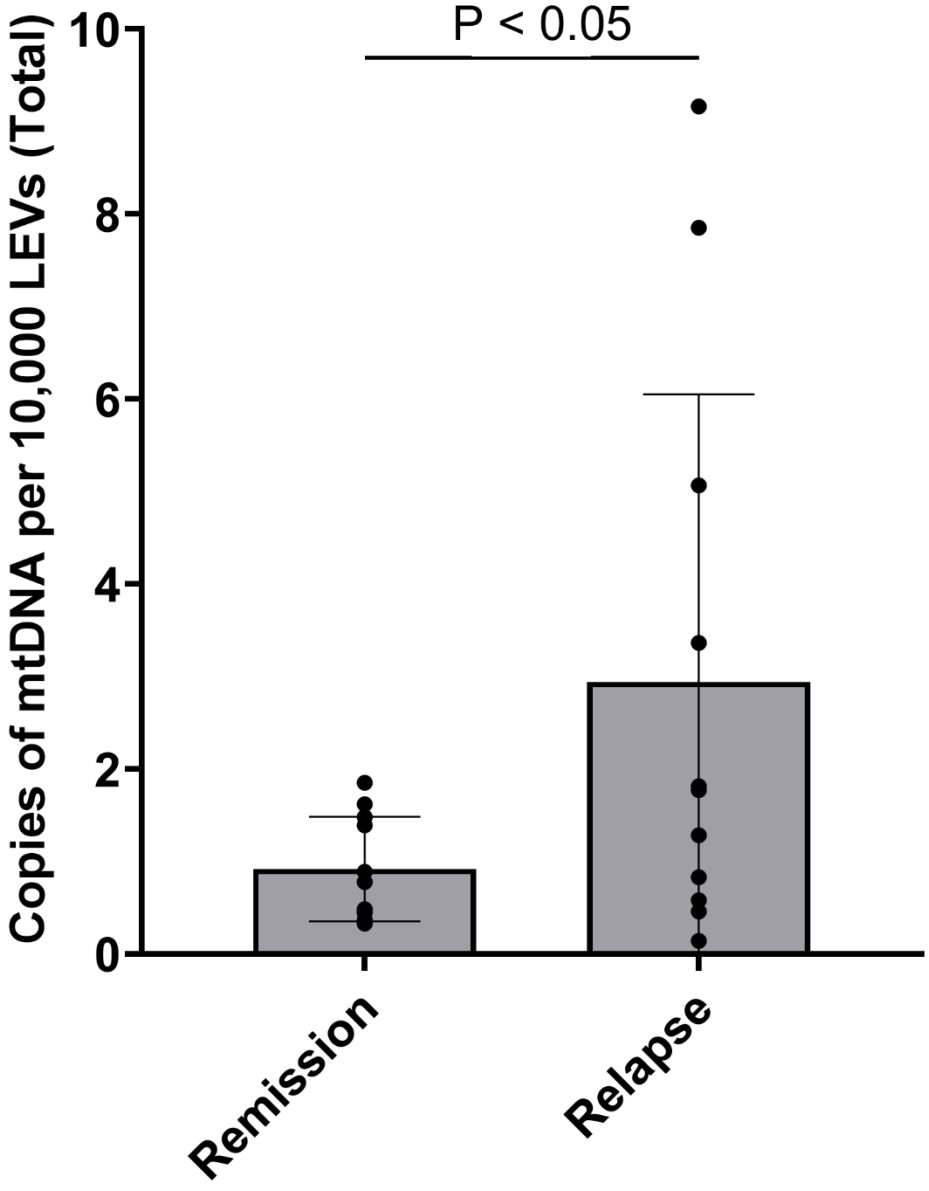
P < 0.05
Copies of mtDNA per 10,000 LEVs (Total)
10
8
6
4
2
0
Remission
Relapse

Figure 3. Large extracellular vesicles (LEVs) from conditionally immortalized human podocytes contain significantly elevated mtDNA content after treatment with PAN, and this is recapitulated in a rat nephrosis model. Further, urinary LEVs from children with nephrotic syndrome also have elevated levels of mtDNA (A) Podocyte LEV mtDNA content is markedly elevated after 24-hours of treatment with PAN (25 μg/mL, N=6) compared to control (N=3). P=0.0002, two tailed t test. **(B)** Sprague-Dawley rats exposed to PAN (100 mg/kg, single injection day 0; N=6) were significantly more albuminuric at Day 9 when compared to control animals (N=6). P=0.0152, two tailed t test. Podocyte foot processes were preserved on electron microscopy for control animals (N=6); however, for PAN-treated animals (N=6), the foot processes were completely effaced. Representative images presented here. This observation was present in all EM images obtained. **(C)** Urinary LEVs from rats were markedly enriched with mtDNA following treatment with PAN (Day 9 shown; N=5 PAN, N=6 control; N=1 PAN removed as outlier). P=0.0095, two tailed t test **(D)** mtDNA in total urinary large extracellular vesicles obtained from children with iNS in both stages of relapse (N=11) and remission (N=11). The results presented are copies of mtDNA per 10,000 total LEVs. $P<0.05$, two tailed t test.

Figure 10. Figure 4. Impact of prednisolone pre-treatment on mitochondrial ROS production, increases in OCR, and mtDNA within LEVs.

Figure 4A

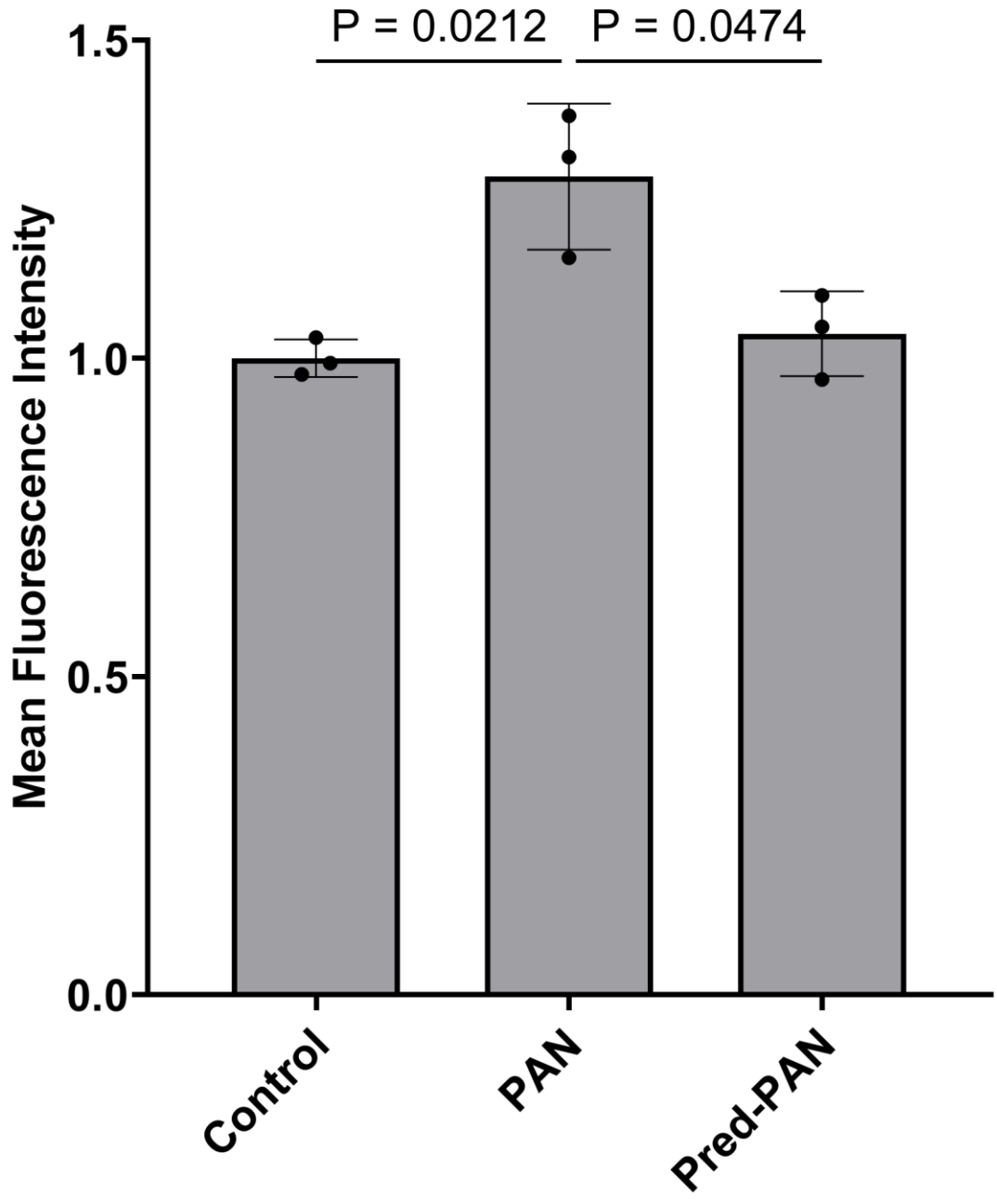

Figure 4B

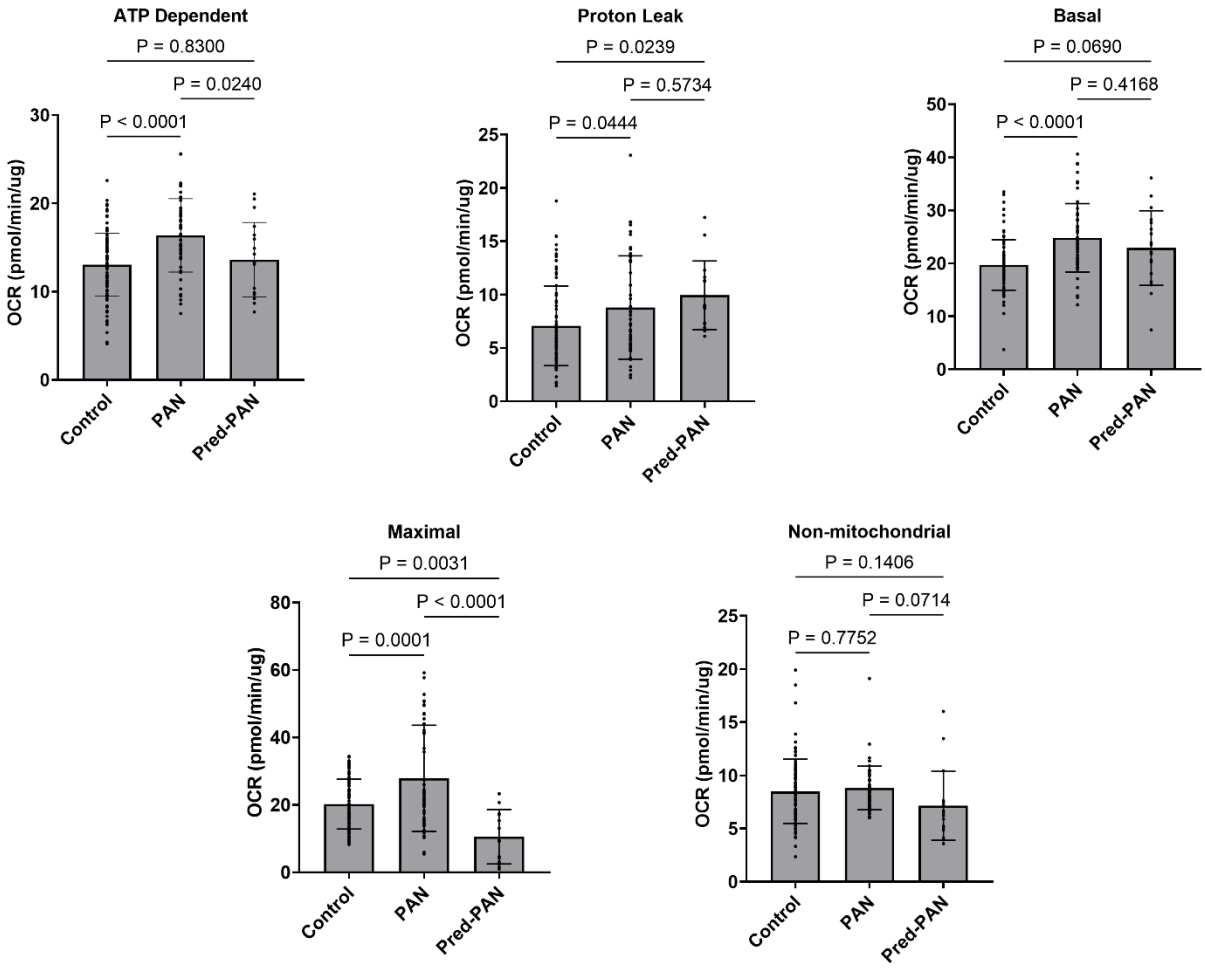
ATP Dependent
P = 0.8300
P = 0.0240
P < 0.0001
OCR (pmol/min/ug)
Control
PAN
Pred-PAN
Proton Leak
P = 0.0239
P = 0.5734
P = 0.0444
Basal
P = 0.0690
P = 0.4168
P < 0.0001
Maximal
P = 0.0031
P < 0.0001
P = 0.0001
Non-mitochondrial
P = 0.1406
P = 0.0714
P = 0.7752

Figure 4C.

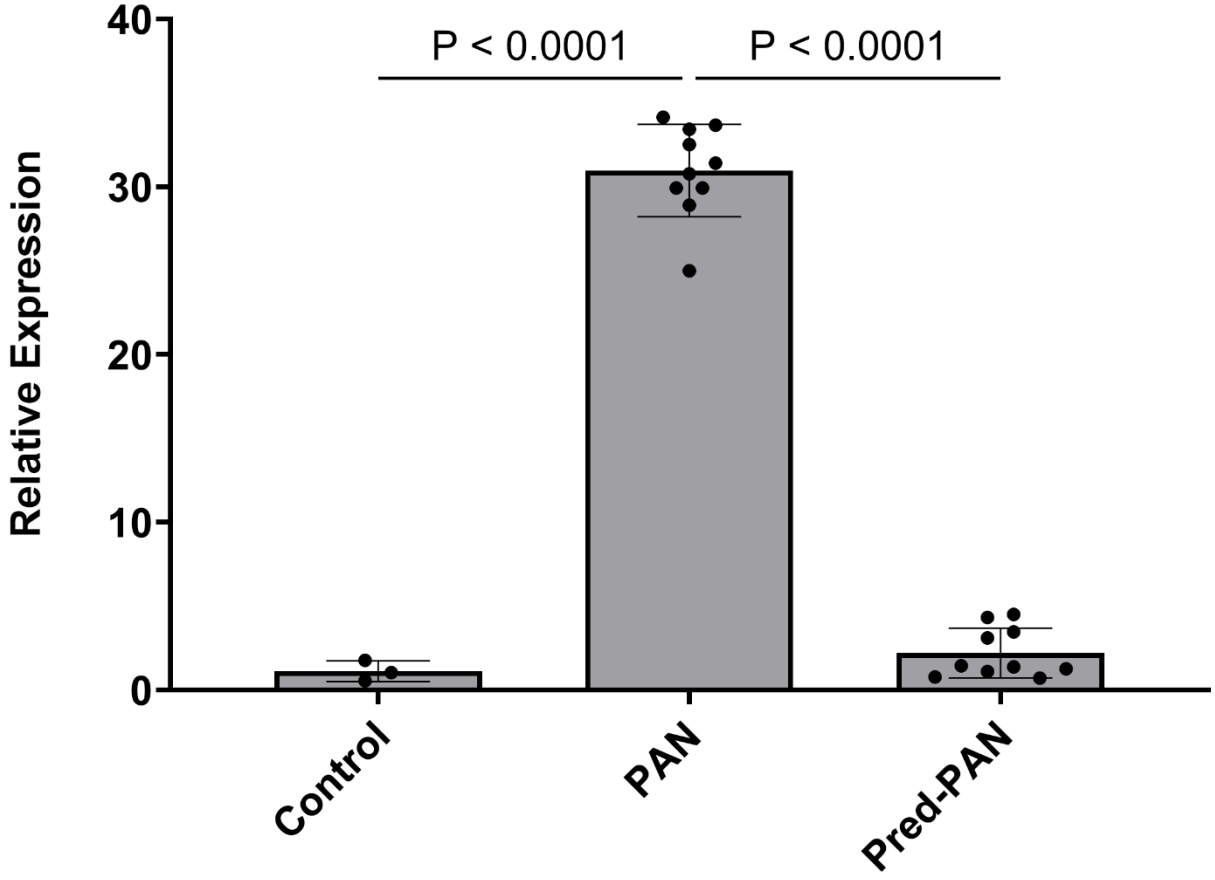
P < 0.0001
P < 0.0001
Relative Expression
40
30
20
10
0
Control
PAN
Pred-PAN

Figure 4. Impact of prednisolone pre-treatment on mitochondrial ROS production, increases in OCR, and mtDNA within LEVs. (A) Pre-treatment with prednisolone (1 μM) prevented the increases in mitoROS observed following treatment with PAN (1-hour, 25 μg/mL, N=6). P=0.0474, one way ANOVA. (B) Similarly, increases in ATP dependent and maximal OCR following PAN treatment (1-hour, 25 μg/mL, N=3) were attenuated with pre-treatment with prednisolone (1 μM, N=3). P<0.0001, one way ANOVA (C) Lastly, a significant reduction in the amount of mtDNA species in LEVs from hPods pre-treated with prednisolone (1 μM; N=6) prior to PAN (25 μg/mL, N=6), relative to control (N=3). P<0.0001, one way ANOVA.

Figure 11. Figure S1. Proteomics of hPods revealed significant alterations in mitochondrial proteins.

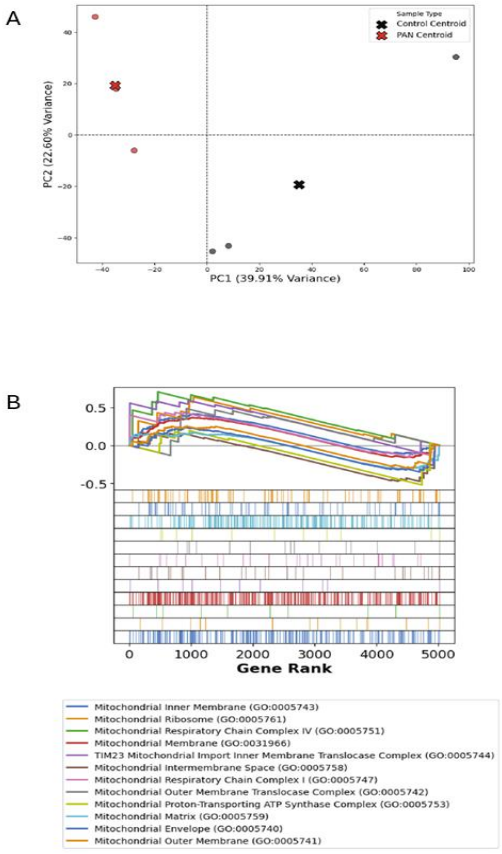

Figure S1. Proteomics of hPods revealed significant alterations in mitochondrial proteins. (A) Principal component analysis. (B) Gene set enrichment analysis.

4 The urinary extracellular vesicle proteome in pediatric nephrotic syndrome

Tyler T. Cooper[1,2], Owen Hovey[2], Gilles A. Lajoie[2], Christopher R.J. Kennedy[3,4], Dylan Burger[3,4], Robert L. Myette[3,4,5]

Under review at Disease Models & Mechanisms at time of submission.

[1]Department of Biomedical and Molecular Sciences, Queen's University, 99 University Avenue, Kingston, Ontario K7L 3N6, Canada.

[2]Department of Biochemistry, The University of Western Ontario, 1151 Richmond Street, London, Ontario N6A 5B7, Canada.

[3]Kidney Research Center, Ottawa Hospital Research Institute, University of Ottawa, Ottawa, Ontario, Canada

[4]Department of Cellular & Molecular Medicine, Faculty of Medicine, University of Ottawa, Ottawa, ON K1H 8M5, Canada.

[5]Children's Hospital of Eastern Ontario Research Institute & Children's Hospital of Eastern Ontario, Division of Pediatric Nephrology, University of Ottawa, Ottawa, Ontario, Canada.

Correspondence: Robert L. Myette, Kidney Research Center, Ottawa Hospital Research Institute, Department of Cellular and Molecular Medicine, University of Ottawa, 2513-451 Smyth Rd. Ottawa, ON, Canada. Email: RMyette@cheo.on.ca

The authors declare no conflicts of interest exist.

Abstract

Idiopathic nephrotic syndrome (NS) is a common glomerulopathy in children and presents with significant proteinuria. There are no reliable clinical or biochemical markers of disease relapse, or prognosis. Extracellular vesicles (EVs) are small, membrane-bound biological effectors released from stressed cells. We previously showed increases in podocyte-specific urinary EVs from children with disease relapse in NS, with numbers returning to near-zero in remission. Herein, we have expanded this work to evaluate proteomic changes of podocytes and their EVs *in vitro* under stress conditions (puromycin aminonucleoside), and in response to the gold standard immunomodulatory agent prednisolone. In addition, we examined proteomic changes in children with NS, comparing the EV proteome between times of remission and relapse. Our key findings reveal significant differential expression of cellular and EV proteomes *in vitro* following treatment with PAN; however, the most marked alterations in the proteome came from treatments with prednisolone. Urinary EV proteomes from children with active NS were significantly different than those in remission, and we identified 645 unique proteins associated with disease and 240 proteins unique to remission.

Introduction

Idiopathic nephrotic syndrome (NS) is a common glomerulopathy in children affecting up to 1:5000 children and presents with significant proteinuria, hypoalbuminemia, and edema [1]. Podocytopathy underlies the etiology of NS and can be confirmed by observing podocyte effacement following kidney biopsy and pathological examination [2]. Current global standards for elucidating the pathophysiology of NS in humans requires the use of both *in vivo* and *in vitro* models that mimic podocyte injury. Chemical insult using puromycin aminonucleoside (PAN) is a widely accepted approach to model podocytopathy in immortalized human podocytes *in vitro* and is a model of nephrosis in rat models *in vivo* [3–5]. PAN is thought to act via an oxidative stress mechanism which in turn 'mimics' renal features of NS by eliciting podocyte injury [6].

Extracellular vesicles (EVs) are membrane-encapsulated vectors released from almost all cell types during times of cellular stress to transfer a diverse range of bioactive cargo [7]. These vesicles contain DNA, miRNA, metabolites, and protein which allow for complex cell-to-cell signaling under both physiological and pathological conditions [7]. A population of large EVs (LEVs), historically referred to as microparticles, are ~100 to 1000 nm in diameter, and are derived predominantly from budding of the plasma membrane [8], retaining characteristics of the parent cell of origin. Recently, we showed that podocyte-specific urinary LEVs from children with NS were increased during times of relapse and returned to near-zero levels during remission [9]. However, comprehensive proteomic characterization of LEVs in pediatric NS is lacking, and their potential as biomarkers for diagnosis and therapeutic response is currently unrealized.

Proteomics is the large-scale study of protein functions, compositions, and interactions, offering unparalleled insights into cellular processes and mechanisms of disease. This approach is particularly valuable for studying EVs, given their diverse protein cargo and multifaceted roles in

intercellular communication [10]. Advances in mass spectrometry-based proteomics, including data-independent acquisition (DIA) methodologies, now enable high-resolution, quantitative analysis of EV proteomes isolated from cell culture or biofluids. These techniques enable unbiased investigations that reveal molecular signatures harbored by tissue-specific EVs, with significant implications for understanding health and disease [11].

Given that NS is a disease of the podocyte and that podocyte-specific LEVs are increased in the urine of children with NS during times of relapse [9], we sought to better characterize LEV levels *in vitro* using conditionally immortalized human podocytes (hPods). We observed that the production of LEVs in hPods increased following treatment with PAN, and this effect was mitigated by prednisolone (PRED), the gold standard therapy for children with NS. To understand the molecular impact of drug treatment on podocyte LEVs, we performed proteomic analyses of hPod-derived LEVs and the hPods themselves *in vitro* following PAN, and PRED exposure. We then compared this *in vitro* model with urinary LEVs isolated from children with NS during both disease and remission, highlighting shared features and significant differences between the cellular model and clinical samples. Herein, we provide the first comprehensive proteomic characterization of urinary LEVs from children with NS, uncovering a diverse array of proteins from both glomerular and tubular origin. Our work provides foundational knowledge on the molecular composition of EVs in pediatric NS, informs future efforts in biomarker discovery, and offers potential for future therapeutic monitoring.

Methodology:

Podocyte Culture: hPods were obtained with permission of Prof. Moin Saleem (University of Bristol, Bristol, UK) [3]. Cells were grown in RPMI-1640 medium supplemented with 10% Fetal Bovine Serum (Invitrogen, Carlsbad, CA) and penicillin-streptomycin (1:100; Invitrogen). Podocytes were proliferated at 33°C in the presence of 10 U/mL Recombinant Human Interferon Gamma (γ-IFN; Invitrogen). For induction of podocyte differentiation, cells were maintained at 38°C for 13-14 days in the absence of γ-IFN, with the experiment performed, in all cases, between days 13-14. PAN (25 μg/mL; Cayman Chemicals, Ann Arbour, Michigan) is a well-characterized podocyte toxin that models NS in the laboratory. PRED pre-treatment occurred 1-hour prior to treatment with PAN. PRED (1 μM; Cayman Chemicals) was resuspended in PBS, aliquoted, and frozen. Dose selection was based on literature review. PAN treatments occurred for 24-hours, as indicated. After treatment, the media was collected, and LEVs were isolated as described. Cell plates were washed with ice cold PBS immediately after media collection and were frozen at -80°C until protein isolation. Protein concentration was determined using the DC protein assay.

Pediatric Nephrotic Syndrome Urine: A prospective study enrolling children with NS is ongoing at the Children's Hospital of Eastern Ontario (REB #18/168X). Urine was obtained from children with NS during both the relapse and remission state. Remission was defined as a urine protein to creatinine ratio of < 0.05 g/mmol. Enrolled children have NS, as defined clinically, and when performed, confirmed by biopsy. Urine samples were freshly obtained and were centrifuged at 2,500 x g for 10 minutes within 4 hours of voiding. Thereafter, urine was frozen at -80 C until used. There were no freeze/thaw events. There were 4 relapse samples, and 4 remission samples evaluated in this study.

Extracellular Vesicles Isolation: LEVs were isolated using sequential centrifugation as described previously [9, 12, 13]. Briefly, cell culture media was centrifuged at 2,500 x *g* for 10 minutes, the supernatant was then collected and centrifuged at 20,000 x *g* for 20 minutes to pellet LEVs. These LEVs were resuspended in sterile, pre-filtered (0.1 μm) phosphate buffered saline (PBS) and frozen at -80°C until analysis.

Nanoparticle Tracking Analysis: NTA was performed as previously described [9]. Briefly, the ZetaView PMX110 Multiple Parameter Particle Tracking Analyzer (Particle Metrix, Meerbusch, Germany) was used. We used size-mode analysis with ZetaView software (version 8.02.28) following calibration with polystyrene beads (105 and 500 nm). Samples were analyzed at 11 camera positions with 2-second video length at 21°C. LEVs were quantified per experiment and expressed as relative to control.

Liquid Chromatography and Tandem Mass Spectrometry: The MS/MS spectra were obtained using the protocol previously reported by our group [11]. Briefly, 10 μg of EV or 50 μg of cell lysates in radioimmunoprecipitation assay buffer (150 mM NaCl, 1% Triton X-100, 0.5% sodium deoxycholate, 0.1% SDS, 50 mM Tris, pH 8.0) were isolated by single-pot protein precipitation (SP3) using 50% Ethanol and proteolysis (50 mM Ammonium Bicarbonate, 1:50 TrypLysC, 18 hours, 37°C) and analyzed on a Thermo Eclipse using Gas-phase Fractionation operating in Data-Independent Acquisition (GPF-DIA). Spectral libraries were first searched in DIA-NN against the human proteome before quantitative analysis using label-free quantification (MaxLFQ). The software parameters were set to a precursor mass tolerance of 20 ppm and a fragment ion mass tolerance of 10 ppm. The search parameters allowed for up to 2 missed cleavages and a maximum

of 2 post-translational modifications per peptide. Missing value imputation, transformations, and proteomic data visualizations were performed using in-house Python code.

Data Analysis: Continuous variables were summarized as mean (±standard deviation, SD) if normally distributed. When non-normally distributed, medians with interquartile ranges were reported. P-values were generated using student t-tests or one-way analysis of variance with multiple comparisons which were corrected using Tukey's method when normally distributed, and Kruskal Wallis and U-test when non-normally distributed. Tests were performed using Prism (version 9.4.1) and Python (version 3.13.1).

Results

PAN-induced injury and, PRED, drive distinct proteomic signatures in immortalized human podocytes: This study evaluated the impact of PAN (25 μg/mL), and PRED (1 μM) treatment on changes to the hPod proteome using four treatment groups, including control, PAN, PRED, and PRED+PAN. Specifically, control hPods did not receive treatment, PAN treatment occurred for 24-hours, PRED treatment occurred for 1 hour, PRED+PAN comprises a 1-hour treatment with PRED prior to a 24-hour treatment with PAN. The combination of 1-hour PRED treatment prior to PAN-induced injury is an accepted model in the field (PRED+PAN; **Figure 1A**).

Overall, we identified and quantified >5000 proteins (**Figure 1B**) with unique proteomic profiles for each experimental condition. Importantly, proteomic transformations did not coincide with an increase or decrease in cell number, as measured using total cellular protein levels between each condition. (**Figure 1C**). Principal component analysis (PCA) revealed distinct proteomic profiles between each of the groups; however, it was observed that PRED treatment alone drove

the largest difference in proteomes (**Figure 1D**). In support of these observations, 226 differentially expressed proteins (DEPs; abs|log2 FC| > 0.6 & log10(p-value) > 1.30) were identified as upregulated in the proteome of hPods treated with PRED compared to Control **(Supplemental Figure 1A**). Notably, we observed induction of cytochrome c oxidase (COX5A), Mitochondrial Translation Peptidase (MTPN), and NADH dehydrogenase (ubiquinone) 1 beta subcomplex, 5, 16kDa (NDUFAB1).

We then sought to determine DEPs unique to PAN-injury, regardless of PRED-treatment, as a means to establish baseline changes that might occur in the absence of PRED. 56 of these DEPs were upregulated in PAN-induced hPod injury relative to control with 111 downregulated (**Figure 1E**). Upregulated DEPs included Tumour protein 53 (TP53), Translocase of Inner Mitochondrial Membrane 17A (TIMM17A), Tropomodulin 2 (TMOD2), Cilia and Flagella Associated Protein 20 (CFAP20), and Cyclin-Dependent Kinase Inhibitor 1A (CDKN1A).

Next, we assessed DEPs in response to PAN vs. PRED+PAN. 300 DEPs were upregulated in PAN-induced hPod injury compared to 282 downregulated DEPs relative to PRED+PAN (**Figure 1F**). This included several upregulated DEPs associating with PAN when compared with PRED+PAN, such as: Metallothionein 1F (MT1F), Gremlin 1 (GREM1), and Angiopoietin-like protein 4 (ANGPTL4), all proteins having been previously described in podocytes [14–16].

Interestingly, DEPs were different when comparing PAN-induced injury with PRED, alone. Specifically, we observed that 159 DEPs were upregulated following PAN injury versus 283 downregulated DEPs relative to PRED (**Supplemental Figure 1B**). We then assessed DEPs under experimental conditions PRED+PAN versus PRED. Interestingly, we observed that 12 DEPs were upregulated under PRED+PAN conditions relative to 26 downregulated DEPs

compared with PRED alone (**Supplemental Figure 1C**). These results further solidify the observation that proteomic transformations driven by PRED were most significant among experimental conditions.

In order to identify proteins with consistent differential expression across experimental conditions, we next assessed for DEPs present in hPods following PAN treatment relative to both control and PRED+PAN (**Figure 1G**). Cross analysis of PAN versus Control (Red) and PAN versus PRED+PAN (Green) revealed TP53 as a highly induced protein following treatment with PAN (**Figure 1G**). Furthermore, we observed an increase in ANGPTL4 following PAN injury, relative to control or PRED+PAN (**Figure 1G**). Comparatively Sphingomyelin Phosphodiesterase Acid-Like 3B (SMPDL3B) expression, among others, was consistently decreased following PAN treatment (**Figure 1G**). Enrichment analysis using Reactome annotations revealed distinct and common protein functions between segregated groups during cross-analysis of DEPs (**Figure 1H**). Specifically, proteins related to cellular response to stimuli, aerobic respiration, neutrophil degranulation, and vesicle-mediated transport were enriched.

Proteomic transformations following PAN-injury are related to EV production and stress, whereas PRED+PAN tends to activate pathways associated with apoptosis and the spliceosome complex: To understand how DEPs confer phenotypic changes, we next used Gene Set Enrichment Analysis (GSEA) to uncover pathways differentially enriched between hPod treatment groups. Initially, we focused on cellular compartments within PAN-injured hPods revealing a significant enrichment in proteins related to stress responses and production of EVs, following treatment with PAN (**Supplemental Figure 2A, B**). Further, we observed enrichment

in other cellular components, including autophagosome membrane, vacuolar membrane, tertiary granule membrane, and endoplasmic reticulum membrane components (**Supplemental Figure 2C**).

Accompanying this, we also examined changes to cellular components between PAN-injury in hPods, and the PRED+PAN group. By pre-treating the hPods with PRED for 1-hour prior to PAN injury, we observed an increase of apoptotic and spliceosome complex proteins, when compared to PAN injury alone. (**Supplemental Figure 2D-F**). Given the results of the GO cellular component analysis, specifically enrichment of EV-related proteins following PAN injury, and further, the recent interest in EVs in renal diseases [17–19], we next evaluated the production of hPod LEVs in the context of PAN-injury, as well as under PRED+PAN conditions.

PAN treatment leads to an increase in hPod LEV formation and release and alters the LEV proteome: Following 24-hours of PAN treatment, hPod LEV release increased ~3-fold compared to control (P=0.0045; **Figure 2A**). There was no apparent increase in LEV production in the presence of PRED. Pretreatment with PRED abrogated the increase in LEV production following PAN injury. There was no apparent impact on LEV size under each treatment condition (**Figure 2B**). Similar to cellular proteomes, LEVs harbour overlapping and unique proteomes between experimental conditions (**Figure 2C**); moreover, PCA determined PRED treatment drives the greatest shifts in LEV proteomes (**Figure 2D**). This was further evaluated by examining volcano plots for different experimental conditions, namely PRED versus control (**Supplemental Figure 3A**), PAN versus PRED (**Supplemental Figure 3B**), and PRED+PAN versus PRED (**Supplemental Figure 3C**). Importantly, EV markers (Albumin, Tissue Factor, CD9, and

Programmed Cell Death 6 Interacting Protein (PDCD6IP or ALIX)) were not different between each experimental condition. This confirms consistent LEV isolation and supports our hypothesis that proteomic cargo in LEVs is unique to experimental conditions (**Figure 2E**).

Next, we sought to determine LEV DEPs present between experimental conditions. PAN-induced injury led to upregulation of 54 unique proteins compared to 138 downregulated proteins under control conditions (**Figure 3A**). Upregulated DEPs included ribosomal proteins, Ribosomal Protein L28, L29, and L35 (RPL28, RPL29, and RPL35 respectively), as well as Small Ubiquitin-like Modifier 2 (SUMO2) and Taxilin Alpha (TXLNA), among others. Downregulated DEPs were more numerous and included Heat Shock Proteins (HSP) and Rho-associated coiled-coil kinase 1 (ROCK1) among others. In support of these observations, GSEA analysis using Reactome and Jensen Compartments annotation revealed a strong enrichment in PAN LEVs of proteins related to Translation, Elongation and Endoplasmic Reticulum, respectively (**Supplemental Figure 4A-B**). Next, we evaluated DEPs between experimental conditions PAN-injury and PRED+PAN (**Figure 3B**). This identified 80 DEPs upregulated by PAN-injury and 375 downregulated DEPs under PRED+PAN conditions. GSEA analysis highlights an enrichment of proteins related to mitochondrial functions in PAN LEVs relative to PRED+PAN LEVs (**Supplemental Figure 4C**). Similar to PAN vs Control LEVs, Jensen Compartment analysis suggests an enrichment of proteins related to Endoplasmic Reticulum in LEVs from PAN vs PRED+PAN (**Supplemental Figure 4D**).

Cross analysis of PAN versus control (Red), PAN versus PRED+PAN (Green), and commonly upregulated DEPs (Blue; **Figure 3C**) revealed upregulated DEPs, FK506-binding protein 9 (FKBP9), Small Ubiquitin-like Modifier 2 (SUMO2), and Cyclin-Dependent Kinase

Inhibitor 2A (CDKN2A). Interestingly, enrichment analysis of these groupings using Reactome annotations uncovered a significant enrichment of proteins with functions related to mitochondrial degradation, vesicle-mediated transport, cellular response to stress, and neutrophil degranulation (**Figure 3D**). Further, we compared the DEPs from hPods following PAN injury with DEPs from hPod-LEVs following PAN injury, in an attempt to determine which proteins are altered in the cells versus their EVs (**Figure 3E**). We identified overlap of 4 proteins, highlighted in Figure 3E.

LEVs from children with NS harbor distinct proteomes reflective of disease status: Building on our *in vitro* analysis of the hPod cellular and LEV proteomes, and our recent work revealing an increase in urinary podocyte-specific LEVs in children with NS during relapse [9], we investigated whether human urinary LEVs from children with NS exhibit significant proteomic differences between disease and remission states. Our analysis identified approximately ~2600 LEV proteins across both conditions, including 645 uniquely associated with disease and 240 proteins unique to remission (**Figure 4A**). Jensen Compartment Analysis revealed that these proteins were predominantly localized to extracellular organelles, extracellular vesicles and exosomes (**Figure 4A**). Proteins unique to disease were significantly associated with an immunological response, vascular endothelial growth factor (VEGF) signaling, and vesicle-mediated transport, whereas proteins unique to remission LEVs were associated with cell-cell adhesion and extracellular matrix reorganization (**Supplemental Figure 5A-B**). PCA revealed distinct proteomic profiles between disease and remission, highlighting the differential LEV proteomes of each condition. (**Figure 4B**). To confirm reproducible LEV isolation from urine, we assessed common EV markers (CD9/81, PDCD6IP, and TSG101) and found no significant difference between conditions (**Figure 4C**). However, higher levels of albumin and tissue factor in disease-state LEVs confirmed their

association with glomerulopathy, and for albumin, likely reflects non-specific binding of albumin in the context of proteinuria.

An in-depth analysis of urinary LEV proteomes identified 512 DEPs being upregulated in patients with active NS disease compared to 350 DEPs downregulated in patients in remission (**Figure 5A**). GSEA identified significant enrichment of Solute Carrier Membrane (SLC) transport proteins under disease conditions (**Figure 5B, C**). Given that these proteins are expressed throughout the nephron, their enrichment likely reflects disease status. In contrast, remission LEVs were enriched in epidermal growth factor (EGF) and COL6A1, two proteins with known functions in tissue regeneration [20]. Collectively, these findings support our hypothesis that the proteomes of LEVs reflect disease status and that several enriched proteins have tissue-specific origins.

There is overlap between discovered hPod-LEV DEPs and DEPs in urinary LEVs from children with NS: After establishing that hPod LEVs exhibit unique proteomes following PAN injury and determining the impact of PRED on the proteome, we evaluated urinary LEVs from children with NS to explore changes in the LEV proteome under PAN-induced injury. We next examined the commonalities between experimental *in vitro* conditions and their impact on the hPod proteome, comparing these findings with urinary-derived LEVs from children with NS. A comparison of urinary LEVs with PAN-injured hPod LEVs and the PRED+PAN treated hPods revealed 44 common DEPs (**Figure 6A**). In these comparisons, 815 DEPs were unique to urinary LEVs (disease versus remission), 106 were unique to PAN-injured hPods (versus control), and 292 were unique to PAN-injury (versus PRED+PAN) (**Figure 6A**). An additional 329 proteins were shared across at least DEP groups. Notably, Jensen Compartment Analysis revealed that these

proteins were enriched in EV-associated proteins, further validating the consistent isolation of LEVs across experimental conditions (**Figure 6A**).

Importantly, we observed conserved protein signatures across LEVs from all three conditions, consisting of 44 proteins (**Figure 6A, B**). Figure 6B illustrates these similarities or differences, with more granular fold-change information. This analysis revealed conserved upregulation of specific DEPs across experimental conditions, along with distinct patterns of up- and down-regulation when compared with urinary LEV DEPs.

There are 36 LEV DEPs identified following treatment with PAN (experimental NS conditions) that were observed in LEVs from children with NS disease: Following a less biased approach to evaluating urinary LEV DEPs, we sought to align those LEV DEPs identified in hPods following PAN injury (versus control), and DEPs present on LEVs from the urine in children with NS disease (versus remission). Specifically, we wanted to directly compare LEV DEPs between experimental NS in the lab, and clinical NS LEVs between disease and remission states. We identified 36 significantly altered DEPs under both conditions. There were commonalities between experimental NS and human NS, specifically Syntaxin 3 (STX3), Regulatory Particle Non-ATPase 2 (RPN2), and Dynactin Subunit 1 (DCTN1) were all commonly upregulated (**Figure 7**). Conversely, Heat Shock Protein Family A member 9 (HSPA9), and phosphate cytidylyltransferase 2, ethanolamine (PCYT2) were downregulated. We did however note certain differences in protein expression patterns between experimental and human NS. In this regard, Prothrombin (F2), and Complement C7 (C7) were differentially regulated, with F2 being upregulated in NS disease LEVs, but downregulated in experimental NS, similar to C7. LEV

C9 was markedly upregulated under NS disease conditions, but in experimental NS, it was mildly downregulated.

Discussion

The overarching goal of this study was to characterize proteomic changes in a cell culture 'experimental' model of NS (the PAN model) in comparison to urine from children with NS. We further assessed the impact of PRED on the hPod proteome. Lastly, we observed that podocyte proteomic transformations are reflected within LEVs. Our group is the first to describe significant urinary LEV proteomic transformations that differ between children with NS disease relapse and remission.

Others have studied the proteomics of urinary EVs in children; however, in the context of childhood NS, there have only been studies linking together urinary EV protein profiles which the authors reported were associated with distinct NS clinical subgroups [21]. While the authors showed characteristic electrophoresis profiles for different clinical subtypes of NS, there was no definitive identification of proteins by mass spectrometry. By linking together *in vitro* and human samples, we have begun to develop an approach for future translational studies.

This was achieved by first determining whether LEVs were released from hPods, as a means to complement our recent observation that urinary podocyte-specific LEVs are associated with disease relapse in children with NS [9]. Secondly, we sought to determine whether changes to the LEV proteome were observed following injury of podocytes *in vitro*, and further, to link this with cellular proteomic changes. Lastly, we unified our findings from *in vitro* cell culture studies with the urinary LEV proteome obtained from children with NS. Overall, we show herein that podocytes increase the production of LEVs in response to PAN injury; however, the exposure to

PRED, or PRED+PAN, also drove distinct cellular and LEV proteome changes. In fact, it was PRED that drove the largest proteomic transformations both in cells and LEVs.

It is notable that we identified significant changes to the podocyte simply from treatment with PRED as it is the gold-standard immunomodulatory medication used in children with NS. The effect of steroids on podocyte function has been described; albeit this was with respect to podocyte motility [22]. However, since podocytes are known to express the Glucocorticoid Receptor (GR), it is not surprising to see significant modifications as a result of treatment with PRED. Further, we assessed the changes induced by treatment with PAN, an experimental toxin which causes hPod injury *in vitro* and nephrosis in rats [6, 23]. Importantly, PAN also induced significant alterations in protein composition relative to control and, PRED+PAN treatments. We identified TP53 as a protein of interest in hPods treated with PAN. The role of TP53 is multifaceted, as it is involved in cell death pathways, and can also act as a master cell cycle regulator, and is involved in DNA repair, and senescence [24]. In the presence of PAN, we speculate that TP53 is upregulated to counteract cellular stressors, such as oxidative stress and DNA damage. Additionally, CDKN1A (p21) was upregulated in PAN-injury LEVs, which is transcriptionally regulated by TP53, and this process is activated under times of cellular stress [24]. Aside from cellular stress response proteins, additionally we observed upregulated proteins associated with cilia and flagella (CFAP20) and actin filaments (TMOD2), which is not surprising given that the podocyte response to cellular stress includes effacement [25]. However, to our knowledge, this is the first observation of such proteins being altered in hPod models.

The effects of PAN, and PRED+PAN have several overlapping DEPs; however, there are several that are uniquely upregulated in PAN treatment when compared to PRED+PAN.

Interestingly, we did not observe a significant differential upregulation of GREM1 or MT1F under PAN conditions alone (versus control). However, we did see an upregulation following PAN treatment when compared to PRED+PAN. This suggests that PRED treatment is at least partly modulating the expression of these targets. GREM1 is a secreted protein which is antagonistic to bone morphogenetic proteins (BMPs) [14]. Importantly GREM1 was shown to be increased in diabetic kidney tissue, and could also inhibit BMP signalling, thought potentially implicated in podocyte injury [14]. Further, MT1F is responsible for binding metals and has been shown to protect against oxidative stress. The overexpression of MT1F in podocytes attenuated severe albuminuria in OVE transgenic mice prone to diabetic kidney disease [15].

We aimed to investigate the effects of PRED, PAN, or PRED+PAN on the hPod LEV proteome to better characterize these *in vitro* models and anticipate their relevance in clinical studies of NS. Our findings show that PAN significantly increased LEV production without affecting their size. Interestingly, while PRED did not independently induce LEV production, it inhibited the PAN-induced increase in LEV release. Despite differences in LEV production, all treatments caused significant transformations to the LEV proteome. Notably, PRED had the most pronounced impact on the hPod LEV proteome, with a substantial number of both upregulated and downregulated DEPs when compared to PAN and PRED+PAN treatments. This observation is novel, as no previous studies have examined the effects of PRED on hPods *in vitro* in relation to LEV proteomics.

As hPods may not accurately represent the glomerular environment, we evaluated LEVs from the urine from children with NS. We have established the feasibility of isolating and analyzing the proteome of urinary-derived LEVs and expanded the existing human urinary LEV

database with details on the NS LEV proteome in children. Such work will serve as the impetus for future studies directed at better understanding the NS urinary LEV proteome in relation to fundamental biologic processes occurring during times of relapse. Indeed, we observed significantly up- and down-regulated DEPs between disease and remission. Importantly, we identified both glomerular and tubular proteins. This is not unexpected given the severity of proteinuria observed in children with NS. It is well characterized that podocytes are effaced, and thus stressed, during times of relapse, and we have already shown that podocyte-specific urinary LEVs are increased during relapse [9]. A novel observation from this study includes the discovery that several tubular proteins are upregulated in urinary LEVs during times of disease relapse in children with NS. We observed significant enrichment of SLC Transporters, which localize mostly to the kidney tubules, and have been described in urinary EVs in the past. Further, their presence has been identified in podocyte-specific EVs, too. Specifically, Prunotto *et al*., analyzed the proteome of podocyte EVs from normal human urine and identified SLC-12A1, -12A3, -13A2, and -23A1 [26]. Consistent with this, we identified SLC13A2 as being upregulated in disease-relapse urinary LEVs. When comparing our results to a study by Gonzales *et al.,* which evaluated urinary EVs without pre-selection for podocyte-specificity, we see more similar trends with a more marked increase in SLC Transporters identified in 'total' urinary LEVs [27]. Specifically, in Gonzales *et al.,* they identified 37 SLC Transporters in the isolated EVs, many of which overlap with our findings (SLC5A8, SLC5A10, SLC22A11, and SLC22A5, among others) [27].

Lastly, we sought to identify podocyte-specific LEV proteomic signatures by comparing our *in vitro* hPod data (PAN versus control) with NS disease LEV data (disease versus remission). In doing so, we identified 36 overlapping, differentially regulated DEPs. This differential regulation speaks to the utility of our *in vitro* model in simulating NS. Importantly, there were

commonly up- and down-regulated proteins across both experimental conditions. STX3 and DCTN1 were identified as upregulated DEPs in both experimental NS as well as in NS disease LEVs. STX7, another of the Syntaxin family, was found abundantly expressed in podocyte clathrin-coated vesicles [28]. Similarly, DCTN1 was also identified in this same study. We speculate these proteins, among many of the other upregulated DEPs in LEVs represent responses to stress or vesiculation.

Our paper is not without its limitations. As discussed extensively, the hPod model is simply a model and cannot definitively recapitulate the glomerular environment [29]. As such, we must interpret these data with caution and use them to guide future studies. A viable next step might include interrogation of directly differentiated podocytes from pluripotent stem cells, or rats subjected to PAN nephrosis. Such studies would allow for perturbation of the system with pharmacological intervention to assess the impact on LEV release, and subsequently the LEV proteome. Another limitation is that the patient-derived urinary LEVs were not podocyte-specific but were a mix of LEVs originating from multiple cellular sources, including tubular.

Strengths of this current paper include the 'ground up' approach taken to interrogate the impact of PAN on hPods *in vitro*, in the context of its use as an experimental NS model. By further understanding the impact of PRED on hPods *in vitro*, we may be able to better understand the urinary LEVs from patients who are routinely exposed to PRED (i.e., children with NS). Next, through evaluation of pure hPod LEVs, and comparing them to urinary-derived LEVs from children with NS, we can attempt to determine truly podocyte specific LEVs in a urinary milieu where LEVs from multiple cellular origins would be present. Ultimately, we observed differential regulation of proteins across *in vitro* conditions and the human LEVs. Several of the identified

proteins have been reported in podocytes, both *in vitro* and *in vivo*, thus confirming that many of our upregulated DEPs are specific to podocytes. Determining their importance, particularly in childhood NS is the obvious next step.

In summary, hPod LEVs are increased *in vitro* following PAN injury. This supports and builds upon our findings of increased podocyte urinary LEVs from children with NS. On further interrogation, podocytes *in vitro* have distinct proteomes when exposed to PAN or PRED. Several differentially regulated proteins have been described previously in podocytes and potentially have important functions therein. By isolating LEVs from the urine of children with NS during both disease and remission, we have developed the first urinary LEV proteome specific to this condition in children. Uncovering the role of these up- and down-regulated DEPs in podocytes and elucidating the significance of their inclusion in LEVs are clear next steps.

References:

1. Noone DG, Iijima K, Parekh R (2018) Idiopathic nephrotic syndrome in children. The Lancet 392:61–74. https://doi.org/10.1016/S0140-6736(18)30536-1

2. Kopp JB, Anders HJ, Susztak K, et al (2020) Podocytopathies. Nat Rev Dis Primers 6:. https://doi.org/10.1038/s41572-020-0196-7

3. Saleem MA, O'Hare MJ, Reiser J, et al (2002) A conditionally immortalized human podocyte cell line demonstrating nephrin and podocin expression. Journal of the American Society of Nephrology 13:630–638. https://doi.org/10.1681/asn.v133630

4. Srivastava T, Sharma M, Yew KH, et al (2013) LPS and PAN-induced podocyte injury in an in vitro model of minimal change disease: Changes in TLR profile. J Cell Commun Signal 7:49–60. https://doi.org/10.1007/s12079-012-0184-0

5. Simic I, Tabatabaeifar M, Schaefer F (2013) Animal models of nephrotic syndrome. Pediatric Nephrology 28:2079–2088. https://doi.org/10.1007/s00467-012-2376-5

6. Marshall CB, Pippin JW, Krofft RD, Shankland SJ (2006) Puromycin aminonucleoside induces oxidant-dependent DNA damage in podocytes in vitro and in vivo. Kidney Int 70:1962–1973. https://doi.org/10.1038/sj.ki.5001965

7. Medeiros T, Myette RL, Almeida JR, et al (2020) Extracellular Vesicles: Cell-Derived Biomarkers of Glomerular and Tubular Injury. Cell Physiol Biochem 54:88–109. https://doi.org/10.33594/000000207

8. Welsh JA, Goberdhan DCI, O'Driscoll L, et al (2024) Minimal information for studies of extracellular vesicles (MISEV2023): From basic to advanced approaches. J Extracell Vesicles 13:e12404. https://doi.org/10.1002/JEV2.12404

9. Myette RL, Xiao F, Geier P, et al (2023) Urinary podocyte-derived large extracellular vesicles are increased in paediatric idiopathic nephrotic syndrome. Nephrology Dialysis Transplantation 38:2089–2091. https://doi.org/10.1093/ndt/gfad086

10. Choi D-S, Kim D-K, Kim Y-K, Gho YS (2015) Proteomics of extracellular vesicles: Exosomes and ectosomes. Mass Spectrom Rev 34:474–490. https://doi.org/10.1002/mas.21420

11. Cooper TT, Dieters-Castator DZ, Liu J, et al (2024) Targeted proteomics of plasma extracellular vesicles uncovers MUC1 as combinatorial biomarker for the early detection of high-grade serous ovarian cancer. J Ovarian Res 17:149. https://doi.org/10.1186/S13048-024-01471-8

12. Lytvyn Y, Xiao F, Kennedy CRJ, et al (2017) Assessment of urinary microparticles in normotensive patients with type 1 diabetes. Diabetologia 60:581–584. https://doi.org/10.1007/s00125-016-4190-2

13. Semenchuk J, Sullivan K, Moineddin R, et al (2022) Urinary interleukin-9 in youth with type 1 diabetes mellitus. Acta Diabetol. https://doi.org/10.1007/s00592-022-01873-4

14. Li G, Li Y, Liu S, et al (2013) Gremlin aggravates hyperglycemia-induced podocyte injury by a TGFβ/smad dependent signaling pathway. J Cell Biochem 114:2101–2113. https://doi.org/10.1002/jcb.24559

15. Carlson EC, Chhoun JM, Laturnus DI, et al (2013) Podocyte-specific overexpression of metallothionein mitigates diabetic complications in the glomerular filtration barrier and glomerular histoarchitecture: A transmission electron microscopy stereometric analysis. Diabetes Metab Res Rev 29:113–124. https://doi.org/10.1002/dmrr.2342

16. Reiser J, Altintas MM (2016) Podocytes. F1000Res 5:. https://doi.org/10.12688/f1000research.7255.1

17. Blijdorp CJ, Burger D, Llorente A, Martens-uzunova ES (2022) Extracellular Vesicles as Novel Players in Kidney Disease

18. Erdbrügger U, Le TH (2016) Extracellular Vesicles in Renal Diseases: More than Novel Biomarkers? Journal of the American Society of Nephrology 27:12–26. https://doi.org/10.1681/asn.2015010074

19. Zhang W, Zhou X, Zhang H, et al (2016) Extracellular vesicles in diagnosis and therapy of kidney diseases. Am J Physiol Renal Physiol 311:F844–F851. https://doi.org/10.1152/ajprenal.00429.2016

20. Harskamp LR, Gansevoort RT, Van Goor H, Meijer E (2016) The epidermal growth factor receptor pathway in chronic kidney diseases. Nature Reviews Nephrology 2016 12:8 12:496–506. https://doi.org/10.1038/nrneph.2016.91

21. Santorelli L, Morello W, Barigazzi E, et al (2021) Urinary Extracellular Vesicle Protein Profiles Discriminate Different Clinical Subgroups of Children with Idiopathic Nephrotic Syndrome. Diagnostics 11:456. https://doi.org/10.3390/diagnostics11030456

22. McCaffrey JC, Webb NJ, Poolman TM, et al (2017) Glucocorticoid therapy regulates podocyte motility by inhibition of Rac1. Sci Rep 7:1–15. https://doi.org/10.1038/s41598-017-06810-y

23. Yamanaka M, Tamura Y, Kuribayashi-Okuma E, et al (2023) Nicorandil protects podocytes via modulation of antioxidative capacity in acute puromycin aminonucleoside-induced nephrosis in rats. Am J Physiol Renal Physiol 324:F168–F178. https://doi.org/10.1152/ajprenal.00144.2022

24. Wang H, Guo M, Wei H, Chen Y (2023) Targeting p53 pathways: mechanisms, structures, and advances in therapy. Signal Transduct Target Ther 8

25. Pavenstädt H, Kriz W, Kretzler M (2003) Cell biology of the glomerular podocyte. Physiol Rev 83:253–307. https://doi.org/10.1152/physrev.00020.2002

26. Prunotto M, Farina A, Lane L, et al (2013) Proteomic analysis of podocyte exosome-enriched fraction from normal human urine. J Proteomics 82:193–229. https://doi.org/10.1016/j.jprot.2013.01.012

27. Gonzales PA, Pisitkun T, Hoffert JD, et al (2009) Large-Scale Proteomics and Phosphoproteomics of Urinary Exosomes. Journal of the American Society of Nephrology 20:363–379. https://doi.org/10.1681/ASN.2008040406

28. Groener M, Wang Y, Cross E, et al (2020) Identification of Podocyte Cargo Proteins by Proteomic Analysis of Clathrin-Coated Vesicles. Kidney360 1:480–490. https://doi.org/10.34067/KID.0000212020

29. Chittiprol S, Chen P, Petrovic-Djergovic D, et al (2011) Marker expression, behaviors, and responses vary in different lines of conditionally immortalized cultured podocytes. Am J Physiol Renal Physiol 301:F660. https://doi.org/10.1152/AJPRENAL.00234.2011

Figure Legends

Figure 1.

A. Cell culture (human podocytes, hPods) conditions and schematic of proteomic workflow. PAN, puromycin aminonucleoside; PRED, prednisolone; GPF-DIA, gas-phase fractionation with data-independent acquisition.
B. Venn diagram showing differentially expressed proteins (DEPs) associated with different experimental conditions from hPods.
C. Protein concentration from cell culture experiments, compared across all four treatment conditions. Protein quantified using the DC protein assay.
D. Principal component analysis for cell culture analysis.
E. Volcano plot comparing DEPs between PAN and control. This revealed an upregulation in 56 DEPs after PAN treatment, while 111 DEPs were downregulated. DEPs: abs|log2 FC| > 0.6 & log10(p-value) > 1.30.
F. Volcano plot comparing DEPs between PAN, and PRED+PAN. This revealed 300 upregulated DEPs following PAN treatment, relative to PRED+PAN, and 282 downregulated DEPs. DEPs: abs|log2 FC| > 0.6 & log10(p-value) > 1.30.
G. Cross analysis of different experimental conditions, including the Log2 Fold Change of DEPs between PAN treatment, and PRED+PAN treatment on the Y axis, compared to PAN versus control, on the X axis.
H. Heat map analysis, highlighting there are more proteins per Reactome term for a given condition. This is observational in nature and should not be compared across columns.

Figure 2.

A. Relative large extracellular vesicle (LEV) production across all experimental conditions. Puromycin aminonucleoside (PAN) treatment led to a significant increase in LEV production (P=0.0045). Prednisolone (PRED) pretreatment (PRED+PAN) attenuated this increase in LEV production (P=0.0007).
B. There were no significant differences in the size of LEVs produced under each experimental condition.
C. Venn diagram showing DEPs from LEVs from each experimental condition.
D. Principal component analysis for LEV DEPs across each experimental condition.
E. Bar chart showing comparisons of specific EV proteins across each experimental condition. No significant differences were observed across each experimental condition for EV-related albumin, tissue factor, CD9 and, Programmed Cell Death 6 Interacting Protein (PDCD6IP; also known as ALIX). This suggests a uniform isolation of EVs across each experimental condition.

Figure 3

A. Volcano plot comparing differentially expressed proteins (DEPs) from large extracellular vesicles (LEVs) between puromycin aminonucleoside (PAN) and control. There were 54 upregulated DEPs in LEVs from human podocytes (hPods) following treatment with PAN, compared to 138 downregulated, relative to control. DEPs: abs|log2 FC| > 0.6 & log10(p-value) > 1.30.

B. Volcano plot comparing DEPs from LEVs from hPods following treatment with PAN, compared to PRED+PAN. This identified 80 upregulated DEPs in LEVs from hPods following PAN treatment compared to 375 downregulated, relative to PRED+PAN. DEPs: abs|log2 FC| > 0.6 & log10(p-value) > 1.30.

C. Cross analysis of DEPs from LEVs from hPods across multiple experimental conditions, including on the Y-axis PAN versus PRED+PAN, and on the X-axis, PAN versus control. This highlights DEPs from LEVs which are specific to PAN versus control, or PAN versus PRED+PAN, versus those that are common across those experimental conditions.

D. Heat map analysis using information from Figure 3C. Heat maps are highlighting there are more proteins per Reactome term for a given condition. This is observational in nature and should not be compared across columns.

E. Cross analysis of DEPs from hPods following PAN injury with DEPs from hPod-LEVs following PAN injury. We observed 4 overlapping proteins between the cells and their LEVs following PAN injury, Complement C5, C7, GDNF Family Receptor Alpha 1 (GFRA1), and Growth Differentiation Factor 15 (GDF15).

Figure 4.

A. Venn diagram showing overlapping and distinct differentially expressed proteins (DEPs) across human nephrotic syndrome (NS) states. Disease, referring to active NS and proteinuria, versus remission, where there is no longer active disease. These are DEPs specific to urinary large extracellular vesicles (LEVs) taken from clinical specimens. We identified 240 DEPs specific to remission, 645 specific to disease, and 2688 overlapping DEPs. Jensen compartment analysis reveals that the LEV DEPs identified are largely specific to extracellular organelle, vesicle, and exosome.

B. Principal component analysis comparing LEVs from urinary specimens between disease and remission conditions.

C. Bar chart showing comparisons of specific EV proteins across disease and remission conditions. There was enrichment in albumin and tissue factor in disease EVs compared to remission. This likely reflects disease status. There were no differences between disease and remission in relation to common EV markers, including CD9, CD81, Programmed Cell Death 6 Interacting Protein (PDCD6IP; also known as ALIX), and Tumour Susceptibility Gene 101 (TSG101). This suggests a uniform isolation of EVs across each disease condition.

Figure 5.

A. Volcano plot comparing large extracellular vesicle (LEV) differentially expressed proteins (DEPs) from urinary specimens from children with nephrotic syndrome (NS) between disease and remission states. We identified 512 upregulated DEPs in disease LEVs compared with 350 downregulated DEPs, relative to remission. DEPs: abs|log2 FC| > 0.6 & log10(p-value) > 1.30.

B. Gene set enrichment analysis revealed upregulated DEPs including Solute Carrier (SLC) transporters, intraflagellar transport, and transport of small molecules.

C. Bar chart showing multiple upregulated DEPs from the SLC transporter family.

Figure 6.

A. Three-way Venn diagram highlighting differentially expressed proteins (DEPs) across experimental nephrotic syndrome (NS) conditions (puromycin aminonucleoside (PAN) treatment versus control; PRED pre-treatment, followed by PAN treatment (PRED+PAN), and clinical NS (disease versus remission large extracellular vesicles (LEVs)). By comparing across experimental NS and clinical NS, we identified 44 overlapping DEPs. Jensen Compartment analysis showing that comparisons across experimental NS and clinical NS again highlighted extracellular organelle, vesicle, and exosome, revealing similarities in the LEVs which supports consistent isolation of similar EV species.
B. Common LEV DEPs between experimental and clinical NS. This heatmap highlights the 44 commonly identified DEPs described in Figure 6A. Fold change is reflected using green for increases, and purple for decreases. Comparisons across columns allow for highlighting of concordant and discordant increases or decreases in proteins across experimental and clinical NS conditions.

Figure 7.

A. Heatmap comparing fold-change in differentially expressed proteins (DEPs) from large extracellular vesicles (LEVs) taken from experimental NS (Puromycin aminonucleoside (PAN) versus control) and compared to clinical samples (disease versus remission). Fold change is highlighted in green for increases, and purple for decreases. This bar chart allows for direct comparison of fold change increases or decreases in proteins of interest between experimental NS (PAN versus control) and clinical NS (disease versus remission).

Supplemental Figure Legends

Supplemental Figure 1

A. Volcano plot of differentially expressed proteins (DEPs) from human podocytes (hPods) following treatment with prednisolone (PRED) versus control. PRED alone caused a significant proteomic shift not explained by protein concentration. Specifically, PRED treatment led to upregulation of 226 DEPs, and 126 downregulated DEPs, relative to control hPods.
B. Volcano plot, as above, comparing puromycin aminonucleoside (PAN) treatment of hPods compared to PRED. These represent hPod DEPs between the two experimental conditions. This revealed an upregulation of 159 DEPs, and a downregulation of 283 DEPs when comparing PAN treatment to PRED alone.
C. Volcano plot, similar to above; however, experimental conditions include PRED+PAN versus PRED. This revealed that 12 DEPs were upregulated, and 26 were downregulated when comparing PRED+PAN with PRED alone. This suggests that many of the above changes are related to the PRED exposure.

Supplemental Figure 2

A. Gene set enrichment analysis (GSEA) from cellular proteome analysis, comparing puromycin aminonucleoside (PAN) treatment with control. GSEA analysis revealed that PAN treatment, relative to control, led to an increase in proteins associated with DNA repair.

B. Similar to A, GSEA data from PAN-treated versus control hPods revealing that PAN led to an increase in proteins associated with microparticles (previous nomenclature for large extracellular vesicles, LEVs).
C. GSEA analysis revealing many different Gene Ontology (GO) components which are enriched in hPods following treatment with PAN, relative to control.
D. GSEA for hPods under experimental conditions PAN versus PRED+PAN. Revealing enrichment in apoptosis-related proteins under PRED+PAN conditions, relative to PAN.
E. Similar to D, GSEA for hPods under PAN versus PRED+PAN, revealing an enrichment in splicesomal complex proteins under PRED+PAN conditions, versus PAN.
F. GSEA for hPods, comparing PAN versus PRED+PAN. GO showed robust enrichment for PRED+PAN versus PAN alone.

Supplemental Figure 3

A. Volcano plots for hPod large extracellular vesicle (LEV) differentially expressed proteins (DEPs) comparing prednisolone (PRED) versus control. This revealed 233 upregulated DEPs, and 123 downregulated DEPs following treatment with PRED when compared to control.
B. Volcano plots for hPod large extracellular vesicle (LEV) differentially expressed proteins (DEPs) comparing PAN versus PRED. This revealed 122 upregulated DEPs, and 368 downregulated DEPs following treatment with PAN when compared to PRED.
C. Volcano plots for hPod large extracellular vesicle (LEV) differentially expressed proteins (DEPs) comparing PRED+PAN versus PRED. This revealed 97 upregulated DEPs, and 33 downregulated DEPs following treatment with PRED+PAN when compared to PRED.

Supplemental Figure 4

A. Gene set enrichment analysis (GSEA; Reactome 2022) for hPod large extracellular vesicles (LEV) comparing PAN versus control experimental conditions.
B. Similar to A; however, using Jensen Compartments.
C. Gene set enrichment analysis (GSEA; Reactome 2022) for hPod large extracellular vesicles (LEV) comparing PRED+PAN versus PAN experimental conditions.
D. Similar to C; however, using Jensen Compartments.

Supplemental Figure 5

A. Heat map (Reactome, Gene Ontology (GO)) comparing urinary large extracellular vesicle (LEV) differentially expressed proteins (DEPs) between clinical specimens taken from children with nephrotic syndrome (NS), comparing those with disease versus remission.
B. Similar to A; however, using only GO terminology.

Figure 12. **Figure 1. hPod cellular proteomic workflow and results.**

Figure 1A

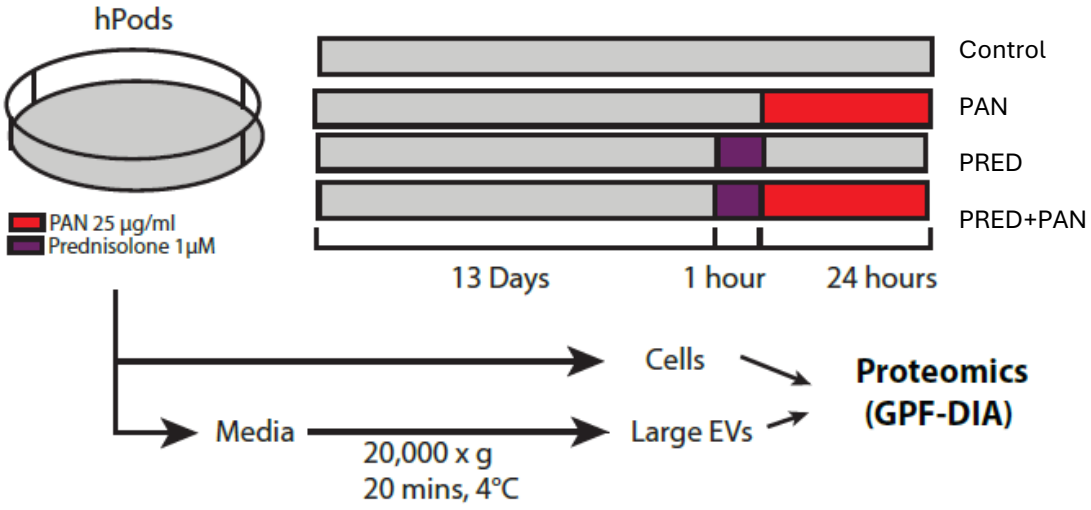

Figure 1B

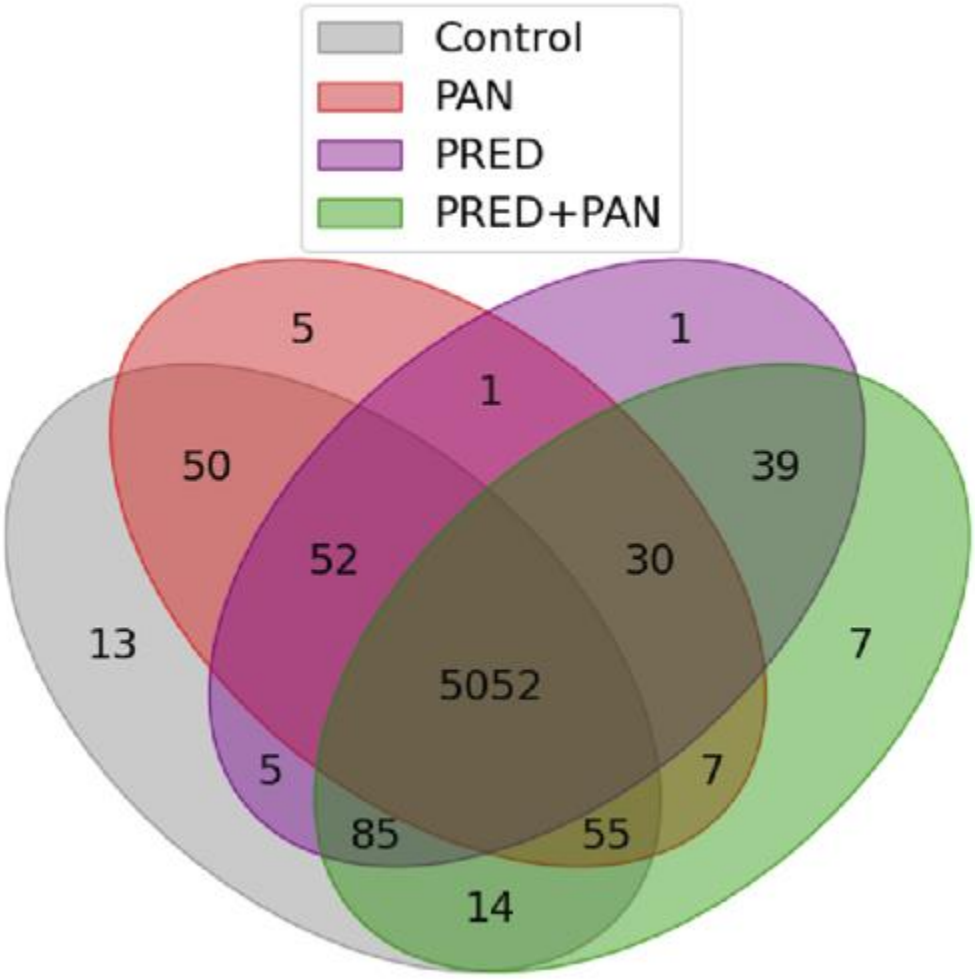

Figure 1C

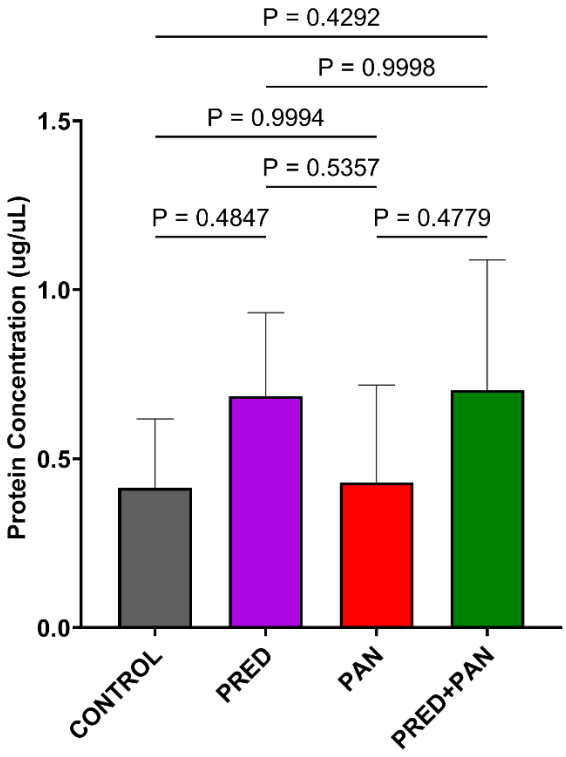
P = 0.4292
P = 0.9998
P = 0.9994
P = 0.5357
P = 0.4847
P = 0.4779
Protein Concentration (ug/uL)
1.5
1.0
0.5
0.0
CONTROL
PRED
PAN
PRED+PAN

Figure 1D

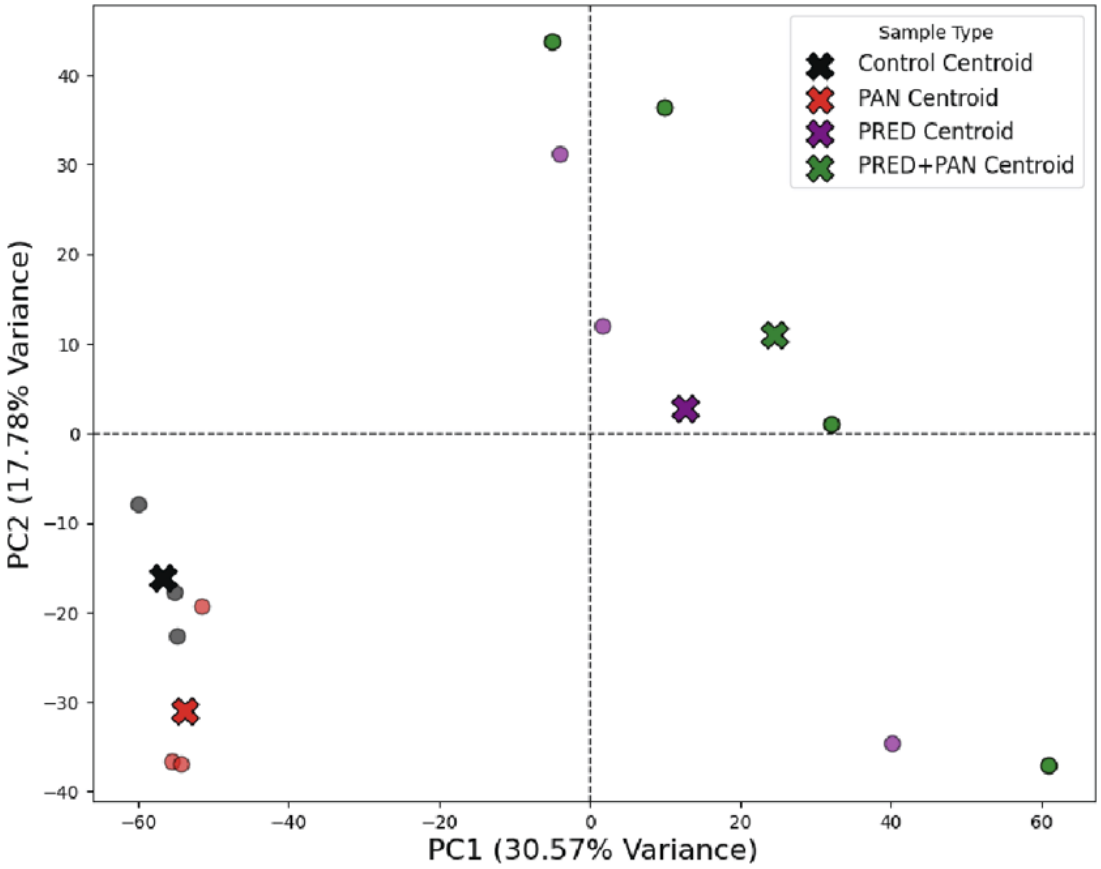
Sample Type
Control Centroid
PAN Centroid
PRED Centroid
PRED+PAN Centroid
PC2 (17.78% Variance)
PC1 (30.57% Variance)
40
30
20
10
0
−10
−20
−30
−40
−60
−40
−20
0
20
40
60

Figure 1E

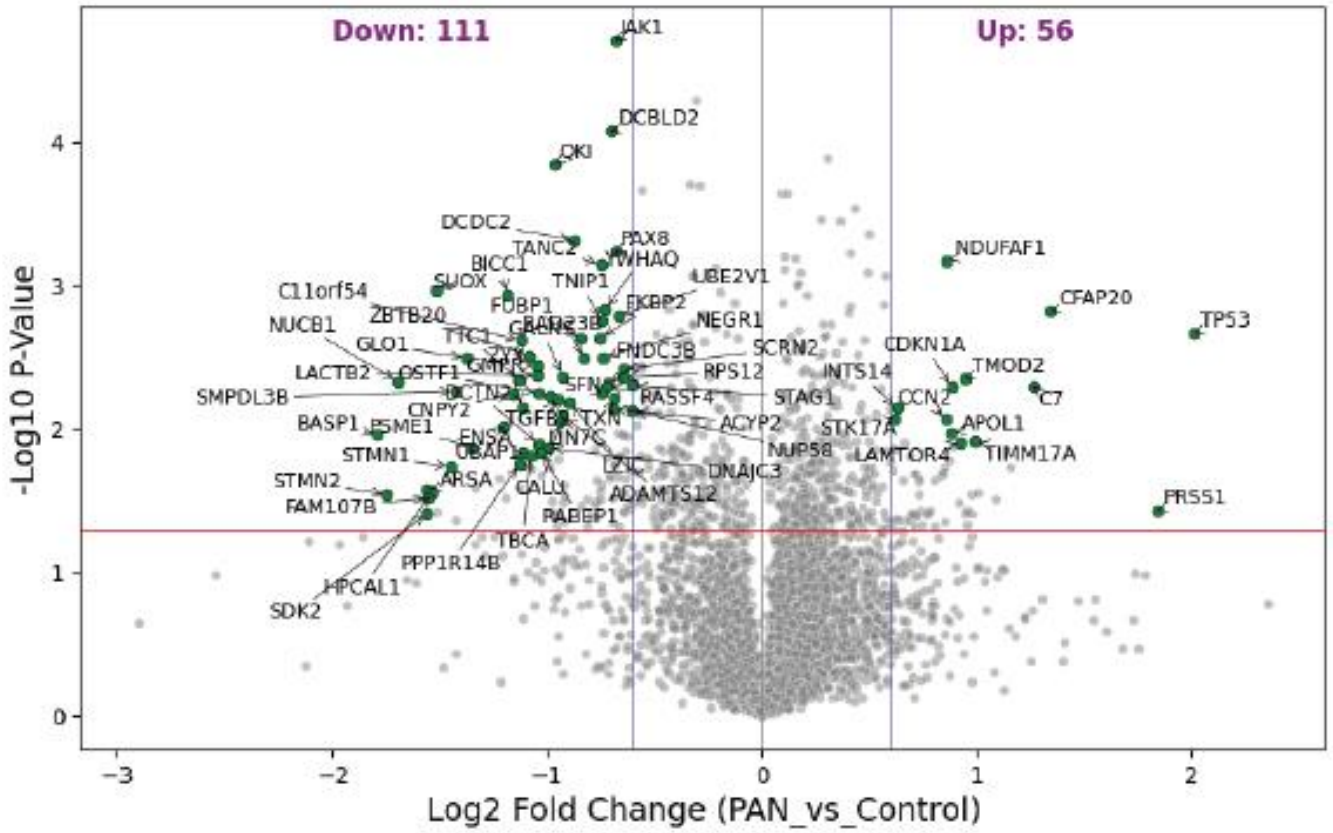
Down: 111
Up: 56
JAK1
DCBLD2
CKI
DCDC2
TANC2
PAX8
WHAQ
BICC1
SUOX
TNIP1
UBE2V1
C11orf54
FUBP1
FKBP2
ZBTB20
NUCB1
NEGR1
GLO1
FNDC3B
SCRN2
LACTB2
OSTF1
RPS12
SMPDL3B
RA5SF4
STAG1
CNPY2
BASP1
PSME1
TGFB2
TXN
ACYP2
ENSA
STMN1
NUP58
LAMTOR4
TIMM17A
DNAJC3
STMN2
ARSA
CALU
ADAMTS12
FAM107B
RABEP1
TBCA
PPP1R14B
HPCAL1
SDK2
NDUFAF1
CFAP20
TP53
CDKN1A
INTS14
TMOD2
C7
CCN2
APOL1
STK17A
PRSS1
-Log10 P-Value
Log2 Fold Change (PAN_vs_Control)

Figure 1F

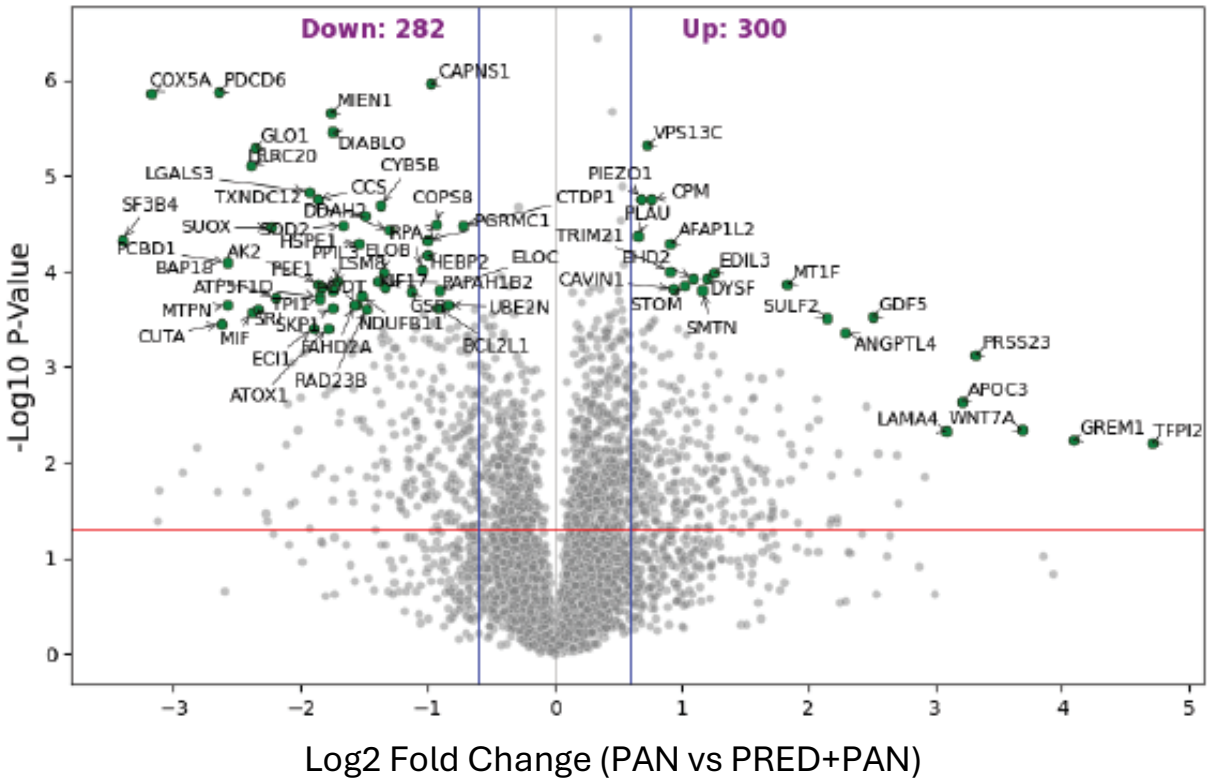
Down: 282
Up: 300
-Log10 P-Value
Log2 Fold Change (PAN vs PRED+PAN)
COX5A
PDCD6
CAPNS1
MIEN1
GLO1
DIABLO
BLRC20
CYB5B
LGALS3
TXNDC12
CCS
COPS8
SF3B4
DDAH2
SUOX
SOD2
RPA3
PSRMC1
PCBD1
HSPE1
AK2
PPIL3
ELOB
BAP18
PEF1
LSM8
HEBP2
ELOC
ATP5F1D
EIF1
PAPAH1B2
MTPN
PPIF
GSR
UBE2N
CUTA
MIF
SKP1
NDUFB11
FAHD2A
BCL2L1
ECI1
RAD23B
ATOX1
VPS13C
PIEZO1
CTDP1
CPM
PLAU
TRIM21
AFAP1L2
EHD2
EDIL3
CAVIN1
DYSF
MT1F
STOM
SMTN
SULF2
GDF5
ANGPTL4
PRSS23
APOC3
LAMA4
WNT7A
GREM1
TFPI2

Figure 1G

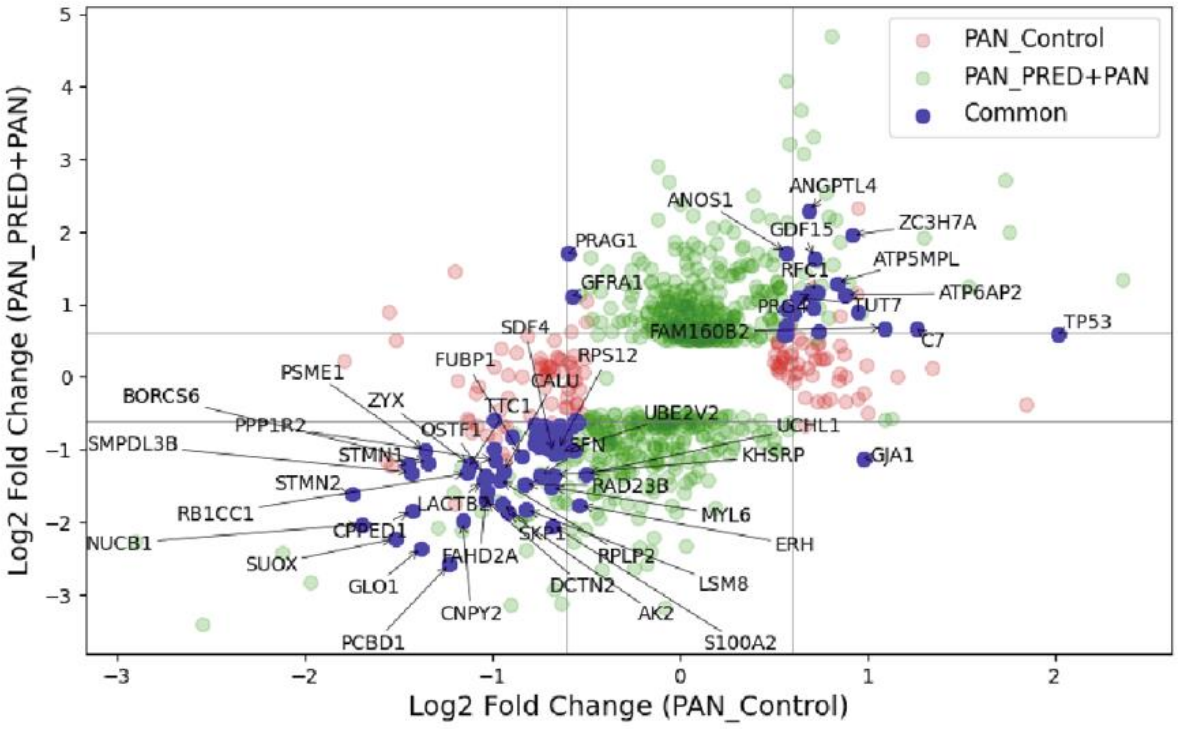
PAN_Control
PAN_PRED+PAN
Common
Log2 Fold Change (PAN_PRED+PAN)
Log2 Fold Change (PAN_Control)
ANGPTL4
ANOS1
GDF15
ZC3H7A
PRAG1
ATP5MPL
RFC1
GFRA1
ATP6AP2
PRG4
TUT7
TP53
SDF4
FAM160B2
C7
FUBP1
RPS12
PSME1
CALU
BORCS6
ZYX
TTC1
UBE2V2
UCHL1
PPP1R2
OSTF1
SMPDL3B
STMN1
SFN
KHSRP
GJA1
STMN2
RAD23B
RB1CC1
LACTB2
MYL6
CPPED1
SKP1
ERH
NUCB1
SUOX
FAHD2A
RPLP2
GLO1
DCTN2
LSM8
CNPY2
AK2
PCBD1
S100A2

Figure 1H

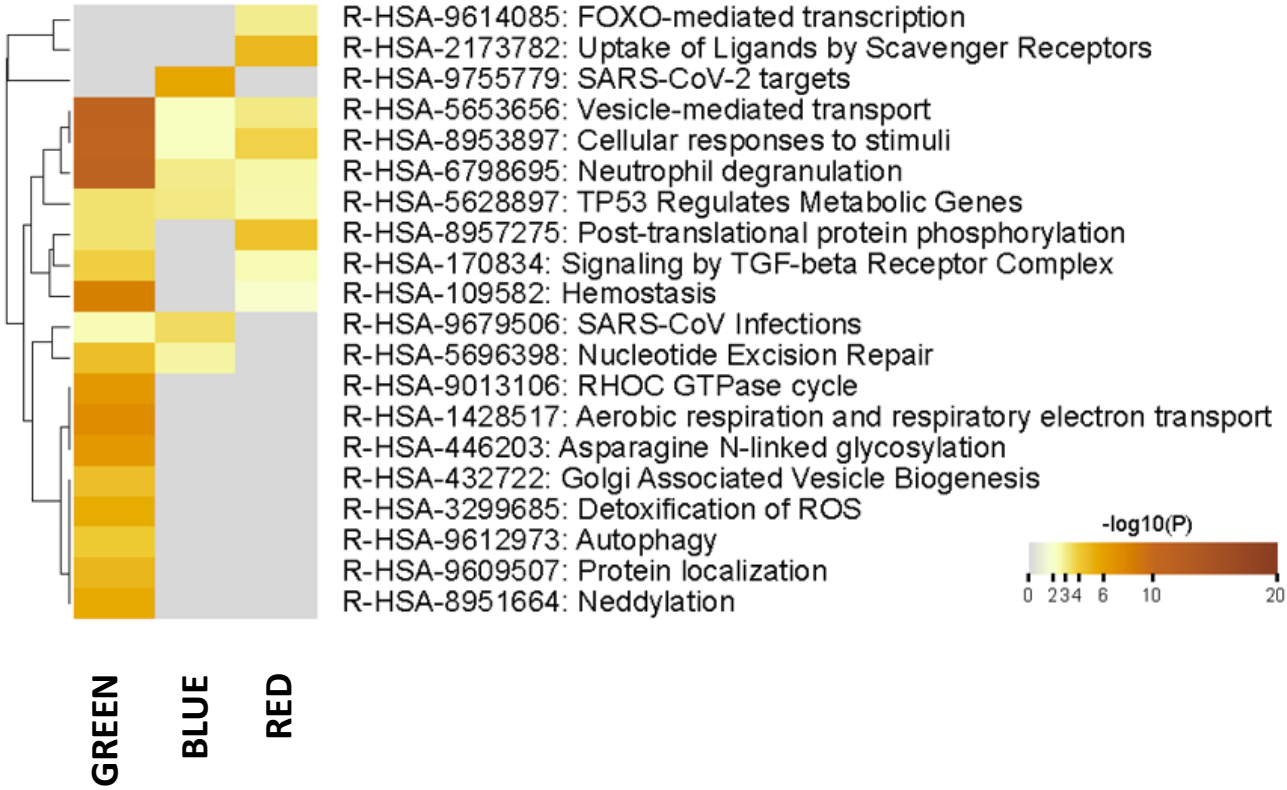
R-HSA-9614085: FOXO-mediated transcription
R-HSA-2173782: Uptake of Ligands by Scavenger Receptors
R-HSA-9755779: SARS-CoV-2 targets
R-HSA-5653656: Vesicle-mediated transport
R-HSA-8953897: Cellular responses to stimuli
R-HSA-6798695: Neutrophil degranulation
R-HSA-5628897: TP53 Regulates Metabolic Genes
R-HSA-8957275: Post-translational protein phosphorylation
R-HSA-170834: Signaling by TGF-beta Receptor Complex
R-HSA-109582: Hemostasis
R-HSA-9679506: SARS-CoV Infections
R-HSA-5696398: Nucleotide Excision Repair
R-HSA-9013106: RHOC GTPase cycle
R-HSA-1428517: Aerobic respiration and respiratory electron transport
R-HSA-446203: Asparagine N-linked glycosylation
R-HSA-432722: Golgi Associated Vesicle Biogenesis
R-HSA-3299685: Detoxification of ROS
R-HSA-9612973: Autophagy
R-HSA-9609507: Protein localization
R-HSA-8951664: Neddylation
-log10(P)
0 234 6 10 20
GREEN
BLUE
RED

Figure 13. **Figure 2. hPod LEV proteomic workflow and results.**

Figure 2A

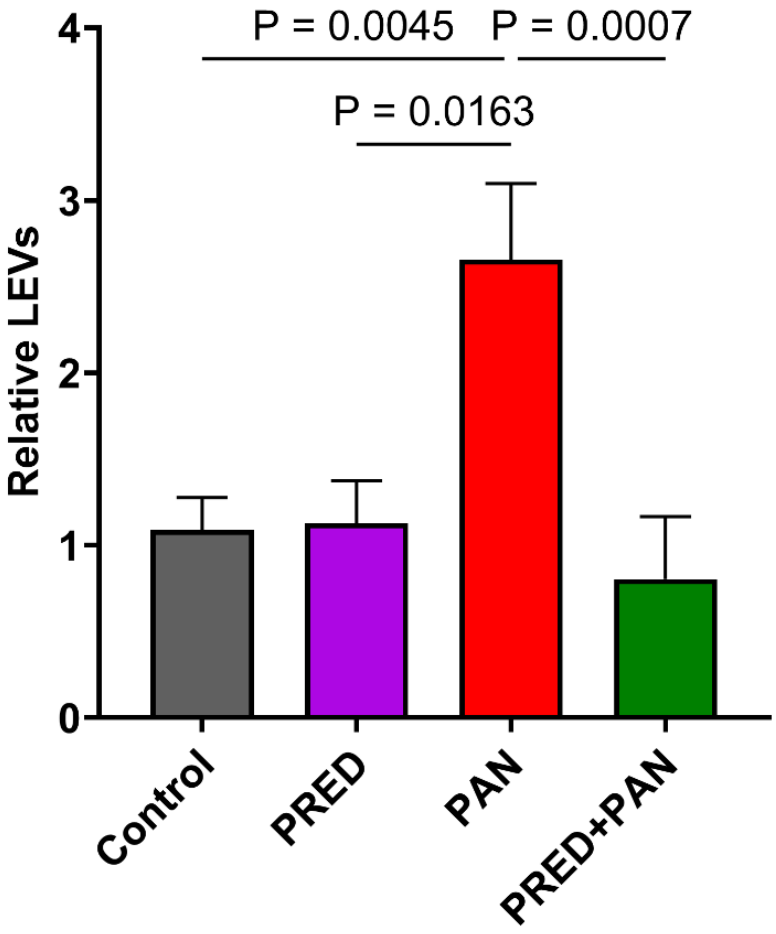

Figure 2B

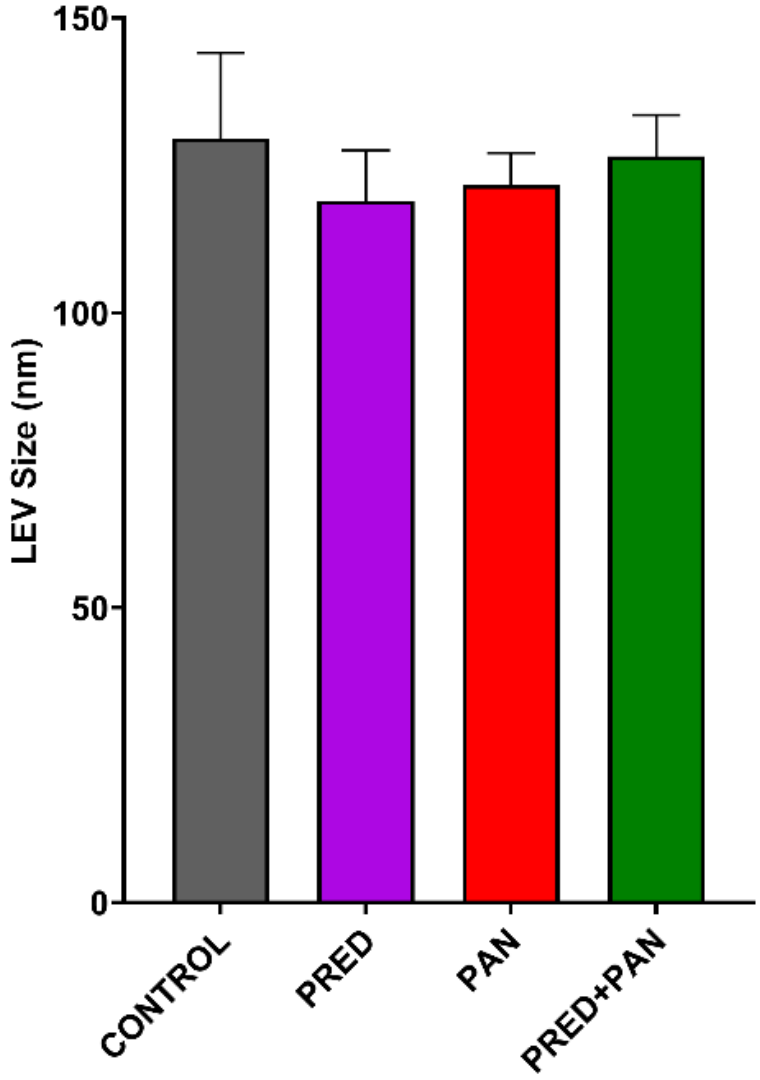

Figure 2C

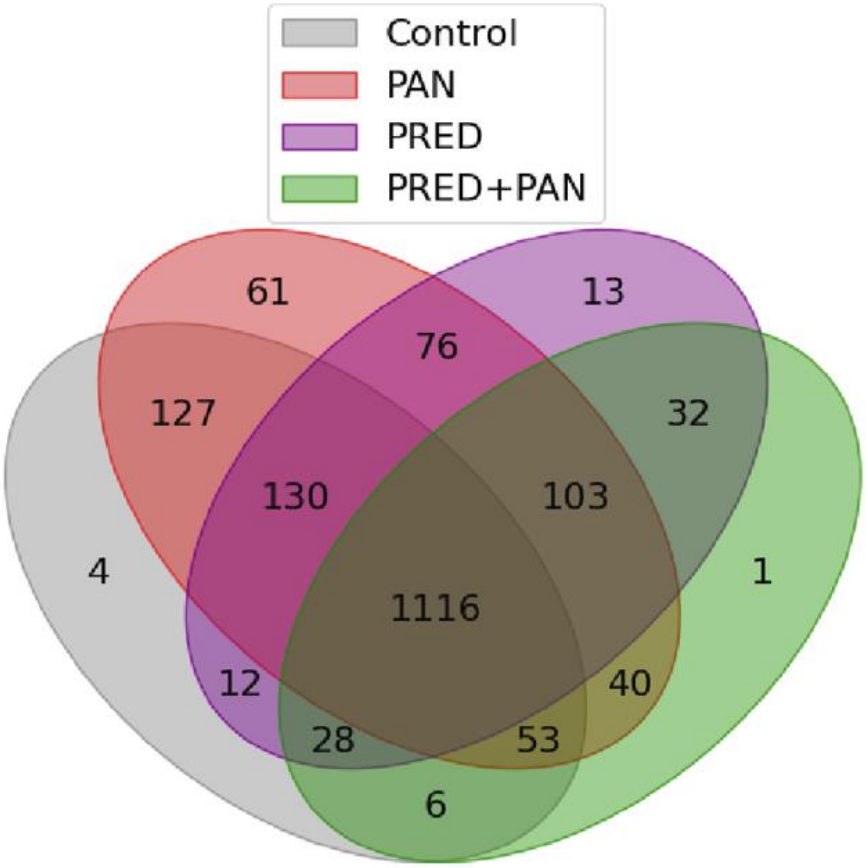
Control
PAN
PRED
PRED+PAN
61
13
76
127
32
130
103
4
1
1116
12
40
28
53
6

Figure 2D

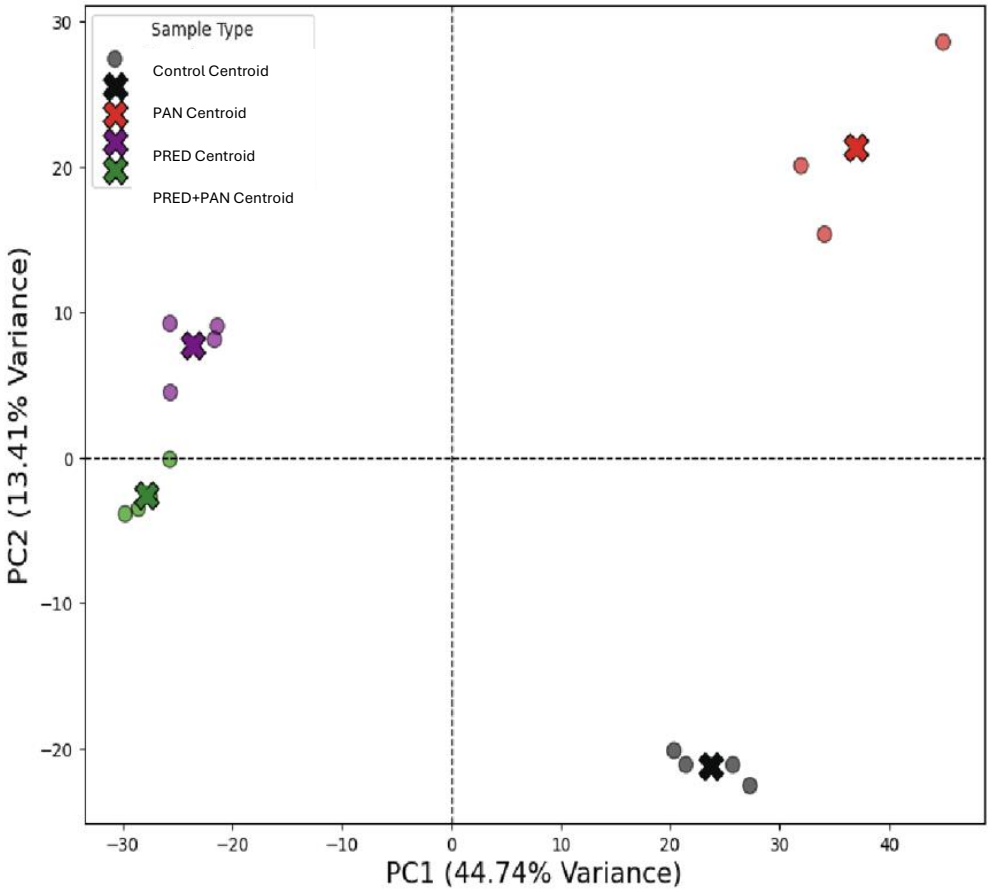
Sample Type
Control Centroid
PAN Centroid
PRED Centroid
PRED+PAN Centroid
PC2 (13.41% Variance)
PC1 (44.74% Variance)
30
20
10
0
−10
−20
−30
−20
−10
0
10
20
30
40

Figure 2E

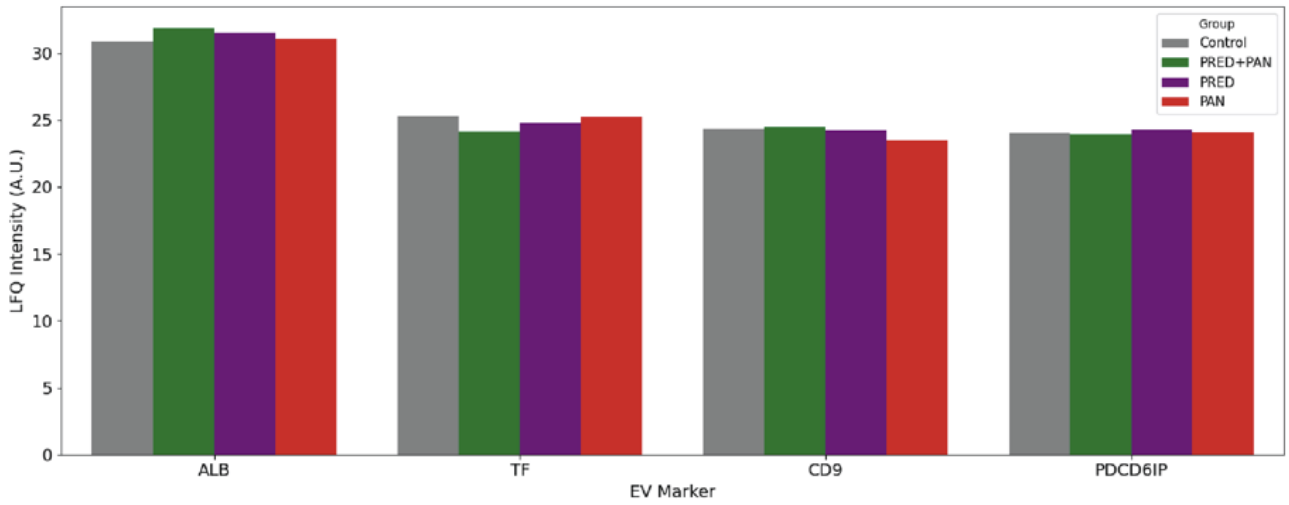
Group
Control
PRED+PAN
PRED
PAN
LFQ Intensity (A.U.)
0
5
10
15
20
25
30
ALB
TF
CD9
PDCD6IP
EV Marker

Figure 14. **Figure 3. Volcano plots and heatmaps for hPod LEV proteomic analysis.**

Figure 3A

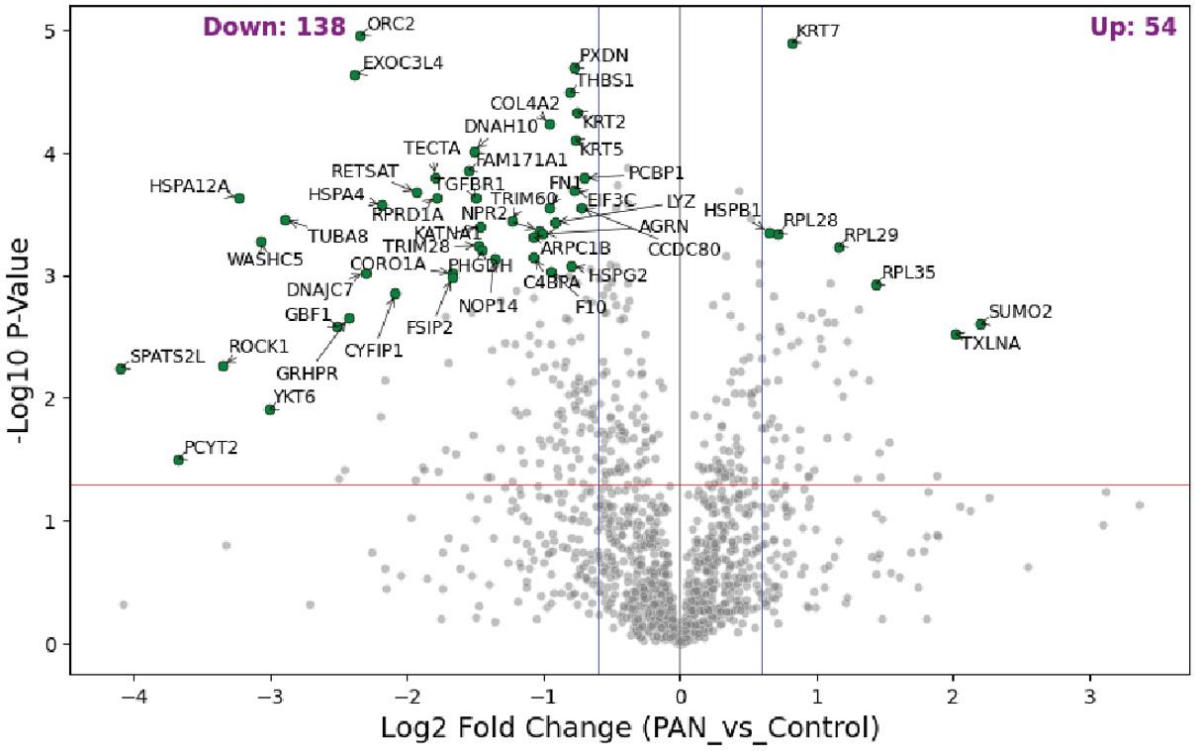

Figure 3B

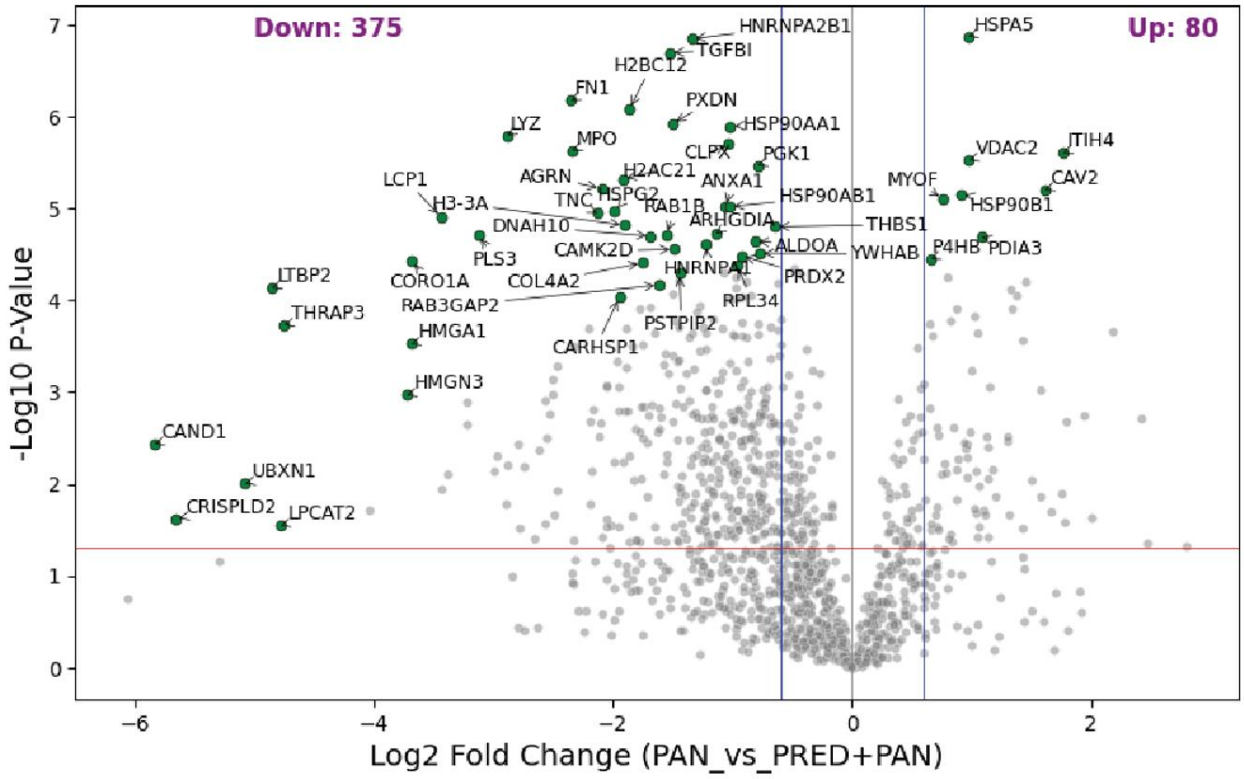
Down: 375
Up: 80
-Log10 P-Value
Log2 Fold Change (PAN_vs_PRED+PAN)
HNRNPA2B1
TGFBI
H2BC12
FN1
PXDN
HSP90AA1
LYZ
MPO
CLPX
PGK1
H2AC21
AGRN
ANXA1
LCP1
H3-3A
TNC
HSPG2
RAB1B
HSP90AB1
DNAH10
ARHGDIA
THBS1
CAMK2D
ALDOA
PLS3
HNRNPA1
PRDX2
LTBP2
CORO1A
COL4A2
RPL34
THRAP3
RAB3GAP2
PSTPIP2
HMGA1
CARHSP1
HMGN3
CAND1
UBXN1
CRISPLD2
LPCAT2
HSPA5
VDAC2
ITIH4
MYOF
CAV2
HSP90B1
YWHAB
P4HB
PDIA3

Figure 3C

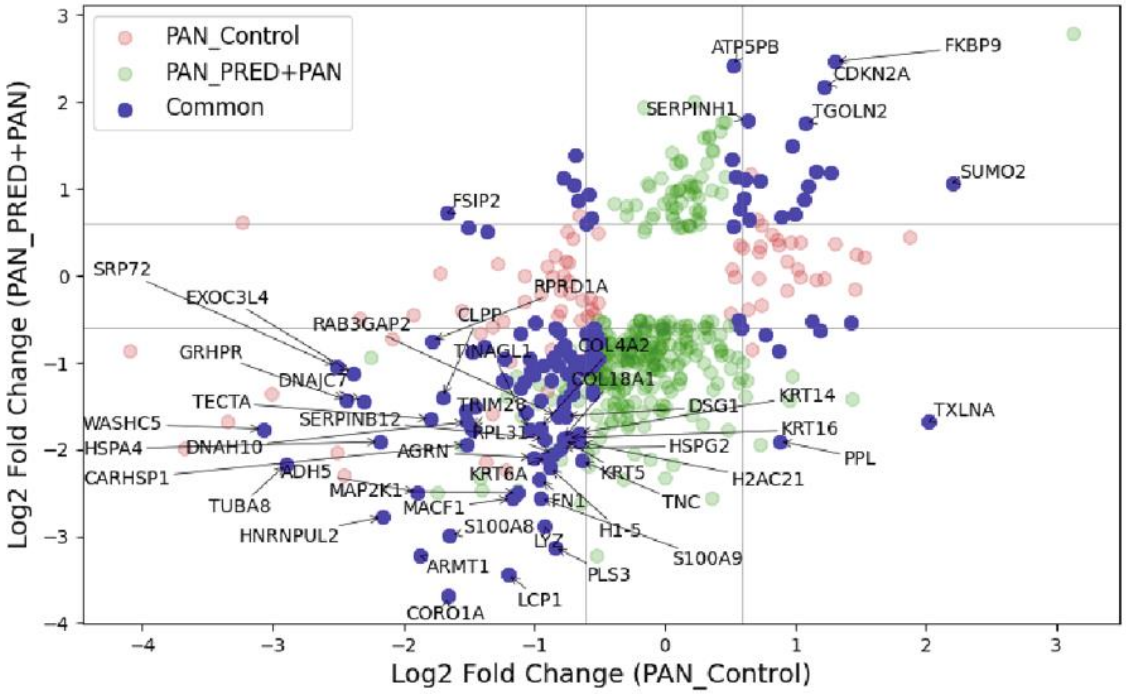
PAN_Control
PAN_PRED+PAN
Common
Log2 Fold Change (PAN_PRED+PAN)
Log2 Fold Change (PAN_Control)
ATP5PB
FKBP9
CDKN2A
SERPINH1
TGOLN2
SUMO2
FSIP2
SRP72
EXOC3L4
RPRD1A
RAB3GAP2
CLPP
GRHPR
TNAGL1
COL4A2
DNAJC7
COL18A1
TECTA
TNIM28
DSG1
KRT14
TXLNA
WASHC5
SERPINB12
RPL31
KRT16
HSPA4
DNAH10
AGRN
HSPG2
PPL
CARHSP1
ADH5
KRT6A
KRT5
H2AC21
MAP2K1
TUBA8
MACF1
FN1
TNC
HNRNPUL2
S100A8
H1-5
LYZ
S100A9
ARMT1
PLS3
LCP1
CORO1A

Figure 3D

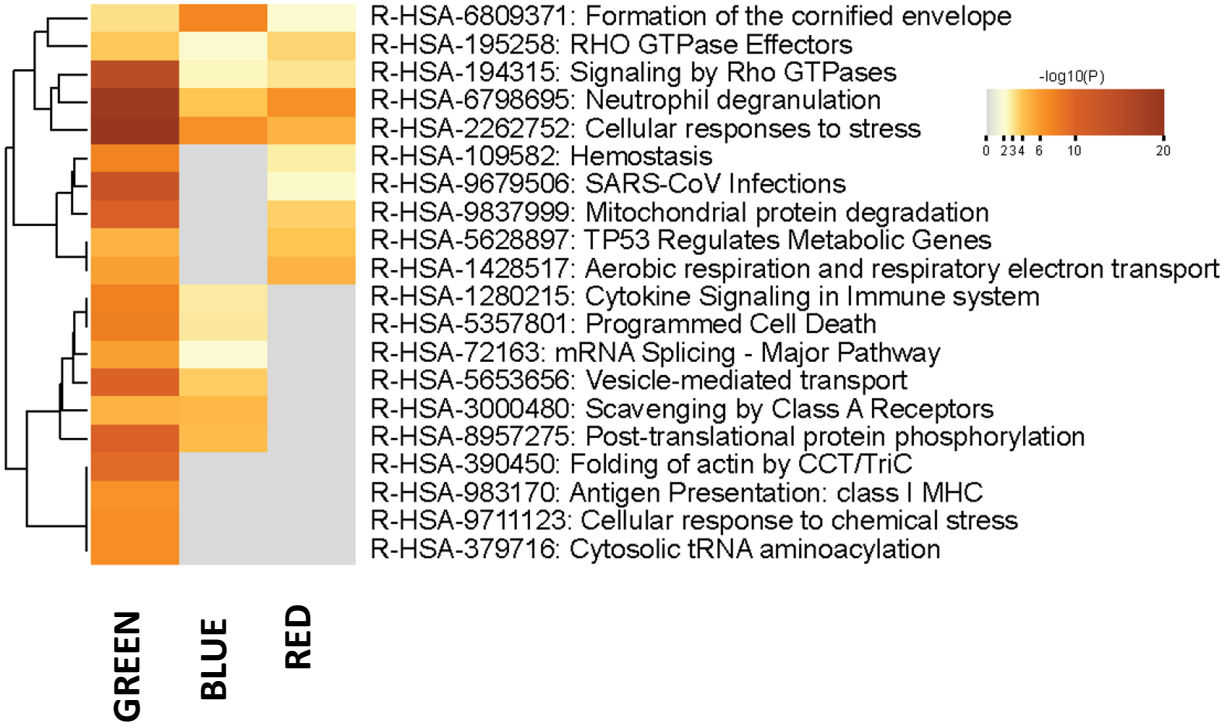
R-HSA-6809371: Formation of the cornified envelope
R-HSA-195258: RHO GTPase Effectors
R-HSA-194315: Signaling by Rho GTPases
R-HSA-6798695: Neutrophil degranulation
R-HSA-2262752: Cellular responses to stress
R-HSA-109582: Hemostasis
R-HSA-9679506: SARS-CoV Infections
R-HSA-9837999: Mitochondrial protein degradation
R-HSA-5628897: TP53 Regulates Metabolic Genes
R-HSA-1428517: Aerobic respiration and respiratory electron transport
R-HSA-1280215: Cytokine Signaling in Immune system
R-HSA-5357801: Programmed Cell Death
R-HSA-72163: mRNA Splicing - Major Pathway
R-HSA-5653656: Vesicle-mediated transport
R-HSA-3000480: Scavenging by Class A Receptors
R-HSA-8957275: Post-translational protein phosphorylation
R-HSA-390450: Folding of actin by CCT/TriC
R-HSA-983170: Antigen Presentation: class I MHC
R-HSA-9711123: Cellular response to chemical stress
R-HSA-379716: Cytosolic tRNA aminoacylation
-log10(P)
0 2 3 4 6 10 20
GREEN
BLUE
RED

Figure 3E

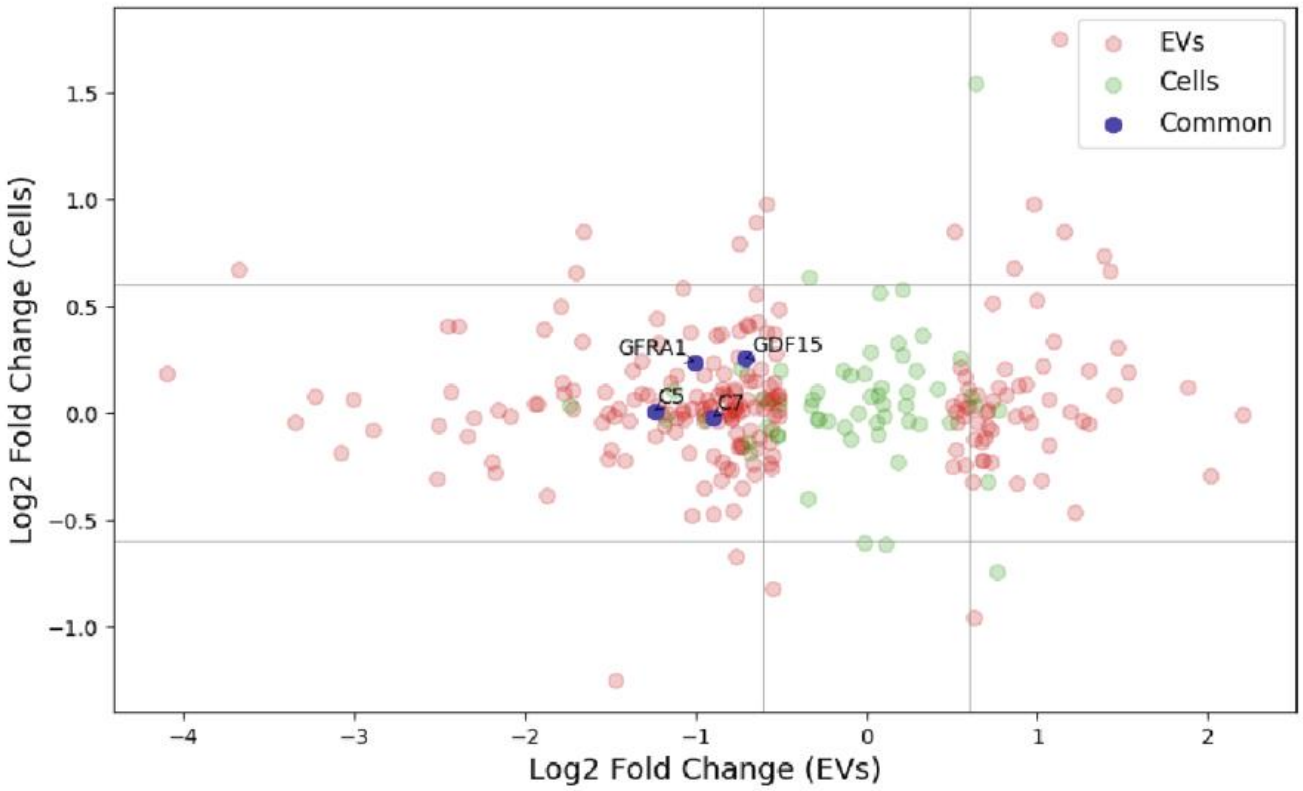
EVs
Cells
Common
GFRA1
GDF15
C5
C7
Log2 Fold Change (Cells)
Log2 Fold Change (EVs)
1.5
1.0
0.5
0.0
−0.5
−1.0
−4
−3
−2
−1
0
1
2

Figure 15. **Figure 4. Human urinary LEV proteomics in children with iNS.**

Figure 4A

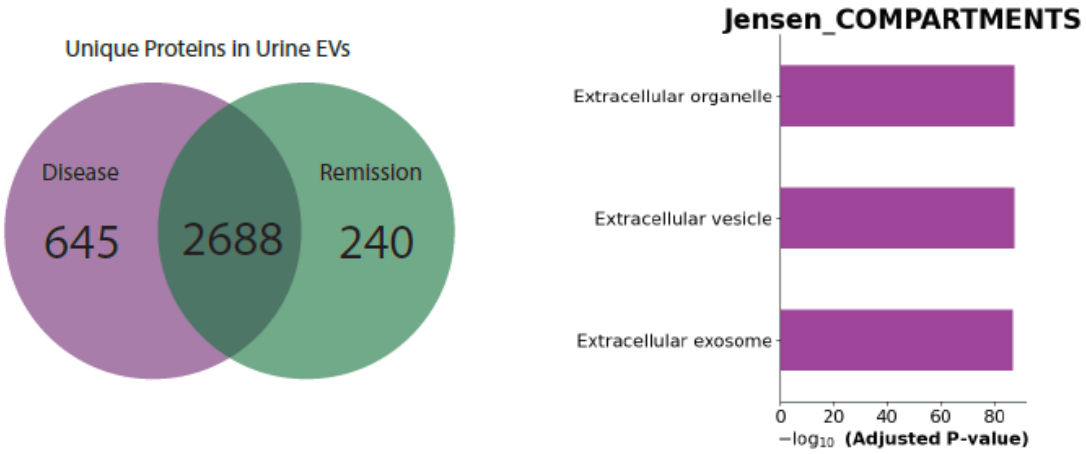

Figure 4B

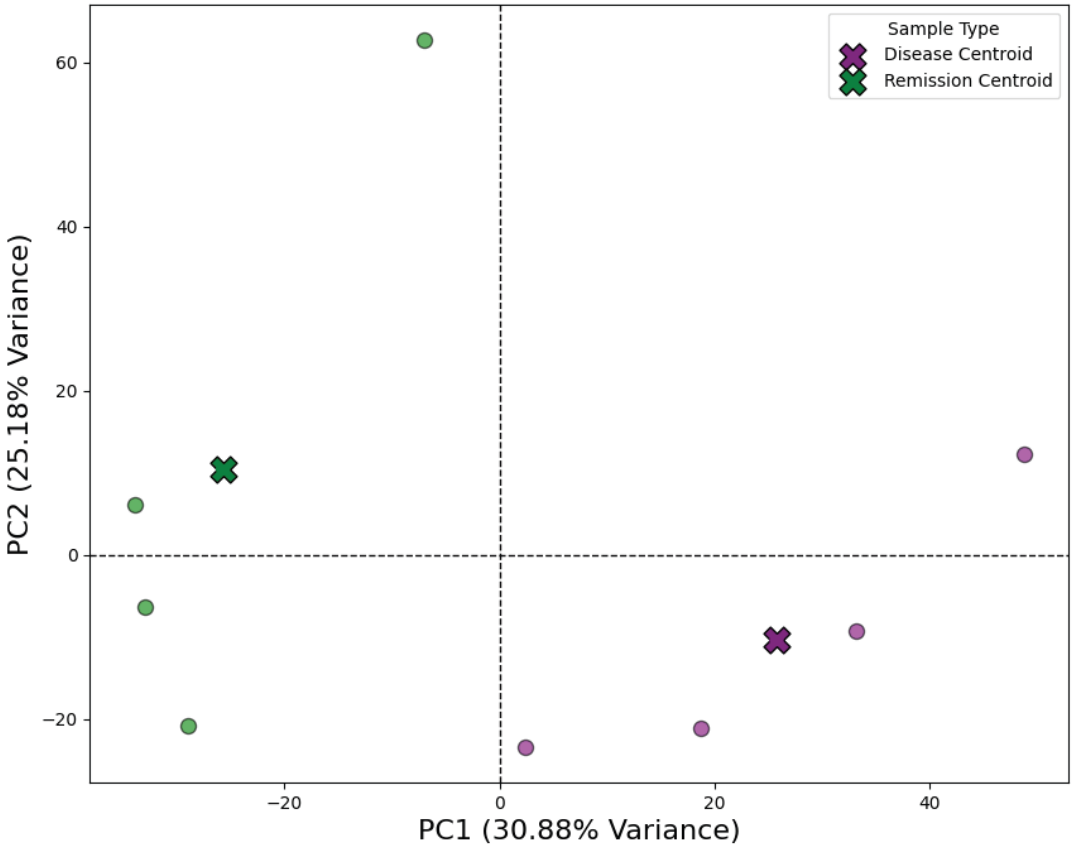
Sample Type
Disease Centroid
Remission Centroid
PC2 (25.18% Variance)
PC1 (30.88% Variance)
60
40
20
0
−20
−20
0
20
40

Figure 4C

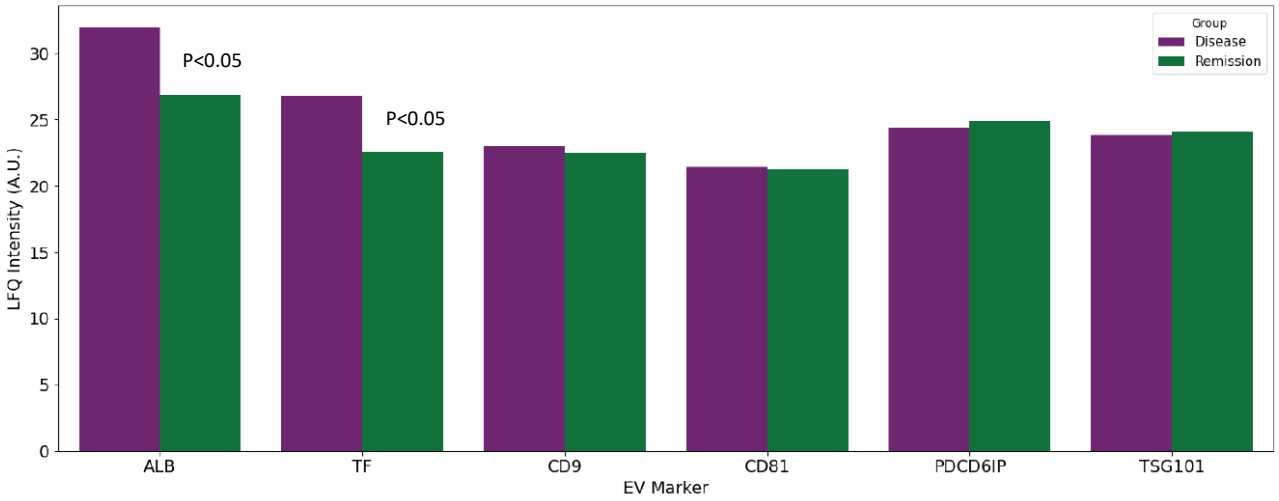
Group
Disease
Remission
P<0.05
P<0.05
LFQ Intensity (A.U.)
0
5
10
15
20
25
30
ALB
TF
CD9
CD81
PDCD6IP
TSG101
EV Marker

Figure 16. **Figure 5. Volcano plots and gene set enrichment analysis for LEVs from the urine of children with iNS.**

Figure 5A

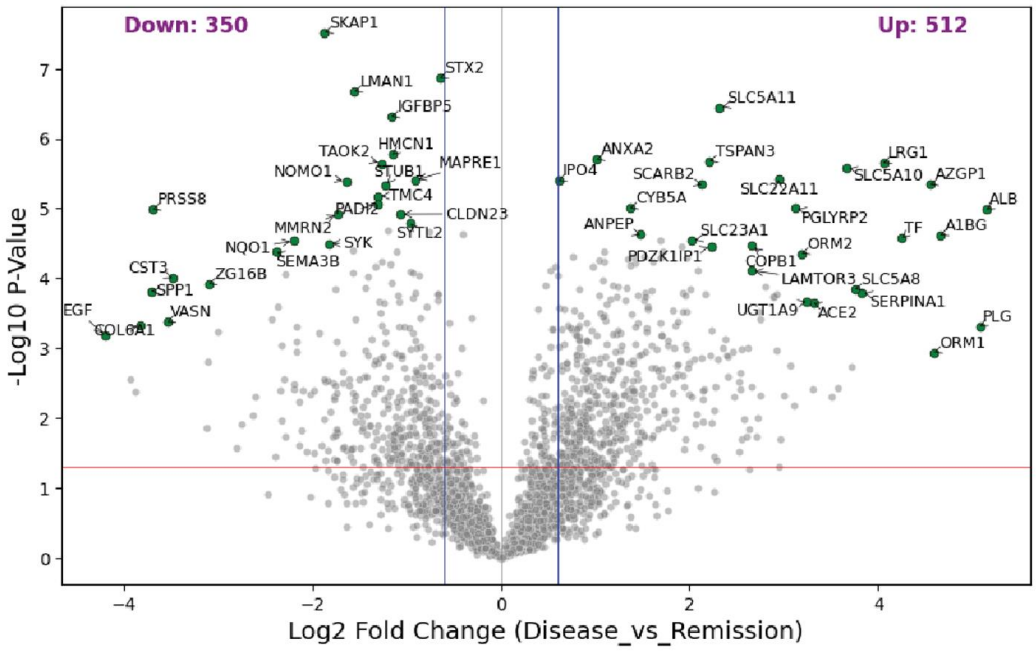

Figure 5B

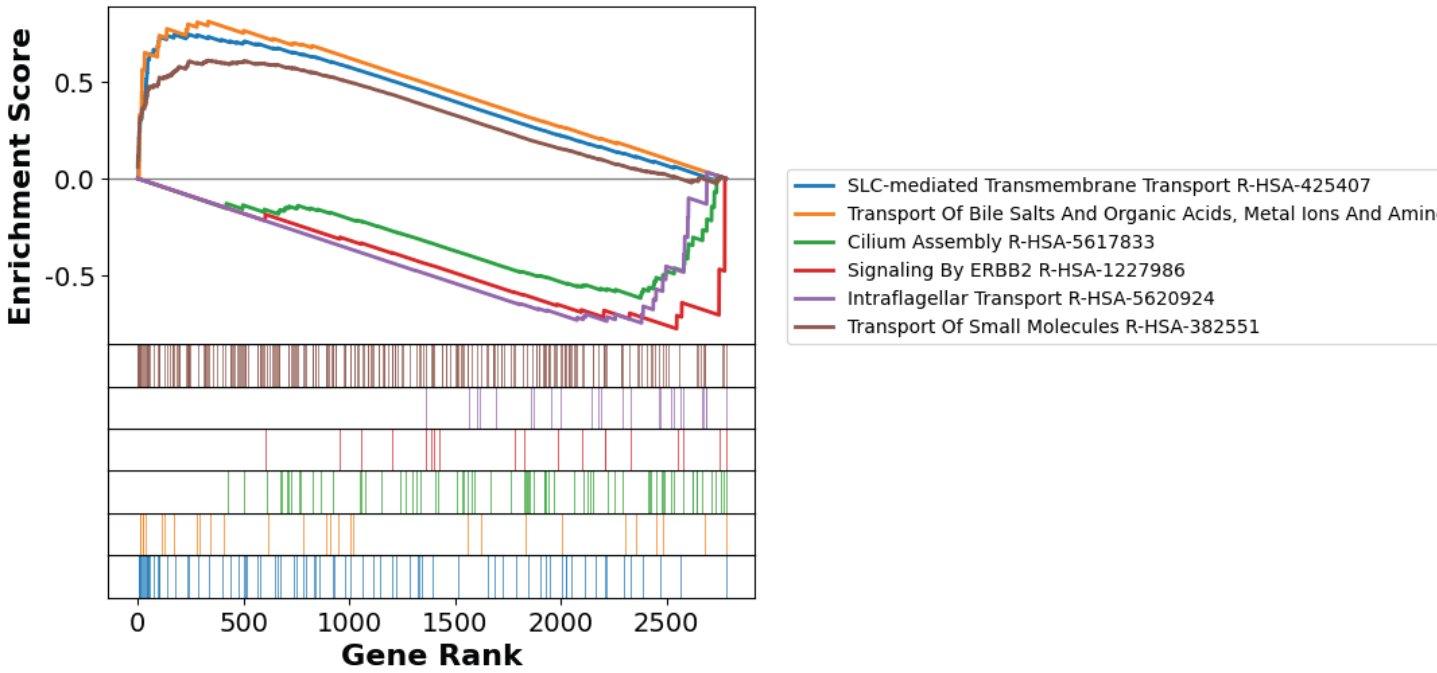
Enrichment Score
0.5
0.0
-0.5
0
500
1000
1500
2000
2500
Gene Rank
SLC-mediated Transmembrane Transport R-HSA-425407
Transport Of Bile Salts And Organic Acids, Metal Ions And Amin
Cilium Assembly R-HSA-5617833
Signaling By ERBB2 R-HSA-1227986
Intraflagellar Transport R-HSA-5620924
Transport Of Small Molecules R-HSA-382551

Figure 5C

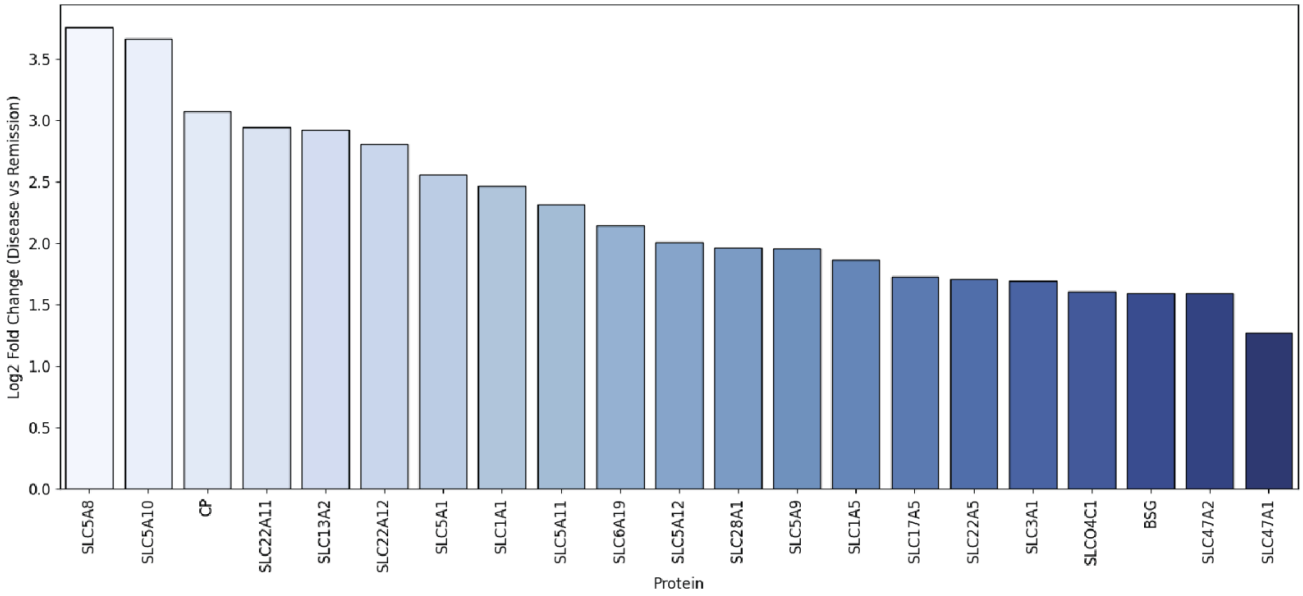
Log2 Fold Change (Disease vs Remission)
3.5
3.0
2.5
2.0
1.5
1.0
0.5
0.0
SLC5A8
SLC5A10
CP
SLC22A11
SLC13A2
SLC22A12
SLC5A1
SLC1A1
SLC5A11
SLC6A19
SLC5A12
SLC28A1
SLC5A9
SLC1A5
SLC17A5
SLC22A5
SLC3A1
SLCO4C1
BSG
SLC47A2
SLC47A1
Protein

Figure 17. **Figure 6. Overlapping LEV DEPs between experimental iNS and clinical specimens.**

Figure 6A

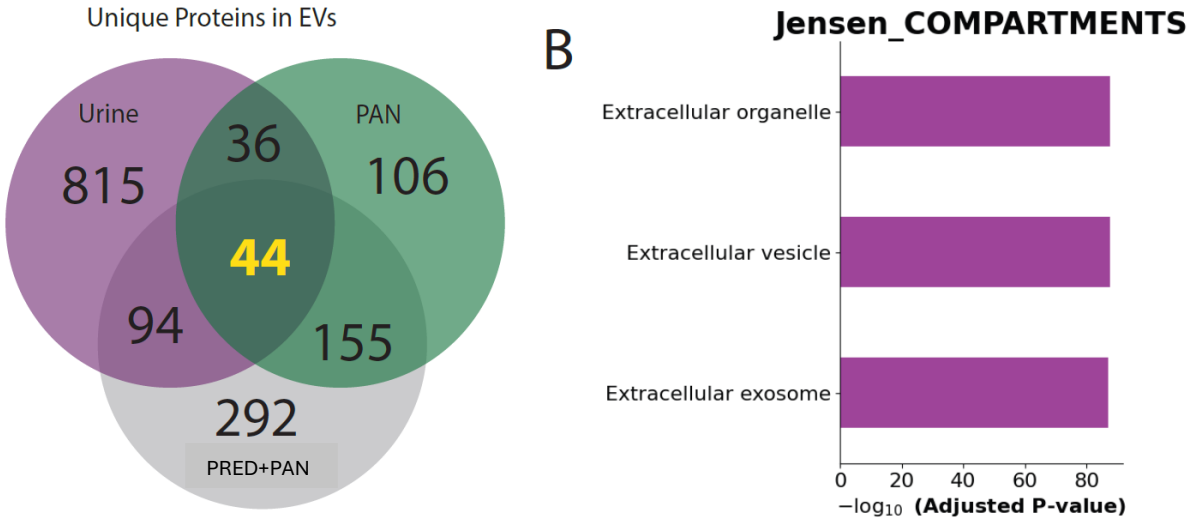

Figure 6B

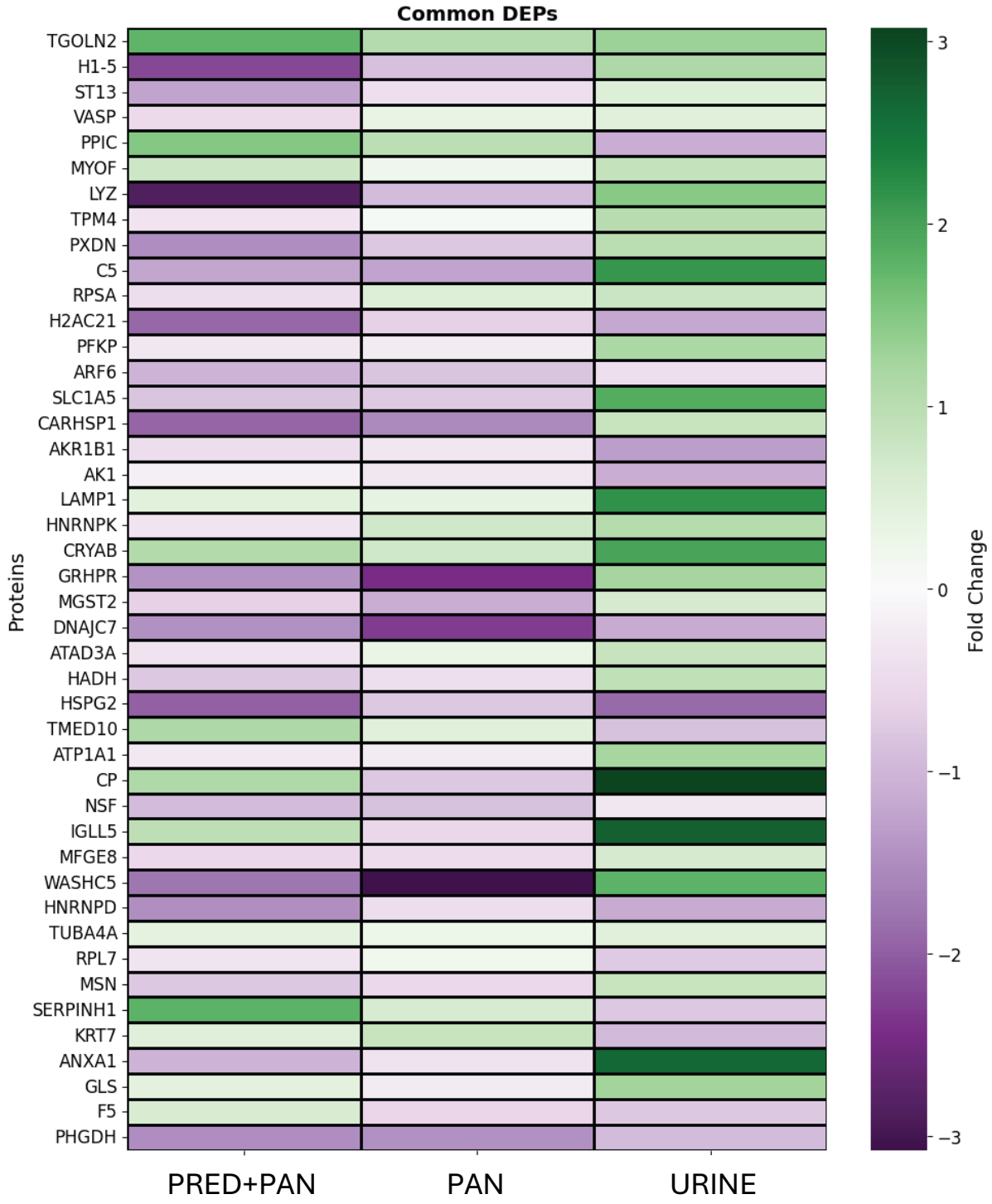
Common DEPs
TGOLN2
H1-5
ST13
VASP
PPIC
MYOF
LYZ
TPM4
PXDN
C5
RPSA
H2AC21
PFKP
ARF6
SLC1A5
CARHSP1
AKR1B1
AK1
LAMP1
HNRNPK
CRYAB
GRHPR
MGST2
DNAJC7
ATAD3A
HADH
HSPG2
TMED10
ATP1A1
CP
NSF
IGLL5
MFGE8
WASHC5
HNRNPD
TUBA4A
RPL7
MSN
SERPINH1
KRT7
ANXA1
GLS
F5
PHGDH
Proteins
PRED+PAN
PAN
URINE
3
2
1
0
−1
−2
−3
Fold Change

Figure 18. Figure 7. Unique and distinct LEV proteomic transformations between experimental iNS and urinary specimens from children with iNS.

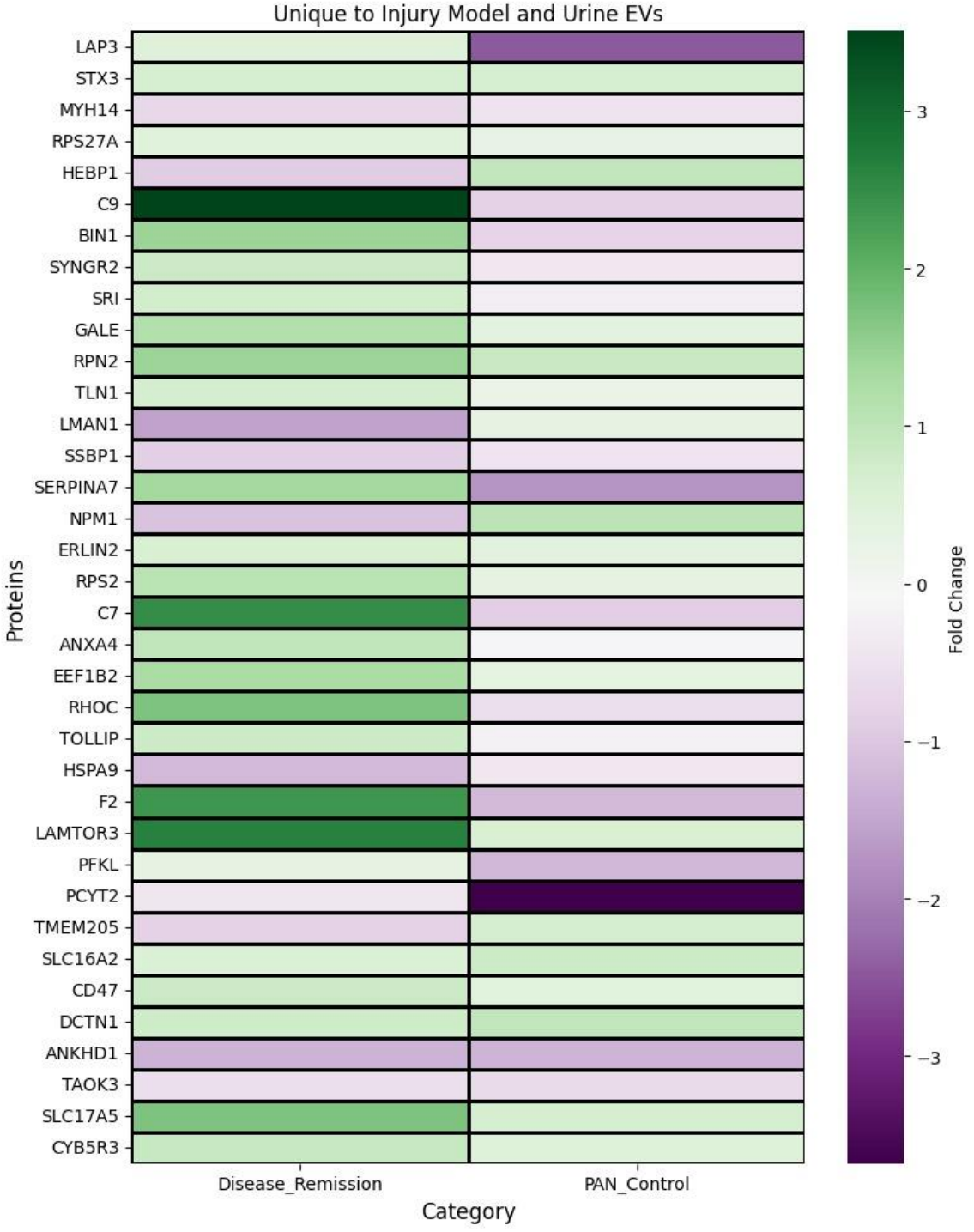

Figure 19. **Supplemental Figure 1. Volcano plots highlighting hPod DEPs under different experimental conditions.**

Supplemental Figure 1A

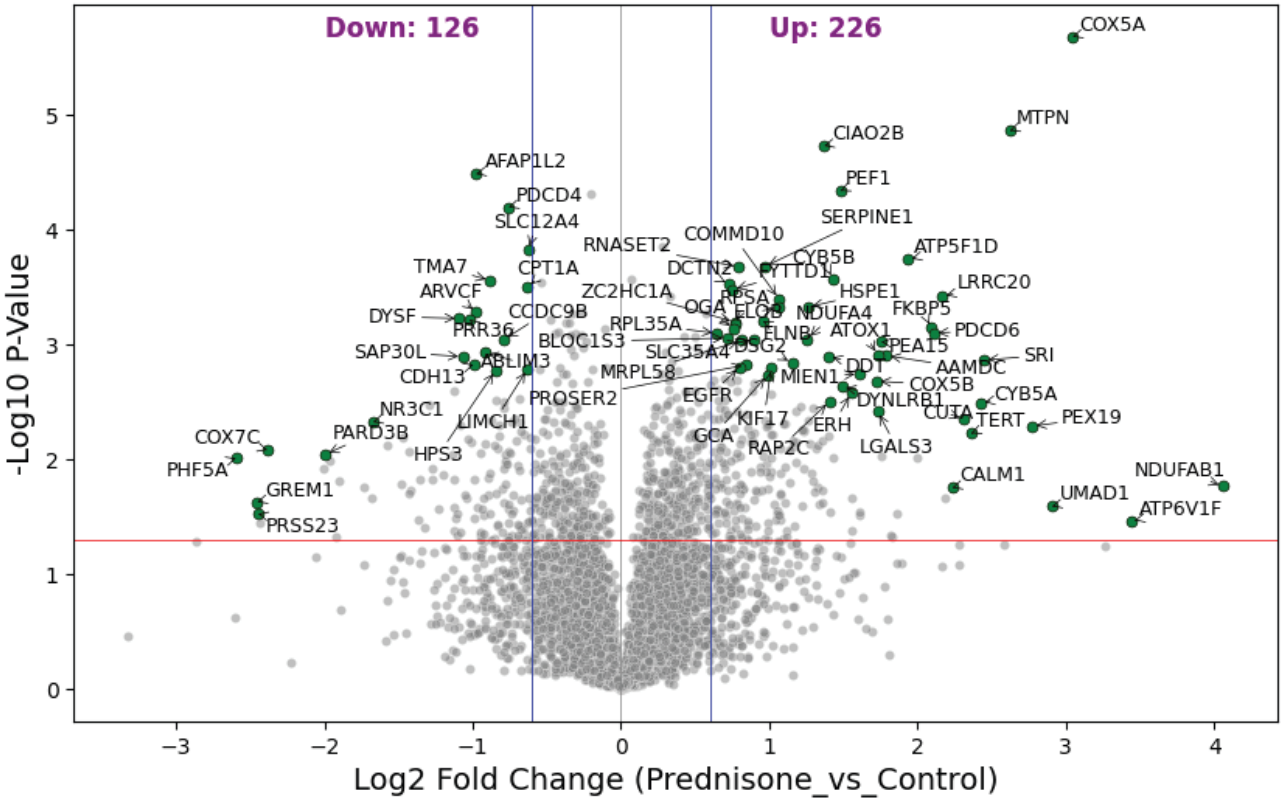

Supplemental Figure 1B

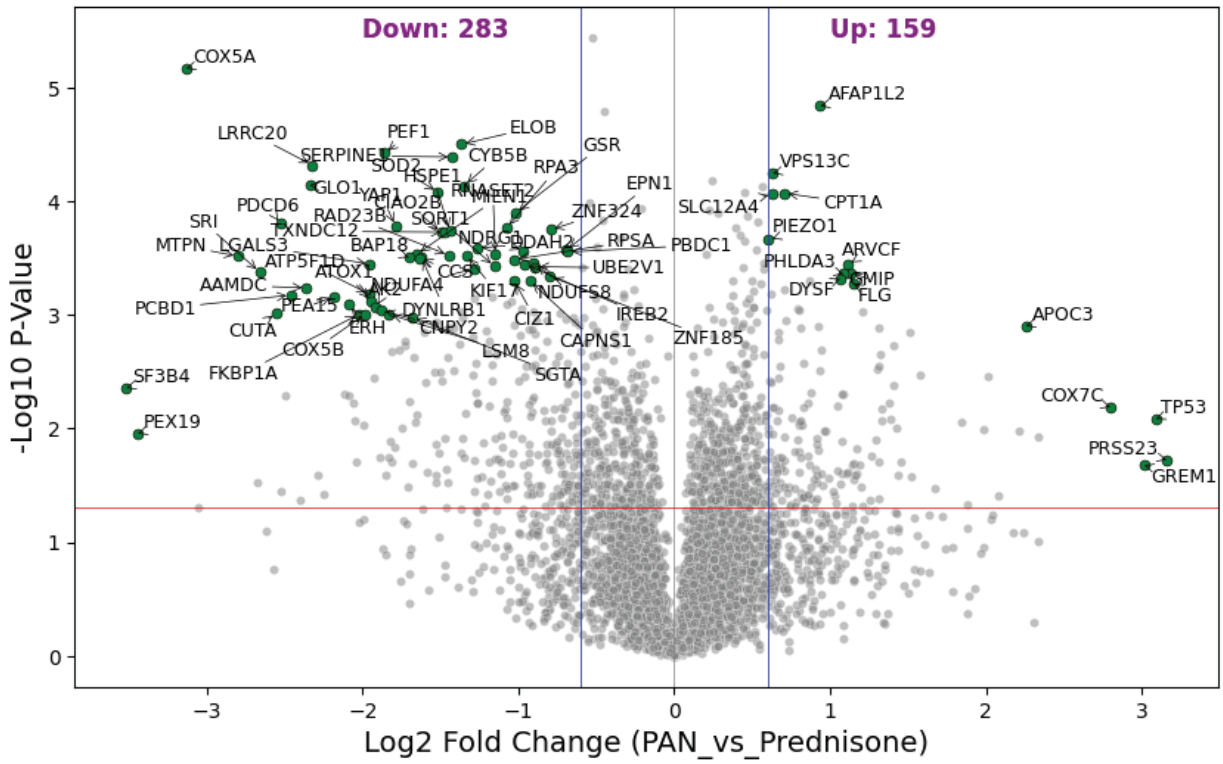

Supplemental Figure 1C

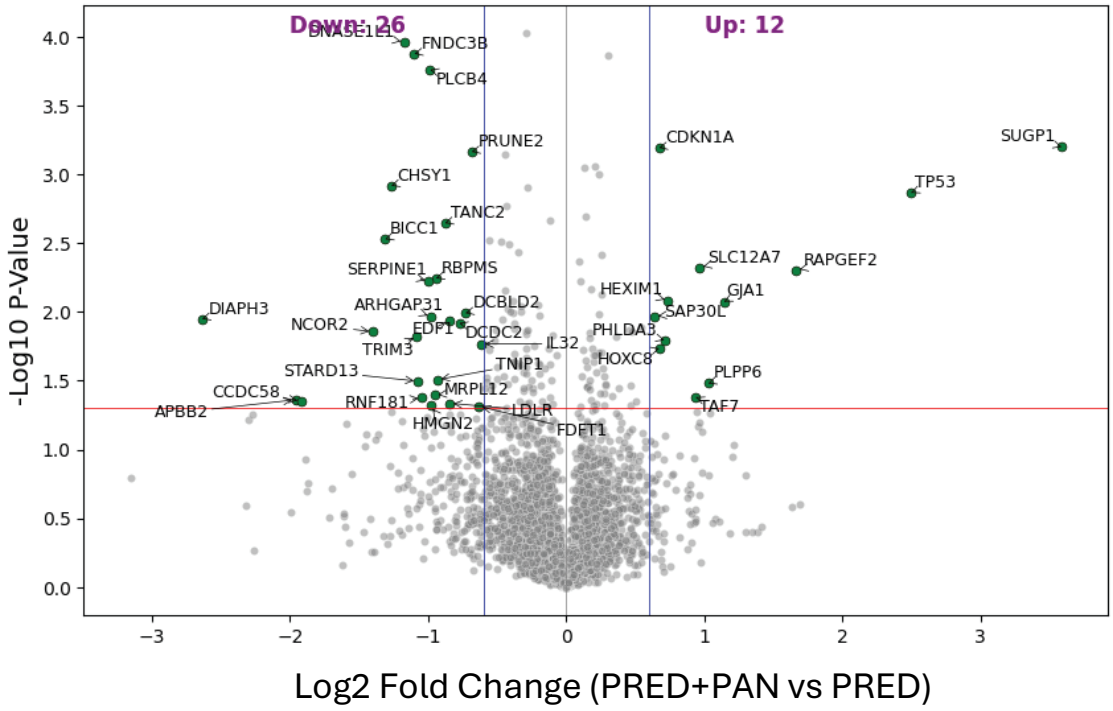

Figure 20. **Supplemental Figure 2. Gene set enrichment analysis for cellular proteomic analyses.**

Supplemental Figure 2A

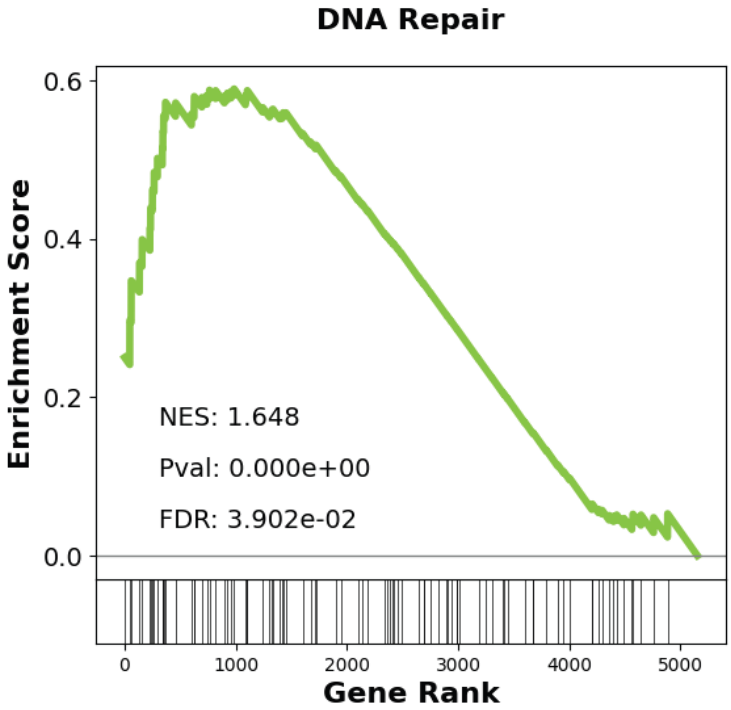

Supplemental Figure 2B

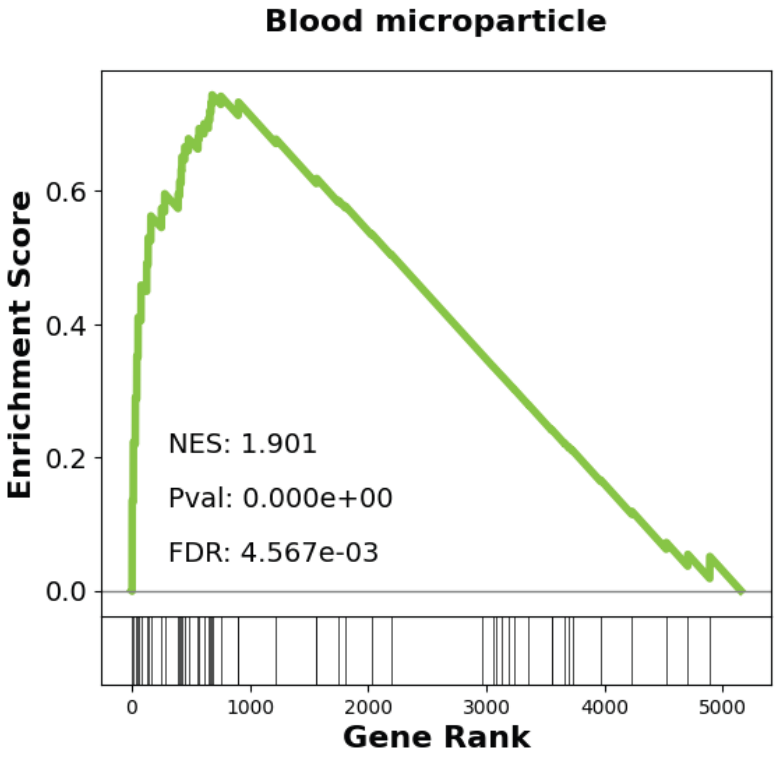

Supplemental Figure 2C

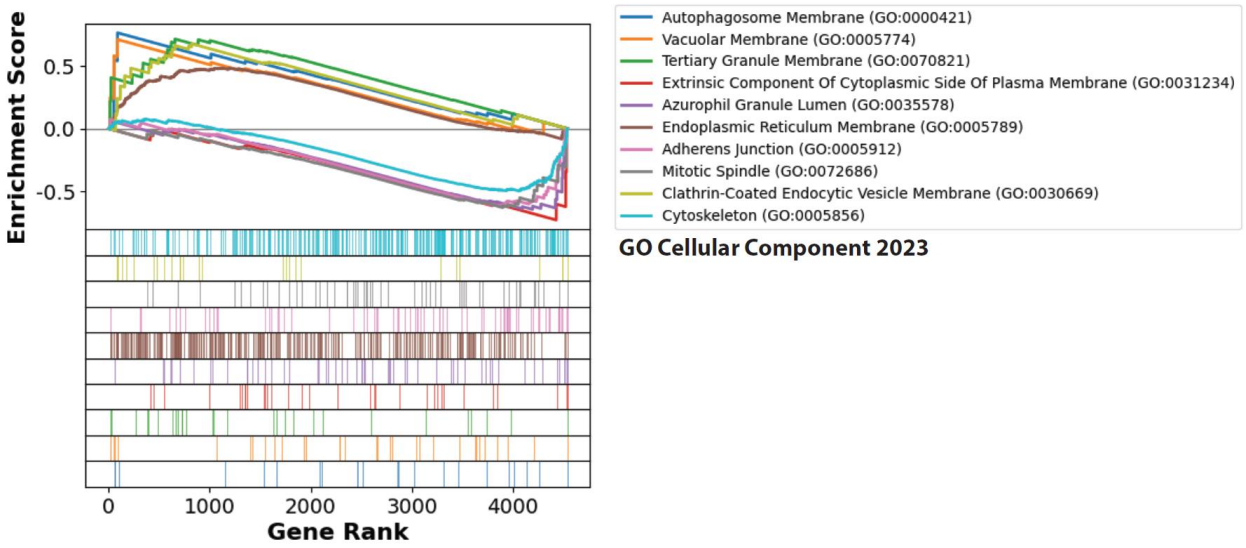

Supplemental Figure 2D

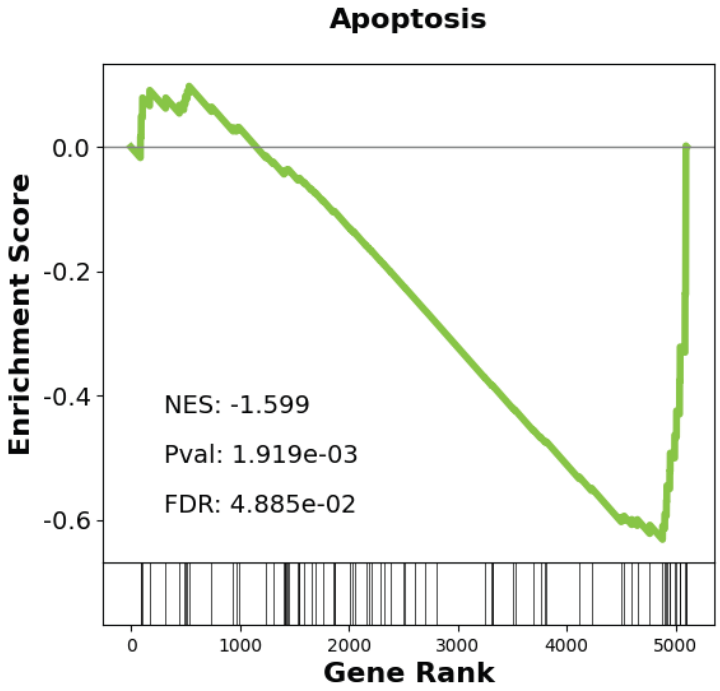

Supplemental Figure 2E

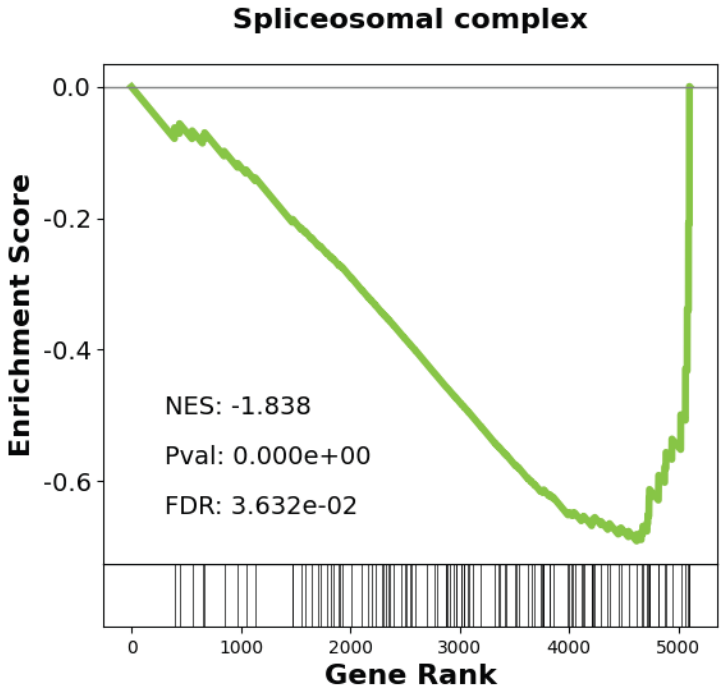

Supplemental Figure 2F

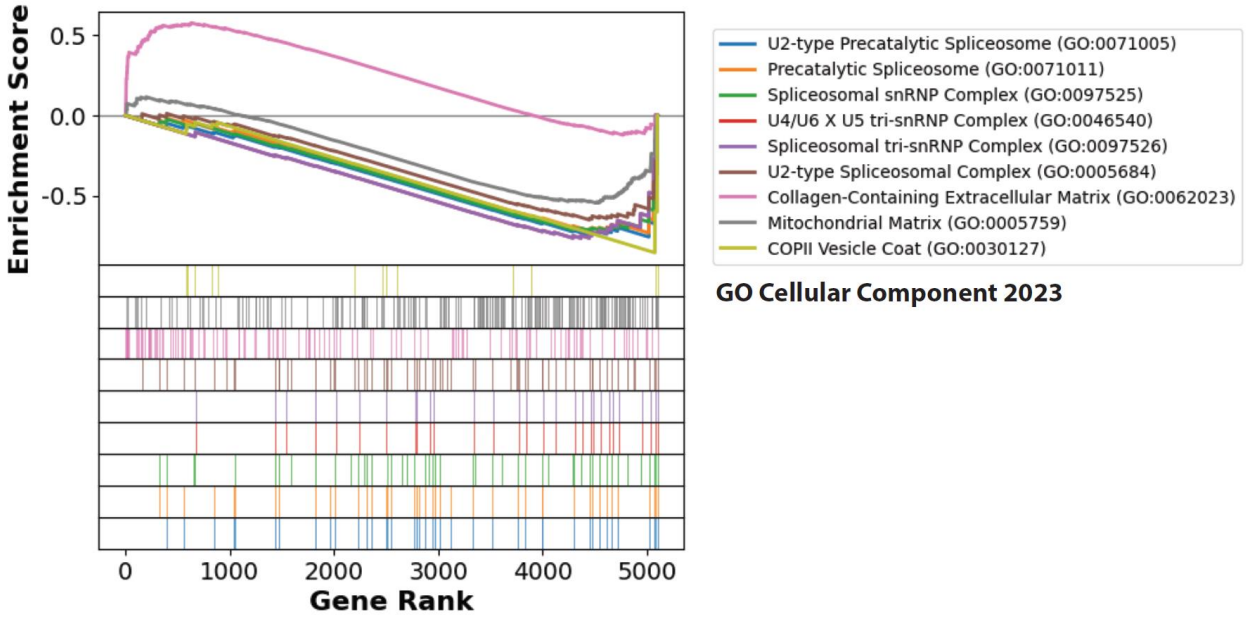

Figure 21. **Supplemental Figure 3. Volcano plots for hPod LEV DEPs under varying experimental conditions.**

Supplemental Figure 3A

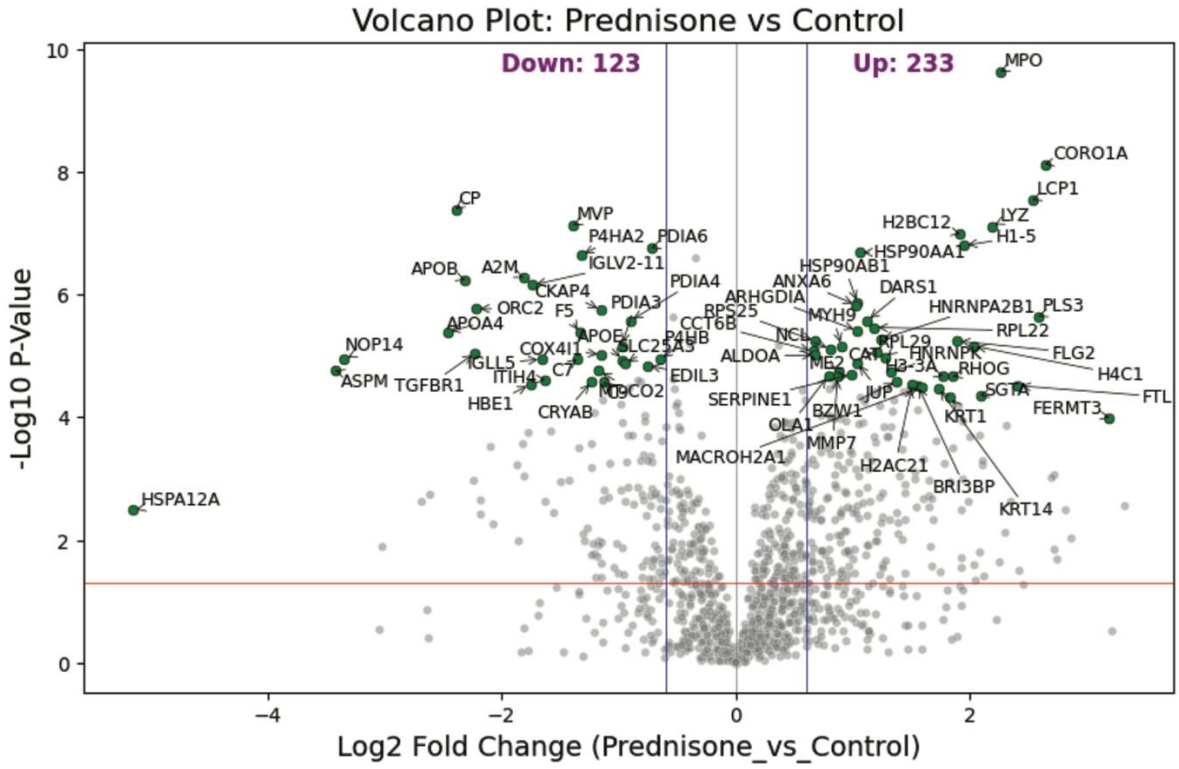

Supplemental Figure 3B

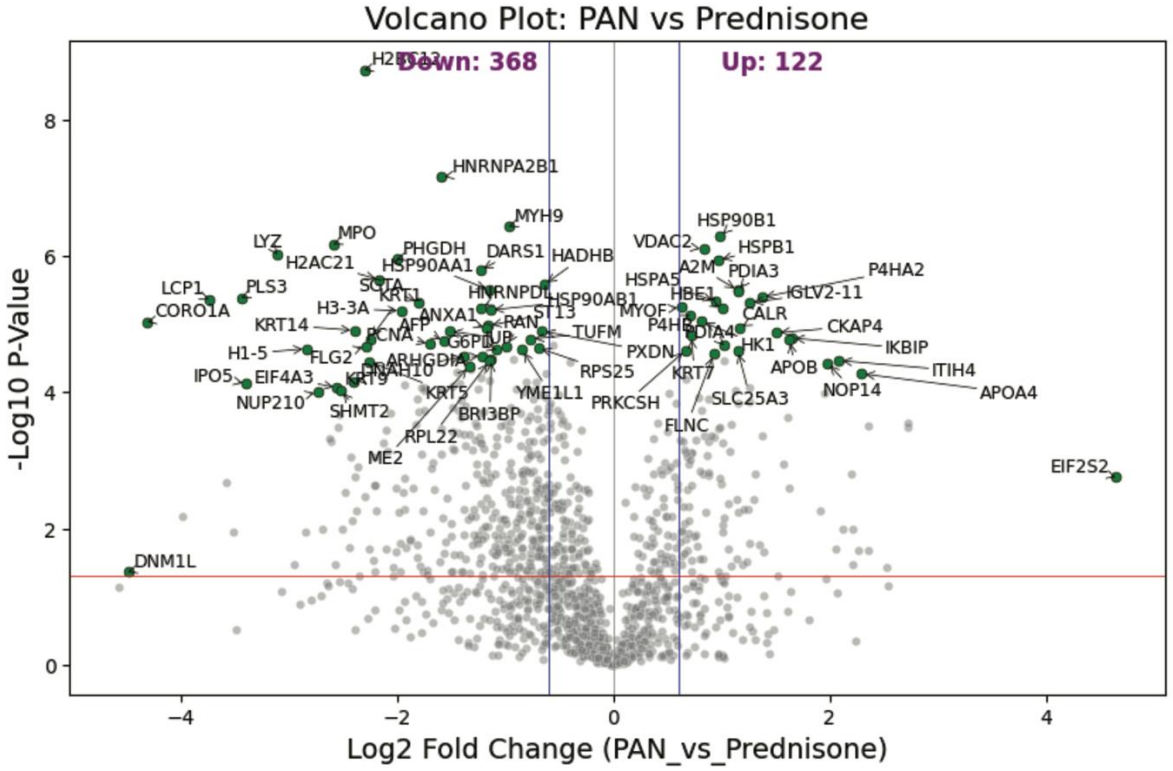

Supplemental Figure 3C

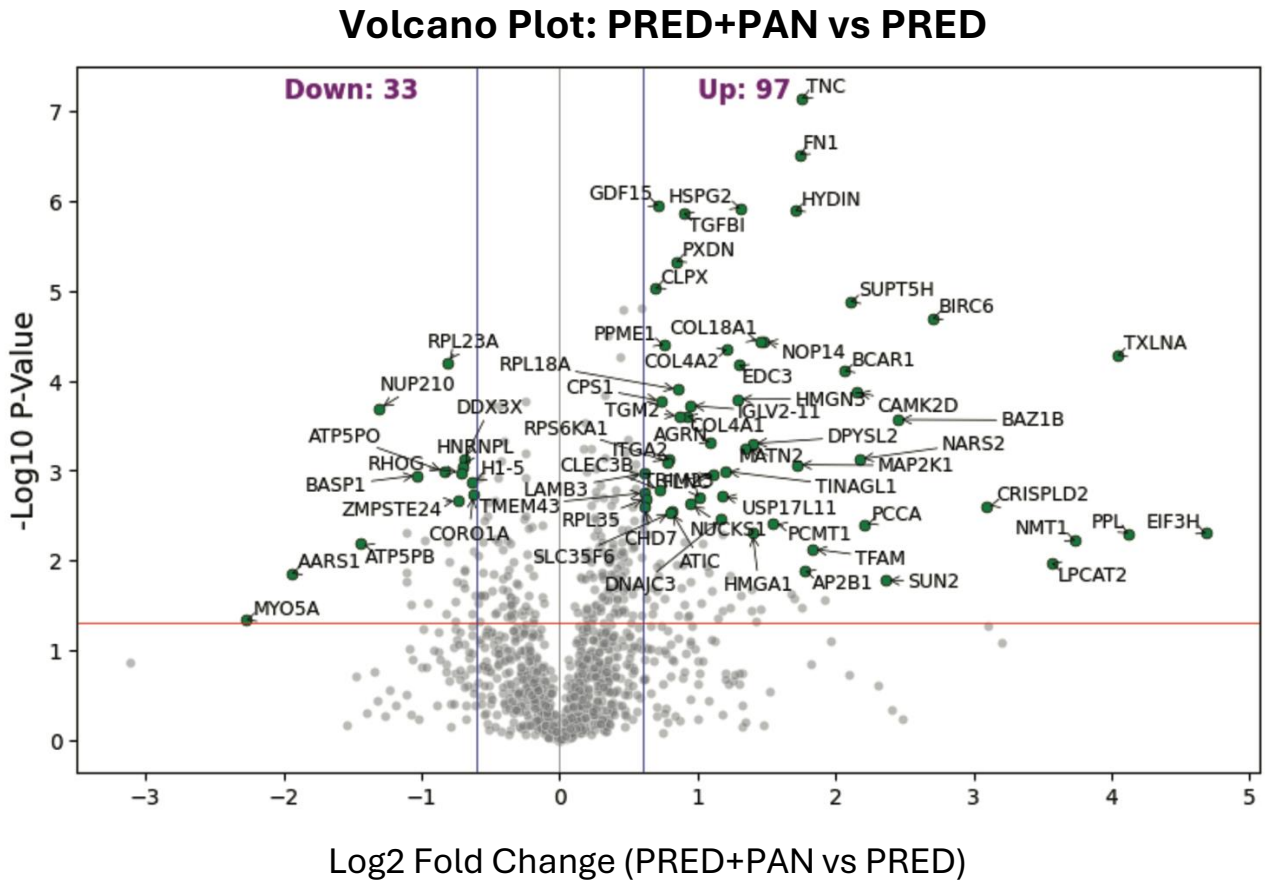

Figure 22. **Supplemental Figure 4. Gene set enrichment analysis for hPod LEVs under various experimental conditions.**

Supplemental Figure 4A

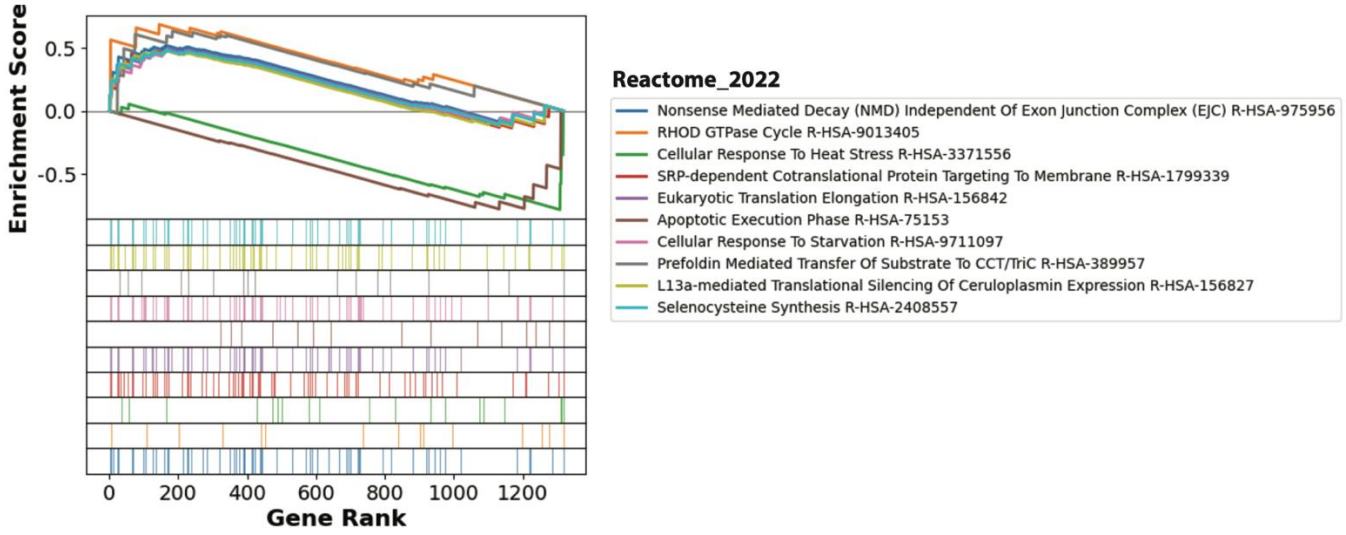

Supplemental Figure 4B

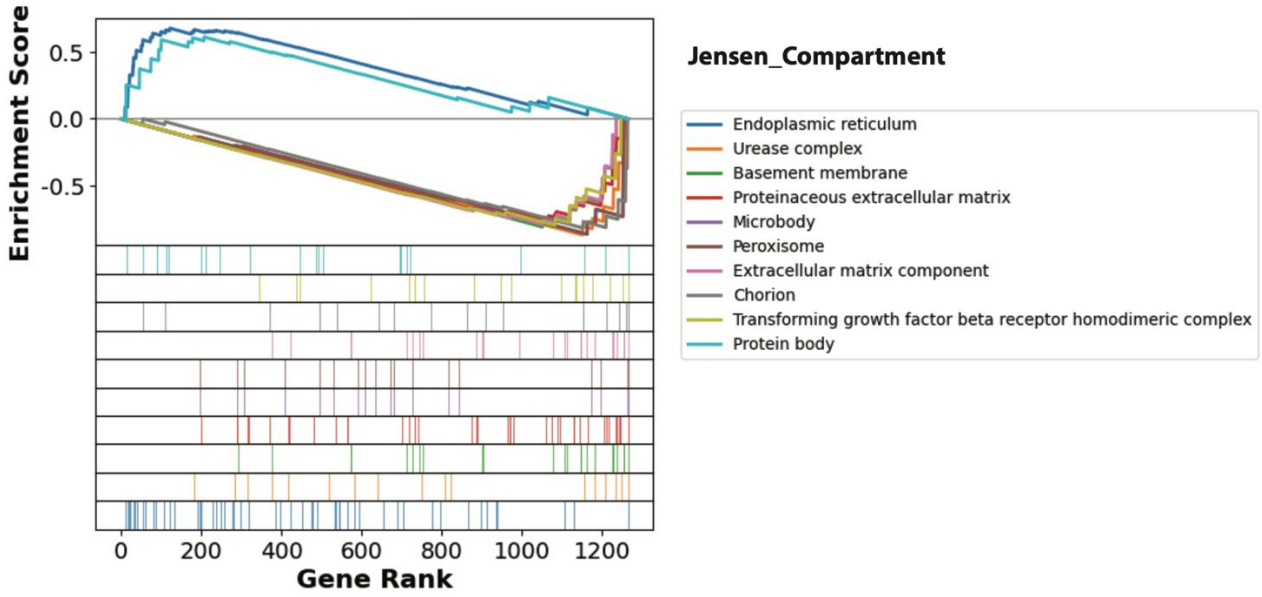

Supplemental Figure 4C

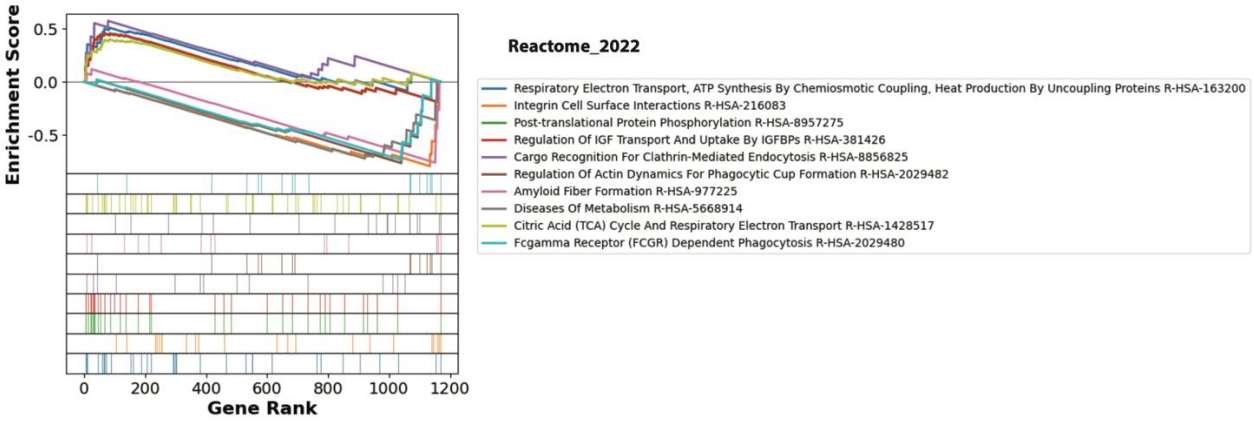

Supplemental Figure 4D

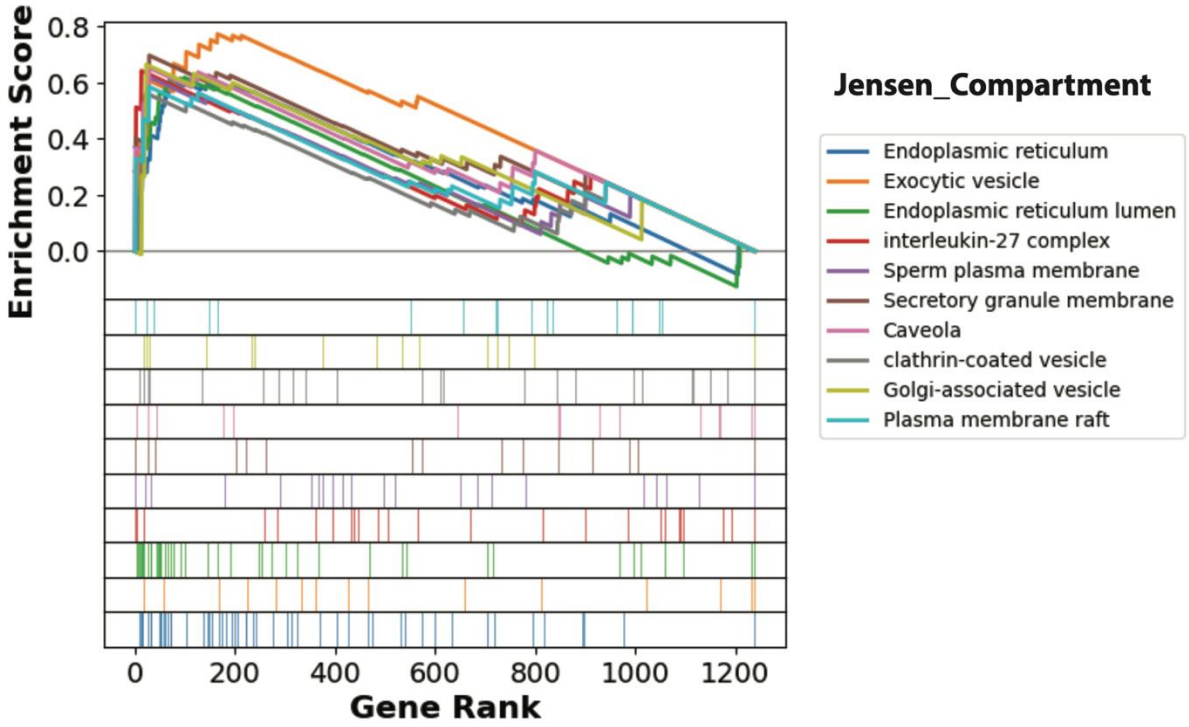

Figure 23. **Supplemental Figure 5. Heat maps comparing urinary LEV DEPs between disease and remission status.**

Supplemental Figure 5A

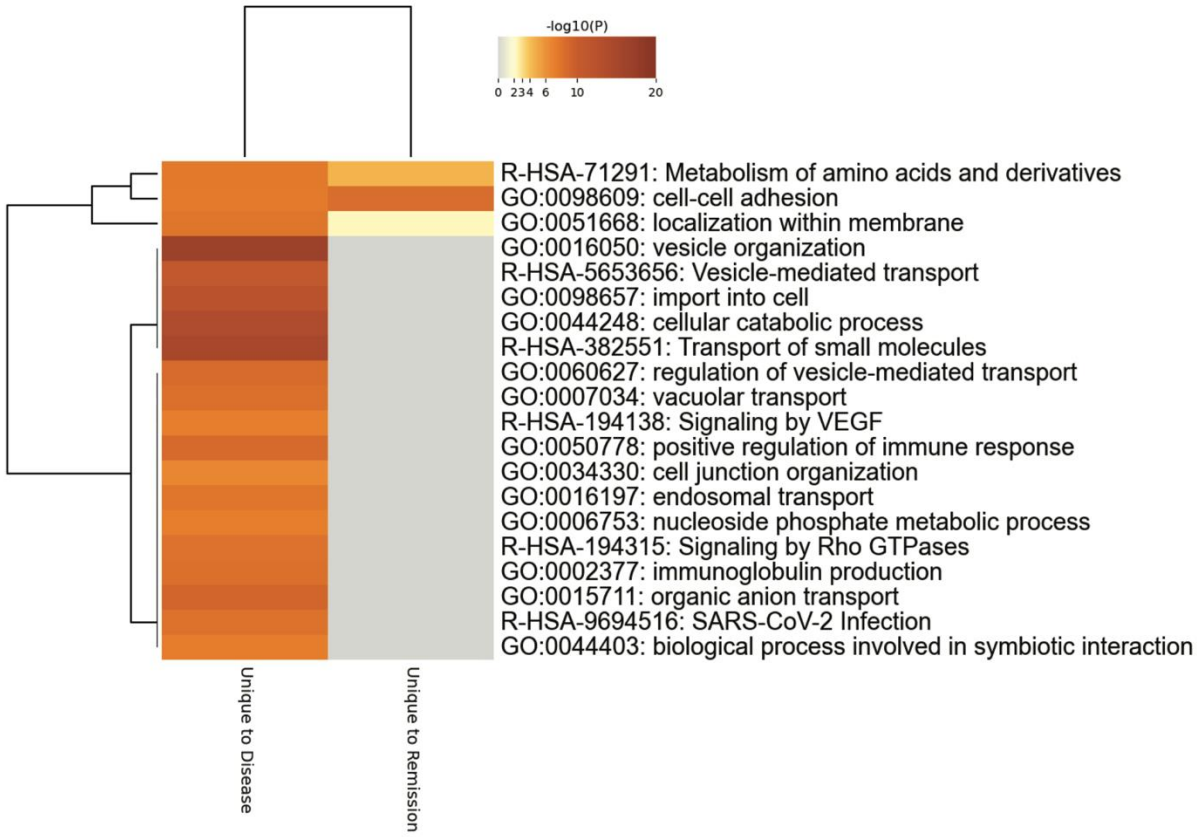

Supplemental Figure 5B

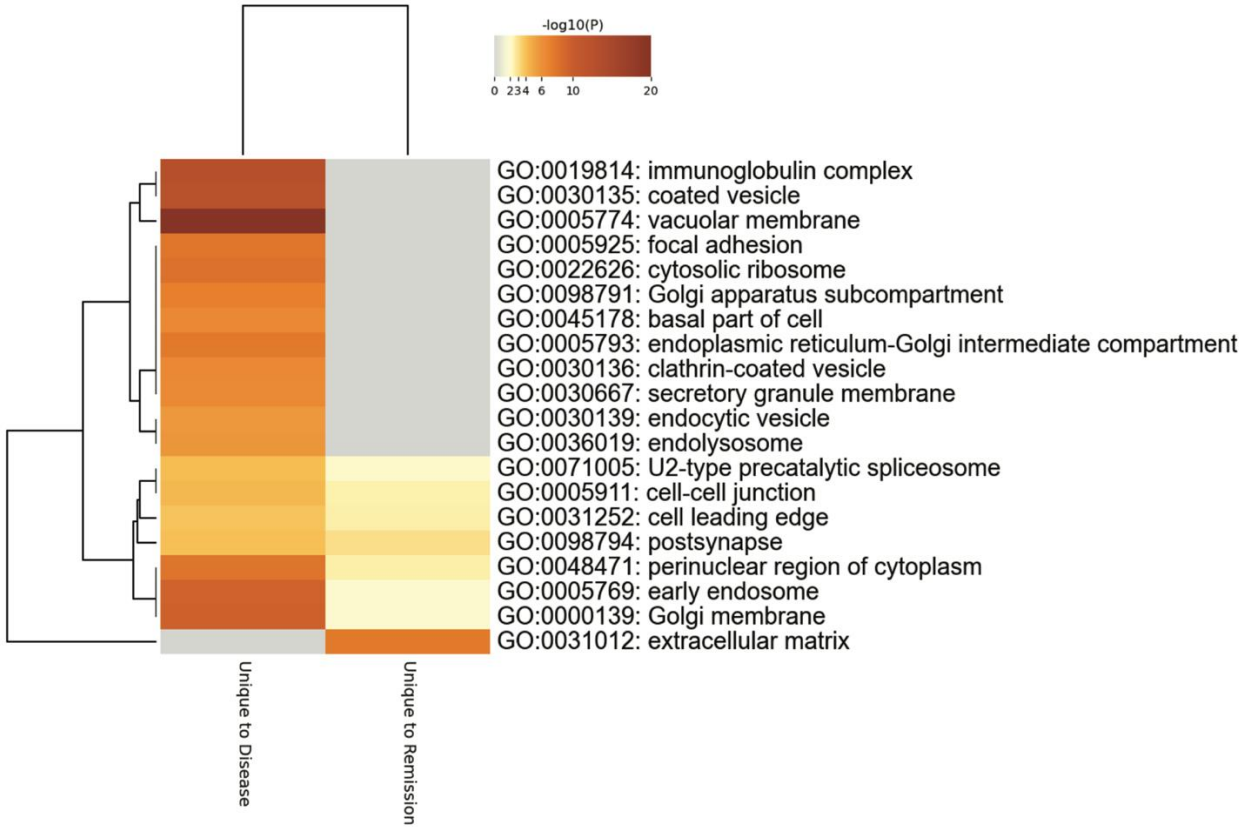

5 Discussion

This thesis focused on urinary LEVs and their cargo, as novel markers of disease in pediatric iNS. Specifically, **Chapter 2** outlined the discovery of LEVs in the urine of children with iNS during relapse; however, these levels were decreased to near-zero during remission. Thereafter, with the knowledge that LEVs in the urine can be collected, quantified, and studied further, I examined the content of LEVs from hPods in cell culture under stress conditions, and tied these observations back to clinical samples. Our novel findings included mtDNA as cargo of LEVs from stressed podocytes, with an association with mitochondrial stress *in vitro* (**Chapter 3**). I further confirmed that this process was conserved in an *in vivo* rat model. Further, through examination of LEVs using proteomics, I discovered that podocyte stress leads to significant alterations in the LEV proteome, as does prednisolone treatment (**Chapter 4**). Altogether, the results of this PhD work will provide the impetus for further mechanistic studies both *in vitro* and *in vivo*.

The search for biomarkers in human disease spans many years; however, it wasn't until recently that EVs were discovered and their potential as biomarkers was revealed. To date, their true potential remains unrealized. Clinical biomarkers in kidney disease are usually limited to products of cellular and biochemical processes in the urine or blood stream. Despite years of research advancements, the most reliable marker of disease activity in pediatric iNS is the rudimentary urine protein level. However, the discovery of EVs may usher in a new era of modern biomarkers. Further, EVs may also offer a more precision-based assessment of injury and recovery. Currently, there are few studies investigating EVs as biomarkers in NS in children. When conducting a PubMed search, as of the writing of this thesis, there are currently 14 results obtained employing the search terms: "Nephrotic Syndrome" AND "Extracellular Vesicles". This suggests

that this field is in its infancy. These studies can be separated into those looking at biomarkers in the serum, and those looking in the urine.

A study examining the role of circulating EVs in patients with SSNS revealed an increase in Rac1 within the EVs [1]. The authors then went on to treat hPods with these EVs containing Rac1 and revealed a recapitulation of a NS phenotype in the cell culture model [1]. This study examined serum EVs following a 100,000 x *g* spin, representing a mixed EV population; however, a lower speed centrifugation step was performed prior to this, eliminating apoptotic bodies, exophers, and blebbisomes. Relapse serum EVs in this population, with a higher level of Rac1, induced enhanced motility and albumin permeability in cultured human podocytes [1]. These observations prompted queries related to how a serum EV would impart its effects at the level of the podocyte in human disease [2]. Specifically, charge- and size-selective properties of the slit diaphragm would have to be overcome by serum-derived EVs to reach the podocyte. There is experimental evidence suggesting this can occur [3]. While my work did not involve serum EVs, this work highlights the advancing field of EV biomarker studies, particularly in NS.

When considering urinary EVs, there are additional studies both in NS and in kidney disease in general. There are reports investigating the role of EVs in the urine as markers of renal allograft injury [4], renal carcinoma [5], and diabetic kidney disease [6], among others [7]. In NS, Santorelli *et al*., studied urinary EVs using gel electrophoresis and discovered unique patterns associated with NS disease phenotypes [8]. Chen *et al* also studied urinary EVs and determined that certain EV-miRNA species were correlated with the degree of proteinuria [9]. Our contribution to this field included the discovery that urinary LEVs, and those derived from podocytes specifically, were increased in urinary specimens from children with iNS relapse. The number of podocyte-specific LEVs returned to nearly zero at the time of remission [10]. While

others have shown general EV population alterations in the urine, our novel observation confirmed that I can isolate and identify LEVs originating from specific renal cell types using surface markers and flow cytometry. Extrapolating further, I hypothesized that since these EVs were increased in the urine of children with NS, and specifically those from the podocyte, the EV cargo provides insights into the underlying mechanism of the disease, at the level of the podocyte. Indeed, I and others have already begun to address this question using podocyte EVs *in vitro*; however, none have done this in the context of NS. Earlier studies examined the effects of podocyte EVs on tubular cells, which are immediately downstream of the glomerulus, and thus the podocyte. Specifically, it was shown that uninjured podocyte derived EVs increased p38 and Smad3 phosphorylation, leading to a pro-fibrotic response in the target tubular cells [11]. Beyond this, it has been shown that EVs released from damaged podocytes can promote apoptosis in tubular cells [12], an observation linked to miRNA content enrichment following injury. Renal tubular cell apoptosis was also observed following treatment with EVs derived from podocytes cultured under diabetic conditions [13]. All three of these examples show the propensity for EVs to elicit deleterious effects on tubular cells, downstream of podocytes, regardless of the nature of the stimulus (i.e., uninjured podocytes, damaged podocytes, or podocytes exposed to diabetic conditions). Whether podocyte-specific EV cargo can have beneficial effects on tubular cells is unclear and requires further study.

To date, it has largely been miRNA content which has been studied as cargo in podocyte EVs *in vitro* and shown to have deleterious effects on tubular cells. Knowing that EVs contain not only miRNA, but also protein, lipids, and DNA, I sought to examine these latter two classes of biomolecules in more detail. mtDNA has been observed in EVs for quite some time and generally has been associated with underlying cellular stress [14–16]. Further, levels of mtDNA in serum

EVs decline with age [17]. It is therefore clear that the presence of mtDNA within EVs likely plays a physiological role and can be modulated during disease or health. The mechanisms that package mtDNA into EVs is also a contentious topic; however, given this has been observed in a variety of cell types, it is likely there is a conserved mechanism for excretion of mtDNA in viable cells, or this is a packaging process that occurs under times of cellular stress or damage. In our study, I found that hPods *in vitro*, when stressed with PAN, a known podocyte toxin, had markedly elevated levels of mtDNA within hPod LEVs. This was associated with mitochondrial stress as evidenced by increased mitoROS, a declining MMP, and a bioenergetic stress. mtDNA levels in LEVs decreased following pre-treatment with prednisolone, the gold standard immunomodulatory agent for children with NS. When examining this observation in a rat model of nephrosis, as well as in urinary samples from children in relapse from iNS, I observed that during disease (proteinuria), the LEVs were significantly enriched in mtDNA, while in control animals, and during remission in children, the LEV mtDNA was measured at significantly lower levels. I am not the first to associate mtDNA levels in EVs with underlying mitochondrial stress. In a model of Huntington's Disease, a defective mitochondrial-lysosomal axis led to enhanced release of EVs containing mtDNA, as well as mitochondrial proteins [18]. Another example includes Behcet's Syndrome, where small EVs are secreted and contain mtDNA. This extrusion of mtDNA in EVs acts to propagate an inflammatory signal via a TLR9-dependent pathway [15]. While the packaging of mtDNA into podocyte LEVs is a unique and novel observation, changes to bioenergetic profiles of podocytes under experimental conditions of stress has been shown before.

Abe *et al.* undertook the first bioenergetic characterization of transformed mouse podocytes in 2010 [19]. It was revealed that basal OCR levels were 55.2 pmol/min, and oligomycin reduced OCR to ~45% of baseline, thus revealing that ~55% of podocyte oxygen consumption

was coupled to ATP synthesis [19]. The conclusions from this study suggested that mitochondria play the primary role in maintaining podocyte energy homeostasis and that glycolysis plays a lesser role [19]. Adding to these observations, Abe *et al.* repeated these experiments in the presence of TGF-β1 which activated mTOR signalling, an increase in MMP, OCR, and intracellular production of ROS [20]. Taken further, Casalena *et al.* revealed that TGF-β1 induced cytoskeletal rearrangements were associated with compensatory adaptations of mitochondrial bioenergetics (ATP synthesis) [21]. High glucose (to mimic hyperglycemia observed in diabetes) also modified the bioenergetic profile of podocytes [22]. Altogether, these findings reveal that a stress event for podocytes induces a bioenergetic adaptation which is sometimes observed as increases in OCR. This is similar to our observation where PAN induced oxidative stress in podocytes, and more specifically mitochondrial stress [23]. I observed increases in mtROS and OCR at 1-hour, suggesting a rapid bioenergetic stress; however, by 24 hours, I detected an adaptation and a return to baseline. This suggests that the podocyte may be responding to buffer this assault, and this may be further evidenced by increases in proton leak at an early point, as well as persistence of this leak at 24-hours. At this time point, I also observed decreases in MMP. Contrary observations were reported by Brinkkoetter *et al*., [24]. Therein, they revealed that deleterious alterations to genes related to mitochondrial biogenesis, fission-fusion capacity, and mtDNA stability did not lead to a pathologic phenotype under physiological and non-stressed conditions. I therefore hypothesize that podocytes rely on anaerobic respiration during times of stability, but switch to a mode requiring more energy, and thus become more dependent on mitochondria, during times of stress. This hypothesis will form the basis of the work I perform as an independent investigator moving forward.

In a rat PAN-nephrosis model [25], I observed significant nephrosis (ascites, increased ACR), foot process effacement on EM, and associated significant elevations in mtDNA within LEVs when compared to control animals. To our knowledge, this is the first time that LEVs have been isolated from rat urine in a nephrosis model, and the first time that mtDNA has been studied within LEVs from nephrotic rats. Prior to our study, an elegant study by Bhayan *et al.* sought to define overlapping transcriptional patterns between steroid-treated, and pioglitazone-treated rats in the same PAN-nephrosis model [26]. Pioglitazone, a Peroxisome Proliferator-Activated Receptor, Gamma (PPARγ) agonist, was shown clinically to decrease proteinuria in children with NS, and to protect podocytes in a preclinical NS model [27, 28]. In comparing PAN-nephrosis rats treated with either Pioglitazone or steroids, the authors discovered 29 commonly regulated genes of interest which pointed to ECM dysregulation as a potential disease mechanism [26]. While this does not directly relate to EVs, it reveals the complexities of the pathomechanism of NS in children, and extrapolations that I can make using the rat nephrosis model.

What is unique about our observation is the presence of mtDNA within LEVs derived from podocytes, and the association with pediatric iNS. Children with iNS currently do not have access to precision medicine treatment approaches, and in turn are treated with a 'one treatment fits all' approach, leading to a significant side effect burden. Our discovery moves us one step closer to more precise diagnostic and therefore treatment approaches in NS. In the setting of our observations discussed to this point, and to further refine the precision approach to understanding NS in children, I then looked at the LEV proteome *in vitro*, as well as in the urine from children with NS. Initially, I examined the podocyte proteome to better understand the parent cell prior to studying LEVs, which are derived from the parent cell of origin. Interestingly, I observed enrichment in mitochondrial proteins in podocytes following PAN treatment, relative to control.

This ties together well with the content of **Paper 2** and further strengthens the idea that podocyte mitochondrial alterations may be associated with cell stress. Using tissue proteomics, Barar *et al.* applied LC-MS/MS to eight formalin-fixed, paraffin embedded tissue samples from patients with MCD (relative to control) [29]. Those with MCD had 11 proteins that were significantly differentially overexpressed. Gene Ontology (GO) Molecular Function analysis showed most proteins were linked with structure and stability of podocytes [29]. Looking specifically at podocytes in culture, Bruschi *et al.* examined proteomic changes in control cells compared to those treated with Everolimus, an mTOR inhibitor [30]. They identified 7786 proteins in podocytes, where in our study of PAN treated podocytes, I identified closer to 5000 proteins. They also interrogated the supernatant from these experimental conditions. According to GO analysis, there were 4 main biological processes altered following treatment with Everolimus. These included proteins involved in epithelial to mesenchymal transition (EMT), metabolism, and kinase signalling. While only briefly commented on, it is possible the supernatant analyses revealed differentially expressed proteins (DEPs) in EVs, as they may have been enriched in the supernatant. Further to this, it was the supernatant which was most enriched in extracellular matrix (ECM) reorganization receptor interaction-related proteins. These observations are consistent with the *in vivo* observations of Bhayan *et al.* [26]. As described above, they examined transcriptional patterns between steroid-treated, and pioglitazone-treated rats in the PAN-nephrosis model, and identified 29 commonly related genes of interest, primarily involving ECM remodelling. In our proteomics study of podocytes, I observed enriched signals related to vesicle generation, mitochondrial proteins, and cellular stress. It was once I examined the proteomes of the EVs generated by hPods following treatment with PAN that I also observed enrichment in proteins associated with ECM organization. However, this was more pronounced in the presence of both

PAN and prednisolone, suggesting that prednisolone is driving the expression more than the injury alone. Speculatively, this increase in ECM organization-related proteins in the setting of prednisolone pre-treatment may be indicative of a reparative process; however, this requires further investigation.

Given the upregulated proteins related to vesicle formation in the podocyte following treatment with PAN, I intuitively examined LEVs from these cells next. Initially, I observed that LEVs are increased *in vitro* following treatment with PAN. These LEVs had unique proteomes under different experimental conditions, with significant DEPs following treatment with PAN and Prednisolone. Others have looked at the proteome of podocytes *in vitro* and have compared them to the urinary EV proteome; however, this was not done specifically in the context of remission versus disease in NS in children. Specifically, Barreiro *et al.* [31] employed an *in vitro* approach to better understand how kidney cells contribute protein and miRNA to urinary EVs. Similar to our study, the authors isolated hPod-EVs and subjected them to either RNA isolation and sequencing, or tandem mass tag proteomics [31]. Further to this, they also interrogated the proteome of several other immortalized kidney cells, including, mesangial cells, proximal tubule cells, and glomerular endothelial cells. This group did not evaluate the proteome of the parent cells, rather, focused their attention on analyzing only the EVs. This group observed significant upregulation of proteins within GO molecular function category 'epithelial cell proliferation'. In contrast, I discovered many different GO categories, including autophagosome membrane, vacuolar membrane, and cytoskeleton. When comparing the podocyte EVs with the urinary EVs, Barreiro *et al.* uncovered an overlap of 7 proteins [31]. Of importance, their urinary EV data was derived from several study databases, including those with healthy controls only, and others which included patients with proteinuria and diabetes [31]. In our study, I was able to compare relapse

EVs from children with NS to PAN treated hPod EVs, as an experimental model of NS. I identified 36 DEPs under experimental conditions of NS that were also observed in EVs from children with NS during disease. Interestingly, I also observed some of the proteins identified in the Barreiro *et al* study, including the following in our NS patient disease EVs: Cullin-2 (CUL2), Phospholipase B domain containing 2 (PLBD2), while the others were found common between disease and remission, included: Proteasome subunit beta type-2 (PSMB2), Complement C3 (C3), Cystatin A (CSTA), Keratin 14 (KRT14), and Endoplasmic reticulum resident protein 44 (ERP44). I further report commonalities between experimental NS and human NS, specifically in Syntaxin 3 (STX3), Regulatory Particle Non-ATPase 2 (RPN2), and Dynactin Subunit 1 (DCTN1) which were all commonly upregulated. Conversely, Heat Shock Protein Family A member 9 (HSPA9), and phosphate cytidylyltransferase 2, ethanolamine (PCYT2) were downregulated. I also noted discrepant differences in protein expression patterns between experimental and human NS. In this regard, Prothrombin (F2), and Complement C7 (C7) were differentially regulated, with F2 being upregulated in NS disease LEVs, but downregulated in experimental NS LEVs, similar to C7. LEV C9 was markedly upregulated under NS disease conditions, but in experimental NS, it was mildly downregulated. This shows the challenges, but also opportunities, in studying LEVs from cells *in vitro* and linking them together with human biospecimens. One obvious consideration is that the PAN model only partially recapitulates iNS, which would be expected.

Overall, this thesis work was successful in first showing that urinary LEVs from children with NS could be isolated, and specifically podocyte LEVs could be studied under both NS disease and remission conditions. Next, I furthered the understanding of the role of the mitochondria in experimental NS, and the potential role of mtDNA within LEVs as a novel marker of disease activity. Lastly, I used data-independent acquisition mass spectrometry proteomics technology to

further our understanding of how both PAN and Prednisolone impact the proteome of not only the hPod, but also the EVs generated *in vitro,* and those from the urine of children with NS. These three studies have contributed overall to further the understanding of pediatric NS, and in particular how I can harness EVs as non-invasive markers of NS in children.

There are obvious future directions which need to be pursued, including bettering the understanding of why the mitochondria may play an important role in NS, and how this links together with the extrusion of mtDNA into EVs. Is this a self-preservation method for the cell? Can I bring urinary EVs to the clinic once I better understand specific signatures under times of podocyte stress? Can they be used to define steroid responsiveness *a priori*? Given these clear questions, I will herein propose and speculate on future research endeavours which I will pursue as an independent investigator.

6 Future Directions

My research program will be dedicated to further understanding the molecular underpinnings of pediatric NS through **3 Pillars**:

1) Mechanistic: Uncovering the mitochondrion's role in NS, specifically through understanding the mechanism of mitochondrial DNA packaging into podocyte EVs and its biological significance.

2) Fundamental: Improving the understanding of fundamental biological processes associated with podocyte EV formation to further inform future clinical utility.

3) Consequential: Understanding the potential deleterious consequences of EVs released from injured podocytes and acting on downstream cells.

References

1. Eroglu FK, Yazar V, Guler U, et al (2021) Circulating extracellular vesicles of patients with steroid-sensitive nephrotic syndrome have higher RAC1 and induce recapitulation of nephrotic syndrome phenotype in podocytes. American Journal of Physiology-Renal Physiology 321:F659–F673. https://doi.org/10.1152/ajprenal.00097.2021

2. Myette R, Burger D (2021) Relapse in steroid-sensitive nephrotic syndrome: are extracellular vesicles the missing link? American Journal of Physiology-Renal Physiology 656–658. https://doi.org/10.1152/ajprenal.00349.2021

3. Oosthuyzen W, Scullion KM, Ivy JR, et al (2016) Vasopressin regulates extracellular vesicle uptake by kidney collecting duct cells. Journal of the American Society of Nephrology 27:3345–3355. https://doi.org/10.1681/ASN.2015050568

4. Sedej I, Štalekar M, Tušek Žnidarič M, et al (2022) Extracellular vesicle-bound DNA in urine is indicative of kidney allograft injury. medRxiv 2022.04.07.22273527. https://doi.org/10.1002/jev2.12268

5. Msaouel P, Malouf GG, Su X, et al (2020) Comprehensive Molecular Characterization Identifies Distinct Genomic and Immune Hallmarks of Renal Medullary Carcinoma. Cancer Cell 37:720-734.e13. https://doi.org/10.1016/j.ccell.2020.04.002

6. Lytvyn Y, Xiao F, Kennedy CRJ, et al (2017) Assessment of urinary microparticles in normotensive patients with type 1 diabetes. Diabetologia 60:581–584. https://doi.org/10.1007/s00125-016-4190-2

7. Ng MSY, Burger D, Svenningsen P, et al (2024) Unlocking the potential of extracellular vesicles in nephrology: what does MISEV2023 add? Kidney Int

8. Santorelli L, Morello W, Barigazzi E, et al (2021) Urinary Extracellular Vesicle Protein Profiles Discriminate Different Clinical Subgroups of Children with Idiopathic Nephrotic Syndrome. Diagnostics 11:456. https://doi.org/10.3390/diagnostics11030456

9. Chen T, Wang C, Yu H, et al (2019) Increased urinary exosomal microRNAs in children with idiopathic nephrotic syndrome. EBioMedicine 39:552–561. https://doi.org/10.1016/j.ebiom.2018.11.018

10. Myette RL, Xiao F, Geier P, et al (2023) Urinary podocyte-derived large extracellular vesicles are increased in paediatric idiopathic nephrotic syndrome. Nephrology Dialysis Transplantation 38:2089–2091. https://doi.org/10.1093/ndt/gfad086

11. Munkonda MN, Akbari S, Landry C, et al (2018) Podocyte-derived microparticles promote proximal tubule fibrotic signaling via p38 MAPK and CD36. J Extracell Vesicles 7:. https://doi.org/10.1080/20013078.2018.1432206

12. Jeon JS, Kim E, Bae YU, et al (2020) microRNA in Extracellular Vesicles Released by Damaged Podocytes Promote Apoptosis of Renal Tubular Epithelial Cells. Cells 9:. https://doi.org/10.3390/cells9061409

13. Huang Y, Li R, Zhang L, et al (2020) Extracellular Vesicles From High Glucose-Treated Podocytes Induce Apoptosis of Proximal Tubular Epithelial Cells. Front Physiol 11:. https://doi.org/10.3389/FPHYS.2020.579296

14. Byappanahalli AM, Omoniyi V, Noren Hooten N, et al (2024) Extracellular vesicle mitochondrial DNA levels are associated with race and mitochondrial DNA haplogroup. iScience 27:. https://doi.org/10.1016/j.isci.2023.108724

15. Konaka H, Kato Y, Hirano T, et al (2023) Secretion of mitochondrial DNA via exosomes promotes inflammation in Behçet's syndrome. EMBO J. https://doi.org/10.15252/embj.2022112573

16. Arance E, Ramírez V, Rubio-Roldan A, et al (2022) Determination of exosome mitochondrial dna as a biomarker of renal cancer aggressiveness. Cancers (Basel) 14:1–13. https://doi.org/10.3390/cancers14010199

17. Lazo S, Noren Hooten N, Green J, et al (2021) Mitochondrial DNA in extracellular vesicles declines with age. Aging Cell 20:1–15. https://doi.org/10.1111/acel.13283

18. Beatriz M, Vilaça R, Anjo SI, et al (2022) Defective mitochondria-lysosomal axis enhances the release of extracellular vesicles containing mitochondrial DNA and proteins in Huntington's disease. Journal of extracellular biology 1:. https://doi.org/10.1002/JEX2.65

19. Abe Y, Sakairi T, Kajiyama H, et al (2010) Bioenergetic characterization of mouse podocytes. Am J Physiol Cell Physiol 299:464–476. https://doi.org/10.1152/ajpcell.00563.2009

20. Abe Y, Sakairi T, Beeson C, Kopp JB (2013) TGF-β1 stimulates mitochondrial oxidative phosphorylation and generation of reactive oxygen species in cultured mouse podocytes, mediated in part by the mTOR pathway. Am J Physiol Renal Physiol 305:. https://doi.org/10.1152/ajprenal.00182.2013

21. Casalena G, Bottinger E, Daehn I (2016) TGFβ-induced actin cytoskeleton rearrangement in podocytes is associated with compensatory adaptation of mitochondrial energy metabolism. Nephron 131:278–284. https://doi.org/10.1159/000442051

22. Stieger N, Worthmann K, Teng B, et al (2012) Impact of high glucose and transforming growth factor-β on bioenergetic profiles in podocytes. Metabolism 61:1073–1086. https://doi.org/10.1016/J.METABOL.2011.12.003

23. Maeda J, Bartlett P (1967) Effects of the potent nephrotogenic aminonucleoside of puromycin on mitochondrial mechanochemistry. Biochem Pharmacol 16:761–768. https://doi.org/10.1016/0006-2952(67)90048-2

24. Brinkkoetter PT, Bork T, Salou S, et al (2019) Anaerobic Glycolysis Maintains the Glomerular Filtration Barrier Independent of Mitochondrial Metabolism and Dynamics. Cell Rep 27:1551-1566.e5. https://doi.org/10.1016/j.celrep.2019.04.012

25. Yamanaka M, Tamura Y, Kuribayashi-Okuma E, et al (2023) Nicorandil protects podocytes via modulation of antioxidative capacity in acute puromycin aminonucleoside-induced nephrosis in rats. Am J Physiol Renal Physiol 324:F168–F178. https://doi.org/10.1152/ajprenal.00144.2022

26. Bhayan S, Dougherty JA, Kamigaki Y, et al (2023) Glucocorticoid- and Pioglitazone-Induced Proteinuria Reduction in Experimental Nephrotic Syndrome Both Correlate with Glomerular ECM Modulation. iScience 108631. https://doi.org/10.1016/j.isci.2023.108631

27. Agrawal S, Chanley MA, Westbrook D, et al (2016) Pioglitazone Enhances the Beneficial Effects of Glucocorticoids in Experimental Nephrotic Syndrome. Sci Rep 6:2–10. https://doi.org/10.1038/srep24392

28. Hunley TE, Hidalgo G, Hui K, et al (2022) Pioglitazone enhances proteinuria reduction in complicated pediatric nephrotic syndrome. Pediatric Nephrology. https://doi.org/10.1007/s00467-022-05637-8

29. Bărar AA, Pralea IE, Maslyennikov Y, et al (2024) Minimal Change Disease: Pathogenetic Insights from Glomerular Proteomics. Int J Mol Sci 25:. https://doi.org/10.3390/IJMS25115613

30. Bruschi M, Granata S, Candiano G, et al (2024) Proteomic Changes Induced by the Immunosuppressant Everolimus in Human Podocytes. Int J Mol Sci 25:. https://doi.org/10.3390/IJMS25137336

31. Barreiro K, Lay AC, Leparc G, et al (2023) An in vitro approach to understand contribution of kidney cells to human urinary extracellular vesicles. J Extracell Vesicles 12:. https://doi.org/10.1002/jev2.12304

7 Significance of studies

Pediatric iNS is a common, but enigmatic glomerulopathy presenting with proteinuria, hypoalbuminemia, and edema. It is histopathologically defined as minimal change disease; however, a more precise description would be iNS with minimal change lesions. Recent evidence suggests this might represent an autoimmune condition; however, regardless of the inciting mechanism, podocyte foot process effacement (podocyte stress) is a central pathological component to this condition. Despite years of study, there remains a lack of prognostic tools, or objective biomarkers of clinical disease, or long-term prognostication. This PhD work, and my future independent work, is directly targeted at addressing this unmet need, while paying particular attention to reducing cumulative steroid exposure for children with iNS. Specifically, by focusing on LEVs as emerging biomarkers of cellular stress, I have furthered the understanding of iNS at the molecular level. Specifically, we now understand that LEVs are released from podocytes under times of stress (both in humans and recapitulated *in vitro*). Understanding this allows for further studies targeted at LEV cargo as markers reflective of podocyte injury, without the need for biopsy. Another major contribution of my work is the discovery that mitochondrial stress in podocytes associates with loading of mtDNA into LEVs. This was further observed not only *in vitro*, but also in a rat model of nephrosis, and in clinical specimens from children with iNS. This novel link between mitochondrial bioenergetic stress and LEV-mtDNA provides potential mechanistic insight which can be ascertained non-invasively. Further, this observation may also allow for future interventions targeted at mitochondrial stress in children with iNS. Lastly, proteomic analysis of vesicles derived from podocytes *in vitro* as well as from clinical urine specimens from children with iNS revealed distinct proteomic transformations under disease conditions. The identification of hundreds of proteins unique to either relapse, remission, or prednisolone therapy

(*in vitro*) offers valuable insight into the pathomechanism of iNS in children. These findings advance a growing view in nephrology that EVs are active players in cell-to-cell communication and disease modulation. Therefore, overall, my work has identified podocyte EVs as emerging tools to further improve our clinical approach to iNS in children, but also contributes to mechanistic, fundamental understanding of podocyte biology in the context of disease.

8 Conclusions

In summary, iNS is the most common glomerulopathy in children and has an unclear etiology. Importantly, children are treated with large doses of steroids at first presentation, and if deemed steroid sensitive, may experience several relapses with resultant iterative treatment courses, resulting in significant cumulative steroid doses with untoward side effects. Clinical and molecular markers for pediatric iNS are lacking; however, herein I have shown the emerging potential of LEVs. These findings lay important groundwork for the development of non-invasive biomarkers which will allow for reduction of cumulative steroid doses in children with iNS.

9 Appendix

9.1 Supplementary papers

9.1.1 Diastolic hypertension is associated with proteinuria in pediatric patients

Myette RL, Burger D, Geier P, Feber J. Diastolic hypertension is associated with proteinuria in pediatric patients. Health Sci Rep. 2021 Aug 9;4(3):e346. doi: 10.1002/hsr2.346. PMID: 34401524; PMCID: PMC8351612. Open access.

Running head: Arterial hypertension in proteinuric pediatric patients

Robert L. Myette[1,2], Dylan Burger[2], Pavel Geier[1], Janusz Feber[1]

[1]Division of Nephrology, Department of Pediatrics, Children's Hospital of Eastern Ontario, University of Ottawa, Ottawa, Canada

[2]Kidney Research Center, Department of Cellular and Molecular Medicine, The Ottawa Hospital Research Institute, University of Ottawa, Ottawa, Canada

Corresponding author

Dr. Janusz Feber

Division of Nephrology, Department of Pediatrics

Children's Hospital of Eastern Ontario, University of Ottawa,

401 Smyth Road

Ottawa, ON, K1H8L1

E-mail: jfeber@cheo.on.ca.

Keywords

Proteinuria, pediatrics, diastolic hypertension

Disclosure and Funding Statement:

The authors have no pertinent disclosures to make. The authors have no source of funding to declare.

Author Contributions:

Conceptualization: Robert Myette, Dylan Burger, Pavel Geier, Janusz Feber

Formal Analysis: Robert Myette, Janusz Feber

Funding Acquisition: not applicable

Writing – review and editing: Robert Myette, Dylan Burger, Pavel Geier, Janusz Feber

Writing –original draft: Robert Myette, Dylan Burger, Pavel Geier, Janusz Feber

All authors have read and approved the final version of the manuscript. Janusz Feber and Robert Myette had full access to all of the data in this study and take complete responsibility for the integrity of the data and the accuracy of the data analysis.

Robert Myette affirms that this manuscript is an honest, accurate and transparent account of the study being reported; that no important aspects of the study have been omitted; and that any discrepancies from the study as planned (and, if relevant) have been explained.

The authors confirm that the data are available upon request.

Abstract

Background and Aims: Blood pressure lability has been observed in certain cohorts of pediatric patients with variable degrees of proteinuria; however, the impact of proteinuria on blood pressure is not fully elucidated. The objective of our study was to analyze blood pressure and heart rate in pediatric patients with proteinuria.

Methods: We performed a retrospective chart review of patients (age 1-18) diagnosed with idiopathic nephrotic syndrome, with varying degrees of proteinuria. Blood pressure and heart rate data were analyzed in relation to anthropometric and biochemical parameters. A total of 72 urine sample analyses, along with associated blood pressure measurements, were obtained from the charts of 33 children (males=25).

Results: Diastolic blood pressure Z-scores were significantly higher in proteinuric patients (urine protein/creatinine > 0.02 g/mmol) compared to non-proteinuric patients (p=0.006; Cohen-d 0.97 (0.41; 1.53)). Systolic blood pressure was also significantly higher in proteinuric patients (p = 0.04), but with a less significant effect size (Cohen-d 0.54 (-0.002; 1.08)). Proteinuria (>0.02g/mmol) was the most significant predictor of diastolic (β=0.79, p=0.04), but not systolic blood pressure elevation on multivariate analysis.

Conclusions: We observed a disproportionate increase in diastolic blood pressure versus systolic blood pressure in patients with proteinuria.

Introduction

Proteinuria in children is defined as a urinary protein to creatinine ratio (UPrCr) > 0.02 g of protein / mmol (1). Proteinuria can reflect glomerular inflammation or injury and is transient, or progressive. One of the most common causes of proteinuria in children is nephrotic syndrome (NS), which has been shown to be associated with hypertension (2).

Traditionally, it is believed that arterial hypertension leads to proteinuria; however, in most instances, children with NS do not suffer from primary hypertension. Yet, they may develop increased arterial blood pressure (BP) throughout the course of NS (2–4). Blood pressure lability has been observed in these cohorts of pediatric patients with variable degrees of proteinuria; however, the impact of proteinuria on blood pressure is not fully elucidated (2–4). Clarifying this further may impact therapeutic approaches for hypertension in patients with proteinuria, even if it is only transient.

Thus, the objective of our study was to analyze BP in proteinuric patients to determine the propensity for isolated systolic, diastolic, or combined arterial hypertension and to assess whether SBP or DBP elevations are associated with the degree of proteinuria.

Methods

Data for this study were collected retrospectively from all patients who had been consecutively enrolled in an ongoing prospective, observational study on NS at The Children's Hospital of Eastern Ontario (CHEO), in Ottawa, Ontario, Canada, between Sept 2019 and March 2020. We enrolled children aged 1-18 with incident or prevalent idiopathic NS. Children with NS secondary to glomerulonephritis, infection or medications were excluded. A research ethics board application (*CHEO REB: 18/168X*) was approved and all patients consented or assented to enrollment in the ongoing prospective, observational trial. If the patients were too young to consent or assent, their parents or guardians consented to their enrolment. This retrospective study is an ancillary analysis of the ongoing, prospective study on NS.

Demographic data, biochemical data, BP and heart rate (HR) measurements were obtained from the chart of enrolled patients. Body mass index (BMI) was calculated from the weight in kilograms and the height in meters (kg/m^2). The BP/HR measurement and biochemical data were associated with the urine sample analysis contributed at the same clinic visit. Because of this, individual patients could have one (or more) urine samples analyzed as proteinuric and one (or more) as non-proteinuric, depending on the degree of proteinuria at the time of the provided urine sample (i.e., Patient 1 can be proteinuric when giving urine sample 1 and 2, but once in remission, can be non-proteinuric for urine sample 3.

Because this was a minimal risk study, blood work obtained for routine clinical practice was evaluated when available, but patients did not provide blood samples for the purpose of the study. The following biochemical results were analyzed: urea, creatinine, Cystatin-C eGFR (GFR), serum sodium, cholesterol, serum albumin and hemoglobin. Urine protein was analyzed using a Roche C401 analyzer. Other information obtained from the charts were: Prednisone exposure

(yes/no; 33 samples obtained from patients on varying doses of prednisone) and Prednisone dose (mg/m^2/day or other day). None of our patients were being treated with antihypertensive agents, but some were on maintenance Tacrolimus (25 samples obtained from patients on tacrolimus, while only 4 were on both Tacrolimus and Prednisone at any one time when a sample was obtained).

Classification of patients/events

All samples came from 33 patients (25 males) with idiopathic NS (1 with query FSGS on biopsy, 21 with biopsy-proven minimal change disease, and 11 with presumed minimal change disease).

We evaluated BP and biochemical parameters in relation to proteinuria based on each random urine sample obtained. Sixteen patients contributed multiple urine samples (range 2-8), while 17 patients contributed a single urine sample. As the median time between repeated samples was 20 days (14;32) and the clinical status of a nephrotic syndrome patient may change very quickly within days, we considered each urine sample as independent (even though some samples were obtained from the same patient) and analyzed for proteinuria in concert with other anthropometric, biochemical and HR/BP data associated with that urine sample (i.e., A patient contributes a urine sample, blood work, a BP and a HR measurement at a single clinic visit).

For the primary analysis, samples were divided based on presence or absence of proteinuria: PROT (UPrCr >0.02g/mmol (>0.2 mg/mg) versus NOPROT (UPrCr ≤0.02 g/mmol (≤0.2 mg/mg)). For the secondary analysis, samples were divided based on the presence of nephrotic range proteinuria: NEPH (UPrCr >0.2g/mmol (>2 mg/mg)) versus NONEPH (UPrCr ≤0.2 g/mmol (≤2 mg/mg)) to observe for the effect of heavy proteinuria on blood pressure. SBP and

DBP Z-scores were then analyzed in relation to UPrCr to assess for influence of the degree of proteinuria on BP.

Blood pressure and heart rate measurement

BP and HR measurements were obtained in the clinic by the same two experienced nurses using an automatic BP device (Dinamap, GE Healthcare). BP was measured 1-3 times within 5 minutes in a quiet position on the non-dominant arm. An average of multiple BP measures obtained during the clinic visit were taken into analysis, unless the patient had a single measurement (only two patients). Although not optimal, we accepted the contribution of a single BP measurement as it is in keeping with published, normative data for BP in children (5).

All BP values (mmHg) and HR values (beats per minute) per a given sample were then converted into Z-scores (5,6). Elevated BP and HR values were defined as Z-scores > 1.65. Pulse pressure (PP) was calculated according to the standard formula (SBP-DBP) and expressed in mmHg.

Statistical analyses

Continuous variables were expressed as mean ± standard deviation (SD) or median (interquartile range, IQR) for non-normal distributions; the normal/non-normal distribution of variables was analyzed with the Shapiro-Wilk test. Group differences between SBP or DBP Z-scores in PROT versus NOPROT and NEPH versus NONEPH events were assessed using Student's t-test for normally distributed variables or the Wilcoxon rank-sum test for non-normally distributed variables. Effect size of the difference between variables was assessed using Cohen-d. The relationship between SBP and DBP Z-scores was analyzed using linear regression. We also performed univariate and multivariate linear regression analysis to analyze predictors of SBP and DBP Z-

score elevations. Lastly, we evaluated a receiver operating characteristic (ROC) curve for categorical outcome variables DBP hypertension (DBP Z-score > 1.65), and SBP hypertension (SBP Z-score > 1.65), using proteinuria as a classifier of these binary outcomes. Areas under the curve (AUC) for DBP and SBP were compared using a bootstrap method with 2000 resamples (pROC package in R). A p-value of <0.05 was considered as statistically significant. All tests were performed using R and Python, and associated packages (7).

Results

A total of 72 urine sample results with associated BP measurements were analyzed. BP and biochemical data associated with the time of urine sample collection are summarized in Table 1.

There was no significant difference between age, height, weight and BMI at the time of urine sample collection in the NOPROT versus PROT groups. Renal function assessed by urea, creatinine and GFR was not significantly different between the NOPROT and PROT groups (Table 1). There was also no difference in serum sodium or hemoglobin levels.

The mean ± SD SBP, and DBP Z-score associated with all samples for the entire cohort of patients was 0.33 ± 0.98 and 0.65 ± 1.0, respectively. In the NOPROT urine sample group, the mean ± SD SBP Z-score was 0.19 ± 0.98 while the PROT urine sample group had a mean ± SD SBP Z-score of 0.72 ± 0.89 (p = 0.042, Cohen-d 0.54 (-0.002; 1.08). The DBP Z-score difference between NOPROT and PROT group samples was even higher with a mean (SD) DBP Z-score of 0.41 ± 0.79 vs 1.33 ± 1.25, (p=0.006; Cohen-d 0.97 (0.41; 1.53)) (Figure 1). In the PROT group, SBP was elevated (>1.65 Z score) in 3/19 (15%) samples, whereas DBP was elevated in 8/19

(42%) samples. Of these 19 PROT group samples, 7 (37%) were associated with only DBP hypertensive values, 1 (5%) was associated with combined SBP and DBP hypertensive values, and 1 (5%) was associated with isolated SBP hypertensive values.

To further analyze the relationship between SBP and DBP Z-scores, we plotted the SBP Z-scores against the DBP Z-scores with a line of identity for reference (Figure 2). The regression analysis showed a significant correlation between DBP and SBP Z-scores ($R = 0.44$, $p < 0.01$), but also a significant skew towards a greater change in DBP Z-scores in relation to the change in SBP Z-scores. Lastly, we used ROC analysis to determine the AUC for proteinuria as a classifier of the binary outcomes, SBP hypertension or DBP hypertension. We noted excellent discriminatory ability between the continuous variable proteinuria, and DBP hypertension (AUC = 0.81), where the association between proteinuria and SBP hypertension was non-discriminatory (AUC = 0.57), the difference between AUCs was significant at p=0.029 (Figure 3).

Additionally, we analyzed the data with nephrotic range proteinuria cut-offs (NEPH and NONEPH). The creatinine, GFR and urea were not significantly different; whereas cholesterol was higher, and serum albumin and serum sodium were lower (data not shown). The NONEPH median (IQR) DBP Z-score was 0.40 (-0.1;1.0) while the NEPH median (IQR) DBP Z-score was 1.6 (0.94;1.84, $p = 0.03$). For SBP, the median (IQR) NONEPH Z-score was 0.40 (-0.5,0.9) and the median (IQR) NEPH Z-score was 0.57 (0.37;0.71, $p = 0.49$).

To better delineate the effect of the degree of proteinuria on BP, we assessed the changes in both SBP and DBP Z-scores vs. UPrCr. On linear regression, there was no statistically significant association between the degree of proteinuria and SBP (p=0.28), but there was a significant association with DBP and UPrCr (p=0.03). We evaluated other clinically relevant parameters in univariate analyses with outcomes of SBP Z-score or DBP Z-score, as outlined in Table 2. Briefly,

we noted no significant relationship between the independent variable prednisone exposure, or varying doses of prednisone on the SBP Z-score but did note a borderline significant association with BMI (p=0.05). Not surprisingly, on multivariate analysis with similar independent variables, there was no signal (p>0.05). On univariate analysis with the dependent variable DBP Z-score, we noted a significant relationship with proteinuria (p=0.03) and 60mg/m^2 prednisone daily (p=0.009). There was a borderline significant association with prednisone (yes/no) (p=0.05). When taking these 3 independent variables into multivariate regression analysis, the only significant association was between proteinuria and DBP Z-score (p=0.04), with high-dose prednisone being borderline significant (p=0.06). We analyzed the effect of Tacrolimus on blood pressure in univariate analysis and found a negative association with SBP Z-score (β= -0.48, p=0.04), and DBP Z-score (β= -0.59, p=0.01).

We observed a significant difference in absolute HR values (p = 0.02) but only a trend in HR Z-score differences (p>0.05) between PROT and NOPROT samples (Table 1). Heart rate Z-score did not correlate with SBP Z-score but correlated well with DBP Z-scores (p = 0.0003).

In considering the impact of body mass on BP in our cohort, we examined the SBP and DBP Z-scores, with cut-offs for BMI above or below 25 kg/m^2. Of importance, there was no statistically significant differences in the SBP Z-scores between those with a BMI>25 kg/m^2, and those with a BMI<25 kg/m^2. When analyzing this for DBP, there was also no significant difference (p=0.55). Taken further, we examined this in NOPROT and PROT groups, and similarly found no significant difference (p>0.05) in either SBP or DBP Z-scores between those patients who had BMI above or below 25 kg/m^2. Similar non-significant results were obtained at a threshold BMI above, or below, 20 kg/m^2. Because of the known association with weight and BP, we analyzed the standard deviation (SD) between weights for children who contributed more than one sample,

as well as the coefficient of variation (CV=SD/mean). There was no significant correlation between SD, or CV, and the SBP and DBP Z-scores.

Discussion

The main finding of our study is that children in our cohort had significantly elevated BPs at the time of proteinuria, and the DBP elevation is disproportionately higher than the SBP elevation.

Previous studies have identified, and attempted to characterize, hypertension in both pediatric and adult patients with nephrotic syndrome (2–4,8,9). Cameron *et al.* noted significantly elevated BP measurements in 31% of patients older than 15 years of age in their study of minimal change disease (10), and this seemed to coincide with the proteinuric state. Additionally, between 10-30% of pediatric patients with steroid-resistant NS, or genetic forms of NS, were hypertensive on presentation on analysis of the PodoNet registry data (9). Shatat *et al*, also highlighted the prevalence of hypertension in a cohort of patients with FSGS (11). These studies did not highlight specific differences between systolic and diastolic hypertension and did not comment whether there was a propensity for disproportionate DBP elevations.

When focusing on DBP elevations, an analysis on the report of the International Study of Kidney Disease in Children (ISKDC) revealed diastolic hypertension, defined as >98th percentile, in 26.2% of patients with heavy proteinuria (12.8% of children with minimal change disease and in 13.4% of those with FSGS) (12). Diastolic hypertension was further described by Flynn (13) on analysis of the Chronic Kidney Disease in Children Study (CKiD) where they noted hypertension in 28% of patients with nephrotic range proteinuria (14% diastolic, 14% systolic). The association between proteinuria and diastolic hypertension was confirmed in our study where the degree of

BP elevation was significantly skewed towards DBP elevations (Figure 2). DBP Z-scores were disproportionately higher than the SBP Z-scores in the PROT group, suggesting proteinuria has a greater impact on DBP. Additionally, we noted a high number of PROT patient samples had isolated DBP elevations (37%), whereas isolated SBP elevation was associated with only 1 (5%) PROT patient sample. In contrast to the aforementioned studies (ISKDC, CKiD), where some patients had renal insufficiency, or were treated for hypertension, all our patients had normal renal function, and none were treated for hypertension at the time of urine sampling, nor were known to be hypertensive prior to entering the study.

The etiology of hypertension in patients with NS is probably multifactorial. It has been suggested that hypertension in proteinuric patients is related to acute issues (fluid shifting), but also may be related to chronic changes, such as renal injury secondary to progression of underlying renal disease (14). We explored the possible impact of weight (fluid) on BP in our cohort. Those patients who contributed more than one sample, also contributed more than one weight. We analyzed the difference in weight, relative to the difference in BP, using absolute weight values, CV and SD, and found no significant correlation with BP.

Taken further, patients with NS have significant co-morbid conditions and medication exposures which may have an impact on BP dynamics. Using univariate regression analysis, we noted a significant relationship between proteinuria ($p=0.03$) and elevations in DBP Z-score, but no impact from steroid exposure as a categorical variable ($p=0.05$). We did, however, note a significant association between high-dose prednisone and DBP Z-score elevation on univariate analysis (Table 2). The apparent negative association with Tacrolimus and SBP and DBP Z-score is likely explained by the fact that most patients on Tacrolimus did not have proteinuria. The multivariate analysis for SBP Z-score elevations (Table 2) revealed no impact from proteinuria, BMI or

prednisone exposure ($p>0.05$). However, the multivariate analysis for the dependent variable DBP Z-score (Table 2), revealed that proteinuria ($p=0.04$) was the only significant variable in the model, with a trend towards an association with high dose prednisone. Taken further, we identified proteinuria as an excellent discriminator for the binary outcome DBP hypertension, whereas it was non-discriminatory for SBP hypertension. This fits with our existing hypothesis that the effect of proteinuria on BP is skewed towards a more significant impact on DBP.

It is tempting to hypothesize that the disproportionately elevated DBP Z-score and absolute HR elevations may be related to endothelial dysregulation and vasoconstriction; however, we were unable to analyze for direct markers of endothelial injury or vasoconstriction. When examining the HR of patients with proteinuria, we did note a significant difference in absolute HR between patients with proteinuria and those without, with a significant effect size (Cohen-d = 0.75). When converted to HR Z-scores, the p value was insignificant, but the effect size was still of medium significance (Cohen-d = 0.45, Table 1). We also noted a significant correlation between HR Z-scores and DBP Z-scores ($p = 0.0002$), but no correlation between SBP Z-scores and HR Z-scores.

Our study is limited due to the retrospective nature of data collection, and the relatively small number of patients. Also, we analyzed proteinuric and non-proteinuric patients with a background of nephrotic syndrome only; whether this applies to other groups of patients with proteinuria remains to be determined. Strengths of our study include a detailed SBP, DBP, PP and HR analysis using classic point estimate assessments and comparison of effect sizes using Cohen-d.

In summary, we observed a disproportionate increase in diastolic versus systolic blood pressure in NS patients with varying degrees of proteinuria.

References

1. Andolino TP, Reid-Adam J. Nephrotic syndrome. Pediatr Rev [Internet]. 2015 Mar;36(3):117–25. Available from: http://www.ncbi.nlm.nih.gov/pubmed/25733763

2. Shatat IF, Becton LJ, Woroniecki RP. Hypertension in childhood nephrotic syndrome. Front Pediatr. 2019;7(JULY):1–9.

3. Monthe Kontchou L, Liccioli G, Pela I, Kontchou LM, Liccioli G, Pela I. Blood Pressure in Children with Minimal Change Nephrotic Syndrome during Oedema and after Steroid Therapy: The Influence of Familial Essential Hypertension. Kidney Blood Press Res. 2009;32(4):258–62.

4. Keshri S, Sharma S, Agrawal N, Bansal S, Guilliani BP, Aggrawal KC. Hypertension and its severity in children with steroid sensitive nephrotic syndrome during remission. Clin Exp Nephrol [Internet]. 2018;22(5):1157–62. Available from: http://dx.doi.org/10.1007/s10157-018-1565-3

5. Flynn JT, Falkner BE. New Clinical Practice Guideline for the Management of High Blood Pressure in Children and Adolescents. Hypertension [Internet]. 2017 Oct;70(4):683–6. Available from: https://www.ahajournals.org/doi/10.1161/HYPERTENSIONAHA.117.10050

6. Ostchega Y, Porter KS, Hughes J, Dillon CF, Nwankwo T. Resting pulse rate reference data for children, adolescents, and adults: United States, 1999-2008. Natl Health Stat Report. 2011;(41):1999–2008.

7. Vallat R. Pingouin: statistics in Python. J Open Source Softw [Internet]. 2018 Nov 19;3(31):1026. Available from: http://joss.theoj.org/papers/10.21105/joss.01026

8. Kuster S, Mehls O, Ritz E. Blood pressure in minimal change and other types of nephrotic syndrome. Clin Exp Hypertens - Part A Theory Pract. 1990;12(3):500.

9. Trautmann A, Bodria M, Ozaltin F, Gheisari A, Melk A, Azocar M, et al. Spectrum of steroid-resistant and congenital nephrotic syndrome in children: The podoNet registry cohort. Clin J Am Soc Nephrol. 2015;10(4):592–600.

10. Cameron JS, Turner DR, Ogg CS, Sharpstone P, Brown CB. The nephrotic syndrome in adults with 'minimal change' glomerular lesions. Qjm. 1974;43(3):461–88.

11. Shatat IF, Schoeneman M, Flynn JT, Woroniecki RP. Association of steroid and cyclosporin resistance in focal segmental glomerulosclerosis. Pediatr Nephrol. 2007;22(6):834–9.

12. Barnett HL, Edelmann CM, Greifer I. Primary nephrotic syndrome in children: Clinical significance of histopathologic variants of minimal change and of diffuse mesangial hypercellularity. Kidney Int. 1981;20(6):765–71.

13. Flynn JT, Mitsnefes M, Pierce C, Cole SR, Parekh RS, Furth SL, et al. Blood pressure in children with chronic kidney disease: A report from the Chronic Kidney Disease in Children study. Hypertension. 2008;52(4):631–7.

14. Laffer CL, Scott RC, Titze JM, Luft FC, Elijovich F. Hemodynamics and Salt-and-Water Balance Link Sodium Storage and Vascular Dysfunction in Salt-Sensitive Subjects. Hypertension. 2016;68(1):195–203.

Tables

Table 4. **Table 1. Biochemical and Clinical Characteristics**

Clinical Information	Overall	NOPROT	PROT	P	Cohen-d (C.I.)
Age (years)	9.0 (5;12)	9.0 (6;13)	9.0 (3;10)	0.131	0.42 (-0.12;0.95)
Height (cm)	135 ± 27	138 ± 25	126 ± 28	0.100	0.48 (-0.05;1.02)
Weight (kg)	31 (21;53)	32 (22;53)	27 (21;51)	0.557	0.19 (-0.35;0.72)
BMI (kg/m^2)	17.6 (16;21)	17 (15;20)	19 (16;22)	0.100	-0.39 (-0.94;0.14)
CysC-eGFR (ml/min/1.73m^2)	94 ± 16	91 ± 13	108 ± 22	0.218	-1.15 (-1.72;-0.58)
Creatinine (umol/L)	48 (37;54)	48 (41;54)	39 (32;48)	0.316	0.49 (-0.05;1.03)
Urea (mmol/L)	4.8 ± 1.2	4.8 ± 1.0	4.9 ± 1.9	0.916	-0.07 (-0.61;0.46)
Na (mmol/L)	140 ± 2.2	140 ± 1.6	139 ± 3.7	0.445	0.59 (0.05;1.13)
Cholesterol (mmol/L)	3.8 (3.6;4.5)	3.8 (3.6;4.4)	3.7 (3.5;12.8)	0.976	-1.52 (-2.11;-0.93)
Serum Albumin (g/L)	42 (40;44)	42 (40;44)	36 (13;44)	0.344	1.41 (0.83;1.99)
Hgb (g/L)	131 ± 12	129 ± 12	138 ± 8.4	0.153	-0.74 (-1.29;-0.19)
SBP (mmHg)	102 (96;107)	102 (96;107)	103 (96;108)	0.758	-0.17 (-0.71;0.36)
SBP Z score	**0.33 ± 0.98**	**0.19 ± 0.98**	**0.72 ± 0.89**	**0.042**	**0.54 (-0.002;1.08)**
DBP (mmHg)	**64 ± 7.9**	**63 ± 7.6**	**68 ± 7.9**	**0.01**	**0.67 (0.13;1.22)**
DBP Z score	**0.65 ± 1.0**	**0.41 ± 0.79**	**1.33 ± 1.25**	**0.006**	**0.97 (0.41;1.53)**
HR (bpm)	**97 ± 19**	**94 ± 17**	**107 ± 22**	**0.02**	**0.75 (0.20;1.30)**
HR Z score	0.99 ± 1.35	0.83 ± 1.27	1.44 ± 1.49	0.135	0.45 (-0.08;0.99)
PP (mmHg)	41 (31;44)	41 (34;44)	36 (31;44)	0.454	0.26 (-0.27;0.80)

Data shown are mean ± SD for normally distributed variables, median (IQR) for non-normally distributed variables. Comparisons are made with unpaired t-tests (normally distributed variables) or Mann-Whitney U-test (non-normally distributed variables). Cohen d expressed as mean effect size with 95%ile confidence intervals in brackets. NOPROT = UPrCr ≤ 0.02 g/mmol of Cr, PROT = UPrCr > 0.02 g/mmol of Cr. BMI = body mass index. CysC-eGFR = Cystatin C estimated glomerular filtration rate. Na = sodium. Hgb = hemoglobin. SBP = systolic blood pressure. DBP = diastolic blood pressure. HR = heart rate. PP = pulse pressure. P<0.05 considered significant.

Table 5. **Table 2. Linear Regression Analysis**

Variable	Estimate	Standard Error	T	P value
A) Univariate Analysis: Outcome SBP Z-score				
Proteinuria	0.43	0.38	1.09	0.28
Prednisone	-0.32	0.23	-1.38	0.17
BMI	0.05	0.03	1.95	0.05
Prednisone 1	0.17	0.30	-0.54	0.58
Prednisone 2	0.04	0.32	0.13	0.90
Prednisone 3	-0.55	0.34	-1.59	0.12
B) Univariate Analysis: Outcome DBP Z-score				
Proteinuria	**0.89**	**0.39**	**2.27**	**0.03**
Prednisone	0.46	0.24	1.98	0.05
BMI	-0.03	0.03	-0.98	0.33
Prednisone 1	**0.80**	**0.30**	**2.68**	**0.009**
Prednisone 2	0.02	0.33	0.05	0.96
Prednisone 3	-0.04	0.36	-0.12	0.90
C) Multivariate Analysis: Outcome DBP Z-Score				
Proteinuria	**0.79**	**0.38**	**2.07**	**0.04**
Prednisone	0.14	0.26	0.52	0.60
Prednisone 1	0.66	0.34	1.95	0.06

Data shown are from the univariate and multivariate regression analysis with Estimate, Standard Error, T-value and p value included. The outcome measure is either SBP Z-score or DBP Z-score, as labelled. A) Univariate analysis with several clinically relevant variables, with an outcome measure of SBP Z-score. B) Univariate analysis with several clinically relevant variables, with an outcome measure of DBP Z-score. C) Multivariate analysis including the significant univariate variables, and the borderline significant variable Prednisone. Significant results bolded, $p<0.05$. BMI=body mass index. Prednisone = yes/no variable. Prednisone 1=60mg/m^2/day. Prednisone 2=40mg/m^2/other day. Prednisone 3=less than 40mg/m^2/day. Proteinuria = UPrCr >0.02 g/mmol.

Figure 24. **Figure 1. SBP and DBP Z-scores in patients with NOPROT versus PROT**

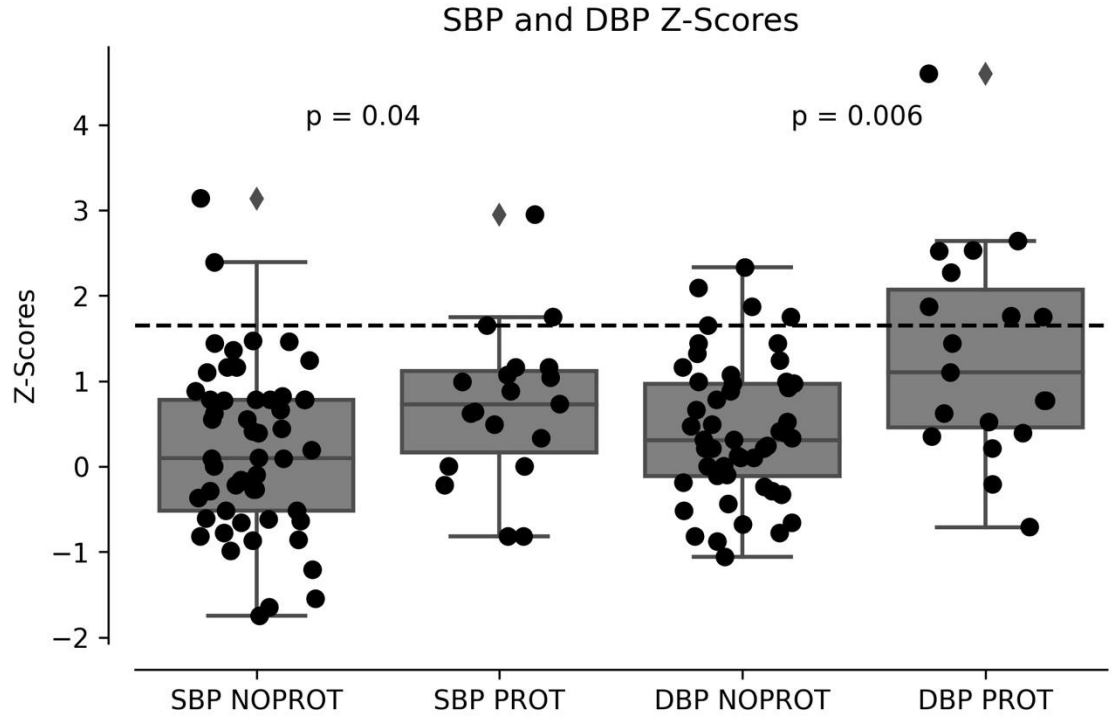

Figure 25. **Figure 2. SBP Z-scores versus DBP Z-scores in comparison with the line of identity as reference**

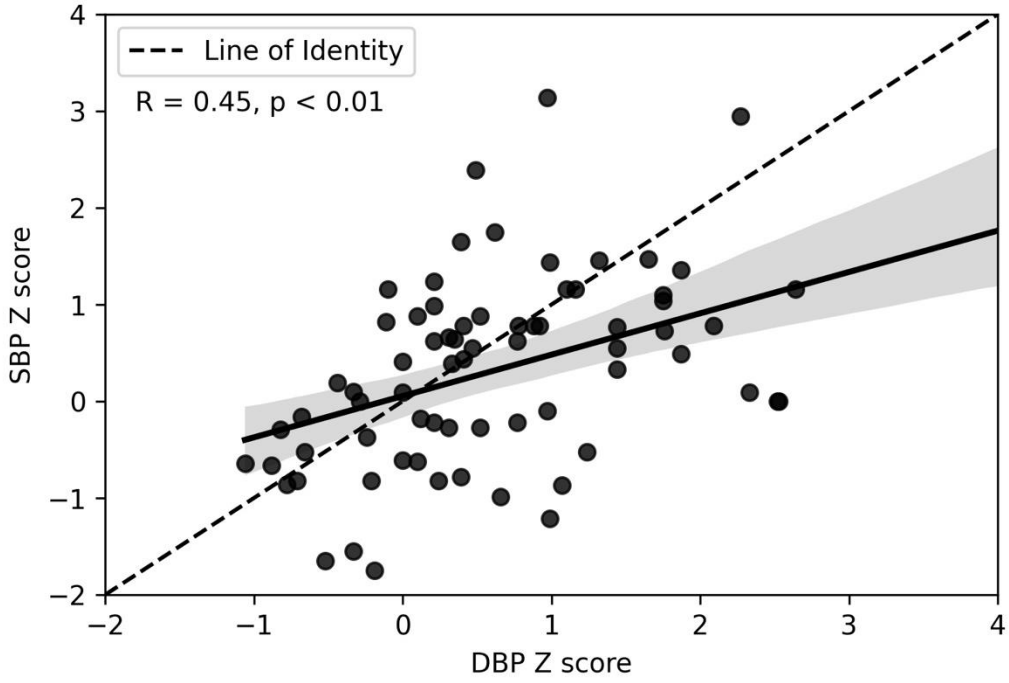

Figure 26. **Figure 3. Receiver operating characteristic analysis for categorical outcome DBP hypertension, or SBP hypertension, with urinary protein to creatinine ratio as a classifier**

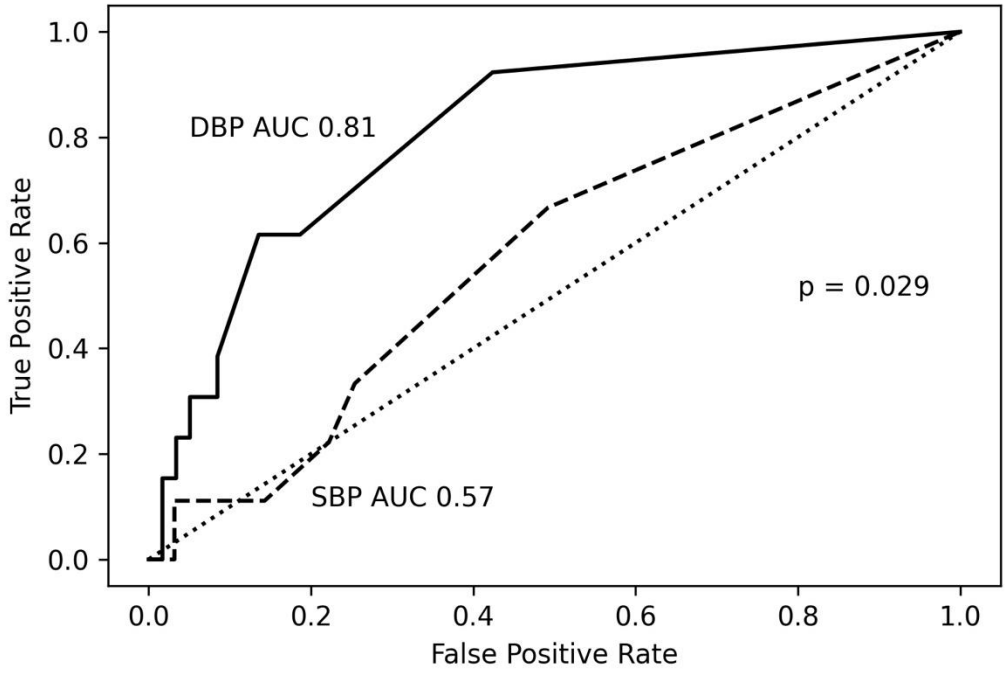

Figure 1. SBP and DBP Z-scores in patients with NOPROT versus PROT. SBP (left) and DBP (right) Z-scores between patients with NOPROT and PROT. Dotted line indicates Z-score 1.65. PROT refers to a UPrCr > 0.02 g/mmol.

Figure 2. SBP Z-scores versus DBP Z-scores in comparison with the line of identity as reference. Shaded area is the 95th percent confidence interval.

Figure 3. Receiver operating characteristic analysis for categorical outcome DBP hypertension, or SBP hypertension, with urinary protein to creatinine ratio as a classifier. DBP = diastolic blood pressure. SBP = systolic blood pressure. AUC = area under the curve. Hypertension defined as Z-score > 1.65.

9.1.2 Relapse in steroid-sensitive nephrotic syndrome: are extracellular vesicles the missing link?

Robert L. Myette MSc, MD, FRCPC[1,2], Dylan Burger, PhD[2]

[1]Division of Nephrology, Department of Pediatrics, Children's Hospital of Eastern Ontario, University of Ottawa, Ottawa, Canada

[2]Kidney Research Center, Department of Cellular and Molecular Medicine, The Ottawa Hospital Research Institute, University of Ottawa, Ottawa, Canada

Corresponding Author:

Dylan Burger, PhD

Senior Scientist and Associate Professor

Kidney Research Centre, The Ottawa Hospital Research Institute

Department of Cellular and Molecular Medicine, University of Ottawa

2513-451 Smyth Rd. Ottawa, ON, Canada

613-562-5800 x8241

dburger@uottawa.ca

This is a non-final version of an article published in final form in AJP-Renal: Relapse in steroid-sensitive nephrotic syndrome: are extracellular vesicles the missing link? Robert L. Myette and Dylan Burger. American Journal of Physiology-Renal Physiology 2021 321:5, F656-F658

Pediatric Nephrotic Syndrome (NS) is a podocytopathy and represents one of the most common forms of glomerular dysfunction in children[1]. Idiopathic NS is the most common form and is comprised of glomerular foot process effacement evident on renal biopsy. Children with idiopathic NS have massive proteinuria with subsequent hypoalbuminemia, and edema. This can lead to secondary issues, including hypercholesterolemia, increased risk of infection and venous thromboembolism and the potential for acute kidney injury[1]. The approach to children with NS is largely the same across the globe. Children with a typical presentation are treated with steroids and assessed for responsiveness across a 4–8-week window. It is only after this window that children can be categorized, broadly speaking, as steroid sensitive or steroid resistant[1]. Complicating the matter further is the yet characterized pathophysiology of idiopathic NS, with no tools available to determine which patients will go on to have a relapsing and remitting course as opposed to those who will be successfully treated after a single course of steroids. This heterogeneity is not otherwise explained by initial presenting features or genetics, and there appears to be subgroups within steroid resistant, or steroid sensitive patients, making prognostication even more difficult[1].

The present understanding of pediatric idiopathic NS is often debated, but most researchers and clinicians agree there appears to be an underlying circulating 'factor' which is important for the development of NS and for relapse. This 'factor' has been purported to be a cytokine[2], a soluble mediator[1], or possibly the Epstein-Barr Virus (EBV)[3], however this remains an active area of investigation.

One possible link is signaling through extracellular vesicles (EVs) such as exosomes, apoptotic bodies, or microparticles[4]. EVs have been extensively studied as surrogate measures of cell stress/injury but also as bioactive factors that exert downstream effects on target cells[4]. The

use of EVs to study pediatric NS is limited. Santorelli *et al*[5], recently investigated urinary EVs (uEV) in children with idiopathic NS, and found specific protein signatures that discriminated various clinical subgroups (steroid sensitive NS, steroid dependent NS and steroid resistant NS). Prior to this, Chen *et al*[6], reported that uEV microRNAs (miR-194-5p, miR-146b-5p, miR-378a-3p, miR-23b-3p and miR-30a-5p) were increased in children with idiopathic NS compared with healthy age- and sex-matched controls. These studies focused on the use of uEVs as biomarkers; however, studies focused on disease mechanisms involving plasma EVs have been lacking.

In the current issue of the *American Journal of Physiology-Renal Physiology,* Eroglu *et al* studied plasma EVs from 20 children with steroid sensitive NS (SSNS) in both relapse and remission, and compared those EVs with 10 healthy controls, and 6 disease controls (a mixture of membranous nephropathy and Henoch-Schonlein Purpura nephritis). The authors isolated and robustly characterized EVs using serial ultracentrifugation and electron microscopy, flow cytometry and western blotting analysis. Further, major proteins isolated from the plasma were identified using mass spectrometry, and gene ontology classification was utilized for assessment of relapse EVs. RAC-GTP was noted to be significantly increased in relapse EVs compared to remission and disease control EVs, highlighting relapse EVs selectively transmit protein signals involved in cytoskeletal rearrangement. Using an immortalized human podocyte culture, treatment with relapse EVs was shown to induce significantly enhanced motility and albumin permeability, recapitulating key features of clinical relapse *in vitro*.

Importantly, with ongoing discussions about the best ways to isolate, characterize and study EVs[7]; the authors have employed best practices for their characterization of the EVs. Their methodology allows for a clear, stepwise understanding of how they have reliably shown relapse

EVs to recapitulate disease *in vitro*. However, important questions remain related to how this putative mechanism could occur in pediatric patients with NS *in vivo.*

The glomerular filtration barrier is a highly specialized and selective filtration barrier responsible for effective filtration and creation of urine consisting mainly of waste products. A healthy glomerular filtration barrier allows for molecular complexes < 6.4 nanometers in diameter, and under 70 kilodaltons in size to traverse it. Given this, one wonders how plasma EVs, whose sizes range from ~20 nm to 1000 nm, would be able to exert an effect on the glomerulus, when approaching from the systemic vasculature (Figure 1). Such an effect would either require that the integrity of the pores be compromised or for a transport system of some kind. While such a system has not been described to date, it is worth noting that there is experimental evidence suggesting that circulating EVs may indeed cross the glomerular filtration barrier. Oosthuyzen *et al.* reported in 2016 that fluorescently labelled EVs appeared in urine as well as kidney tissue when injected systemically in mice[8]. More directly, the Bussolati group employed a 3-dimensional perfused glomerulus model and observed that mesenchymal stromal cell EVs could pass through the filtration barrier[9]. Thus, there exists, at least a theoretical mechanism by which systemic EVs may influence podocyte function.

Taken together, this novel and exhaustive characterization of plasma "relapse EVs", highlights their effect on *in vitro* podocyte culture. The concept of a circulating factor has dominated the Pediatric NS literature for decades; however, to date, no candidate mediator has been successfully, or convincingly, isolated. Eroglu and colleagues bring the field forward with their study and show that EVs may potentially represent the missing link to better understand relapsing disease. Nevertheless, further studies are needed to verify that circulating EVs can influence podocyte signaling and to confirm the *in vivo* relevance of this novel signaling pathway.

Citations:

1. Noone, D. G., Iijima, K. & Parekh, R. Idiopathic nephrotic syndrome in children. *Lancet* **392**, 61–74 (2018).
2. Agrawal, S. *et al.* Plasma Cytokine Profiling to Predict Steroid Resistance in Pediatric Nephrotic Syndrome. *Kidney Int. Reports* **6**, 785–795 (2021).
3. Dossier, C., Jamin, A. & Deschênes, G. Idiopathic nephrotic syndrome: The EBV hypothesis. *Pediatr. Res.* **81**, 233–239 (2017).
4. Medeiros, T., Myette, R. L., Almeida, J. R., Silva, A. A. & Burger, D. Extracellular Vesicles: Cell-Derived Biomarkers of Glomerular and Tubular Injury. *Cell. Physiol. Biochem.* **54**, 88–109 (2020).
5. Santorelli, L. *et al.* Urinary Extracellular Vesicle Protein Profiles Discriminate Different Clinical Subgroups of Children with Idiopathic Nephrotic Syndrome. *Diagnostics* **11**, 456 (2021).
6. Chen, T. *et al.* Increased urinary exosomal microRNAs in children with idiopathic nephrotic syndrome. *EBioMedicine* **39**, 552–561 (2019).
7. Erdbrügger, U. *et al.* Urinary extracellular vesicles: A position paper by the Urine Task Force of the International Society for Extracellular Vesicles. *J. Extracell. Vesicles* **10**, (2021).
8. Oosthuyzen, W. *et al.* Vasopressin regulates extracellular vesicle uptake by kidney collecting duct cells. *J. Am. Soc. Nephrol.* **27**, 3345–3355 (2016).
9. Bellucci, L., Montini, G., Collino, F. & Bussolati, B. Mesenchymal Stromal Cell-Derived Extracellular Vesicles Pass through the Filtration Barrier and Protect Podocytes in a 3D Glomerular Model under Continuous Perfusion. *Tissue Eng. Regen. Med.* **18**, 549–560 (2021).

Figure 27. Figure 1. Possible mechanisms of EV-mediated induction of NS.

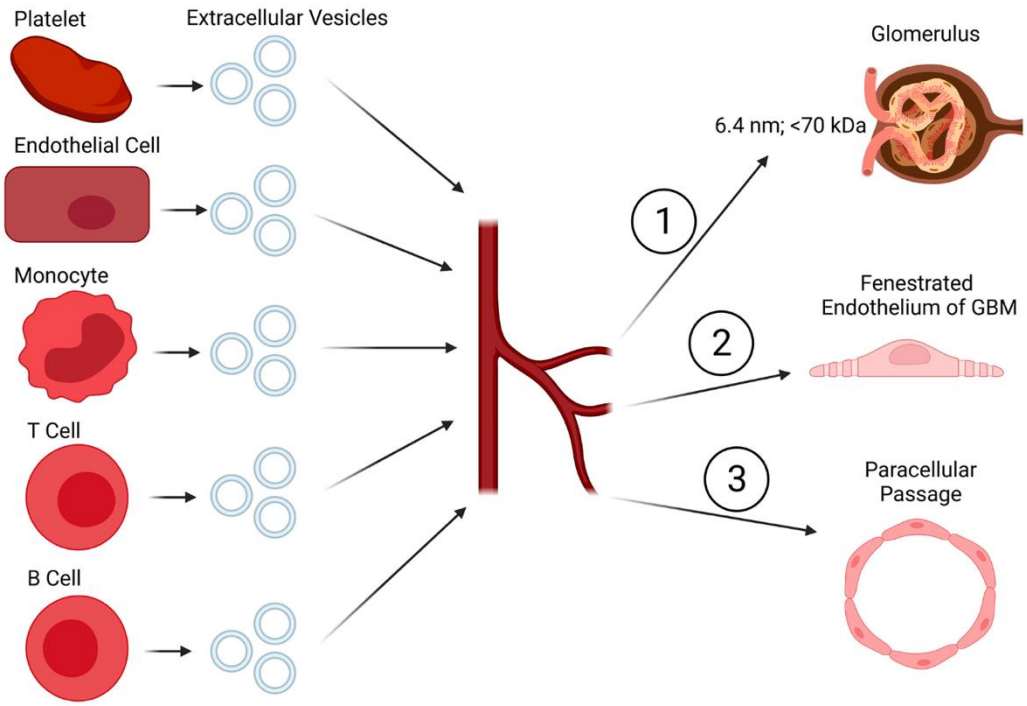

Figure 1. Possible mechanisms of extracellular vesicle (EV)-mediated induction of nephrotic syndrome (NS). The source of EVs responsible for this effect is presently unknown but may include platelet, endothelial, and/or leukocytes (monocyte, T-cell, and B-cell). Possible mechanisms by which circulating EVs could access podocytes and influence function include: *1*) direct filtration whereby EVs enter the urinary space and interact with podocytes on the apical surface, *2*) crossage of endothelial fenestrations and glomerular basement membrane whereby EVs interact with the basolateral surface, or *3*) paracellular movement and interaction with either the apical or basolateral surface of podocytes. Created with BioRender.com.

9.1.3 Damage associated molecular patterns and pattern recognition receptors in the podocyte (DOI: 10.1681/ASN.0000000531)

Robert L. Myette[1,2,3,4], Mayra Trentin-Sonoda[3], Chloé Landry[3,4], Chet E. Holterman[3], Tony Lin[3], Dylan Burger[3,4†] & Christopher R.J. Kennedy[3,4†]

[1]Children's Hospital of Eastern Ontario, Division of Pediatric Nephrology, University of Ottawa, Ottawa, Ontario, Canada.

[2]Children's Hospital of Eastern Ontario Research Institute, University of Ottawa, Ottawa, Ontario, Canada

[3]Kidney Research Center, Ottawa Hospital Research Institute, University of Ottawa, Ottawa, Ontario, Canada.

[4]Department of Cellular and Molecular Medicine, University of Ottawa, Ottawa, Ontario, Canada.

†Senior authors contributed equally

Correspondence: Dr. Robert L. Myette, Kidney Research Center, Ottawa Hospital Research Institute, Department of Cellular and Molecular Medicine, University of Ottawa, 2513-451 Smyth Rd. Ottawa, ON, Canada. Email: rmyet077@uottawa.ca

This is a non-final version of an article published in final form in JASN. Myette, Robert L.1,2,3,4; Trentin-Sonoda, Mayra3; Landry, Chloé3,4; Holterman, Chet E.3; Lin, Tony3; Burger, Dylan3,4; Kennedy, Christopher R.J.3,4. Damage-Associated Molecular Patterns and Pattern Recognition Receptors in the Podocyte. Journal of the American Society of Nephrology 36(1):p 136-143, January 2025. | DOI: 10.1681/ASN.0000000531

Abbreviation List (alphabetical order)

AGE - advanced glycation end products
AMP – adenosine monophosphate
AOPPs - advance oxidation protein products
ASC - apoptosis-associated speck-like protein with a caspase recruitment domain
BIM - Bcl-2-like protein 11
CCR or CXCR – chemokine receptor
C/EBPβ - CCAAT/enhancer-binding protein β
cGAS - cyclic GMP-AMP synthase
CLEC-2 – C-type lectin-like receptor 2
CML - Nε-carboxymethyl-lysine
DAMPs - damage associated molecular patterns
db/db – diabetic mouse model
DKD - diabetic kidney disease
DNA - deoxyribonucleic acid
EMT – epithelial-to-mesenchymal transition
ER – Endoplasmic Reticulum
FOXOA – Forkhead Box OA
GBM - glomerular basement membrane
GMP – Guanosine monophosphate
HMGB1 - high mobility group box 1
IgA - immunoglobulin A
IgG - immunoglobulin G
IL – interleukin
LPS - lipopolysaccharide
LRR - Leucine rich repeat
MCC950 - potent and specific NLRP3 inhibitor
Myd88 - myeloid differentiation primary response 88
NOD - Nucleotide-binding oligomerization domain-like
NOXs – NADPH oxidases
NRP1 – neuropilin 1
Nf-kβ p65 - Nuclear factor kappa-light-chain-enhancer of activated B cells
NLRP3 - NOD-, LRR-, and pyrin domain-containing protein 3
PAMP - pathogen associated molecular pattern
PENT – pentosidine
PRR – pattern recognition receptor
RAAS - renin-angiotensin-aldosterone system
RAGE - receptor for advanced glycation end products
RIG-1 - Retinoic acid-inducible gene 1
ROS - reactive oxygen species
STING - stimulator of interferon genes
STZ - streptozotocin

TBK-1 - TANK-binding kinase 1
TLR - toll like receptor
TNFα – Tumour necrosis factor, alpha
TRIF - toll/IL1 receptor domain-containing adaptor inducing interferon β
TRAM - TRIF-related adaptor molecule
ZEB2 - Zinc finger E-box-binding homeobox 2

Abstract

Podocytes possess immune system components allowing for a variety of innate responses to endogenous and exogenous stimuli. Recently, several groups have linked inappropriate innate immune signaling to podocyte injury, particularly chronic, sustained injury; however, the immune capabilities of podocytes have not been fully elucidated. Damage associated molecular patterns (DAMPs) are endogenous danger molecules released from damaged cells, including podocytes, and can elicit an inflammatory response and recruit immune cells to areas of injury. This is done through binding to pattern recognition receptors (PRR). Thought largely to be protective and responsive to injury or infection, recent evidence suggests signaling via DAMP pathways can aggravate and promote chronic diseases already associated with inflammation. The purpose of this narrative review is to highlight current knowledge with respect to specific podocyte DAMPs and PRRs, and to provide insight into ongoing work and possible future research avenues to advance our understanding of podocyte immune mechanisms.

Damage associated molecular patterns (DAMPs) and pattern recognition receptors (PRRs)

DAMPs are endogenous 'danger' molecules that elicit a large variety of downstream innate immune effects via interaction with PRRs [1]. Such immunostimulatory DAMPs come in the form of proteins, nucleic acids, ions, glycans, and metabolites that have sustained a change in position, concentration, and/or properties, enabling them to activate their respective PRRs [2]. This is in contrast to pathogen associated molecular patterns (PAMPs) which are exogenous, usually microbial, danger molecules sensed by their respective receptors whereby they elicit downstream inflammatory and immune signaling [3]. The main function of DAMPs and PAMPs is to bind with their respective PRRs to act as ligands for downstream signaling. Upon their release, a chemotactic gradient emanating from the injury site is established, allowing for the migration of immune cells to the area [3, 4]. Once DAMPs and PAMPs are cleared, the recruited immune cells may begin a reparative process [3].

DAMPs can enter the extracellular space as a result of cell death, organelle damage and/or metabolic dysregulation [2]. They can be released passively from necrotic cells or, alternatively, through active mechanisms such as the exocytosis of secretory lysosomes, exosomes, ectosomes, or the activation of membrane channel pores in live cells [5]. These signals can also originate from the extracellular matrix, as is the case with proteoglycans which are released following tissue injury [1, 6]. Intracellular DAMPs are more numerous, and include mitochondrial DAMPs, autophagy-related DAMPs, nuclear DAMPs, and cytosolic DAMPs (Table 1) [1]. Mitochondrial deoxyribonucleic acid (DNA) is considered a mitochondrial DAMP, along with formylated peptides, adenosine triphosphate (ATP), and the mitochondria themselves which are consumed by macrophages and can induce an inflammatory response through binding to PRRs [7]. When cells undergo autophagy without cell death, studies have shown the release of high mobility group box

1 (HMGB1), ATP, interleukin 1β (IL-1β), and DNA which act as DAMPs in their interactions with PRRs [1, 8]. Nuclear DAMPs are released during cell death processes or inflammation, with HMGB1 being the most studied nuclear DAMP [1, 9]. Cytosolic DAMPs include the S100 proteins which are released from immune cells when under stress [10]. PRRs are various in nature, but all have the unifying feature of eliciting downstream effector responses geared towards immune and inflammatory pathways [11–13]. Toll Like Receptors (TLRs), Nucleotide-binding oligomerization domain-like (NOD)-, Leucine rich repeat (LRR)-, and pyrin domain-containing protein 3 (NLRP3), cyclic guanosine monophosphate-adenosine monophosphate (GMP-AMP) synthase-stimulator of interferon genes (cGAS-STING), and the Receptor for Advanced Glycation End Products (RAGE), among others including Retinoic Acid Inducible Gene 1 (RIG-1), and Podoplanin/C-type Lectin-like Receptor 2 (CLEC-2), are arms of effector pathways that are responsive to DAMPs (Figure 1), and all these pathways are present in the podocyte.

The kidney, glomerulus, and podocyte

The kidney has several interlinked, yet exclusive functional compartments. The renal tubules are enriched in transport proteins and are involved in mineral and electrolyte homeostasis, as well as appropriate fluid balance. The glomerulus is comprised of several cell types of varying origins. Podocytes are terminally differentiated, and highly specialized epithelial cells located within the glomerulus [14]. They are uniquely positioned to form a size- and charge-selective barrier which is responsible for appropriate filtration [15]. Podocytes possess foot processes, each characterized by an extensive actin cytoskeleton, which interconnects with foot processes of neighboring podocytes [16]. These foot processes are connected by specialized cell-cell junctions known as slit diaphragms, functionally forming the glomerular filtration apparatus. Beyond serving as a size and charge-selective barrier to prevent the filtration of large molecules, the

podocyte, and the slit diaphragm proteins function as a signaling apparatus for self and neighboring podocytes. Specifically, podocyte and slit diaphragm proteins can regulate the actin cytoskeleton, cell-cell interactions, motility, and immune processes [17].

The podocyte has been shown to possess functional arms of the immune system [18, 19]. Podocytes exhibit the capacity to recognize and respond to various signaling molecules associated with inflammation and express several cytokines and their receptors, including interleukin 1 alpha (IL-1α), IL-1β, and tumour necrosis factor alpha (TNF-α) [20–22]. Moreover, podocytes express chemokine receptor 1 (CCR1), CCR2, and CXCR4 which play a pivotal role in immune cell recruitment [21]. Podocytes also express major histocompatibility complex (MHC) class I and II genes, key components of the adaptive immune system [23]. Lastly, and most importantly for this review, podocytes possess functional TLRs, NLRP3, cGAS-STING, RAGE, RIG-1, and Podoplanin (which is PRR-like in its interaction with CLEC-2). The function of these specific PRRs and their roles as innate immune effectors in podocytes is narrowly defined at present and current knowledge is summarized here.

TLRs

In humans, the TLR family consists of 10 members (TLR1-10) whereas mice have TLR 1-9, 11, 12 and 13, but lack TLR 10 [11]. TLRs play a critical role in early responses to infectious pathogens as well as cellular damage. These transmembrane signaling molecules are located in various cellular compartments including but not limited to the plasma membrane, endoplasmic reticulum (ER), and endosomes [24]. In the kidney, TLRs can be found in a variety of cell types including proximal tubular epithelial cells, mesangial cells, and podocytes, and they play a role in damage response and disease progression [25–28]. Activation of TLRs via binding of DAMPs results in downstream signaling via myeloid differentiation primary response 88 (MyD88) and

toll/IL1 receptor domain-containing adaptor inducing interferon β / TRIF-related adaptor molecule (TRIF/TRAM)-dependent pathways that are capable of inducing and regulating production of pro-inflammatory cytokine expression [29]. TLR ligands include DNA, S100 proteins, and HMGB1 which elicit downstream effectors, including MYD-88, Interleukin 6 (IL-6), and TNFα, among others (Table 1).

A growing body of work implicates TLRs in immune-mediated glomerulonephritis. In Immunoglobulin A (IgA) and IgG nephropathy, increased expression of TLR9 and TLR4 has been demonstrated, primarily in podocytes [30, 31]. Interestingly, a link between TLR9 and TLR4 signaling, and increased activity of the renin-angiotensin-aldosterone system (RAAS) pathway has also been demonstrated in this setting [30, 32]. Furthermore, increased expression and activity of several TLR family members appears to play a role in progression of mouse models of lupus nephritis, minimal change disease, and membranoproliferative glomerulonephritis [28, 33–35].

In vitro cell culture studies using mouse podocytes, as well as rodent models of diabetic kidney disease (DKD) have demonstrated increased expression and activation of TLR4, as well as TLR2, upon exposure to high glucose conditions [36–38]. Interestingly, modulation of several micro-RNAs (miRNAs; miRs) targeting TLR4 mRNA stability has been demonstrated to impact TLR4 expression. Further, extracellular vesicles containing miR-26a-5p, derived from adipose mesenchymal stem cells, were shown to reduce TLR4 expression and increase viability of mouse podocytes exposed to high glucose [38, 39]. HMGB1, an endogenous TLR4 ligand also appears to play key roles in TLR4 signaling in both streptozotocin (STZ)-induced type 1 diabetes in mice, as well as type II diabetic *db/db* mice [40, 41]. Interestingly, both genetic deletion of TLR4 in mice, as well as the use of a competitive antagonist of HMGB1 binding resulted in decreased kidney injury in an STZ model of DKD [40].

Work from our group identified that NADPH-oxidase 5 (NOX5) expression in mouse podocytes elicited an inflammatory phenotype via TLR signaling. Importantly, mice do not express NOX5, so a transgenic model was developed [42]. Using this transgenic NOX5^{pod+} mouse model, we showed that compared to control, these mice demonstrated greater glomerular inflammation, increased TLR1 expression, and increased proinflammatory cytokine production [43]. Further, incubating immortalized human podocytes with lipopolysaccharide (LPS) resulted in TLR induction, and increased NOX5 expression [43]. Increased urinary excretion of HMGB1 was also observed in NOX5^{pod+} mice compared to wild-type controls, following an LPS challenge. Altogether, this evidence suggests some TLRs are present within the podocyte and their activity is associated with injury.

NLRP3 Inflammasome

Similar to TLRs, inflammasomes provide surveillance for potential PAMPs and DAMPs. Inflammasomes are an assembly of proteins, typically composed of (1) a sensor protein that recognizes molecules associated with pathogens or cell death/stress, (2) an adaptor protein that recruits caspases, and (3) the effector, *i.e.*, a proinflammatory caspase. The NLRP3 inflammasome has NLRP3 (or cryopyrin) as the sensor protein, along with the adaptor apoptosis-associated speck-like protein with a caspase recruitment domain (ASC) protein and procaspase-1, and finally, the effector caspase 1 which acts on pro-IL-1β, creating IL-1β [44]. Activation of the NLRP3 inflammasome requires a priming step, usually in the form of an inflammatory signal, and subsequently an activation signal, usually in the form of a DAMP. The main DAMPs which interact with NLRP3 include reactive oxygen species (ROS), and DNA, which are sensed by NLRP3 and promote oligomerization into the inflammasome [45]. Ultimately, NLRP3 engagement leads to activation of the pro-inflammatory cytokines IL-1β and IL-18. Such cytokines

have been shown to decrease glomerular nephrin content in several disease models, including DKD [46], and aldosterone-induced podocyte injury [47].

Xiong *et al*., showed that NLRP3 and caspase-1 mRNA expression levels are upregulated in renal tissue samples from individuals with primary glomerulonephritis, along with increased protein expression in the glomeruli [48]. The same pattern was observed in glomeruli from individuals with nephrotic syndrome [47]. Furthermore, a study performed with publicly available RNA sequencing data showed that adriamycin-induced focal segmental glomerulosclerosis promotes upregulation of NLRP3 [49].

Higher expression of NLRP3 is closely related to podocyte injury in individuals with lupus nephritis [50]. Activation of the NLRP3 inflammasome was shown to be increased in podocytes from lupus-prone mice whereas inhibition of NLRP3 by MCC950 reduces caspase-1 activity. This led to protection against proteinuria and renal injury [51]. CCAAT/enhancer-binding protein β (C/EBPβ) is a regulator of the NLRP3 inflammasome. *In vitro*, knockdown of C/EBPβ in a model of lupus nephritis promoted downregulation of the NLRP3 inflammasome proteins in the podocytes, alleviating inflammation [52]. In addition, other studies have shown the protective effect of MITOtempo on podocyte injury through inhibition of the NLRP3 inflammasome [51, 53].

Moreover, the NLRP3 inflammasome is also associated with aging, podocyte heath, and lifespan. While NLRP3 expression in the podocytes of a young patient, as well as young mice, was virtually absent, an increase in expression was detected in a sample from an 82-year-old individual and in aged mice [54]. In aged mice, inhibition, or knockdown of NLRP3 improved podocyte senescence and health, prolonging podocyte lifespan [54].

It is therefore clear that activation of the NRLP3 inflammasome is associated with deterioration of renal function in glomerular disease, and age also appears to play a factor in its expression.

cGAS-STING

cGAS is another integral part of the innate immune response through its recognition of pathogens and viruses. It is capable of sensing and binding to DNA (foreign or self) whereby cGAS is activated and enzymatically generates cGAMP [55]. cGAMP binds to STING leading to a signaling cascade with downstream activation of inflammatory genes, type I interferon production, autophagy, and cell death [55, 56].

Podocyte cGAS-STING signaling has been implicated in laboratory models of DKD. Mitrofanova *et al.,* showed that both human and murine podocytes express all components of the cGAS-STING system [57]. Agonism of STING in wild-type mice led to albuminuria and podocyte loss while the cGAS-STING pathway was upregulated in their model of DKD. Further, Zang *et al.,* showed that lipotoxicity-related mitochondrial DNA leakage led to activation of STING and downstream effectors TANK-binding kinase 1 (TBK1) and nuclear factor kappa-light-chain-enhancer of activated B cells (NF-kB p65) [58]. Both groups showed that blockage of the cGAS-STING pathway was nephroprotective in their models. The protective effects of Sacubitril/Valsartan in DKD mouse models via modulation of the cGAS-STING pathway has also been shown [59]. cGAS-STING signaling, and blockade, is an emerging area of research with potential for widespread impact for individuals with DKD.

RAGE

RAGE is a multi-ligand PRR of the immunoglobulin superfamily. It can be activated by a variety of ligands, of which advanced glycation end products (AGEs) are the most widely studied

[60]. AGEs are a heterogenous population composed of proteins, lipids and nucleic acids subjected to non-enzymatic glycation by reducing sugars. Although AGE formation is known to gradually increase with physiological aging, this process can be accelerated by diabetes, renal failure, and inflammation [61].

RAGE-ligand interactions trigger various proinflammatory cascades through the induction of ROS by NOXs and subsequent NF-kB signaling, leading to the upregulation of RAGE itself [62]. In the kidney, RAGE is predominantly expressed in podocytes, rendering the glomerular filtration barrier vulnerable to the activation of the AGE-RAGE axis [60, 63].

Indeed, RAGE-induced podocyte activation has been shown to impact the structural integrity of the glomerular filtration barrier, through podocyte loss and reorganization. Podocyte apoptosis can be induced via several RAGE-dependent pathways. By activating Forkhead Box OA (FOXOA) transcriptional activity, RAGE can increase Bcl-2-like protein 11 (BIM) expression, leading to podocyte apoptosis [64]. Activation of RAGE by advanced oxidation protein products (AOPPs) has also been shown to lead to podocyte apoptosis by inducing ER-stress that activates the unfolded protein response [65].

Alterations in the cytoskeletal structure of podocytes can also impair the proper function of the glomerular filtration barrier. RAGE activation leads to loss of nephrin expression in podocytes, resulting in changes in the slit diaphragm [66]. Proper actin distribution may also be impaired by the suppression of alpha-actinin-4 observed following AGE exposure [67]. By downregulating the expression of the transmembrane glycoprotein Neuropilin 1 (NRP1), RAGE also impairs podocyte migration, causing nude areas to form along the glomerular basement membrane (GBM). It does this by reducing the binding ability of the Sp1 transcription factor to the NRP1 promoter [68].

In DKD, podocyte RAGE expression is increased along with an accumulation of RAGE ligands (i.e. Nε-carboxymethyl-lysine (CML), Pentosidine (PENT)) at the GBM [62]. CML is the most predominant AGE to accumulate in renal compartments in the context of diabetes and has been shown to induce epithelial-mesenchymal transition (EMT) in podocytes, leading to their detachment from the GBM. Experimental evidence supports that this is mediated by the transcription factor Zinc finger E-box-binding homeobox 2 (ZEB2), which is activated following exposure to CML, leading to increased glomerular permeability [69]. Increased glomerular filtration barrier permeability can also be the result of increased vascular endothelial growth factor expression which has been linked to RAGE activation [70]. Accordingly, both pharmacological inhibition and genetic deletion of RAGE can prevent podocyte effacement and proteinuria in AGE-mediated kidney injury [71]. RAGE-dependent mechanisms have thus been linked to glomerular perturbations in DKD and other glomerular diseases.

Other PRRs in the podocyte

In addition to TLRs, cGAS-STING, NLRP3, and RAGE, there exist other DAMP-PRR axes which have been identified in the podocyte. Retinoic acid-inducible gene 1 (RIG-1) is expressed in podocytes [72, 73] and acts as a PRR when binding to double stranded RNA, which is a byproduct of viral replication. This is thought to represent a potential mechanism for podocyte inflammation in the context of viral infection. Taken further, whether misprocessed self-RNA, released during cellular injury, could bind with RIG-1 and induce an inflammatory response is an area of intense study [74].

Further, C-type Lectin Receptor 2 (CLEC-2) is a ligand for Podoplanin. Podoplanin is a mucin-type integral membrane protein found abundantly in the podocyte. Recombinant CLEC-2 was shown to bind to Podoplanin *in vitro* and induce significant podocyte morphological changes

[75]. Thus, it seems CLEC-2, despite being a receptor on platelets, can act as a DAMP and bind with Podoplanin (acting as a PRR). This would of course only occur under conditions where the glomerular filtration barrier is disrupted thus allowing for platelet CLEC-2 exposure to podocytes.

Future directions

As a central component of the glomerular filtration barrier, podocytes play a critical role in preventing protein loss in the urine. Recent evidence suggests that podocytes possess several key immune system components. Indeed, signaling via the TLR-, NLRP3-, cGAS-STING-, RAGE-, RIG-1- and Podoplanin/CLEC-2-axes have been implicated in podocyte disease, and in some instances, these PRR-ligand interactions may be targeted to reduce proteinuria in experimental glomerular disease.

Outside of the scope of this review would be the implications for DAMP-signaling inhibition and its impact on immune cell infiltration, and further, the impact of genetic polymorphisms in PRR genes which may give rise to aberrant signalling in podocytopathies. The latter consideration is important as specific genetic polymorphisms in NLRP3 and TLRs have been studied, and in some cases in the context of kidney disease. Specifically, NLRP3 polymorphisms have been shown to associate with susceptibility to chronic kidney disease [76], lupus nephritis [77], and early kidney transplant rejection [78]. Similarly, TLR polymorphisms have been associated with early kidney transplant rejection [79] and the development of post-transplant diabetes [80]. However, there do not appear to be any studies specifically linking genetic polymorphisms in PRRs within podocytes at the molecular or clinical level.

Another important consideration is the obvious redundancy associated with multiple receptors binding the same target(s). In this case, a common ligand is DNA which can activate several PRRs within the podocyte, and elsewhere. This redundancy may stem from an evolutionary

protective mechanism, as perhaps each receptor can bind specific DNA or RNA segments but have all evolved to be promiscuous and bind DNA. What is yet to be discovered is whether these PRRs can also bind DNA-binding proteins, allowing for further selection of pathway activation, or to distinguish between physiologic and pathologic signalling. Complex crosstalk between different DAMPs and PRRs is likely occurring; however, this has not been clearly described in the literature, particularly in the context of podocyte signalling pathways.

Important, and key unanswered questions remain in this field including how can we discover novel therapeutic targets and study their effects in such a complex system? Another unanswered question is whether these signalling pathways are protective in any manner. Is the maladaptive response a result of the disease, or the cause of the disease? What happens to DAMPs and PRRs as we age, are they more likely to cause disease? Would repeated injury, such as a relapsing and remitting podocytopathy, lead to a more vulnerable podocyte with time? And lastly, do genetic polymorphisms in genes found in DAMP / PRR pathways render the podocyte more vulnerable to injury, or could they be protective?

Conclusion

Given that DAMP signaling is implicated in inflammatory responses, and particularly that recent evidence suggests maladaptive signaling in the context of sterile inflammation associated with chronic disease, it is certainly possible DAMP pathways can be targeted at multiple levels. New mechanistic insights into podocyte biology, and the role of DAMPs and PRRs, will allow for more personalized medicine approaches, particularly with the creation of targeted therapies.

Figure 28. ***Figure 1.*** *A selection of damage associated molecular pattern receptors and some of their key ligands in podocytes*

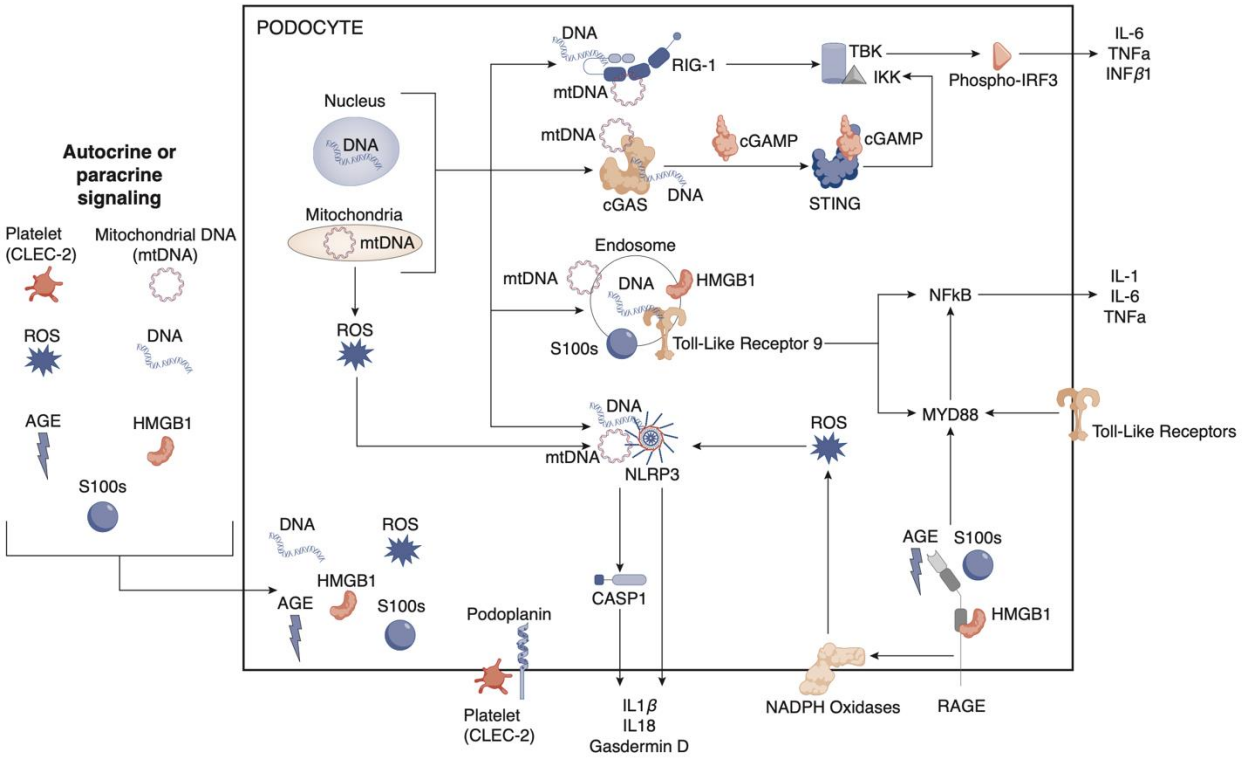

Figure 1. A selection of damage associated molecular pattern receptors and some of their key ligands in podocytes. DNA, deoxyribonucleic acid; RNA, ribonucleic acid; HMGB1, High mobility group box 1; MYD-88, Myeloid differentiation primary response 88; NF-kB, Nuclear factor kappa-light-chain-enhancer of activated B cells; ROS, reactive oxygen species; IL-1β, Interleukin 1 beta; IL-6, Interleukin 6; TNF-α, Tumour Necrosis Factor, alpha; INFB-1, Interferon beta; TLR, toll like receptor; IL-18, Interleukin 18; AGE, advanced glycation end products; C1q, complement component 1q; DIAPH1, Protein diaphanous homolog 1; Ras-related C3 botulinum toxin substrate 1; NOX2, NADPH-oxidase 2; TRCP6, Transient receptor potential cation channel, subfamily C, member 6; RIG-1, Retinoic acid-inducible gene 1; CLEC-2, C-type lectin-like

receptor 2; cGAS, cyclic GMP-AMP synthase; STING, stimulator of interferon genes; CASP1, caspase 1.

Table 6. **Table 1.** A list of the common pattern recognition receptors and damage associated molecular patterns in the podocyte, along with some of their downstream effectors.

PRR	DAMP	Downstream Effectors	References
Toll Like Receptors	DNA, RNA, S100 proteins, HMGB1, protein	MYD-88, NF-kB, IL-1, IL-6, TNFα	[81, 82]
NLRP3	DNA, ROS	Caspase-1, IL-1β, IL-18	[82, 83]
cGAS-STING	DNA	IL-6, TNFα, INFB-1	[82, 84]
RAGE	AGE, S100 proteins, HMGB1, C1q	DIAPH1, RAC1, NOX2, TRCP6	[85]
RIG-1	Double-stranded RNA	IL-6, TNFα, INFB-1	[72, 73]
Podoplanin (PRR-like)	C-type Lectin-like Receptor 2	Ezrin, radixin, moesin	[75]

DNA, deoxyribonucleic acid; RNA, ribonucleic acid; HMGB1, High mobility group box 1; MYD-88, Myeloid differentiation primary response 88; NF-kB, Nuclear factor kappa-light-chain-enhancer of activated B cells; ROS, reactive oxygen species; IL-1β, Interleukin 1 beta; IL-6, Interleukin 6; TNF-α, Tumour Necrosis Factor, alpha; INFB-1, Interferon beta; TLR, toll like receptor; IL-18, Interleukin 18; AGE, advanced glycation end products; C1q, complement component 1q; DIAPH1, Protein diaphanous homolog 1; Ras-related C3 botulinum toxin substrate 1; NOX2, NADPH-oxidase 2; TRCP6, Transient receptor potential cation channel, subfamily C, member 6; RIG-1, Retinoic acid-inducible gene 1.

Citations

1. Schaefer L (2014) Complexity of danger: The diverse nature of damage-associated molecular patterns. Journal of Biological Chemistry 289:35237–35245

2. Ma M, Jiang W, Zhou R (2024) DAMPs and DAMP-sensing receptors in inflammation and diseases. Immunity 57:752–771. https://doi.org/10.1016/j.immuni.2024.03.002

3. Bianchi ME (2007) DAMPs, PAMPs and alarmins: all we need to know about danger. J Leukoc Biol 81:1–5. https://doi.org/10.1189/jlb.0306164

4. McDonald B, Pittman K, Menezes GB, et al (2010) Intravascular danger signals guide neutrophils to sites of sterile inflammation. Science 330:362–6. https://doi.org/10.1126/science.1195491

5. Murao A, Aziz M, Wang H, et al (2021) Release mechanisms of major DAMPs. Apoptosis 26:152–162. https://doi.org/10.1007/s10495-021-01663-3

6. Frey H, Schroeder N, Manon-Jensen T, et al (2013) Biological interplay between proteoglycans and their innate immune receptors in inflammation. FEBS J 280:2165–79. https://doi.org/10.1111/febs.12145

7. Maeda A, Fadeel B (2014) Mitochondria released by cells undergoing TNF-α-induced necroptosis act as danger signals. Cell Death Dis 5:e1312. https://doi.org/10.1038/cddis.2014.277

8. Hou W, Zhang Q, Yan Z, et al (2013) Strange attractors: DAMPs and autophagy link tumor cell death and immunity. Cell Death Dis 4:e966. https://doi.org/10.1038/cddis.2013.493

9. Pisetsky DS (2014) The translocation of nuclear molecules during inflammation and cell death. Antioxid Redox Signal 20:1117–25. https://doi.org/10.1089/ars.2012.5143

10. Donato R, R. Cannon B, Sorci G, et al (2013) Functions of S100 Proteins. Curr Mol Med 13:24–57. https://doi.org/10.2174/156652413804486214

11. Kawasaki T, Kawai T (2014) Toll-like receptor signaling pathways. Front Immunol 5:1–8. https://doi.org/10.3389/fimmu.2014.00461

12. Fritz G (2011) RAGE: A single receptor fits multiple ligands. Trends Biochem Sci 36:625–632. https://doi.org/10.1016/j.tibs.2011.08.008

13. Kim SM, Kim YG, Kim DJ, et al (2018) Inflammasome-independent role of NLRP3 mediates mitochondrial regulation in renal injury. Front Immunol 9:1–14. https://doi.org/10.3389/fimmu.2018.02563

14. Reiser J, Altintas MM (2016) Podocytes. F1000Res 5:114 https://doi.org/10.12688/f1000research.7255.1

15. Kopp JB, Anders HJ, Susztak K, et al (2020) Podocytopathies. Nat Rev Dis Primers 6:. https://doi.org/10.1038/s41572-020-0196-7

16. Blaine J, Dylewski J (2020) Regulation of the Actin Cytoskeleton in Podocytes. Cells 9:1–27. https://doi.org/10.3390/cells9071700

17. Grahammer F, Schell C, Huber TB (2013) The podocyte slit diaphragm--from a thin grey line to a complex signalling hub. Nat Rev Nephrol 9:587–98. https://doi.org/10.1038/nrneph.2013.169

18. Bruno V, Mühlig AK, Oh J, Licht C (2023) New insights into the immune functions of podocytes: the role of complement. Mol Cell Pediatr 10

19. Bhargava R, Tsokos GC (2019) The immune podocyte. Curr Opin Rheumatol 31:167–174. https://doi.org/10.1097/BOR.0000000000000578

20. Niemir ZI, Stein H, Dworacki G, et al (1997) Podocytes are the major source of IL-1 alpha and IL-1 beta in human glomerulonephritides. Kidney Int 52:393–403. https://doi.org/10.1038/ki.1997.346

21. Huber TB, Reinhardt HC, Exner M, et al (2002) Expression of Functional CCR and CXCR Chemokine Receptors in Podocytes. The Journal of Immunology 168:6244–6252. https://doi.org/10.4049/jimmunol.168.12.6244

22. Srivastava T, Sharma M, Yew KH, et al (2013) LPS and PAN-induced podocyte injury in an in vitro model of minimal change disease: Changes in TLR profile. J Cell Commun Signal 7:49–60. https://doi.org/10.1007/s12079-012-0184-0

23. Coers W, Brouwer E, Vos JT, et al (1994) Podocyte expression of MHC class I and II and intercellular adhesion molecule-1 (ICAM-1) in experimental pauci-immune crescentic glomerulonephritis. Clin Exp Immunol 98:279–86. https://doi.org/10.1111/j.1365-2249.1994.tb06138.x

24. Fitzgerald KA, Kagan JC (2020) Toll-like Receptors and the Control of Immunity. Cell 180:1044–1066. https://doi.org/10.1016/j.cell.2020.02.041

25. Krüger B, Krick S, Dhillon N, et al (2009) Donor Toll-like receptor 4 contributes to ischemia and reperfusion injury following human kidney transplantation. Proc Natl Acad Sci U S A 106:3390–5. https://doi.org/10.1073/pnas.0810169106

26. Kaur H, Chien A, Jialal I (2012) Hyperglycemia induces Toll like receptor 4 expression and activity in mouse mesangial cells: relevance to diabetic nephropathy. Am J Physiol Renal Physiol 303:F1145-50. https://doi.org/10.1152/ajprenal.00319.2012

27. Wolf G, Bohlender J, Bondeva T, et al (2006) Angiotensin II upregulates toll-like receptor 4 on mesangial cells. J Am Soc Nephrol 17:1585–93. https://doi.org/10.1681/ASN.2005070699

28. Banas MC, Banas B, Hudkins KL, et al (2008) TLR4 links podocytes with the innate immune system to mediate glomerular injury. J Am Soc Nephrol 19:704–13. https://doi.org/10.1681/ASN.2007040395

29. Akira S, Uematsu S, Takeuchi O (2006) Pathogen recognition and innate immunity. Cell 124:783–801. https://doi.org/10.1016/j.cell.2006.02.015

30. Jin L-W, Pan M, Ye H-Y, et al (2019) Down-regulation of the long non-coding RNA XIST ameliorates podocyte apoptosis in membranous nephropathy via the miR-217-TLR4 pathway. Exp Physiol 104:220–230. https://doi.org/10.1113/EP087190

31. Zhang Q, Shi SF, Zhu L, et al (2012) Tacrolimus improves the proteinuria remission in patients with refractory IgA nephropathy. Am J Nephrol 35:312–320. https://doi.org/10.1159/000337175

32. Sha W, Shen L, Zhou L, et al (2015) Down-regulation of miR-186 contributes to podocytes apoptosis in membranous nephropathy. Biomed Pharmacother 75:179–84. https://doi.org/10.1016/j.biopha.2015.07.021

33. Masum MA, Ichii O, Hosny Ali Elewa Y, et al (2018) Overexpression of toll-like receptor 9 correlates with podocyte injury in a murine model of autoimmune membranoproliferative glomerulonephritis. Autoimmunity 51:386–398. https://doi.org/10.1080/08916934.2018.1549234

34. O'Sullivan KM, Ford SL, Longano A, et al (2018) Intrarenal Toll-like receptor 4 and Toll-like receptor 2 expression correlates with injury in antineutrophil cytoplasmic antibody-associated vasculitis. Am J Physiol Renal Physiol 315:F1283–F1294. https://doi.org/10.1152/ajprenal.00040.2018

35. Kimura J, Ichii O, Miyazono K, et al (2014) Overexpression of Toll-like receptor 8 correlates with the progression of podocyte injury in murine autoimmune glomerulonephritis. Sci Rep 4:7290. https://doi.org/10.1038/srep07290

36. Wang Y, Liu J, Zhang Q, et al (2021) Human umbilical cord mesenchymal stem cells attenuate podocyte injury under high glucose via TLR2 and TLR4 signaling. Diabetes Res Clin Pract 173:108702. https://doi.org/10.1016/j.diabres.2021.108702

37. Ma J, Chadban SJ, Zhao CY, et al (2014) TLR4 activation promotes podocyte injury and interstitial fibrosis in diabetic nephropathy. PLoS One 9:e97985. https://doi.org/10.1371/journal.pone.0097985

38. Yao T, Zha D, Gao P, et al (2018) MiR-874 alleviates renal injury and inflammatory response in diabetic nephropathy through targeting toll-like receptor-4. J Cell Physiol 234:871–879. https://doi.org/10.1002/jcp.26908

39. Duan Y, Luo Q, Wang Y, et al (2020) Adipose mesenchymal stem cell-derived extracellular vesicles containing microRNA-26a-5p target TLR4 and protect against diabetic nephropathy. J Biol Chem 295:12868–12884. https://doi.org/10.1074/jbc.RA120.012522

40. Chen X, Ma J, Kwan T, et al (2018) Blockade of HMGB1 Attenuates Diabetic Nephropathy in Mice. Sci Rep 8:8319. https://doi.org/10.1038/s41598-018-26637-5

41. Xu C, Chen Y, Liu Z, Fu X (2023) Hedysarum polybotrys polysaccharide attenuates renal inflammatory infiltration and fibrosis in diabetic mice by inhibiting the HMGB1/RAGE/TLR4 pathway. Exp Ther Med 26:493. https://doi.org/10.3892/etm.2023.12192

42. Holterman CE, Thibodeau JF, Towaij C, et al (2014) Nephropathy and elevated BP in mice with podocyte-specific NADPH oxidase 5 expression. Journal of the American Society of Nephrology 25:784–797. https://doi.org/10.1681/ASN.2013040371

43. Holterman CE, Boisvert NC, Thibodeau JF, et al (2019) Podocyte NADPH Oxidase 5 Promotes Renal Inflammation Regulated by the Toll-Like Receptor Pathway. Antioxid Redox Signal 30:1817–1830. https://doi.org/10.1089/ars.2017.7402

44. Schroder K, Tschopp J (2010) The inflammasomes. Cell 140:821–32. https://doi.org/10.1016/j.cell.2010.01.040

45. Swanson K V., Deng M, Ting JPY (2019) The NLRP3 inflammasome: molecular activation and regulation to therapeutics. Nature Reviews Immunology 2019 19:8 19:477–489. https://doi.org/10.1038/s41577-019-0165-0

46. Hou Y, Lin S, Qiu J, et al (2020) NLRP3 inflammasome negatively regulates podocyte autophagy in diabetic nephropathy. Biochem Biophys Res Commun 521:791–798. https://doi.org/10.1016/j.bbrc.2019.10.194

47. Bai M, Chen Y, Zhao M, et al (2017) NLRP3 inflammasome activation contributes to aldosterone-induced podocyte injury. Am J Physiol Renal Physiol 312:F556–F564. https://doi.org/10.1152/ajprenal.00332.2016

48. Xiong J, Wang Y, Shao N, et al (2015) The Expression and Significance of NLRP3 Inflammasome in Patients with Primary Glomerular Diseases. Kidney Blood Press Res 40:344–54. https://doi.org/10.1159/000368511

49. Hu H, Li M, Chen B, et al (2022) Activation of necroptosis pathway in podocyte contributes to the pathogenesis of focal segmental glomerular sclerosis. Clin Exp Nephrol 26:1055–1066. https://doi.org/10.1007/s10157-022-02258-1

50. Chen F-F, Liu X-T, Tao J, et al (2023) Renal NLRP3 Inflammasome activation is associated with disease activity in lupus nephritis. Clin Immunol 247:109221. https://doi.org/10.1016/j.clim.2022.109221

51. Fu R, Guo C, Wang S, et al (2017) Podocyte Activation of NLRP3 Inflammasomes Contributes to the Development of Proteinuria in Lupus Nephritis. Arthritis Rheumatol 69:1636–1646. https://doi.org/10.1002/art.40155

52. Wang X, Cheng W, Chen X, et al (2022) Inhibition of CEBPB Attenuates Lupus Nephritis via Regulating Pim-1 Signaling. Mediators Inflamm 2022:2298865. https://doi.org/10.1155/2022/2298865

53. Liu B, Wang D, Cao Y, et al (2022) MitoTEMPO protects against podocyte injury by inhibiting NLRP3 inflammasome via PINK1 / Parkin pathway-mediated mitophagy. Eur J Pharmacol 929:175136. https://doi.org/10.1016/j.ejphar.2022.175136

54. Kaverina N, Schweickart RA, Chan GC, et al (2023) Inhibiting NLRP3 signaling in aging podocytes improves their life- and health-span. Aging 15:6658–6689. https://doi.org/10.18632/aging.204897

55. Zierhut C, Funabiki H (2020) Regulation and Consequences of cGAS Activation by Self-DNA. Trends Cell Biol 30:594–605

56. Li X-D, Wu J, Gao D, et al (2013) Pivotal Roles of cGAS-cGAMP Signaling in Antiviral Defense and Immune Adjuvant Effects. Science (1979) 341:1390–1394. https://doi.org/10.1126/science.1244040

57. Mitrofanova A, Fontanella A, Tolerico M, et al (2022) Activation of Stimulator of IFN Genes (STING) Causes Proteinuria and Contributes to Glomerular Diseases. Journal of the American Society of Nephrology 33:2153–2173. https://doi.org/10.1681/ASN.2021101286

58. Zang N, Cui C, Guo X, et al (2022) cGAS-STING activation contributes to podocyte injury in diabetic kidney disease. iScience 25:105145. https://doi.org/10.1016/J.ISCI.2022.105145

59. Myakala K, Jones BA, Wang XX, Levi M (2021) Sacubitril/valsartan treatment has differential effects in modulating diabetic kidney disease in db/db mice and KKAy mice compared with valsartan treatment. Am J Physiol Renal Physiol 320:F1133–F1151. https://doi.org/10.1152/AJPRENAL.00614.2020

60. Kim W, Hudson BI, Moser B, et al (2005) Receptor for advanced glycation end products and its ligands: a journey from the complications of diabetes to its pathogenesis. Ann N Y Acad Sci 1043:553–61. https://doi.org/10.1196/annals.1338.063

61. Shen C-Y, Lu C-H, Wu C-H, et al (2020) The Development of Maillard Reaction, and Advanced Glycation End Product (AGE)-Receptor for AGE (RAGE) Signaling Inhibitors as Novel Therapeutic Strategies for Patients with AGE-Related Diseases. Molecules 25:. https://doi.org/10.3390/molecules25235591

62. Parwani K, Mandal P (2023) Role of advanced glycation end products and insulin resistance in diabetic nephropathy. Arch Physiol Biochem 129:95–107. https://doi.org/10.1080/13813455.2020.1797106

63. D'Agati V, Yan SF, Ramasamy R, Schmidt AM (2010) RAGE, glomerulosclerosis and proteinuria: roles in podocytes and endothelial cells. Trends Endocrinol Metab 21:50–6. https://doi.org/10.1016/j.tem.2009.07.003

64. Chuang PY, Yu Q, Fang W, et al (2007) Advanced glycation endproducts induce podocyte apoptosis by activation of the FOXO4 transcription factor. Kidney Int 72:965–976. https://doi.org/10.1038/sj.ki.5002456

65. Rong G, Tang X, Guo T, et al (2015) Advanced oxidation protein products induce apoptosis in podocytes through induction of endoplasmic reticulum stress. J Physiol Biochem 71:455–70. https://doi.org/10.1007/s13105-015-0424-x

66. Ha T-S (2006) High glucose and advanced glycosylated end-products affect the expression of alpha-actinin-4 in glomerular epithelial cells. Nephrology (Carlton) 11:435–41. https://doi.org/10.1111/j.1440-1797.2006.00668.x

67. Doublier S, Salvidio G, Lupia E, et al (2003) Nephrin expression is reduced in human diabetic nephropathy: evidence for a distinct role for glycated albumin and angiotensin II. Diabetes 52:1023–30. https://doi.org/10.2337/diabetes.52.4.1023

68. Bondeva T, Wolf G (2009) Advanced glycation end products suppress neuropilin-1 expression in podocytes by a reduction in Sp1-dependent transcriptional activity. Am J Nephrol 30:336–345. https://doi.org/10.1159/000227762

69. Kumar PA, Welsh GI, Raghu G, et al (2016) Carboxymethyl lysine induces EMT in podocytes through transcription factor ZEB2: Implications for podocyte depletion and proteinuria in diabetes mellitus. Arch Biochem Biophys 590:10–19. https://doi.org/10.1016/j.abb.2015.11.003

70. Wendt TM, Tanji N, Guo J, et al (2003) RAGE drives the development of glomerulosclerosis and implicates podocyte activation in the pathogenesis of diabetic nephropathy. Am J Pathol 162:1123–37. https://doi.org/10.1016/S0002-9440(10)63909-0

71. Guo J, Ananthakrishnan R, Qu W, et al (2008) RAGE mediates podocyte injury in adriamycin-induced glomerulosclerosis. J Am Soc Nephrol 19:961–72. https://doi.org/10.1681/ASN.2007101109

72. Yamashita M, Millward CA, Inoshita H, et al (2013) Antiviral innate immunity disturbs podocyte cell function. J Innate Immun 5:231–241. https://doi.org/10.1159/000345255

73. Nakata M, Shimada M, Narita-Kinjo I, et al (2021) PolyIC Induces Retinoic Acid-inducible Gene-I and Melanoma Differentiation-associated Gene 5 and Modulates Inflammation in Podocytes. In Vivo (Brooklyn) 35:147. https://doi.org/10.21873/INVIVO.12242

74. Zhao Y, Ye X, Dunker W, et al (2018) RIG-I like receptor sensing of host RNAs facilitates the cell-intrinsic immune response to KSHV infection. Nat Commun 9:. https://doi.org/10.1038/S41467-018-07314-7

75. Tanaka K, Tanaka M, Watanabe N, et al (2022) C-type lectin-like receptor (CLEC)-2, the ligand of podoplanin, induces morphological changes in podocytes. Scientific Reports 2022 12:1 12:1–12. https://doi.org/10.1038/s41598-022-26456-9

76. La Russa A, Lofaro D, Montesanto A, et al (2023) Association between NLRP3 rs10754558 and CARD8 rs2043211 Variants and Susceptibility to Chronic Kidney Disease. Int J Mol Sci 24:. https://doi.org/10.3390/ijms24044184

77. da Cruz HLA, Cavalcanti CAJ, de Azêvedo Silva J, et al (2020) Differential expression of the inflammasome complex genes in systemic lupus erythematosus. Immunogenetics 72:217–224. https://doi.org/10.1007/s00251-020-01158-6

78. Dessing MC, Kers J, Damman J, et al (2016) Donor and recipient genetic variants in NLRP3 associate with early acute rejection following kidney transplantation. Sci Rep 6:36315. https://doi.org/10.1038/srep36315

79. Abdolvahabi R, Sarrafnejad A, Nafar M, et al (2018) Association Between TLR2, TLR4, and CD14 Gene Polymorphisms and Acute Rejection in Kidney Transplant. Exp Clin Transplant 16:31–37. https://doi.org/10.6002/ect.2016.0115

80. Kim JS, Kim SK, Park JY, et al (2016) Significant Association between Toll-Like Receptor Gene Polymorphisms and Posttransplantation Diabetes Mellitus. Nephron 133:279–86. https://doi.org/10.1159/000446570

81. Yu L, Wang L, Chen S (2010) Endogenous toll-like receptor ligands and their biological significance. J Cell Mol Med 14:2592–603. https://doi.org/10.1111/j.1582-4934.2010.01127.x

82. Burke GW, Mitrofanova A, Fontanella A, et al (2023) The podocyte: glomerular sentinel at the crossroads of innate and adaptive immunity. Front Immunol 14

83. Jo E-K, Kim JK, Shin D-M, Sasakawa C (2016) Molecular mechanisms regulating NLRP3 inflammasome activation. Cell Mol Immunol 13:148–59. https://doi.org/10.1038/cmi.2015.95

84. Decout A, Katz JD, Venkatraman S, Ablasser A (2021) The cGAS-STING pathway as a therapeutic target in inflammatory diseases. Nat Rev Immunol 21:548–569. https://doi.org/10.1038/s41577-021-00524-z

85. Curran CS, Kopp JB (2022) RAGE pathway activation and function in chronic kidney disease and COVID-19. Front Med (Lausanne) 9:970423. https://doi.org/10.3389/fmed.2022.970423